Novel treatment targets for pulmonary arterial hypertension and right ventricular failure

Sun, Xiaoqing

2021

document version
Publisher's PDF, also known as Version of record

Novel treatment targets for pulmonary arterial hypertension and right ventricular failure

Xiaoqing Sun

孙晓晴

Novel treatment targets for pulmonary arterial hypertension and right ventricular failure

Xiaoqing Sun

孙晓晴

Novel treatment targets for pulmonary arterial hypertension and right ventricular failure
Thesis, VU University, Amsterdam, the Netherlands

Cover design	**Xiaoqing Sun, Ivor Burgos**
Layout	**Harma Makken / persoonlijkproefschrift.nl**
Printing	**Ridderprint / ridderprint.nl**
ISBN	**978-94-6416-581-4**

VRIJE UNIVERSITEIT

NOVEL TREATMENT TARGETS FOR PULMONARY ARTERIAL HYPERTENSION AND RIGHT VENTRICULAR FAILURE

ACADEMISCH PROEFSCHRIFT

ter verkrijging van de graad Doctor of Philosophy aan
de Vrije Universiteit Amsterdam,
op gezag van de rector magnificus
prof.dr. V. Subramaniam,
in het openbaar te verdedigen
ten overstaan van de promotiecommissie
van de Faculteit der Geneeskunde
op woensdag 2 juni 2021 om 11.45 uur
in de aula van de universiteit,
De Boelelaan 1105

door

Xiaoqing Sun

geboren te Shandong, China

promotoren:	prof.dr. H.J. Bogaard prof.dr. M.J.T.H. Goumans
copromotor:	dr. F.S. Handoko-de Man

欲穷千力目, 更上一层楼

~王之涣

One can enjoy a grander sight

by climbing to a greater height

~Zhihuan Wang

Voorzitter promotiecommissie:	prof. dr. B.J.J.M. Brundel
Overige leden promotiecommissie:	prof. dr. S. Bonnet
	prof. dr. R.A. de Boer
	associate prof. dr. B. Bartelds
	associate prof. dr. A. Andersen
	assistant prof. dr. G. Sánchez-Duffhues

paranimfen:	Eva L Peters
	Rahana Yasmeen Parbhudayal

The research presented in this thesis was performed at the Department of Pulmonology and Physiology of VU University Medical Center / Amsterdam Cardiovascular Sciences, Amsterdam.

The research described in this thesis was supported by Dutch Cardiovascular Alliance: the Dutch Heart Foundation, Dutch Federation of University Medical Centers, the Netherlands Organization for Health Research and Development, and the Royal Netherlands Academy of Sciences (CVON-2012-08 PHAEDRA, CVON-2018-29 PHAEDRA-IMPACT), the Netherlands Organization for Scientific Research (NWO-VICI: 918.16.610, NWO-VIDI: 917.18.338).

Financial support by the Dutch Heart Foundation for the publication of this thesis is gratefully acknowledged.

Additional financial support for printing this thesis was kindly provided by:
Pfizer PFE bv

CONTENTS

Part IV: Treatment and the right ventricle

Part V: Summary and general discussion

Part I

General introduction and scope of the thesis

CHAPTER 1

General Introduction and thesis outline

ABBREVIATIONS

BMPR2	bone morphogenetic protein type 2 receptor
DCA	dichloroacetate
EC	endothelial cell
FGF	fibroblast growth factor
HDAC	histone deacetylases
IPF	idiopathic pulmonary fibrosis
MAO	monoamine oxidase
MCT	monocrotaline
MCTP	monocrotaline pyrrole
MnTBAP	Manganese (III) tetrakis (4-benzoic acid) porphyrin
mPAP	mean pulmonary artery pressure
PAB	pulmonary artery banding
PAH	pulmonary arterial hypertension
PASMC	pulmonary arterial smooth muscle cell
PDGF	platelet derived growth factor
PH	pulmonary hypertension
RV	Right ventricle
SuHx	SU5416 plus hypoxia
TGF	transforming growth factor
VEGF	vascular endothelial growth factor
WHO	World Health Organization

1. PULMONARY ARTERIAL HYPERTENSION

Pulmonary hypertension (PH) is a hemodynamic state, regardless of its etiology characterized by chronic elevation of pulmonary artery pressure and pulmonary vascular resistance, and ultimately leading to right ventricular (RV) failure.[1] The new definition of PH was discussed in 2018, during the 6th World Symposium on PH, which led to a revision of the hemodynamic threshold of mean pulmonary artery pressure (mPAP) from ≥ 25 mmHg to > 20 mmHg.[2, 3]

PH is classified into five groups roughly based on pathophysiology, the so-called World Health Organization (WHO) groups (Table 1). The term pulmonary arterial hypertension (PAH) specifically refers to WHO group 1, which is hemodynamically distinguished by precapillary PH, with mPAP ≥ 20 mmHg, pulmonary wedge pressure

≤ 15 mmHg, and pulmonary vascular resistance > 3 wood units measured by right heart catheterization.[2] PAH is a relatively rare disease, affecting approximately 6.6 to 26 people per million.[4-6]

Table 1. WHO clinical classification of pulmonary hypertension[7]

WHO group 1. Pulmonary arterial hypertension (PAH)
1.1 Idiopathic PAH
1.2 Heritable PAH
1.3 Drug and toxin induced
1.4 Associated with:
1.4.1 Connective tissue disease
1.4.2 Congenital heart disease
1.4.3 Portal hypertension
1.4.4 Human immunodeficiency virus infection
1.4.5 Schistosomiasis
WHO group 1. pulmonary veno-occlusive disease/pulmonary capillary hemangiomatosis
WHO group 2. PH secondary to left heart disease
WHO group 3. PH secondary to lung diseases/hypoxemia
WHO group 4. chronic thromboembolic pulmonary hypertension
WHO group 5. PH of miscellaneous or uncertain causes

PAH is characterized by a proliferative vasculopathy and excessive remodeling in the distal pulmonary arterial bed, resulting in high pulmonary artery pressure and RV afterload.[8] The progressive increase in RV afterload leads to RV failure, which is the major cause of mortality. Currently, therapies for PAH are limited to vasodilators, which can dilate the partially occluded vessels and relieve disease symptoms. However, they cannot reverse pulmonary vascular remodeling or stop the progression of RV failure, and PAH still remains a progressive lethal disease.[9] The NIH registry in 1984 was the first large registry to provide data on survival of PAH patients, showing 1-, 3- and 5-year survival rates of 68%, 48% and 34%, respectively.[10] Despite the progress in PAH specific therapies and support strategies, recent registries show that PAH survival remains poor with 1-, 3- and 5-year survival rates of 88-96%, 72-77% and 59-64%, respectively.[11-13]

Therefore, new treatments targeting pulmonary vascular remodeling and the RV are urgently required. The overall aim of this thesis is to investigate novel promising treatment strategies for PAH and RV failure, based on multiple pathological mechanisms underlying the disease, including bone morphogenetic protein type 2

receptor (BMPR2) signaling pathway (***Chapter 2-4***), growth factors (***Chapter 5***), histone acetylation (***Chapter 6***), as well as treatment targeting the RV (***Chapter 7-9***).

2. PROMISING TREATMENT TARGETS FOR PAH

2.1 BMPR2 signaling pathway

BMPR2 is a transmembrane serine/threonine kinase receptor involved in the BMP signaling pathway, which is essential for embryogenesis, development and tissue homeostasis. Upon ligand-induced formation of a heteromeric receptor complex of consisting of a type 2 and a type 1 receptor, BMPR2 activates the BMPR type 1 receptor, BMPR1, by phosphorylation of specific residues in its kinase domain. The activated BMPR1 propagates the signal towards the nucleus through phosphorylation of the BMP specific transcription factors SMAD1, -5 and/or 8.

More than 70% of patients with hereditary PAH show heterozygous mutations in BMPR2, and about 40% of all subjects carrying BMPR2 mutations resulting in haplo-insufficiency will ultimately develop PAH.[14, 15] More interestingly, non-genetic forms of PAH have also been related to a reduction in BMPR2 levels and BMP signaling.[16] Loss of BMPR2 has been linked to increased inflammation and proliferation of pulmonary endothelial cells (ECs) as well as pulmonary arterial smooth muscle cells (PASMCs).[17-19] Based on this, modulation of BMPR2 signaling is considered a promising treatment strategy for PAH. In ***Part II*** of the thesis, I investigate novel PAH treatment strategies related to modulating the BMPR2 pathway.

Although many translational researchers have sought to treat PAH by restoring BMPR2 signaling, basic characterization of BMPR2 expression and activity in the lungs of PAH patients and animals with experimental PAH is far from complete. In only a few studies, BMPR2 expression was assessed in the lungs of patients with PAH. Moreover, the methodology used to study BMPR2 expression varied between studies. Therefore, in ***Chapter 2***, we describe BMPR2 receptor expression and downstream signaling in animal models most commonly used to study experimentally induced PH and compare these findings to altered BMPR2 signaling in the lungs of PAH patients.

In ***Chapter 3***, we investigate the role of the orphan nuclear receptor Nur77 as a promising treatment target for PAH. Nur77 plays a key role in a wide array of cellular

processes such as proliferation, apoptosis and inflammation, and it is implicated in several cardiovascular diseases.[20-24] Interestingly, in a cell-and context-dependent manner Nur77 modulates the transforming growth factor (TGF)-β pathway, which has a strong connection with BMPR2 signaling.[25, 26] Therefore, we hypothesized that activation of Nur77 by 6-mercaptopurine would improve PAH by reducing proliferation, inflammation and increasing BMPR2 signaling.

In ***Chapter 4***, we tested Manganese (III) tetrakis (4-benzoic acid) porphyrin (MnTBAP) as another potential PAH treatment acting on the BMPR2 pathway. MnTBAP is a synthetic metalloporphyrin which has been shown to have beneficial effects in bleomycin-induced pulmonary fibrosis, carrageenan-induced pleurisy, lung contusion, renal fibrosis and renal injury.[27-30] Besides its effects on oxidative stress and inflammation, MnTBAP has been shown to increase BMPR2 in human umbilical vein endothelial cells.[31] Therefore, we hypothesized that MnTBAP might be a potential therapeutic treatment for PAH.

2.2 Growth factor signaling

Dysregulated signaling by growth factors and their receptors has been found to contribute to remodeling in PAH in both the pulmonary vasculature and the RV. Growth factors of interest include platelet derived growth factor (PDGF), fibroblast growth factor (FGF), vascular endothelial growth factor (VEGF) and TGF-β.[32]

In ***Chapter 5***, we tested Nintedanib to treat PAH. Nintedanib is a tyrosine kinase inhibitor that targets primarily PDGF-, FGF-, and VEGF-mediated proliferation in pulmonary fibroblasts, and possibly TGF-β-mediated transformation to myofibroblasts.[33] Moreover, nintedanib was approved for the treatment of idiopathic pulmonary fibrosis (IPF).[33] The anti-proliferative properties of nintedanib may have a potential beneficial effect on pulmonary vascular remodeling by reversing the associated PH in patients with IPF. We hypothesized that nintedanib could also have favorable effects on PAH by reducing vascular remodeling.

2.3 Histone acetylation

Acetylation of lysine residues on the N-terminal tails of histones modulates chromatin structure and accessibility of the genome by altering DNA-histone interactions. Among the two enzymes families regulating histone acetylation, histone deacetylases (HDACs) regulate several key cellular processes and are implicated in several cardiovascular

diseases.[34] Given the effects of HDACs on proliferation, apoptosis and inflammation of ECs and SMCs, we hypothesized that HDAC inhibition may treat PAH. Therefore, in ***Chapter 6***, we studied the effects of the efficient second-generation HDAC inhibitor quisinostat in experimental PAH.

3. PAH THERAPIES AND RV FAILURE

Although the initial insult in PAH involves the pulmonary vasculature, RV failure is the most important determinant of mortality in patients with PAH.[35-37] 5-year survival in PAH patients is strongly correlated with RV ejection fraction, independent of changes in pulmonary vascular resistance or pressures.[37] Therefore, it is important for drugs used in the treatment of PAH to be beneficial or at least non-toxic to the RV. In ***Part IV*** of the thesis, ***Chapters 7-9***, I review RV failure mechanisms and investigate the effects of novel PAH therapies on the RV.

3.1 Pathogenesis of RV failure

Many questions regarding the mechanisms underlying RV failure remain unclear. Recent clinical and pre-clinical studies have identified several key structural and molecular determinants that are associated with RV failure, including inflammation, metabolic shift from oxidative metabolism towards glycolysis, oxidative stress, capillary rarefaction, neurohormonal activation, and upregulation of profibrotic pathways (Figure 1).[38-42]

Among these factors, the role of inflammation has been highlighted in the initiation and maintenance of pulmonary vascular remodeling in PAH. Less is known about the possible role of inflammation in the development of RV failure. Inflammation is considered a *double-edged sword*, as it stimulates the immune response to microbial infection while it may also lead to further injuries in noninfectious conditions, such as cardiovascular diseases.[43] The "Cytokine Hypothesis" is regarded as one of the basic mechanisms for the development of heart failure, and states that a cardiac event triggers systemic activation of pro-inflammatory cytokines, which in turn accelerate the progression of heart failure.[44] In ***Chapter 7,*** we review the available evidence of inflammation in the pressure overloaded RV and discuss the potential role of inflammation in the pathogenesis and progression of RV failure. Based on available

evidence, we propose a key role for inflammation and neurohormonal signaling in the vicious circle of pulmonary vascular remodeling and RV failure (Figure 1).

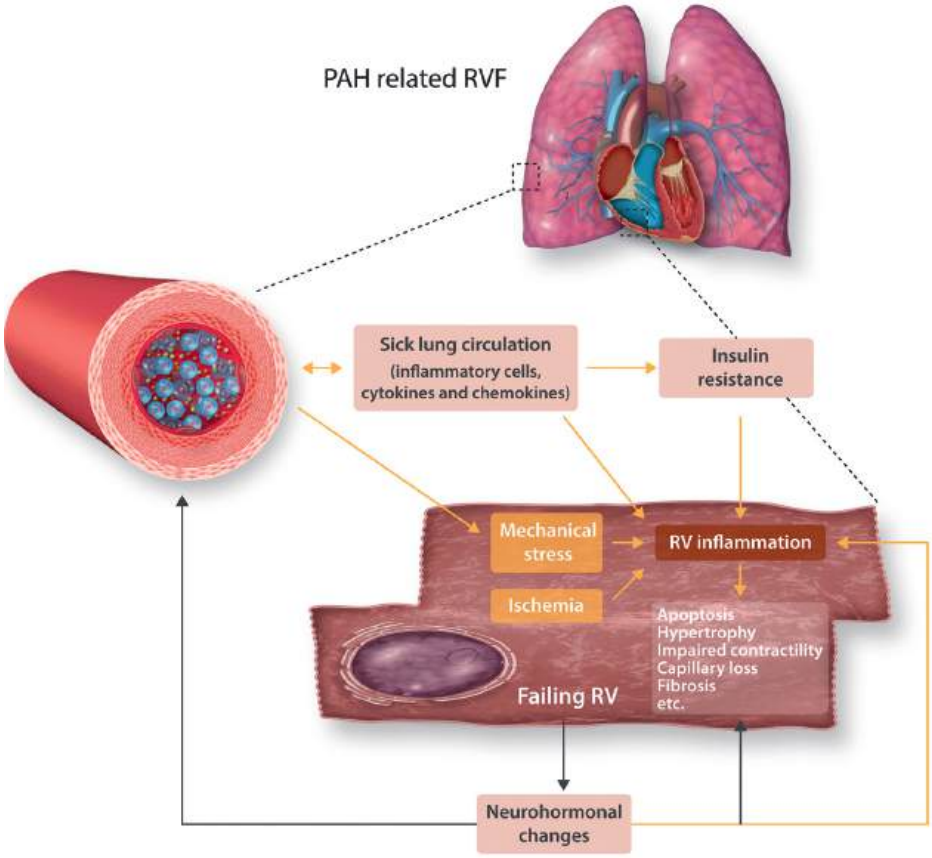

Figure 1. The role of inflammation in the vicious circle between pulmonary vascular remodeling and RV failure (taken from Chapter 7).
In PAH, perivascular inflammation plays a role in pulmonary vascular remodeling, leading to increased RV mechanical stress, ischemia, and systemic inflammation spilling over into the RV. Increased activity of the neurohormonal system is another trigger of RV inflammation. While RV inflammation may lead to the progression of RV failure, the failing heart will further increase neurohormonal activity, which promotes pulmonary vascular remodeling. Altogether, a vicious circle is formed between RV inflammation, RV failure and pulmonary vascular remodeling.

3.2 The effect of novel PAH treatments on the RV

The current treatment paradigm of RV failure has a focus on supportive and symptom-based care. After reducing RV afterload and optimizing preload, it may be desirable to

increase RV contractility.[45] Until now, there have been no therapies directly targeting the RV.

In ***Chapter 8***, we evaluate the effects of dichloroacetate (DCA) on RV remodeling, specially focused on myocardial apoptosis. DCA was shown to target the mitochondria and inhibit pyruvate dehydrogenase kinase, promoting RV function by increasing glucose oxidation.[46, 47] As DCA can target mitochondrial related pathways of apoptosis, it can be speculated that at least some of DCA's beneficial effects in the RV may come about through modulation of myocardial apoptosis. However, previous studies on DCA and apoptosis have been controversial.

In ***Chapter 9***, we investigate the treatment effects of monoamine oxidase A (MAO-A) inhibitor on experimental PAH and RV failure. MAO-A, as a class of enzyme bound to the outer mitochondrial membrane, is an important source of reactive oxygen species.[48] Increased MAO-A activity in ECs and cardiomyocytes contributes to vascular dysfunction and progression of left heart failure.[49-51] Moreover, MAO-A catalyzes preferentially serotonin and norepinephrine, two monoamines with widely recognized roles in PAH and RV failure. Therefore, we hypothesized that MAO-A can be a novel promising target for PAH and RV failure treatment.

4. ANIMAL MODELS OF PH AND RV FAILURE

In my thesis, I use three experimental rodent models to investigate new treatments for PAH and RV failure: the Sugen 5416 + hypoxia (SuHx) rat model, the monocrotaline (MCT) rat model and the pulmonary artery banding (PAB) rat model.

SuHx PAH rat model is a "second hit" model which exhibits many features of severe PAH in humans. The model relies on a single subcutaneous injection of the VEGF receptor inhibitor Sugen (SU-5416), which is followed by exposure to chronic hypoxia for 2-4 weeks. SU-5416 induces EC apoptosis and causes mild PAH without any other second hit.[52] But under chronic hypoxic conditions, hyper-proliferation of a subset of apoptosis-resistant ECs is stimulated leading to severe, irreversible angio-obliterative PAH.[52] Importantly, the SuHx rat model has shown to be a particularly robust PAH model, as drugs with demonstrated efficacy in other PH rodent models have little effect in SuHx rats.[53] Moreover, SuHx induces RV failure with death of some but not all animals,

which is somewhat similar to the disease progression of PAH patients.[54] Considering the similarities with human PAH, the SuHx rat model is the most commonly used model in this thesis, including ***Chapter 2-6*** and ***Chapter 9***.

An older and even more frequently used model of PH is exposure to MCT. Advantages of the model include its technical simplicity, reproducibility and low cost.[55] In this model, PH is induced by a single subcutaneous injection of MCT, which is a toxic pyrrolizidine alkaloid derived from the seeds of the *Crotalaria spectabilis* plant. After injection, MCT is activated into the reactive pyrrole metabolite dehydromonocrotaline (MCTP) in the liver, which is highly reactive and instable with a short half-life of a few seconds. MCTP is then temporarily stabilized by binding to erythrocytes, and it is detached from its carrier during gas-exchange to enter the lungs.[55] Although the exact mechanism is unknown, it is speculated by many that MCTP causes direct EC damage that then triggers the inexorable development and progression of severe PH, which eventually leads to RV failure.[54, 55] In this thesis, we used MCT rat model in ***Chapter 2*** and ***Chapter 8***.

In contrast to the SuHx and MCT models which cause pulmonary vascular remodeling, the PAB rat model is characterized by a preserved pulmonary vasculature. RV dysfunction in the PAB model therefore is not sensitive to any effects of drugs on the pulmonary vasculature. PAB is usually performed by placing a suture, clip, or inflatable ring around the pulmonary trunk proximally to the RV. In the presence of severe PAB, the mortality can reach 40% in adult rodents.[38] Importantly, use of the PAB model allows for the demonstration of afterload-independent myocardial effects of new therapeutic approaches.[56] Therefore, in order to confirm the independent effect and safety of new therapies on the RV, we used PAB rat model in ***Chapter 9***.

5. SUMMARY

PAH is a progressive and fatal disease characterized by pulmonary vascular remodeling, increased pulmonary vascular resistance and ultimately leads to RV failure and premature death. Unfortunately, current treatments for PAH are limited to pharmacological vasodilation to dilate the partially occluded vessels and weak anti-proliferative agents, and they have been proved to be ineffective in reversing vascular remodeling and preventing deterioration and the need for lung transplant.

Therefore, new treatments interfering with different mechanisms of PAH pathogenesis are required.

This thesis aimed to investigate novel promising treatment strategies for PAH and PAH induced RV failure, based on multiple pathological mechanisms underlying the disease. Therefore, I investigated drugs impacting on BMPR2 signaling pathway (***Chapter 2-4***), on growth factor signaling (***Chapter 5***), on histone acetylation (***Chapter 6***), as well as several therapeutic strategies specifically targeting the RV (***Chapter 7-9***).

REFERENCES

1. Vonk Noordegraaf A, Groeneveldt JA and Bogaard HJ. Pulmonary hypertension. *Eur Respir Rev*. 2016;25:4-11.
2. Condon DF, Nickel NP, Anderson R, Mirza S and de Jesus Perez VA. The 6th World Symposium on Pulmonary Hypertension: what's old is new. *F1000Res*. 2019;8.
3. Simonneau G, Montani D, Celermajer DS, Denton CP, Gatzoulis MA, Krowka M, Williams PG and Souza R. Haemodynamic definitions and updated clinical classification of pulmonary hypertension. *Eur Respir J*. 2019;53.
4. Peacock AJ, Murphy NF, McMurray JJ, Caballero L and Stewart S. An epidemiological study of pulmonary arterial hypertension. *Eur Respir J*. 2007;30:104-9.
5. Humbert M, Sitbon O, Chaouat A, Bertocchi M, Habib G, Gressin V, Yaici A, Weitzenblum E, Cordier JF, Chabot F, Dromer C, Pison C, Reynaud-Gaubert M, Haloun A, Laurent M, Hachulla E and Simonneau G. Pulmonary arterial hypertension in France: results from a national registry. *Am J Respir Crit Care Med*. 2006;173:1023-30.
6. Escribano-Subias P, Blanco I, Lopez-Meseguer M, Lopez-Guarch CJ, Roman A, Morales P, Castillo-Palma MJ, Segovia J, Gomez-Sanchez MA, Barbera JA and investigators R. Survival in pulmonary hypertension in Spain: insights from the Spanish registry. *Eur Respir J*. 2012;40:596-603.
7. Kim D and George MP. Pulmonary Hypertension. *Med Clin North Am*. 2019;103:413-423.
8. Wilkins MR. Pulmonary hypertension: the science behind the disease spectrum. *Eur Respir Rev*. 2012;21:19-26.
9. Lajoie AC, Lauziere G, Lega JC, Lacasse Y, Martin S, Simard S, Bonnet S and Provencher S. Combination therapy versus monotherapy for pulmonary arterial hypertension: a meta-analysis. *Lancet Respir Med*. 2016;4:291-305.
10. Rich S, Dantzker DR, Ayres SM, Bergofsky EH, Brundage BH, Detre KM, Fishman AP, Goldring RM, Groves BM, Koerner SK and et al. Primary pulmonary hypertension. A national prospective study. *Annals of internal medicine*. 1987;107:216-23.
11. Benza RL, Miller DP, Barst RJ, Badesch DB, Frost AE and McGoon MD. An evaluation of long-term survival from time of diagnosis in pulmonary arterial hypertension from the REVEAL Registry. *Chest*. 2012;142:448-456.
12. Gall H, Felix JF, Schneck FK, Milger K, Sommer N, Voswinckel R, Franco OH, Hofman A, Schermuly RT, Weissmann N, Grimminger F, Seeger W and Ghofrani HA. The Giessen Pulmonary Hypertension Registry: Survival in pulmonary hypertension subgroups. *The Journal of heart and lung transplantation : the official publication of the International Society for Heart Transplantation*. 2017;36:957-967.
13. Strange G, Lau EM, Giannoulatou E, Corrigan C, Kotlyar E, Kermeen F, Williams T, Celermajer DS, Dwyer N, Whitford H, Wrobel JP, Feenstra J, Lavender M, Whyte K, Collins N, Steele P, Proudman S, Thakkar V, Keating D and Keogh A. Survival of Idiopathic Pulmonary Arterial Hypertension Patients in the Modern Era in Australia and New Zealand. *Heart, lung & circulation*. 2018;27:1368-1375.

14. K.B. L, R.D M, Pauciulo MW, Thomson JR, Phillips JA, 3rd, Loyd JE, Nichols WC and Trembath RC. Heterozygous germline mutations in BMPR2, encoding a TGF-beta receptor, cause familial primary pulmonary hypertension. *Nat Genet*. 2000;26:81-84.
15. Deng ZM, Morse JH, Slager SL, Cuervo N, Moore KJ, Venetos G, Kalachikov S, Cayanis E, Fischer SG, Barst RJ, Hodge SE and Knowles JA. Familial primary pulmonary hypertension (gene PPH1) is caused by mutations in the bone morphogenetic protein receptor-II gene. *Am J Hum Genet*. 2000;67:737-744.
16. Machado RD, Southgate L, Eichstaedt CA, Aldred MA, Austin ED, Best DH, Chung WK, Benjamin N, Elliott CG, Eyries M, Fischer C, Graf S, Hinderhofer K, Humbert M, Keiles SB, Loyd JE, Morrell NW, Newman JH, Soubrier F, Trembath RC, Viales RR and Grunig E. Pulmonary Arterial Hypertension: A Current Perspective on Established and Emerging Molecular Genetic Defects. *Hum Mutat*. 2015;36:1113-27.
17. Hansmann G, de Jesus Perez VA, Alastalo TP, Alvira CM, Guignabert C, Bekker JM, Schellong S, Urashima T, Wang L, Morrell NW and Rabinovitch M. An antiproliferative BMP-2/PPARgamma/apoE axis in human and murine SMCs and its role in pulmonary hypertension. *J Clin Invest*. 2008;118:1846-57.
18. de Jesus Perez VA, Alastalo TP, Wu JC, Axelrod JD, Cooke JP, Amieva M and Rabinovitch M. Bone morphogenetic protein 2 induces pulmonary angiogenesis via Wnt-beta-catenin and Wnt-RhoA-Rac1 pathways. *J Cell Biol*. 2009;184:83-99.
19. Soon E, Crosby A, Southwood M, Yang P, Tajsic T, Toshner M, Appleby S, Shanahan CM, Bloch KD, Pepke-Zaba J, Upton P and Morrell NW. Bone morphogenetic protein receptor type II deficiency and increased inflammatory cytokine production. A gateway to pulmonary arterial hypertension. *Am J Respir Crit Care Med*. 2015;192:859-72.
20. Nie X, Tan J, Dai Y, Mao W, Chen Y, Qin G, Li G, Shen C, Zhao J and Chen J. Nur77 downregulation triggers pulmonary artery smooth muscle cell proliferation and migration in mice with hypoxic pulmonary hypertension via the Axin2-beta-catenin signaling pathway. *Vascul Pharmacol*. 2016;87:230-241.
21. Pires NM, Pols TW, de Vries MR, van Tiel CM, Bonta PI, Vos M, Arkenbout EK, Pannekoek H, Jukema JW, Quax PH and de Vries CJ. Activation of nuclear receptor Nur77 by 6-mercaptopurine protects against neointima formation. *Circulation*. 2007;115:493-500.
22. You B, Jiang YY, Chen S, Yan G and Sun J. The orphan nuclear receptor Nur77 suppresses endothelial cell activation through induction of IkappaBalpha expression. *Circ Res*. 2009;104:742-9.
23. Moll UM, Marchenko N and Zhang XK. p53 and Nur77/TR3 - transcription factors that directly target mitochondria for cell death induction. *Oncogene*. 2006;25:4725-43.
24. Medzikovic L, Schumacher CA, Verkerk AO, van Deel ED, Wolswinkel R, van der Made I, Bleeker N, Cakici D, van den Hoogenhof MM, Meggouh F, Creemers EE, Remme CA, Baartscheer A, de Winter RJ, de Vries CJ, Arkenbout EK and de Waard V. Orphan nuclear receptor Nur77 affects cardiomyocyte calcium homeostasis and adverse cardiac remodelling. *Sci Rep*. 2015;5:15404.

25. Palumbo-Zerr K, Zerr P, Distler A, Fliehr J, Mancuso R, Huang J, Mielenz D, Tomcik M, Fürnrohr BG, Scholtysek C, Dees C, Beyer C, Krönke G, Metzger D, Distler O, Schett G and Distler JH. Orphan nuclear receptor NR4A1 regulates transforming growth factor-β signaling and fibrosis. *Nature medicine*. 2015;21:150-8.
26. Zhou F, Drabsch Y, Dekker TJ, de Vinuesa AG, Li Y, Hawinkels LJ, Sheppard KA, Goumans MJ, Luwor RB, de Vries CJ, Mesker WE, Tollenaar RA, Devilee P, Lu CX, Zhu H, Zhang L and Dijke PT. Nuclear receptor NR4A1 promotes breast cancer invasion and metastasis by activating TGF-β signalling. *Nature communications*. 2014;5:3388.
27. Venkatadri R, Iyer AK, Ramesh V, Wright C, Castro CA, Yakisich JS and Azad N. MnTBAP Inhibits Bleomycin-Induced Pulmonary Fibrosis by Regulating VEGF and Wnt Signaling. *J Cell Physiol*. 2017;232:506-516.
28. Suresh MV, Yu B, Lakshminrusimha S, Machado-Aranda D, Talarico N, Zeng L, Davidson BA, Pennathur S and Raghavendran K. The protective role of MnTBAP in oxidant-mediated injury and inflammation in a rat model of lung contusion. *Surgery*. 2013;154:980-90.
29. Bi X, Wang J, Liu Y, Wang Y and Ding W. MnTBAP treatment ameliorates aldosterone-induced renal injury by regulating mitochondrial dysfunction and NLRP3 inflammasome signalling. *Am J Transl Res*. 2018;10:3504-3513.
30. Batinic-Haberle I, Cuzzocrea S, Reboucas JS, Ferrer-Sueta G, Mazzon E, Di Paola R, Radi R, Spasojevic I, Benov L and Salvemini D. Pure MnTBAP selectively scavenges peroxynitrite over superoxide: comparison of pure and commercial MnTBAP samples to MnTE-2-PyP in two models of oxidative stress injury, an SOD-specific Escherichia coli model and carrageenan-induced pleurisy. *Free Radic Biol Med*. 2009;46:192-201.
31. Zhou Q, Einert M, Schmitt H, Wang Z, Pankratz F, Olivier CB, Bode C, Liao JK and Moser M. MnTBAP increases BMPR-II expression in endothelial cells and attenuates vascular inflammation. *Vascul Pharmacol*. 2016;84:67-73.
32. Hassoun PM, Mouthon L, Barbera JA, Eddahibi S, Flores SC, Grimminger F, Jones PL, Maitland ML, Michelakis ED, Morrell NW, Newman JH, Rabinovitch M, Schermuly R, Stenmark KR, Voelkel NF, Yuan JX and Humbert M. Inflammation, growth factors, and pulmonary vascular remodeling. *J Am Coll Cardiol*. 2009;54:S10-9.
33. Wollin L, Wex E, Pautsch A, Schnapp G, Hostettler KE, Stowasser S and Kolb M. Mode of action of nintedanib in the treatment of idiopathic pulmonary fibrosis. *European Respiratory Journal*. 2015;45:1434-1445.
34. Rosa-Garrido M, Chapski DJ and Vondriska TM. Epigenomes in Cardiovascular Disease. *Circ Res*. 2018;122:1586-1607.
35. van Wolferen SA, Marcus JT, Boonstra A, Marques KM, Bronzwaer JG, Spreeuwenberg MD, Postmus PE and Vonk-Noordegraaf A. Prognostic value of right ventricular mass, volume, and function in idiopathic pulmonary arterial hypertension. *European heart journal*. 2007;28:1250-7.
36. van de Veerdonk MC, Kind T, Marcus JT, Mauritz GJ, Heymans MW, Bogaard HJ, Boonstra A, Marques KM, Westerhof N and Vonk-Noordegraaf A. Progressive right ventricular dysfunction in patients with pulmonary arterial hypertension responding to therapy. *J Am Coll Cardiol*. 2011;58:2511-9.

37. Mauritz GJ, Kind T, Marcus JT, Bogaard HJ, van de Veerdonk M, Postmus PE, Boonstra A, Westerhof N and Vonk-Noordegraaf A. Progressive changes in right ventricular geometric shortening and long-term survival in pulmonary arterial hypertension. *Chest*. 2012;141:935-943.
38. Bogaard HJ, Natarajan R, Henderson SC, Long CS, Kraskauskas D, Smithson L, Ockaili R, McCord JM and Voelkel NF. Chronic pulmonary artery pressure elevation is insufficient to explain right heart failure. *Circulation*. 2009;120:1951-60.
39. Bogaard HJ, Natarajan R, Mizuno S, Abbate A, Chang PJ, Chau VQ, Hoke NN, Kraskauskas D, Kasper M, Salloum FN and Voelkel NF. Adrenergic receptor blockade reverses right heart remodeling and dysfunction in pulmonary hypertensive rats. *Am J Respir Crit Care Med*. 2010;182:652-60.
40. Ciarka A, Doan V, Velez-Roa S, Naeije R and van de Borne P. Prognostic significance of sympathetic nervous system activation in pulmonary arterial hypertension. *Am J Respir Crit Care Med*. 2010;181:1269-75.
41. Campian ME, Hardziyenka M, de Bruin K, van Eck-Smit BL, de Bakker JM, Verberne HJ and Tan HL. Early inflammatory response during the development of right ventricular heart failure in a rat model. *European journal of heart failure*. 2010;12:653-8.
42. Neubauer S. The failing heart--an engine out of fuel. *The New England journal of medicine*. 2007;356:1140-51.
43. Frangogiannis NG. The inflammatory response in myocardial injury, repair, and remodelling. *Nat Rev Cardiol*. 2014;11:255-65.
44. Seta Y, Shan K, Bozkurt B, Oral H and Mann DL. Basic mechanisms in heart failure: the cytokine hypothesis. *J Card Fail*. 1996;2:243-9.
45. Konstam MA, Kiernan MS, Bernstein D, Bozkurt B, Jacob M, Kapur NK, Kociol RD, Lewis EF, Mehra MR, Pagani FD, Raval AN and Ward C. Evaluation and Management of Right-Sided Heart Failure: A Scientific Statement From the American Heart Association. *Circulation*. 2018;137:e578-e622.
46. Piao L, Fang YH, Cadete VJ, Wietholt C, Urboniene D, Toth PT, Marsboom G, Zhang HJ, Haber I, Rehman J, Lopaschuk GD and Archer SL. The inhibition of pyruvate dehydrogenase kinase improves impaired cardiac function and electrical remodeling in two models of right ventricular hypertrophy: resuscitating the hibernating right ventricle. *Journal of molecular medicine (Berlin, Germany)*. 2010;88:47-60.
47. Piao L, Sidhu VK, Fang YH, Ryan JJ, Parikh KS, Hong Z, Toth PT, Morrow E, Kutty S, Lopaschuk GD and Archer SL. FOXO1-mediated upregulation of pyruvate dehydrogenase kinase-4 (PDK4) decreases glucose oxidation and impairs right ventricular function in pulmonary hypertension: therapeutic benefits of dichloroacetate. *Journal of molecular medicine (Berlin, Germany)*. 2013;91:333-46.
48. Kaludercic N, Mialet-Perez J, Paolocci N, Parini A and Di Lisa F. Monoamine oxidases as sources of oxidants in the heart. *J Mol Cell Cardiol*. 2014;73:34-42.
49. Deshwal S, Di Sante M, Di Lisa F and Kaludercic N. Emerging role of monoamine oxidase as a therapeutic target for cardiovascular disease. *Curr Opin Pharmacol*. 2017;33:64-69.

50. Lighezan R, Sturza A, Duicu OM, Ceausu RA, Vaduva A, Gaspar M, Feier H, Vaida M, Ivan V, Lighezan D, Muntean DM and Mornos C. Monoamine oxidase inhibition improves vascular function in mammary arteries from nondiabetic and diabetic patients with coronary heart disease. *Can J Physiol Pharmacol*. 2016;94:1040-1047.
51. Kaludercic N, Takimoto E, Nagayama T, Feng N, Lai EW, Bedja D, Chen K, Gabrielson KL, Blakely RD, Shih JC, Pacak K, Kass DA, Di Lisa F and Paolocci N. Monoamine oxidase A-mediated enhanced catabolism of norepinephrine contributes to adverse remodeling and pump failure in hearts with pressure overload. *Circ Res*. 2010;106:193-202.
52. Taraseviciene-Stewart L, Kasahara Y, Alger L, Hirth P, Mc Mahon G, Waltenberger J, Voelkel NF and Tuder RM. Inhibition of the VEGF receptor 2 combined with chronic hypoxia causes cell death-dependent pulmonary endothelial cell proliferation and severe pulmonary hypertension. *FASEB J*. 2001;15:427-38.
53. Nicolls MR, Mizuno S, Taraseviciene-Stewart L, Farkas L, Drake JI, Al Husseini A, Gomez-Arroyo JG, Voelkel NF and Bogaard HJ. New models of pulmonary hypertension based on VEGF receptor blockade-induced endothelial cell apoptosis. *Pulm Circ*. 2012;2:434-42.
54. Stenmark KR, Meyrick B, Galie N, Mooi WJ and McMurtry IF. Animal models of pulmonary arterial hypertension: the hope for etiological discovery and pharmacological cure. *Am J Physiol Lung Cell Mol Physiol*. 2009;297:L1013-32.
55. Gomez-Arroyo JG, Farkas L, Alhussaini AA, Farkas D, Kraskauskas D, Voelkel NF and Bogaard HJ. The monocrotaline model of pulmonary hypertension in perspective. *Am J Physiol Lung Cell Mol Physiol*. 2012;302:L363-9.
56. Guihaire J, Bogaard HJ, Flecher E, Noly PE, Mercier O, Haddad F and Fadel E. Experimental models of right heart failure: a window for translational research in pulmonary hypertension. *Semin Respir Crit Care Med*. 2013;34:689-99.

Part II

Novel treatment targeting BMPR2 pathway

CHAPTER 2

The BMP receptor 2 in pulmonary arterial hypertension: when and where the animal model matches the patient?

C.M. Happé[1]*, K. Kurakula[2]*, XQ. Sun[1], D. Bos[1], N. Rol[1], C. Guignabert[3,4], L. Tu[3,4], I. Schalij[1], K.C. Wiesmeijer[1], Olga Tura-Ceide[5,6], A. Vonk-Noordegraaf[1], F.S. de Man[1], H.J. Bogaard[1], M.J. Goumans[2]

*Both authors contributed equally

[1]Amsterdam UMC, Vrije Universiteit Amsterdam, Department of Pulmonology, Amsterdam Cardiovascular Sciences, Amsterdam, the Netherlands. [2]Laboratory for cardiovascular cell biology, Department of Cell and Chemical Biology, Leiden University Medical Center, Leiden, the Netherlands. [3]INSERM UMR_S 999, LabEx LERMIT, Centre Chirurgical Marie Lannelongue, Le Plessis-Robinson and Université Paris-Sud, [4]DHU TORINO, Le Kremlin-Bicêtre, Paris, France. [5]Department of Pulmonary Medicine, Hospital Clínic-Institut d'Investigacions Biomèdiques August Pi I Sunyer (IDIBAPS), University of Barcelona, Barcelona, Spain. [6]Biomedical Research Networking center on Respiratory diseases (CIBERES), Madrid, Spain.

Cells. 2020 Jun 8;9(6):1422

ABSTRACT

Background: Mutations in Bone morphogenetic protein receptor type II (BMPR2) are leading in the development of hereditary pulmonary arterial hypertension (PAH). In non-hereditary forms of PAH, perturbations in the Transforming Growth Factor-β (TGF-β)/BMP-axis are believed to cause deficient BMPR2 signaling by changes in receptor expression, activity of the receptor and/or downstream signaling. To date, BMPR2 expression and its activity in the lungs of patients with non-hereditary PAH is poorly characterized. Over the last decades, different animal models have been used to understand the role of BMPR2 signaling in PAH pathophysiology. Especially the Monocrotaline (MCT) and Sugen-Hypoxia (SuHx) models are extensively used in interventional studies to examine if restoring BMPR2 signaling result in PAH disease reversal. While PAH is assumed to develop in patients over months or years, pulmonary hypertension in experimental animal models develops in days or weeks. It is therefore likely that modifications in BMP and TGF-β signaling in these models do not fully recapitulate those in patients. In order to determine the translational potential of the MCT and SuHx models, we analyzed BMPR2 expression and activity in the lungs of rats with experimental induced PAH and compared this to BMPR2 expression and activity in the lungs of PAH patients.

Methods: BMPR2 expression was analyzed by western blot analysis and immunofluorescence (IF) microscopy to determine the quantity and localization of the receptor in lung tissue from normal control subjects and patients with hereditary or idiopathic PAH, as well as in the lungs of control rats and rats with MCT or SuHx- induced PAH. Activation of the BMP pathway was analyzed by determining the level and localization of phosphorylated Smad1/5/8 (pSmad 1/5/8), a downstream mediator of the canonical BMPR2 signaling.

Results: While BMPR2 and pSmad 1/5/8 expression levels were unaltered in whole lung lysates/homogenates from patients with hereditary and idiopathic PAH, IF analysis showed that BMPR2 and pSmad 1/5/8 levels were markedly decreased in the pulmonary vessels of both PAH patient groups. Whole lung BMPR2 expression was variable in the two PAH rat models, while in both experimental models the expression of BMPR2 in the lung vasculature was increased. However, in the human PAH lungs, expression of pSmad 1/5/8 was downregulated in the lung vasculature of both experimental models.

Conclusion: BMPR2 receptor expression and downstream signaling is reduced in the lung vasculature of patients with idiopathic and hereditary PAH, which is cannot be appreciated when using human whole lung lysates. Despite increased BMPR2 expression in the lung vasculature, the MCT and SuHx rat models did develop PAH and impaired downstream BMPR2-Smad signaling similar to our findings in the human lung.

Keywords: pulmonary arterial hypertension, BMPR2, BMP and TGF-β signaling, animal models of pulmonary hypertension

1. INTRODUCTION

Mutations in the *BMPR2* gene were the first genetic perturbations implicated in the pathophysiology of pulmonary arterial hypertension (PAH) and are still responsible for most cases of hereditary PAH (hPAH) to date[1–3]. PAH patients with a BMPR2 mutation present at a younger age with a more severe phenotype and an increased risk of death[4]. Aside from mutations in the *BMPR2* gene other genes related to BMPR2 signaling such as *ALK1, CAV1, ENG, SMAD4, SMAD8 , SMAD9*, *BMPR1* and *BMP9* are implicated in hPAH, albeit less frequent[5–10]. Furthermore, aberrant BMPR2 signaling has been described in non-hereditary subtypes of PAH, although descriptions of defective BMPR2 expression in human tissue remain relatively scarce[11]. Reduced or absent BMPR2 expression was observed in the lung vasculature of patients with idiopathic PAH (iPAH, then called primary pulmonary hypertension) and hPAH. Decreased levels of BMPR2 were also observed in blood-outgrowth endothelial cells (BOECs) from hPAH and iPAH patients[12,13]. Levels of phosphorylated Smad 1/5/8 (pSmad) were altered in pulmonary artery endothelial cells (PAEC) of iPAH patients compared to controls, indicative of altered BMP signaling[14]. Dewachter et al. showed lower mRNA expression of BMPR2 in whole lung lysates from hPAH. In both hPAH and iPAH BMPR2 mRNA expression was lower in isolated pulmonary artery smooth muscle cells (PASMCs). The reduced BMPR2 mRNA expression was not observed in isolated PAEC from iPAH and hPAH patients. In the same study, reduced BMPR2 protein (molecular weight 75kDa) was observed in whole lung lysates of patients with hPAH but not iPAH patients[11]. Together, these findings put aberrant BMPR2 signaling at the center of the pathobiology of many if not most forms of PAH. However, the number of studies assessing BMPR2 expression in the PAH lung remains limited and the methodology used to study BMPR2 expression varies among studies.

It is currently hypothesized that a decrease in BMPR2 signaling leads to a disturbance in the TGF-β/BMP balance favoring activation of the TGF-β signaling pathway[15]. Increased TGF-β signaling can result in pro-proliferative and anti-apoptotic responses in PAECs and PASMCs, and increased inflammatory cytokine and chemokine production**[16–19]**. Although the BMP receptors typically activate Smad1/5/8 and TGFβ receptors phosphorylate Smad2/3, depending on the cell type and the genetic disorder, TGFβ can induce pSmad 1/5/8, albeit with a different affinity and kinetics as BMP ligands do. Restoring BMPR2 signaling is therefore of interest from a treatment perspective, to stop progression of the disease. Although in several translational studies, drugs

were tested that were hypothesized to restore the TGF-β/BMP balance and reverse experimentally induced PH, basic characterization of BMPR2 expression and activity in the most commonly used PH animal models is currently still very limited [20,21]. The two most used animal models for PAH preclinical research are the monocrotaline (MCT) and Sugen-hypoxia (SuHx) rat models. MCT is an alkaloid derived from the seeds of *Crotalaria spectabilis*. Once injected, MCT is metabolized in the liver to its active form and induces PAEC damage followed by the induction of pulmonary hypertension[22]. The SuHx model depends on a single injection of the vascular endothelial growth factor receptor inhibitor Sugen to induce PAEC damage combined with a 4 week hypoxic (10% of oxygen) stimulus[23]. Because both the MCT and SuHx rat models rely on chemically and hypoxia induced hits for the subsequent development of PAH in the following weeks rather than decades, it is likely that the BMP signaling pathway in experimentally induced PAH acts different than observed in the human disease, and might even vary between models. Since in translational research, using the most representative animal model to test new compounds is crucially important, the aim of this study is to describe BMPR2 receptor expression and downstream signaling in the MCT and SuHx rat model for experimentally induced PAH and to compare these findings to altered BMPR2 signaling in the lungs of iPAH and hPAH patients. Additionally, we will compare the expression levels in whole lung lysates, as determined by western blot, versus vascular expression only.

2. MATERIALS AND METHODS

Patient tissue samples and animal experiments

Human lung tissue samples were obtained from hPAH (n=7) and iPAH (n=7) patients upon autopsy. Control lung tissue samples (n=8) were obtained from patients who had died from non-pulmonary causes (cancer, suicide) as previously reported[24]. Usage of samples was approved by the Institutional Review Board of the VU University Medical Center and Comite de ´Protection des Personnes (CPP) Ile-de-France VII, Paris. All samples were formalin fixed and paraffin embedded according to common tissue-processing protocols. Animal experiments were approved by the animal welfare committee of the VU university and were conducted in accordance with the European convention for the protection of vertebrate animals used for experimental and other scientific purposes. Male Wistar rats (MCT model n=8 / control n=5) and male Sprague Dawley rats (SuHx model n=8 / control n=5) (Charles River, the Netherlands) were

housed in groups of 3-4 under controlled conditions (22 degrees, 12:12 h light/dark cycle). Food and water were available ad libitum.

Study design

Rats were randomly divided in three groups: Control (Con), SuHx and MCT, and results were compared to both iPAH and hPAH. Control group consisted of a 50/50 mix of Wistar and Sprague Dawley rats. The SuHx protocol was followed as described previously[25]. Briefly, Sprague-Dawley animals were injected with SU5416 (25 mg/kg s.c.), Tocris Bioscience, #3037, Bristol, United Kingdom dissolved in carboxymethylcellulose (CMC)) and exposed to hypoxia (10%) for four weeks followed by re-exposure to normoxia for 6 weeks. Wister rats received a single dose of monocrotaline (60 mg/kg s.c.) to initiate development of PAH. The CON group received a single shot of the solvent CMC (SuHx) or sterile saline (MCT). Experiments were terminated 4 weeks post-MCT injection or 6 weeks post-hypoxia. The timing of end-experiments was chosen to ensure full development of PAH and end-stage pulmonary vascular remodeling[25,26]. Animals were killed via exsanguination and organs were weighed and processed for analysis.

Right ventricle pressure measurements

Prior to termination of the experiment, open-chest RV catheterization was performed under general anesthesia in all animals (3,0 % isoflurane, 1:1 O_2/air mix) as described before[27]. The catheter was inserted through the RV wall. Rats were intubated (Teflon tube, 16 gauge) and attached to a mechanical ventilator (Micro-Ventilator, UNO, Zevenaar, the Netherlands; ventilator settings: breathing frequency, 70 breaths per minute; pressures, 12/0 cm H_2O; inspiratory/expiratory ratio, 1:1). RV pressures were recorded using of a microtip pressure-volume conductance catheter (Millar Instruments, Houston, TX). Analyses were performed when a steady state was reached over an interval of at least 10 seconds.

Histology and morphometry

Lungs were weighed and the airways of the right middle lobe were filled with 0.5% low-melt agarose in saline under constant pressure of 25 mmHg and stored in formalin (#4169-30, Klinipath BV, Duiven, the Netherlands). The remaining lobes were stored in liquid nitrogen for future processing. The heart was perfused with tyrode solution, weighed, dissected, snap-frozen in liquid nitrogen and stored in -80°C. Transversally cut lung sections (4µm) were stained with Elastica van Gieson (EvG) for analysis of vascular

dimensions. The degree of vascular occlusion was expressed by the percentage of occluded vessels determined on a minimum of 30 vessels per animal per group[27].

Western Blot

RIPA lysis buffer (89900, Thermofisher scientific) with protease inhibitors (PMSF, Thermofisher scientific / complete mini protease inhibitor cocktail, Sigma-Aldrich) was added to lung tissue and homogenized with a tissue lyser (Qiagen, Venlo, the Netherlands). Protein concentration was quantified by (Pierce 660nm protein assay kit, Thermo Scientific, Pierce Biotechnology, Rockford, USA). Samples (10 µg) were separated on a gradient gel (Bis-Tris 4-12% gel, Life technologies). XCell blot module was used for protein transfer from the gel to an ECL membrane (Hybond ECL Nitrocellulose Membrane, GE Healthcare). Primary antibody for BMPR2 (1:1000, MA5-15827, Thermo scientific) / phospho-Smad 1/5/8 (#12656, Cell Signaling)) diluted in phosphate buffered saline with bovine serum albumin (5%) (PBS-A) was incubated overnight at 4°C. Appropriate secondary antibody (1:4000, Polyclonal rabbit anti-mouse, Z0259, DAKO) diluted in PBS-A was incubated for 1 hour. Blots were re-incubated with β-actin (1:50000, A3854, Sigma) or GAPDH diluted in PBS for 1 hour to correct for unequal loading. An internal control composed of a mix of protein supernatants from all groups is used to correct for inter-blot variation.

Immunofluorescence staining and quantitative analysis

After deparaffinization and hydration, epitope retrieval was performed by immersing the slides in antigen unmasking solution (H3300, Vector Laboratories) for 20 minutes. Blocking steps with 1% bovine serum albumin were performed for 90 minutes, before incubating the sections with primary antibodies BMPR2 (MA5-15827, Thermo scientific or 612292, BD Biosciences, 1:50) and phospho-Smad 1/5/8 (#12656, Cell Signaling, 1:50) overnight at 4^0C. For the negative controls the primary antibody was omitted to account for nonspecific binding of the secondary antibody. Labeling with appropriate secondary antibody conjugated to Cy5 followed for 90 minutes. Additional overnight staining with pre-conjugated anti-actin α-smooth-muscle-actin – Cy3 (α-SMA, C6198, Sigma), Von Willebrand Factor FITC (VWF, ab8822, Abcam) was performed before a 10 min incubation with 4'6-diamidino-2-phenylindole (DAPI, H-1200, Vector Labs) prior to sealing. Image acquisition was performed on a ZEISS Axiovert 200M Marianas inverted microscope. All BMPR2 and psmad 1/5/8 images were acquired in a single session. Exposure time for the protein of interest was determined automatically by software (Slidebook 6, Intelligent imaging innovations) once and used for all subsequent slides.

The negative control was used to determine and set a low signal threshold. Figures were assembled using Adobe Illustrator (AI, version 23.03).

BMPR2 expression was determined per high power field (at 400X) and corrected for vessel area by assigning a region of interest (ROI) using FIJI software[28]. ROI was created by manually drawing the vessel circumference subtracted by vessel lumen (if applicable). Average intensity of the BMPR2 signal in ROI was used to quantify the expression per vessel. A minimum of 20 vessels per section were measured. Only vessels in rats ranging from a 50-100 um diameter were included for analysis.

Statistical Analysis

All analyses were performed in a blinded fashion. All data were verified for normal distribution. A *p*-value <0,05 was considered significant. All data are presented as mean ±SEM. Parameters were analyzed by one-way ANOVA with Bonferroni post-hoc testing (GraphPad Prism for Windows 6, San Diego CA).

3. RESULTS

BMPR2 levels are not decreased in whole lung lysates of iPAH and hPAH patients

We first analyzed the protein levels of BMPR2 and pSmad 1/5/8 in whole lung homogenates of samples derived from human PAH patients and controls subjects. Western blot analysis showed that BMPR2 was similar in iPAH and hPAH compared to control lung tissues (Fig 1A). In contrast, semi-quantitative analysis of the expression of BMPR2 in lung vessels by immunofluroscence (IF) revealed reduced expression of the receptor in the vessels of both iPAH and hPAH patients compared to control regardless of the mutational status (p=<0.05)(Fig 1B,C).

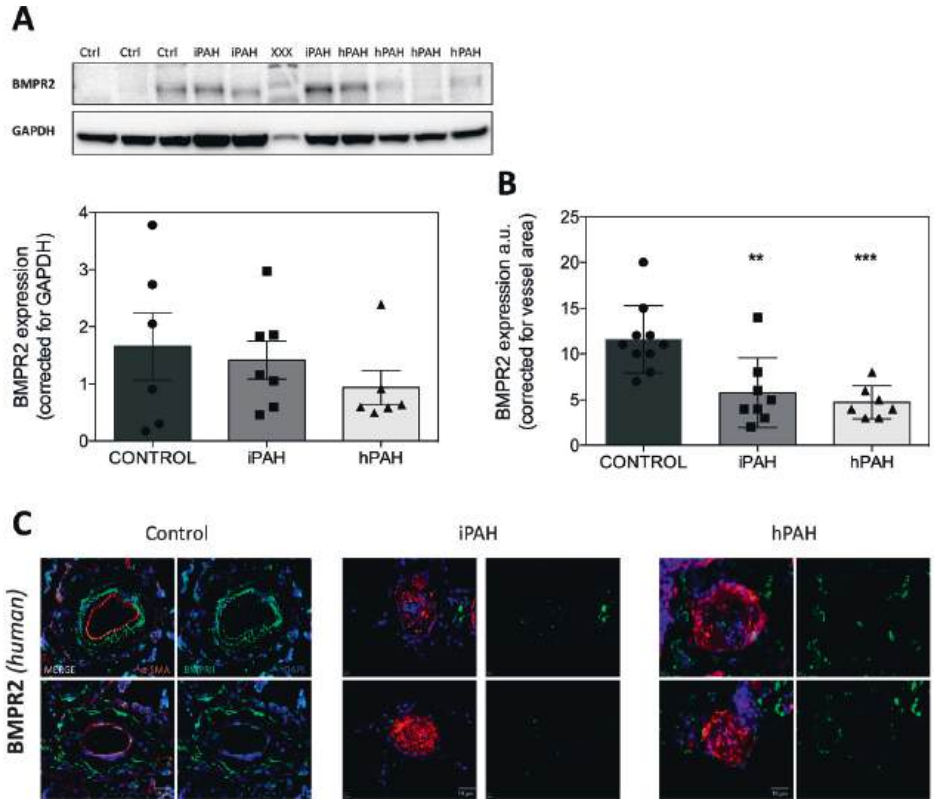

Figure 1 Western blot analysis of BMPR2 protein expression in whole lung homogenates.
A: BMPR2 expression in whole lung homogenates. xxx=non-relevant sample. B: BMPR2 expression corrected for vessel area. C: Typical examples of vessels are shown. Green = BMPR2; Red = smooth-muscle-actin (α-SMA); Blue = nuclei. ** = p<0.01 / ***= p<0.001

Decreased levels of pSmad 1/5/8 in the lung vasculature of iPAH and hPAH patients

Analyzing the levels of phosphorylated Smad 1/5/8 protein in whole lung homogenates showed no significant differences (Fig2A). However, there was a clear reduction in the expression of vascular pSmad 1/5/8 when comparing both iPAH and hPAH to control vessels (p<0,05) (Fig 2BC).

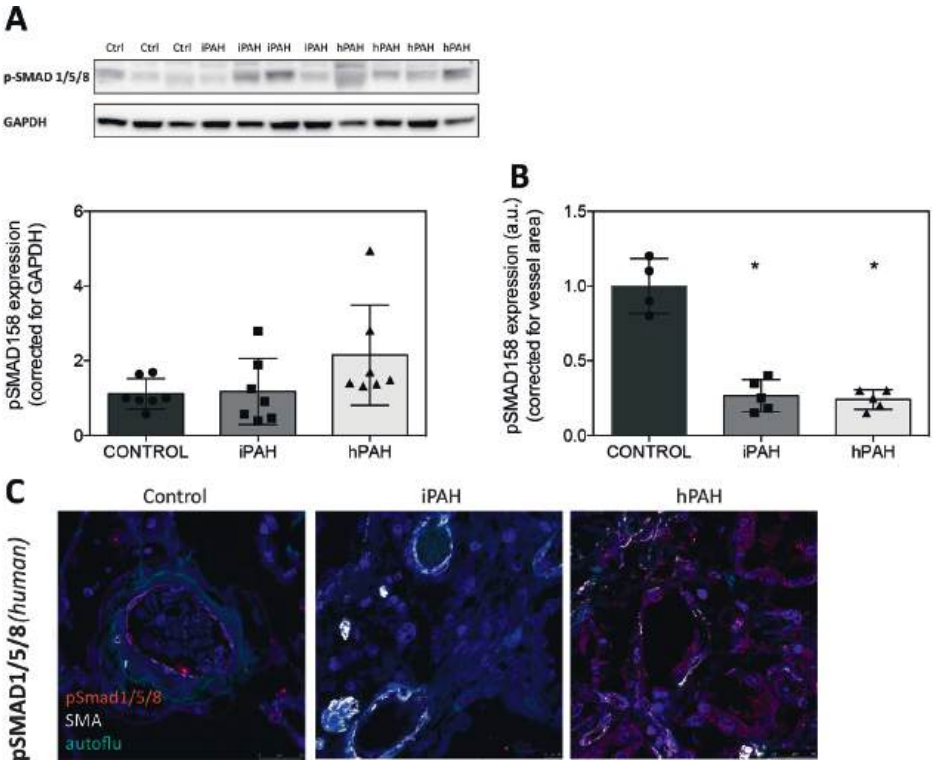

Figure 2 Analysis of Smad 1/5/8/ phosphorylation in whole lung homogenates.
A: pSmad 1/5/8 in whole lung homogenates B: pSmad 1/5/8 expression corrected for vessel area. C: Typical examples of vessels are shown. Green = pSmad 1/5/8; red = smooth-muscle-actin; blue = nuclei. autoflu=autofluroscence. * = $p<0.05$.

Development of PAH in animal models

Next, we sought to compare BMPR2-Smad signaling in human PAH with PAH induced in rats. Therefore, we first confirmed the development of PAH in our animal models by the increase in right ventricle systolic pressure (RVSP), increased RV hypertrophy (RV/LV+S) and increased vascular remodeling (Fig 3).

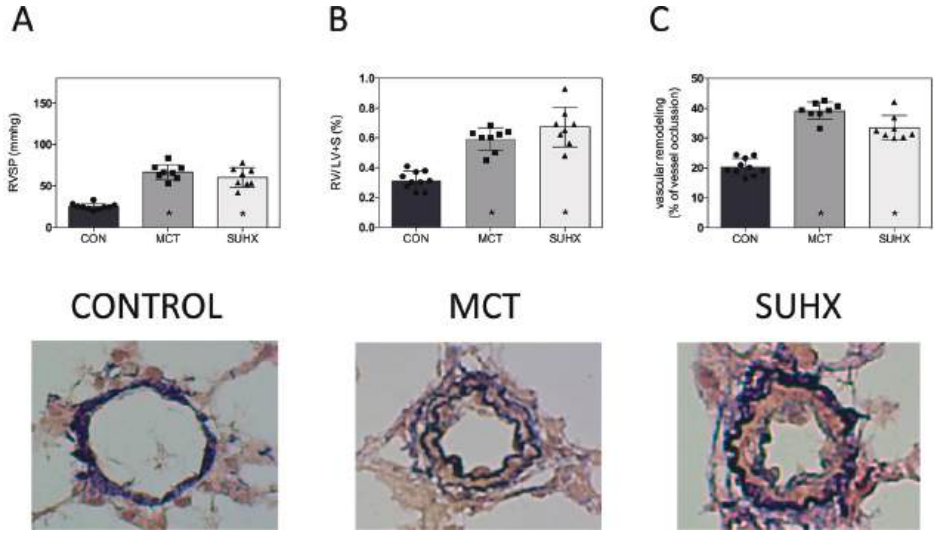

Figure 3 Characteristics of PAH animal model with A: RVSP = right ventricle systolic pressure, B: Fulton index (RV/LV+S) and C: vascular remodeling. Typical examples of vessel remodeling are shown below (EvG staining, 400x magnification). *= p<0.05.

BMPR2 expression is increased in MCT and SuHx lung vasculature

Whole lung BMPR2 protein expression level was reduced in MCT (p<0,05) but did not change in the SuHx model when compared to control (Fig 4A). Using IF quantification corrected for vessel area, we observed a notable increase in the expression of BMPR2 in both the MCT and SuHx lung vasculature (Fig 4B, E). The ratio of pSmad 1/5/8 versus total Smad 1/5/8, indicating BMPR2 activation, was similar in whole lung homogenates of MCT rats and SuHx rats (Fig 4C). However, the ratio of pSmad 1/5/8 versus β-actin is reduced in whole lung homogenates of MCT rats (data not shown) indicating that reduced levels of pSmad1/5/8 is due to reduced total Smad levels and not due to impaired receptor activation/signaling. IF analysis demonstrated reduced expression of vascular pSmad 1/5/8 in both PAH models (Fig 4D-F). As we opted to use both Wistar and Sprague-Dawley rats in our control group we tested for statistical difference of whole lung lysate BMPR2 protein expression between both strains. No difference in BMPR2 protein expression was observed in separate control group analysis (data not shown).

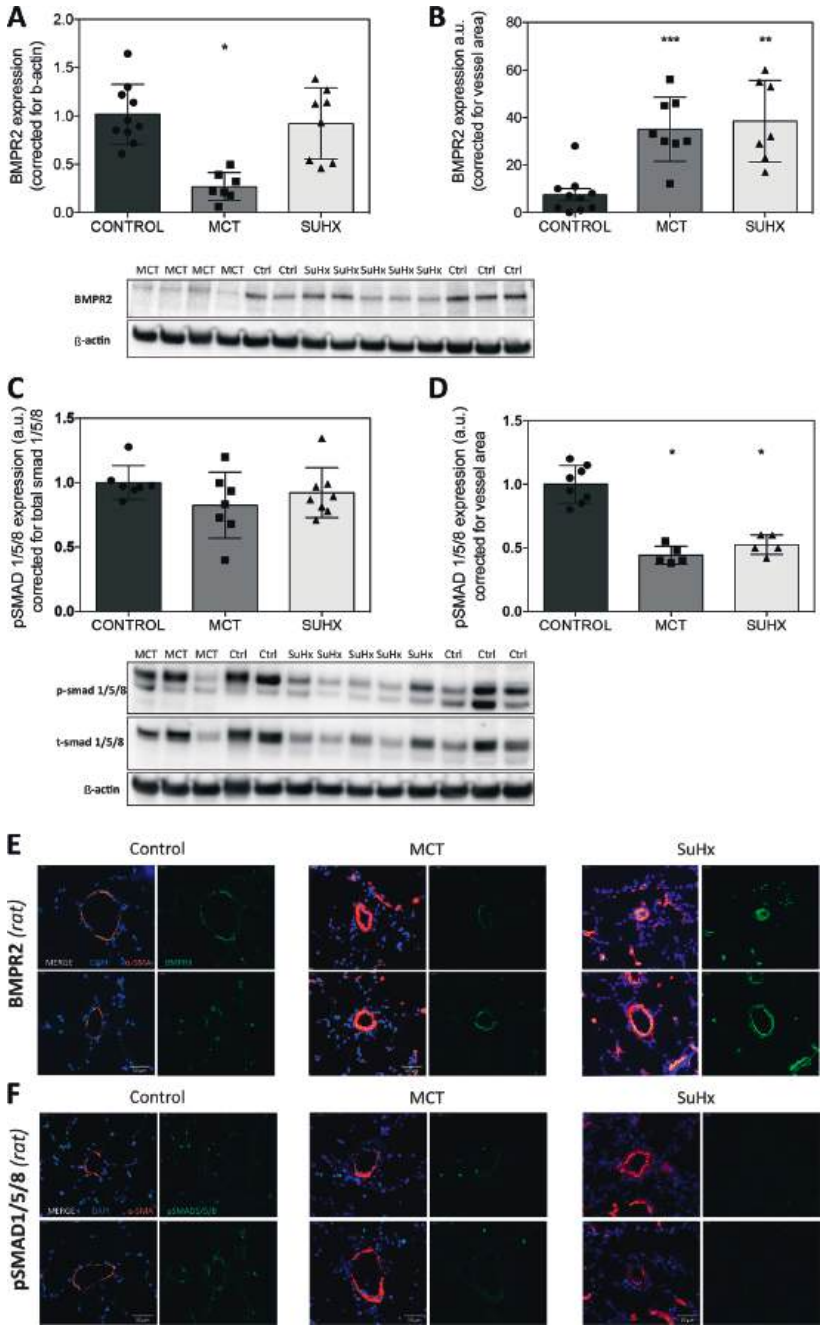

Figure 4. BMPR2 and pSmad 1/5/8 protein expression in whole lung homogenates vs. immunofluorescence.

A-B: Analysis of protein expression by Western Blot and C-D: immunofluorescence. E: Typical examples are shown. Green = pSmad 1/5/8 or BMPR2; red = smooth-muscle-actin (α-SMA); blue = nuclei. * = p<0.05 / ** = p<0.01 / ***= p<0.001

4. DISCUSSION

This study describes the expression levels of BMPR2 and its downstream signaling component pSmad 1/5/8 in lung tissue and more specifically in the lung vasculature of PAH patients as well as in two established animal models of PAH. We confirmed reduced protein expression of BMPR2 and its downstream signaling component pSmad 1/5/8 in both hPAH and iPAH, but surprisingly, both the MCT and SuHx rat model for experimentally induced PAH showed increased vascular expression of BMPR2 in end stage disease. Downstream BMPR2 activity, as assessed by pSmad 1/5/8 expression, was decreased in the lung vasculature of both PAH models, consistent with the patient situation.

Disturbed BMP signaling in iPAH and hPAH

Analysis of IF images showed a reduced vascular expression of BMPR2 in both iPAH and hPAH, which is in concordance with a previous report of reduced expression of BMPR2 in hPAH and iPAH determined by immunohistochemistry (IHC)[13]. While reduced BMPR2 expression in whole lung tissue samples from hPAH but not iPAH was reported in a previous study using western blot analysis[11], we did not observe a difference in BMPR2 expression in hPAH/iPAH vs control in this study. An explanation for our findings perhaps lies in different type of mutations that allow for BMPR2 protein to be formed but incorrectly expressed or unable to induce Smad 1/5/8 phosphorylation. Another possible explanation is that we detected 115kDa protein of BMPR2 (predicted BMPR2 size is 115kDa) whereas in the other study reported 75kDa protein of BMPR2. Of note, we confirmed the specificity of the BMPR2 antibody by 1) knock-down studies using BMPR2 shRNAs in PAECs and PASMCs, 2) using a different BMPR2 antibody, and 3) using BMP9 stimulated PAEC lysates.

Previous studies showed that missense mutations in the ligand-binding domain by cysteine substitutions impair BMP signaling by mutant receptor mislocalisation in the cytosol[29]. Furthermore, as autopsy material was used, it is possible that the cause and time of death may have inferred with BMPR2 signaling in non-vascular cells (e.g. epithelial or macrophage). The phosphorylation of Smad 1/5/8 was decreased in the vasculature of both iPAH and hPAH lungs suggesting that even in the absence of a BMPR2 mutation, BMP signaling is reduced. This observation is in line with another study showing reduced number of Smad 1/5 positive cells by IHC in the vascular intimal and medial layer of iPAH and hPAH[30]. Richter and colleagues found the expression of phosphorylated Smad 1/5/8 in luminal endothelial cells in plexiform lesions, but

pSmad1/5/8 was not present in core endothelial cells. Unfortunately the IHC data was not quantified[14].

Reduced BMPR2 and pSmad 1/5/8 expression in MCT and SuHx animal models of PAH

Remarkably, using IF we observed increased levels of BMPR2 in the lung vasculature of MCT and SuHx rats, while protein levels in whole lung lysates were only reduced in the MCT model. Previously Ramos et al[31]. reported reduced levels of BMPR2 protein by western blot analysis using whole lung lysates 14 days after MCT injection. Others have described a brief initial increase in BMPR2 protein expression two days after MCT injection, with a subsequent decrease in BMPR2 protein levels after seven and twenty-one days[32–34] in whole lung homogenates by Western blot analysis. Impaired BMP signal transduction was confirmed in our study by reduced pSmad 1/5/8 expression in both MCT and SuHx. A recent study assessing the increase of BMPR2 signaling upon BMP9 stimulation, observed reduced levels of BMPR2 and pSmad 1/5/8 in the MCT model. For SuHx, only a reduction in the expression of pSmad 1/5/8 was reported[35]. Other additional studies have also reported decreases in protein expression of pSmad 1/5/8[31,36]. In contrast to these and our studies, one study reported augmented Smad1 signaling[31]. One difference in the methodological setup between this study and ours is the time post-MCT injection when the analysis was performed (14 vs. 28 days post-MCT). Since BMPR2 expression varies over the course of disease progression in the MCT model, the time difference is likely to explain the difference in Smad1 signaling[33]. Our study opted for prolonged disease development before analysis of the experimental PAH models as at that time-point it more closely resembles human end-stage disease. One explanation for the seemingly normal vascular BMPR2 expression in the SuHx model might be the role of vascular endothelial growth factor receptor 3 (VEGFR3). Blocking of VEGFR3 by Sugen contributes to the vascular remodeling observed in the SuHx model, but recently VEGFR3 has also been linked to BMPR2 and PAH[37,38]. Hwangbo et al. propose a VEGFR3-BMPR2 interaction that is crucial for receptor endocytosis and subsequent induction of phosphorylation of Smads[39]. Inhibition of endocytosis by blocking VEGFR3 by Sugen might therefore result in an increased BMPR2 vascular expression observed in PAH.

Analyzing vessels in more detail showed that in both MCT and SuHx animals, pSmad 1/5/8 is reduced while BMPR2 expression is increased. This increase in BMPR2 levels might be a feedback mechanism to restore endogenous BMP signaling and prevent

disease progression, a process that has failed in end-stage lung tissue of iPAH patients. It could also imply differences in BMPR2 and-or the type I receptor kinase activity[15] or the presence of inhibitors preventing BMPs to bind to the receptor[15,40]. While our study was able to distinguish between vascular vs. non-vascular expression of BMP signaling, it will be worthwhile to differentiate between the different vascular cell types. Even within the population of endothelial cells, the expression of phosphorylated Smad 1/5/8 was shown to differ upon location within a plexiform lesion[14]. In addition, characterization of BMP signaling throughout disease development might give more insight into the role of BMP signaling in vascular remodeling in PAH. Perros et al. recently published their findings from a novel BMPR2 mutant rat model aimed to specifically model hPAH. These BMPR2 mutated rats spontaneously develop PAH between six and twelve months of age. Whole lung BMPR2 and pSmad 1/5/8 protein expression was lowered by fifty percent as measured by western blot analysis[41]. Analyzing the lung vascular BMPR2 and pSmad 1/5/8 expression in this novel model would inform us if expression is indeed similar to human disease.

Interventions aimed to restore the TGF-β/BMP balance in experimental PAH

Inhibition of lysosomal degradation of BMPR2 by chloroquine prevented the progression of PAH in the monocrotaline (MCT) model[42,43]. Restoration of downregulated BMPR2 signaling via targeted gene delivery of *BMPR2* revealed therapeutic potential in the MCT model[32]. Sildenafil, a phosphodiesterase type 5 inhibitor currently registered for the treatment of PAH, was demonstrated to restore MCT induced PH in association with increased whole lung pSmad 1/5/8 expression[44]. Using laser dissection microscopy, Mcmurtry et al. showed decreased BMPR2 mRNA expression in the MCT lung vasculature. Additionally, they showed a gradient in lung vascular BMPR2 mRNA expression with distal vessels having to highest expression levels compared to mid or proximal vessels. Gene therapy with BMPR2 distributed BMPR2 to resistance PAs but did not ameliorate PAH in the MCT model[34]. Further, in a study assessing the effect of a selective TGF-β ligand trap, decreased levels of BMPR2 mRNA in SuHx and MCT lungs were unaffected by this treatment despite effective reversal of PH[45]. Post or propter activation of BMPR2, FK506 (known as tacrolimus) reversed established PAH in the SuHx and MCT models[20,46]. In another study, selective enhancement of BMPR2 signaling using BMP9 was shown to reverse disease in the MCT and SuHx model. In this study, whole lung pSmad 1/5 was reduced before treatment in both the MCT and SuHx model, while only in the MCT model lower whole lung BMPR2 protein expression was reported[35]. A multitude of other studies investigating compounds

targeting BMPR2 signaling regulation, protein processing regulation, translational regulation, transcriptional regulation and genetic based therapies were performed or are currently ongoing[47–49].

The aim of this study was to give insights in the translational capability of two animal models commonly used to study new treatment modalities for PAH. Focusing on the BMPR2 signaling pathway as the main driver of the disease, both animal models only partly recapitulate the human situation. This study reconfirmed and add to the still limited body of evidence describing decreased vascular BMPR2 expression in PAH. Our contrasting findings of increased BMPR2 observed in the SuHx and MCT lung vasculature emphasizes the inadequacy of using whole lung lysates. We propose for future studies to not use whole lung lysates to determine BMPR2 levels but more suitable techniques such as IF or IHC, which will allow to take into account the spatial localization of BMPR2 expression. Since expression levels of BMPR2 are different in both MCT and SuHx models compared to hPAH or iPAH, this should be taken into consideration when performing preclinical studies using a candidate compound to target BMPR2 or its downstream signaling component.

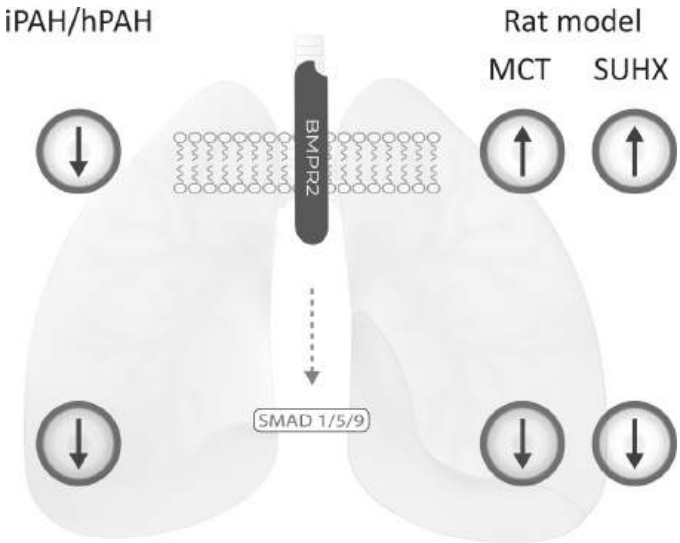

Figure 5. Schematic overviews summarizing imaging results of this study.
While BMPR2 protein expression is decreased in PAH along with decreased pSMAD 1/5/8 signaling, animal BMPR2 expression is increased in the lung vasculature.

In conclusion, our findings confirm decreased BMPR2 receptor expression and downstream signaling activity in the lung vasculature of patients with idiopathic and hereditary PAH. At the same time, our study indicates that whole lung lysates are not representative of vascular BMPR2 and pSmad 1/5/8 expression in the lung. Finally, despite an increased BMPR2 expression in the lung vasculature, PAH developed in the MCT and SuHx rat models and the downstream BMPR2 signaling activity resemble that of human PAH (fig 5.).

Funding: This work was supported by the Dutch CardioVascular Alliance (DCVA): the Dutch Heart Foundation, Dutch Federation of University Medical Centers, the Netherlands Organization for Health Research and Development, and the Royal Netherlands Academy of Sciences Grant 2012-08 and 2018-2023 awarded to the Phaedra consortium (http://www.phaedraresearch.nl). We also acknowledge support for KK by the Dutch Lung Foundation (Longfonds) grant number-5.2.17.198J0 and by the Leiden University Foundation grant (W18378-2-32).

Acknowledgments: We thank Prof. Peter ten Dijke for critical reading of the manuscript and providing valuable feedback. The authors also thank Prof. Marc Humbert, Prof. Elie Fadel, and their clinical and surgical teams for their expertise and support.

Conflicts of Interest: The authors declare no conflict of interest

REFERENCES

1. Simonneau, G.; Gatzoulis, M.A.; Adatia, I.; Celermajer, D.; Denton, C.; Ghofrani, A.; Gomez Sanchez, M.A.; Krishna Kumar, R.; Landzberg, M.; Machado, R.F.; et al. Updated Clinical Classification of Pulmonary Hypertension. *J. Am. Coll. Cardiol.* **2013**, *62*.
2. Thomson, J.R.; Machado, R.D.; Pauciulo, M.W.; Morgan, N.V.; Humbert, M.; Elliott, G.C.; Ward, K.; Yacoub, M.; Mikhail, G.; Rogers, P.; et al. Sporadic primary pulmonary hypertension is associated with germline mutations of the gene encoding BMPR-II, a receptor member of the TGF-β family. *J. Med. Genet.* **2000**, *37*, 741–745.
3. Lane, K.B.; Machado, R.D.; Pauciulo, M.W.; Thomson, J.R.; Phillips, J.A.; Loyd, J.E.; Nichols, W.C.; Trembath, R.C. Heterozygous germline mutations in *BMPR2*, encoding a TGF-β receptor, cause familial primary pulmonary hypertension. *Nat. Genet.* **2000**, *26*, 81–84.
4. Evans, J.D.W.; Girerd, B.; Montani, D.; Wang, X.-J.; Galiè, N.; Austin, E.D.; Elliott, G.; Asano, K.; Grünig, E.; Yan, Y.; et al. BMPR2 mutations and survival in pulmonary arterial hypertension: an individual participant data meta-analysis. *Lancet Respir. Med.* **2016**.
5. Austin, E.D.; Ma, L.; LeDuc, C.; Rosenzweig, E.B.; Borczuk, A.; Phillips, J.A.; Palomero, T.; Sumazin, P.; Kim, H.R.; Talati, M.H.; et al. Whole Exome Sequencing to Identify a Novel Gene (Caveolin-1) Associated With Human Pulmonary Arterial HypertensionClinical Perspective. *Circ. Cardiovasc. Genet.* **2012**, *5*, 336–343.
6. Wang, G.; Fan, R.; Ji, R.; Zou, W.; Penny, D.J.; Varghese, N.P.; Fan, Y. Novel homozygous BMP9 nonsense mutation causes pulmonary arterial hypertension: a case report. *BMC Pulm. Med.* **2016**, *16*, 17.
7. Girerd, B.; Montani, D.; Coulet, F.; Sztrymf, B.; Yaici, A.; Jaïs, X.; Tregouet, D.; Reis, A.; Drouin-Garraud, V.; Fraisse, A.; et al. Clinical outcomes of pulmonary arterial hypertension in patients carrying an ACVRL1 (ALK1) mutation. *Am. J. Respir. Crit. Care Med.* **2010**, *181*, 851–861.
8. Shintani, M.; Yagi, H.; Nakayama, T.; Saji, T.; Matsuoka, R. A new nonsense mutation of SMAD8 associated with pulmonary arterial hypertension. *J. Med. Genet.* **2009**, *46*, 331–337.
9. Drake, K.M.; Dunmore, B.J.; McNelly, L.N.; Morrell, N.W.; Aldred, M.A. Correction of Nonsense *BMPR2* and *SMAD9* Mutations by Ataluren in Pulmonary Arterial Hypertension. *Am. J. Respir. Cell Mol. Biol.* **2013**, *49*, 403–409.
10. Pousada, G.; Baloira, A.; Fontán, D.; Núñez, M.; Valverde, D. Mutational and clinical analysis of the ENG gene in patients with pulmonary arterial hypertension. *BMC Genet.* **2016**, *17*.
11. Dewachter, L.; Adnot, S.; Guignabert, C.; Tu, L.; Marcos, E.; Fadel, E.; Humbert, M.; Dartevelle, P.; Simonneau, G.; Naeije, R.; et al. Bone morphogenetic protein signalling in heritable versus idiopathic pulmonary hypertension. *Eur. Respir. J.* **2009**, *34*, 1100–1110.
12. Lavoie, J.R.; Ormiston, M.L.; Perez-Iratxeta, C.; Courtman, D.W.; Jiang, B.; Ferrer, E.; Caruso, P.; Southwood, M.; Foster, W.S.; Morrell, N.W.; et al. Proteomic Analysis Implicates Translationally Controlled Tumor Protein as a Novel Mediator of Occlusive Vascular Remodeling in Pulmonary Arterial Hypertension. *Circulation* **2014**, *129*, 2125–2135.
13. Atkinson, C. Primary Pulmonary Hypertension Is Associated With Reduced Pulmonary Vascular Expression of Type II Bone Morphogenetic Protein Receptor. *Circulation* **2002**, *105*, 1672–1678.

14. Richter, A.; Yeager, M.E.; Zaiman, A.; Cool, C.D.; Voelkel, N.F.; Tuder, R.M. Impaired Transforming Growth Factor-β Signaling in Idiopathic Pulmonary Arterial Hypertension. *Am. J. Respir. Crit. Care Med.* **2004**, *170*, 1340–1348.
15. Morrell, N.W.; Bloch, D.B.; ten Dijke, P.; Goumans, M.-J.T.H.; Hata, A.; Smith, J.; Yu, P.B.; Bloch, K.D. Targeting BMP signalling in cardiovascular disease and anaemia. *Nat. Rev. Cardiol.* **2016**, *13*, 106–120.
16. Nasim, M.T.; Ogo, T.; Chowdhury, H.M.; Zhao, L.; Chen, C.; Rhodes, C.; Trembath, R.C. BMPR-II deficiency elicits pro-proliferative and anti-apoptotic responses through the activation of TGFβ-TAK1-MAPK pathways in PAH. *Hum. Mol. Genet.* **2012**, *21*, 2548–2558.
17. Soon, E.; Crosby, A.; Southwood, M.; Yang, P.; Tajsic, T.; Toshner, M.; Appleby, S.; Shanahan, C.M.; Bloch, K.D.; Pepke-Zaba, J.; et al. BMPR-II Deficiency Promotes Pulmonary Hypertension via Increased Inflammatory Cytokine Production. *Am. J. Respir. Crit. Care Med.* **2015**.
18. Upton, P.D.; Morrell, N.W. The transforming growth factor-β–bone morphogenetic protein type signalling pathway in pulmonary vascular homeostasis and disease. *Exp. Physiol.* **2013**, *98*, 1262–1266.
19. Dorfmüller, P.; Perros, F.; Balabanian, K.; Humbert, M. Inflammation in pulmonary arterial hypertension. *Eur. Respir. J.* **2003**, *22*, 358–363.
20. Spiekerkoetter, E.; Tian, X.; Cai, J.; Hopper, R.K.; Sudheendra, D.; Li, C.G.; El-Bizri, N.; Sawada, H.; Haghighat, R.; Chan, R.; et al. FK506 activates BMPR2, rescues endothelial dysfunction, and reverses pulmonary hypertension. *J. Clin. Invest.* **2013**, *123*, 3600–3613.
21. Nickel, N.P.; Spiekerkoetter, E.; Gu, M.; Li, C.G.; Li, H.; Kaschwich, M.; Diebold, I.; Hennigs, J.K.; Kim, K.-Y.; Miyagawa, K.; et al. Elafin Reverses Pulmonary Hypertension via Caveolin-1–Dependent Bone Morphogenetic Protein Signaling. *Am. J. Respir. Crit. Care Med.* **2015**, *191*, 1273–1286.
22. Kay, J.M.; Harris, P.; Heath, D. Pulmonary hypertension produced in rats by ingestion of Crotalaria spectabilis seeds. *Thorax* **1967**, *22*, 176–179.
23. Taraseviciene-Stewart, L.; Kasahara, Y.; Alger, L.; Hirth, P.; Mahon, G.M.; Waltenberger, J.; Voelkel, N.F.; Tuder, R.M. Inhibition of the VEGF receptor 2 combined with chronic hypoxia causes cell death-dependent pulmonary endothelial cell proliferation and severe pulmonary hypertension. *FASEB J.* **2001**, *15*, 427–438.
24. Overbeek, M.J.; Mouchaers, K.T.B.; Niessen, H.M.; Hadi, A.M.; Kupreishvili, K.; Boonstra, A.; Voskuyl, A.E.; Belien, J.A.M.; Smit, E.F.; Dijkmans, B.C.; et al. Characteristics of Interstitial Fibrosis and Inflammatory Cell Infiltration in Right Ventricles of Systemic Sclerosis-Associated Pulmonary Arterial Hypertension Available online: https://www.hindawi.com/journals/ijr/2010/604615/abs/ (accessed on Apr 20, 2019).
25. de Raaf, M.A.; Schalij, I.; Gomez-Arroyo, J.; Rol, N.; Happé, C.; de Man, F.S.; Vonk-Noordegraaf, A.; Westerhof, N.; Voelkel, N.F.; Bogaard, H.J. SuHx rat model: partly reversible pulmonary hypertension and progressive intima obstruction. *Eur. Respir. J.* **2014**, *44*, 160–168.
26. Handoko, M.L.; Man, F.S. de; Happé, C.M.; Schalij, I.; Musters, R.J.P.; Westerhof, N.; Postmus, P.E.; Paulus, W.J.; Laarse, W.J. van der; Vonk-Noordegraaf, A. Opposite Effects of Training in Rats With Stable and Progressive Pulmonary Hypertension. *Circulation* **2009**, *120*, 42–49.

27. Happé, C.M.; de Raaf, M.A.; Rol, N.; Schalij, I.; Vonk-Noordegraaf, A.; Westerhof, N.; Voelkel, N.F.; de Man, F.S.; Bogaard, H.J. Pneumonectomy combined with SU5416 induces severe pulmonary hypertension in rats. *Am. J. Physiol.-Lung Cell. Mol. Physiol.* **2016**, *310*, L1088–L1097.
28. Schindelin, J.; Arganda-Carreras, I.; Frise, E.; Kaynig, V.; Longair, M.; Pietzsch, T.; Preibisch, S.; Rueden, C.; Saalfeld, S.; Schmid, B.; et al. Fiji: an open-source platform for biological-image analysis. *Nat. Methods* **2012**, *9*, 676–682.
29. Rudarakanchana, N.; Flanagan, J.A.; Chen, H.; Upton, P.D.; Machado, R.; Patel, D.; Trembath, R.C.; Morrell, N.W. Functional analysis of bone morphogenetic protein type II receptor mutations underlying primary pulmonary hypertension. *Hum. Mol. Genet.* **2002**, *11*, 1517–1525.
30. Yang, X. Dysfunctional Smad Signaling Contributes to Abnormal Smooth Muscle Cell Proliferation in Familial Pulmonary Arterial Hypertension. *Circ. Res.* **2005**, *96*, 1053–1063.
31. Ramos, M.F.; Lamé, M.W.; Segall, H.J.; Wilson, D.W. Smad Signaling in the Rat Model of Monocrotaline Pulmonary Hypertension. *Toxicol. Pathol.* **2008**, *36*, 311–320.
32. Reynolds, A.M.; Holmes, M.D.; Danilov, S.M.; Reynolds, P.N. Targeted gene delivery of BMPR2 attenuates pulmonary hypertension. *Eur. Respir. J.* **2012**, *39*, 329–343.
33. Long, L.; Crosby, A.; Yang, X.; Southwood, M.; Upton, P.D.; Kim, D.-K.; Morrell, N.W. Altered Bone Morphogenetic Protein and Transforming Growth Factor- Signaling in Rat Models of Pulmonary Hypertension: Potential for Activin Receptor-Like Kinase-5 Inhibition in Prevention and Progression of Disease. *Circulation* **2009**, *119*, 566–576.
34. McMurtry, M.S.; Moudgil, R.; Hashimoto, K.; Bonnet, S.; Michelakis, E.D.; Archer, S.L. Overexpression of human bone morphogenetic protein receptor 2 does not ameliorate monocrotaline pulmonary arterial hypertension. *Am. J. Physiol.-Lung Cell. Mol. Physiol.* **2007**, *292*, L872–L878.
35. Long, L.; Ormiston, M.L.; Yang, X.; Southwood, M.; Gräf, S.; Machado, R.D.; Mueller, M.; Kinzel, B.; Yung, L.M.; Wilkinson, J.M.; et al. Selective enhancement of endothelial BMPR-II with BMP9 reverses pulmonary arterial hypertension. *Nat. Med.* **2015**.
36. Harper, R.L.; Reynolds, A.M.; Bonder, C.S.; Reynolds, P.N. BMPR2 gene therapy for PAH acts via Smad and non-Smad signalling. *Respirology* **2016**, *21*, 727–733.
37. Al-Husseini, A.; Kraskauskas, D.; Mezzaroma, E.; Nordio, A.; Farkas, D.; Drake, J.I.; Abbate, A.; Felty, Quentin; Voelkel, N.F. Vascular endothelial growth factor receptor 3 signaling contributes to angioobliterative pulmonary hypertension. *Pulm. Circ.* **2015**, *5*, 101–116.
38. Hwangbo, C.; Lee, H.-W.; Kang, H.; Ju, H.; Wiley, D.S.; Papangeli, I.; Han, J.; Kim, J.-D.; Dunworth, W.P.; Hu, X.; et al. Modulation of Endothelial Bone Morphogenetic Protein Receptor Type 2 Activity by Vascular Endothelial Growth Factor Receptor 3 in Pulmonary Arterial Hypertension. *Circulation* **2017**, *135*, 2288–2298.
39. Lee, H.-W.; Jin, S.-W. VEGFR3 as a novel modulator for PAH. *Oncotarget* **2017**, *8*, 84610–84611.
40. Goumans, M.-J.; Zwijsen, A.; Dijke, P. ten; Bailly, S. Bone Morphogenetic Proteins in Vascular Homeostasis and Disease. *Cold Spring Harb. Perspect. Biol.* **2018**, *10*, a031989.
41. Hautefort Aurélie; Mendes-Ferreira Pedro; Sabourin Jessica; Manaud Grégoire; Bertero Thomas; Rucker-Martin Catherine; Riou Marianne; Adão Rui; Manoury Boris; Lambert Mélanie; et al. Bmpr2 Mutant Rats Develop Pulmonary and Cardiac Characteristics of Pulmonary Arterial Hypertension. *Circulation* **2019**, *139*, 932–948.

42. Long, L.; Yang, X.; Southwood, M.; Lu, J.; Marciniak, S.J.; Dunmore, B.J.; Morrell, N.W. Chloroquine Prevents Progression of Experimental Pulmonary Hypertension via Inhibition of Autophagy and Lysosomal Bmpr-II Degradation. *Circ. Res.* **2013**.
43. Dunmore, B.J.; Drake, K.M.; Upton, P.D.; Toshner, M.R.; Aldred, M.A.; Morrell, N.W. The lysosomal inhibitor, chloroquine, increases cell surface BMPR-II levels and restores BMP9 signalling in endothelial cells harbouring BMPR-II mutations. *Hum. Mol. Genet.* **2013**, *22*, 3667–3679.
44. Yang Jun; Li Xiaohui; Al-Lamki Rafia S.; Wu Changxin; Weiss Astrid; Berk Joachim; Schermuly Ralph T.; Morrell Nicholas W. Sildenafil Potentiates Bone Morphogenetic Protein Signaling in Pulmonary Arterial Smooth Muscle Cells and in Experimental Pulmonary Hypertension. *Arterioscler. Thromb. Vasc. Biol.* **2013**, *33*, 34–42.
45. Yung, L.-M.; Nikolic, I.; Paskin-Flerlage, S.D.; Pearsall, R.S.; Kumar, R.; Yu, P.B. A Selective TGFβ Ligand Trap Attenuates Pulmonary Hypertension. *Am. J. Respir. Crit. Care Med.* **2016**.
46. Spiekerkoetter, E.; Sung, Y.K.; Sudheendra, D.; Scott, V.; Del Rosario, P.; Bill, M.; Haddad, F.; Long-Boyle, J.; Hedlin, H.; Zamanian, R.T. Randomised placebo-controlled safety and tolerability trial of FK506 (tacrolimus) for pulmonary arterial hypertension. *Eur. Respir. J.* **2017**, *50*.
47. Orriols, M.; Gomez-Puerto, M.C.; ten Dijke, P. BMP type II receptor as a therapeutic target in pulmonary arterial hypertension. *Cell. Mol. Life Sci.* **2017**, *74*, 2979–2995.
48. Kurakula, K.; Sun, X.-Q.; Happé, C.; Bos, D. da S.G.; Szulcek, R.; Schalij, I.; Wiesmeijer, K.C.; Lodder, K.; Tu, L.; Guignabert, C.; et al. 6-mercaptopurine, an agonist of Nur77, reduces progression of pulmonary hypertension by enhancing BMP signalling. *Eur. Respir. J.* **2019**, 1802400.
49. Van der Feen, D.E.; Kurakula, K.; Tremblay, E.; Boucherat, O.; Bossers, G.P.; Szulcek, R.; Bourgeois, A.; Lampron, M.-C.; Habbout, K.; Martineau, S.; et al. Multicenter Preclinical Validation of BET Inhibition for the Treatment of Pulmonary Arterial Hypertension. *Am. J. Respir. Crit. Care Med.* **2019**.

SUPPLEMENT FIGURE

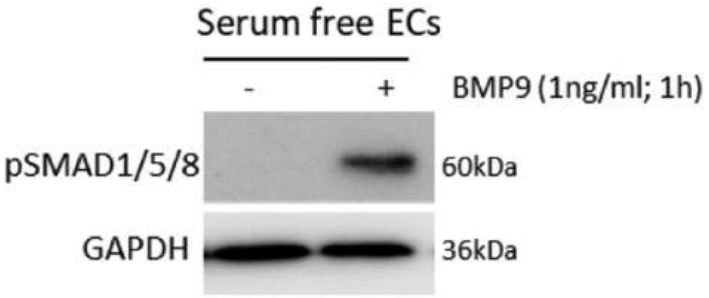

Figure S1: pSMAD1/5/8 levels in MVECs.
pSMAD1/5/8 levels in serum starved MVECs treated with or without BMP9 (1 ng/mL) for 1 hour, indicating BMP9 can induce pSMAD1/5/8 in these cells. MVECs: microvascular endothelial cells

CHAPTER 3

Prevention of progression of pulmonary hypertension by the Nur77 agonist 6-mercaptopurine: role of BMP signaling

Kondababu Kurakula[1,7], Xiao-Qing Sun[2,7], Chris Happé[2], Denielli da Silva Goncalves Bos[2], Robert Szulcek[2], Ingrid Schalij[2], Karien C. Wiesmeijer[1], Kirsten Lodder[1], Ly Tu[3,4], Christophe Guignabert[3,4], Carlie J.M. de Vries[5], Frances S. de Man[2], Anton Vonk Noordegraaf[2], Peter ten Dijke[6], Marie-José Goumans[1,8], Harm Jan Bogaard[2,8]

[7]These two authors contributed equally to this work.

[8]These two authors jointly supervised this work.

[1]Department of Cell and Chemical Biology, Leiden University Medical Center, Leiden, The Netherlands. [2]Pulmonary Hypertension Knowledge Center, Department of Pulmonology, VU University Medical Center/Institute for Cardiovascular Research, Amsterdam, The Netherlands. [3]INSERM UMR_S 999, LabEx LERMIT, Hôpital Marie Lannelongue, Le Plessis-Robinson, France. [4]Université Paris-Sud et Université Paris-Saclay, Le Kremlin-Bicêtre, France. [5]Department of Medical Biochemistry, Academic Medical Center, Amsterdam, The Netherlands. [6]Department of Cell and Chemical Biology, Oncode institute, Leiden University Medical Center, Leiden, The Netherlands.

Eur Respir J. 2019 Sep 29;54(3).

ABSTRACT

Pulmonary arterial hypertension (PAH) is a progressive fatal disease characterized by abnormal remodelling of pulmonary vessels, leading to increased vascular resistance and right ventricle failure. This abnormal vascular remodelling is associated with endothelial cell dysfunction, increased proliferation of smooth muscle cells, inflammation, and impaired bone morphogenetic protein (BMP) signalling. Orphan nuclear receptor Nur77 is a key regulator of proliferation and inflammation in vascular cells, but its role in the impaired BMP signaling and vascular remodelling in PAH is unknown.

We hypothesized that activation of Nur77 by 6-mercaptopurine would improve the PAH by inhibiting endothelial cell dysfunction and vascular remodelling.

Nur77 expression is decreased in cultured pulmonary microvascular endothelial cells (MVECs) and lungs of PAH patients. Nur77 significantly increased BMP signaling and strongly decreased proliferation and inflammation in MVECs. In addition, conditioned medium from PAH MVECs overexpressing Nur77 inhibited the growth of healthy smooth muscle cells. Pharmacological activation of Nur77 by 6-mercaptopurine markedly restored MVEC function by normalizing proliferation, inflammation and BMP signaling. Finally, 6-mercaptopurine prevented and reversed abnormal vascular remodelling and right ventricle hypertrophy in the sugen-hypoxia rat model of severe angioproliferative PAH.

Our data demonstrate that Nur77 is a critical modulator in PAH by inhibiting vascular remodelling and increasing BMP signalling, and activation of Nur77 could be a promising option for the treatment of PAH.

INTRODUCTION

Pulmonary arterial hypertension (PAH) is a progressive fatal disease caused by abnormal proliferation of pulmonary vascular cells, resulting in remodelling of small pulmonary arteries (PAs), increased pulmonary vascular resistance, right ventricular (RV) failure, and ultimately death [1-4]. In hereditary PAH, mutations in the gene encoding for bone morphogenetic protein receptor 2 (BMPR2) or in genes encoding for downstream SMAD transcriptional effectors lead to impaired BMP signaling [4-7]. Interestingly, Impaired BMP signalling also occurs in non-hereditary forms of PAH [6, 8]. Despite advances in the treatment of PAH, current therapies still fail to reverse the established abnormal remodelling present in the lungs. Therefore, new molecular targets for development of remodelling-focused therapeutics are urgently needed.

Pulmonary artery endothelial cells (PA-ECs), pulmonary artery smooth muscle cells (PA-SMCs), pericytes and fibroblasts all play crucial roles in the pathobiology of PAH [5, 9-12]. PAH PA-ECs are hyperproliferative and contribute to the decrease in luminal diameter of the pulmonary micro-vessels. Additionally, PAH PA-ECs secrete factors such as inflammatory cytokines and growth factors which in turn induce proliferation and migration of PA-SMCs and fibroblasts and contribute to the progression of PAH [13-17]. A loss of BMPR2 in the endothelium can initiate and sustain the development of PAH [18, 19], but the driving transcriptional mechanisms remain poorly understood. Here we identify a central role for the orphan nuclear receptor Nur77 (NR4A1) in EC dysfunction, aberrant BMP signalling and vascular remodelling in PAH.

The transcription factor Nur77 plays a key role in a wide array of cellular processes such as proliferation, apoptosis, and inflammation [20-24]. Nur77 is implicated in several cardiovascular diseases such as atherosclerosis, restenosis, and cardiac hypertrophy [20, 22, 25]. In ECs, Nur77 decreases endothelin-1 expression and attenuates pro-inflammatory responses via inhibition of the nuclear factor (NF)κB pathway [26, 27]. Activation of Nur77 by Cytosporone B (CsnB) was shown to ameliorate experimental pulmonary hypertension (PH) in mice by decreasing PA-SMC proliferation [28, 29]. Interestingly, Nur77 modulates the transforming growth factor β (TGFβ) pathway in a cell-and context- dependent manner [30, 31]. 6-Mercaptopurine (6-MP), a well-established immunosuppressive drug to treat various autoimmune and chronic inflammatory diseases, is a non-traditional agonist of Nur77 [21, 22, 32]. 6-MP mediates a genotoxic stress response which in turn activates transcription of all three members

of the NR4A nuclear hormone receptor family, including Nur77, NOR-1, and Nurr1 [32]. We and others have shown that 6-MP inhibits activation of immune cells and also reduces the inflammatory response of ECs and the proliferation of vascular SMCs in Nur77 dependent manner [33-35]. Here, we show that Nur77 is a key player in PAH, involved in PA-EC dysfunction, proliferation of PA-SMCs and impaired BMP signalling, and that pharmacological targeting of Nur77 by 6-MP presents a novel therapeutic concept in PAH.

METHODS

See supplementary material for detailed methods.

Human lung samples and cell culture

PAH lung tissues were collected with patients' consent and approval from the local ethics committees at Free medical center, Amsterdam and Comite de ´Protection des Personnes (CPP) Ile-de-France VII, Paris. Control lung tissue was from patients undergoing a surgical procedure for cancer. Isolation and culturing of microvascular endothelial cells (MVECs) and pulmonary artery smooth muscle cells (PA-SMCs) was described previously [36, 37].

Plasmids, chemicals, Quantitative Real Time-PCR (qRT-PCR), western blot and luciferase assays

See supplementary material for details.

Lenti-viral transduction and proliferation assays

Lenti-viral transduction of cells, and cell proliferation (MTT) assays were performed as described previously [21, 23].

SuHx rat model of pulmonary hypertension (PH)

SU5416+Hypoxia (SuHx)-mediated PH in male Sprague-Dawley rats was induced as described previously [38, 39]. In the prevention study, rats received 6-MP (1 mg/kg/day) in drinking water from day 0 to day 42. In the reversal study, after randomization (treatment vs vehicle), animals were divided into two groups receiving 6-MP (1 mg/kg/day or 7.5 mg/kg/day) or vehicle (DMSO) in the drinking water from day 42 to day 70. Power calculation was performed to determine the appropriate sample size for

both prevention and reversal studies. Echocardiography, hemodynamic evaluation and RV hypertrophy were blinded to the condition, followed an unbiased approach and performed as described previously [38-40].

Statistical analysis

Statistical analyses were performed using Graphpad Prism 7 for Windows (GraphPad Software). Student's t-tests were used for comparisons between two groups. Multiple comparisons were assessed by one-way ANOVA, followed by Bonferroni post-hoc test. p-values < 0.05 were considered significant. All statistical tests used two-sided tests of significance. Data are presented as mean ± SEM.

RESULTS

Nur77 expression is impaired in PAH MVECs

Immunofluorescent staining showed that Nur77 is expressed in ECs, SMCs, fibroblasts, and epithelial cells in the lungs of control, idiopathic PAH (iPAH) and hereditary PAH (HPAH) patients (Fig. 1A). Transcript levels of Nur77 were significantly decreased in lungs of both iPAH and HPAH compared to controls, as shown by qPCR (Fig. 1B). Consistent with this observation, mRNA levels of Nur77 were markedly decreased in cultured human pulmonary microvascular ECs (MVECs) of both iPAH and HPAH compared to controls (Fig. 1C). Furthermore, protein levels of Nur77 were significantly decreased in MVECs of iPAH compared to controls (Fig. 1D). Taken together, these data suggest that Nur77 is involved in PA-EC function in PAH.

Nur77 modulates BMP/SMAD signalling in MVECs

Confirming previous studies, levels of BMPR2 and Id1 were significantly decreased in iPAH MVECs compared to control cells (Fig. 1E). Ectopic expression of Nur77 modestly, but significantly augmented BMPR2 mRNA levels in MVECs (Fig. 1F). Conversely, knock-down of Nur77 decreased BMPR2 protein levels in MVECs (Fig. 1G). To investigate the effect of Nur77 on canonical BMP signalling, we determined the phosphorylation of Smad1/5/8 following ectopic expression of Nur77. Nur77 markedly increased the phosphorylation of Smad1/5/8 under serum, BMP9 and TNFα-stimulated conditions (Fig. 1H). Ectopic expression of Nur77 augmented BMP9-induced BMP/SMAD reporter (BRE-luc) activity [40] (Fig. 1I) and Id3 mRNA expression (Fig. 1J), while knock-down of Nur77 decreased BMP9-induced BRE-luciferase activity in MVECs (Fig. 1K). Nur77 also

augmented the expression level of Id1 in PAH MVECs (Fig. 1L). Taken together, our data demonstrated that Nur77 increases BMP/SMAD signalling in MVECs.

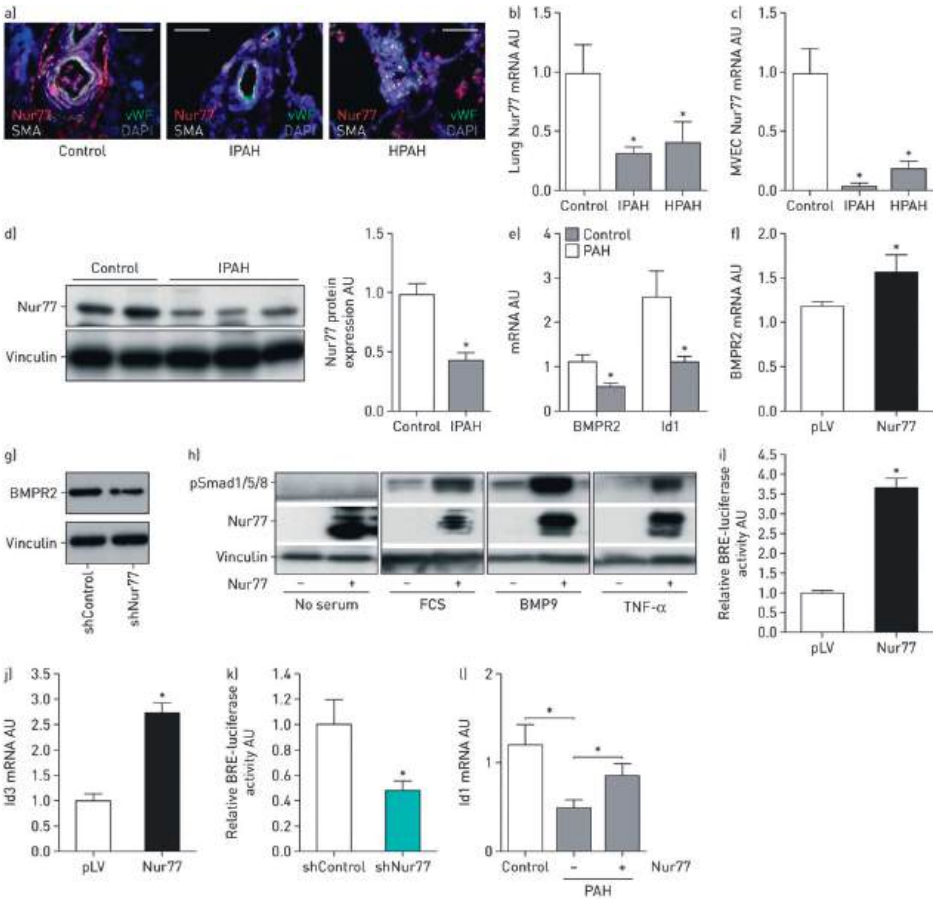

Figure 1. Nur77 expression is reduced in pulmonary arterial hypertension (PAH) and Nur77 enhances bone morphogenetic protein (BMP) signalling in microvascular endothelial cells (MVECs). vWF: von Willebrand factor; DAPI: 4′,6-diamidino-2-phenylindole; SMA: α-smooth muscle actin; IPAH: idiopathic PAH; HPAH: hereditary PAH; AU: arbitrary units; BMPR2: BMP receptor 2; pLV: control lentivirus; sh: short hairpin; pSmad1/5/8: phosphorylated Smad1/5/8; TNF: tumour necrosis factor; qRT: quantitative real-time. a) Representative immunofluorescence photomicrographs of Nur77 (red), vWF (green) and SMA (white) in human pulmonary arteries from control, IPAH and HPAH lungs (n=4). DAPI (blue): nuclei. Scale bar: 50 µm. b, c) qRT-PCR was performed to assess mRNA expression of Nur77 in b) control, IPAH and HPAH lungs (n=6 per group) and in c) MVECs from control, IPAH and HPAH patients (n=4 per group). d) Representative Western blots with relative densitometricanalyses showing Nur77 in total lung from control and IPAH patients (n=3). e) qRT-PCR was performed to assess mRNA expression of BMPR2 and Id1 in MVECs from control and PAH patients (n=6 per group). f) qRT-PCR was performed to assess mRNA expression of BMPR2 in MVECs following overexpression of Nur77 (n=3). g) Representative Western blots showing BMPR2 in MVECs following knockdown of Nur77 by shNur77 lentivirus (n=3). h) Representative Western blots showing pSmad1/5/8 following overexpression of Nur77

Figure 1 *(continued)*
and stimulation with vehicle (no serum), serum (10% FCS), BMP9 (1 ng·mL–1) and TNF-α (50 ng·mL–1) in MVECs (n=3). i) BRE-luciferase activity in MVECs was measured following overexpression of Nur77 and stimulation with BMP9 (1 ng·mL–1) for 16 h (n=3). j) qRT-PCR was performed to assess mRNA expression of Id3 in MVECs following ectopic expression of Nur77 (n=3). k) BRE-luciferase activity in MVECs was measured following knockdown of Nur77 and stimulation with BMP9 (1 ng·mL–1) for 16 h (n=3). l) qRT-PCR was performed to assess mRNA expression of Id1 in control and PAH MVECs following ectopic expression of Nur77 (n=3). *: $p<0.05$. The t-test was used for comparisons between two groups. Multiple comparisons were assessed by one-way ANOVA followed by Bonferroni's post hoc test. Data are presented as mean ± SEM.

Nur77 reduces inflammation of MVECs by inhibiting NFκB activity

As expected, PAH MVECs have higher mRNA levels of the pro-inflammatory cytokines IL-6 and RANTES after TNFα stimulation when compared to control cells (Fig. 2A). Knock-down of Nur77 markedly increased TNFα-induced expression of TNFα, IL-1β and IL-6 at mRNA level (Fig. 2B), while ectopic expression of Nur77 decreased the protein levels of MCP-1 and IL-6 in MVECs (Fig. 2C-D). Furthermore, knock-down of Nur77 significantly increased (Fig. 2E), while ectopic expression of Nur77 strongly decreased the transcriptional activity of the NFκB promoter (Fig. 2F), suggesting that in PA-MVECs Nur77 decreases the expression of pro-inflammatory cytokines through inhibition of the NFκB pathway.

Nur77 attenuates proliferation of MVECs through inhibiting CyclinD1

Both cultured MVECs from control and PAH patients display a cobble stone morphology (Fig. 2G). However, PAH MVECs grow faster as demonstrated by an MTT assay (Fig. 2H). Since Nur77 is reported to decrease cell proliferation by inhibiting CyclinD1 [29], we explored whether loss of Nur77 could explain the hyper-proliferation of PAH MVECs. Over-expression of Nur77 reduced proliferation of both PAH and control MVECs (Fig. 2H), while knock-down of Nur77 stimulated their growth. Furthermore, we found that over-expression of Nur77 decreased (Fig. 2J), while knock-down of Nur77 significantly increased CyclinD1 promoter activity (Fig. 2K). Altogether, these data suggest that Nur77 is involved in PAH MVEC proliferation via modulation of CyclinD1.

Since the interplay between ECs and SMCs is crucial in the pathogenesis of PAH, we next investigated the role of Nur77 in ECs-SMCs interaction. Addition of conditioned medium from TNFα-pre-treated PAH PA-ECs transduced with Nur77 inhibited the growth of healthy PA-SMCs (Fig. 2L), indicating that Nur77 plays an important role not only in PA-ECs but also in the cross-talk between ECs and SMCs.

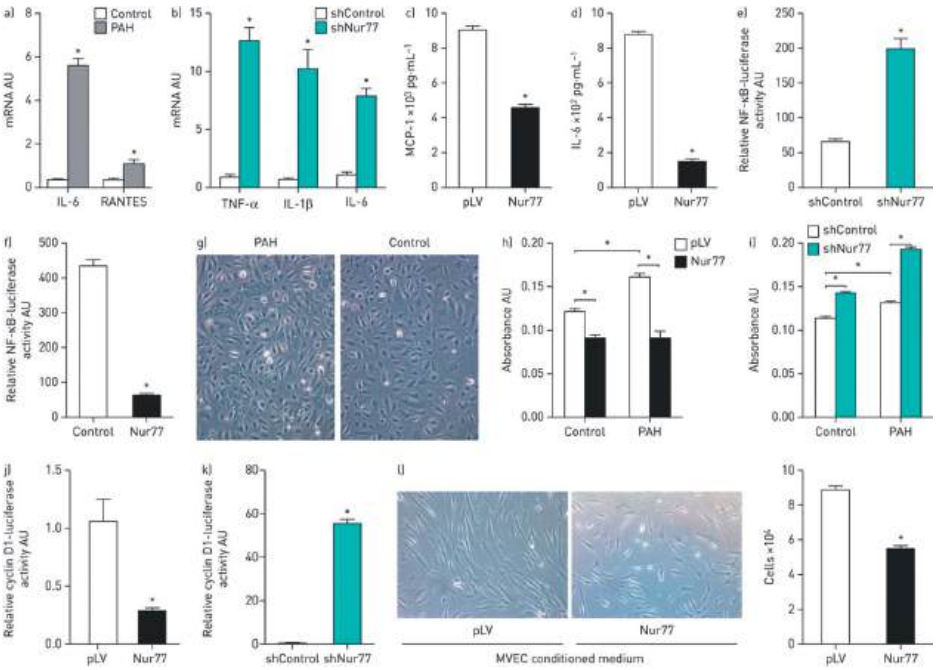

Figure 2. Nur77 inhibits inflammation and proliferation of microvascular endothelial cells (MVECs). AU: arbitrary units; PAH: pulmonary arterial hypertension; IL: interleukin; sh: short hairpin; TNF: tumour necrosis factor; MCP: monocyte chemoattractant protein; pLV: control lentivirus; qRT: quantitative real-time; MTT: 3-(4,5-dimethylthiazol-2-yl)-2,5-diphenyltetrazolium bromide. a) qRT-PCR was performed to assess mRNA expression of IL-6 and RANTES in TNF-α-stimulated MVECs (6 h) from control and idiopathic PAH patients (n=3). b) qRT-PCR was performed to assess mRNA expression of TNF-α, IL-1β and IL-6 in TNF-α-stimulated MVECs (6 h) (n=3). c, d) ELISAs for c) MCP-1 and d) IL-6 were performed using supernatants from MVECs following ectopic expression of Nur77 and stimulation with TNF-α for 6 h (n=4). e, f) TNF-α-induced NF-κB-luciferase activity in HEK293T cells was measured following e) knockdown and f) ectopic expression of Nur77 (n=3). g) Morphological appearance of control and PAH MVECs. h, i) MTT assays were performed to assess proliferation of control and PAH MVECs following h) knockdown and i) ectopic expression of Nur77 (n=3). j, k) Cyclin D1 promoter-luciferase activity in HEK293T cells was measured following j) ectopic expression and k) knockdown of Nur77. The data shown are representative of three experiments. l) Assessment of serum-starved pulmonary artery smooth muscle cell proliferation following incubation with conditioned medium from PAH MVECs without and with ectopically expressed Nur77 and stimulated with TNF-α (n=3). *: $p<0.05$. The t-test was used for comparisons between two groups. Multiple comparisons were assessed by one-way ANOVA followed by Bonferroni's post hoc test. Data are presented as mean±sem.

Nur77 is required for 6-MP-induced activation of BMP signalling

To increase Nur77 activity we stimulated PAH MVECs with two known agonists of Nur77, CsnB and 6-MP [21, 41] and found that both agonists increased the protein levels (Fig. 3A) and mRNA expression of Nur77 (Fig. 3B) in PAH MVECs. Since the transcriptional activity of Nur77 determines its function, we determined the transcriptional activity

of Nur77 using a Nur77 specific luciferase reporter (NurRE-luc) [23] in MVECs, and observed that both agonists increased the activity of the Nur77 reporter (Fig. 3C). Interestingly, CsnB and 6-MP also significantly increased the BRE-luc activity (Fig. 3D). To determine whether the observed increase in BRE-luc activity required Nur77, we knocked-down Nur77 and found that both agonists were no longer able to activate the BMP reporter (Fig. 3D). This confirmed our previous observation that Nur77 activates the BMP/Smad signaling pathway. In line with the increased BRE luciferase activity, both agonists also increased the mRNA levels of the down-stream target Id1 (Fig. 3E). Moreover, treatment of PAH MVECs with both agonists decreased proliferation (Fig. 3F) and attenuated CyclinD1-promoter luciferase activity (Fig. 3G). We also found that both CsnB and 6-MP require Nur77 to reduce pro-inflammatory cytokine IL-6 expression (data not shown).Taken together, we show that both CsnB and 6-MP require Nur77, at least partly, to exhibit their function in restoring the behavior of PAH MVECs. Although both agonists of Nur77 displayed similar potential in vitro, we assessed whether 6-MP could prevent development of PH in the SuHx rat model for angioproliferative PH [42], because i) 6-MP is used in the clinic for decades [21, 32], ii) decreased inflammation in cultured MVECs (Supplementary Fig. 1A-B), iii) increased the expression levels of Id3 and BMPR2 in PAH MVECS (Supplementary Fig. 1C-D), and iv) decreased proliferation of healthy human PASMCs (Supplementary Fig. 1E).

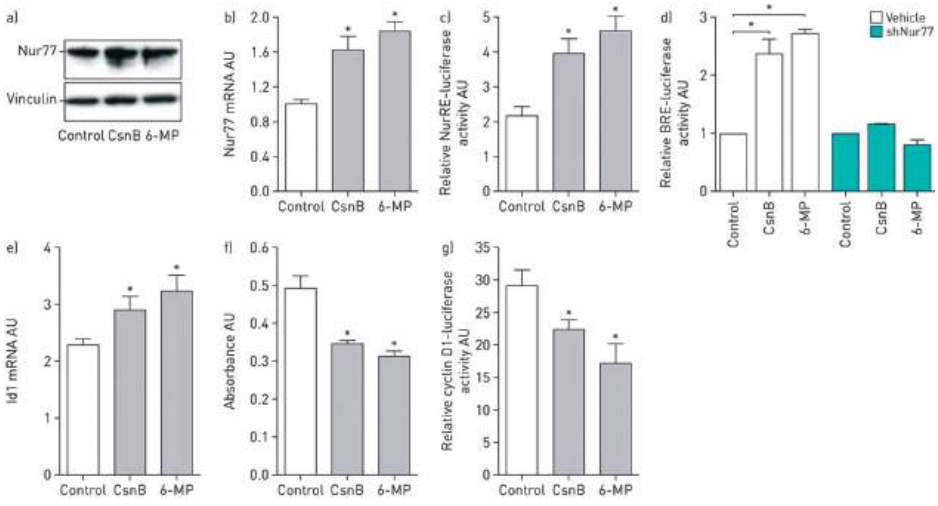

Figure 3. Upregulated Nur77 is involved in the 6-mercaptopurine (6-MP)-mediated effect on bone morphogenetic protein (BMP) signalling in microvascular endothelial cells (MVECs).
CsnB: cytosporone B; AU: arbitrary units; qRT: quantitative real-time; MTT: 3-(4,5-dimethylthiazol-2-yl)-2,5-diphenyltetrazolium bromide; PAH: pulmonary arterial hypertension. a) Western blot (n=3) and b) qRT-PCR (n=3) analysis was performed to measure the expression of Nur77 in MVECs that were

Figure 3 *(continued)*
pre-treated with CsnB (5 μM) or 6-MP (10 μM) for 16 h. c) The activity of Nur77 was monitored in MVECs expressing the NurRE-luciferase reporter following treatment with CsnB (5 μM) or 6-MP (10 μM). The data shown are representative of three experiments. d) Overall BRE-luciferase activity was measured in MVECs transduced with control or shNur77 lentivirus for 48 h followed by treatment with CsnB (5 μM) or 6-MP (10 μM) in the presence of BMP9 (1 ng·mL–1) for 16 h (n=3). e) qRT-PCR was performed to assess mRNA expression of Id1 following treatment with CsnB (5 μM) or 6-MP (10 μM) for 16 h (n=3). f) MTT assays were performed to assess PAH MVEC proliferation following treatment with CsnB (5 μM) or 6-MP (10 μM) for 24 h (n=3). g) Cyclin D1 promoter-luciferase activity in PAH MVECs was measured following treatment with CsnB (5 μM) or 6-MP (10 μM) for 16 h (n=3). *: $p<0.05$. Multiple comparisons were assessed by one-way ANOVA followed by Bonferroni's post hoc test. Data are presented as mean±sem.

6-MP treatment prevents the development of PH

When treating the animals with 1 mg/kg 6-MP per day orally from the start of the experiment till day 42 we found that 6-MP was able to maintain RV function by significantly decreasing RVSP, arterial-elastance (Ea), RV end-diastolic-elastance (stiffness, Eed) while increasing RV-arterial-coupling (Ees/Ea) (Fig. 4A). Moreover, 6-MP treatment significantly increased stroke volume (SV) and RV systolic function (TAPSE) while significantly decreasing RV free-wall thickness (RVWT) and RV end-diastolic diameter (RVEDD) (Fig. 4B). Consistent with our in vitro findings, 6-MP treatment also decreased serum levels of inflammatory cytokines IL-6 and MCP-1 (Fig. 4C). However, no significant effect of 6-MP on the levels of phospho-IKK α/β was observed (Supplementary Fig. 2A). Furthermore, 6-MP significantly reduced the number of occlusive lesions and fully muscularized arteries, and reduced the thickness of both the intimal and medial layers (Fig. 4D; data not shown). The number of proliferating cells was decreased in 6-MP treated rats compared to vehicle, as determined by immunofluorescent staining for Ki67 (Fig. 4E). Furthermore, 6-MP treatment attenuated the recruitment of CD68 positive macrophages to the lungs (Fig. 4F), while no significant effect of 6-MP on number of B-cells and T-cells was observed (Supplementary Fig. 2B-C). We found no evidence of 6-MP changing the composition of blood cells or systemic blood pressure (Supplementary Fig. 2D; data not shown). Finally, but importantly, RV hypertrophy and RV fibrosis were significantly decreased in the 6-MP-treated PH rats (Fig. 4G-H). Taken together, 6-MP treatment from the start of the experiment prevents the development of PH in the SuHx rat model.

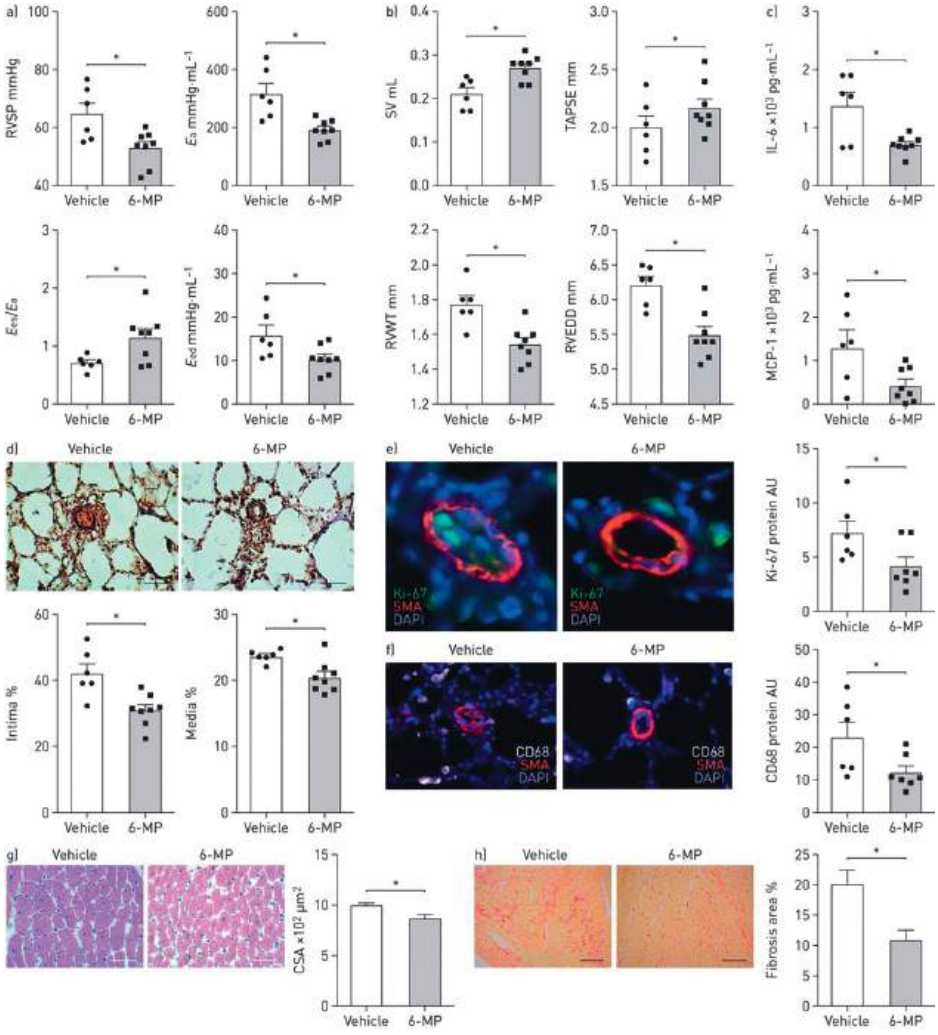

Figure 4. 6-Mercaptopurine (6-MP) prevents the development of pulmonary hypertension (PH) and improves cardiac function in Sugen/hypoxia (SuHx)-induced PH in rats.

RVSP: right ventricular systolic pressure; Ea: arterial elastance; Ees: end-systolic elastance; Eed: end-diastolic elastance; SV: stroke volume; TAPSE: tricuspid annular plane systolic excursion; RVWT: right ventricular wall thickness; RVEDD: right ventricular end-diastolic diameter; IL: interleukin; MCP: monocyte chemoattractant protein; SMA: α-smooth muscle actin; DAPI: 4′,6-diamidino-2-phenylindole; AU: arbitrary units; CSA: cross-sectional area. a) SuHx rats were treated with 6-MP in drinking water from the start till the end of the experiment. Echocardiography, followed by physiological measurements, was carried out at the day of termination (day 42). RVSP (top left), Ea (top right), Ees/Ea (bottom left) and Eed (bottom right) are shown for the indicated groups of rats (n=6 rats for vehicle and n=8 rats for 6-MP per group). b) SV (top left), TAPSE (top right), RVWT (bottom left) and RVEDD (bottom right) are shown for the indicated groups (n=6–8 lungs per group). c) ELISAs for IL-6 (top) and MCP-1 (bottom) were performed in serum from the indicated groups (n=6–8 lungs per group). d) The neointima to media ratio of pulmonary arteries (<90 µm in diameter) from lung sections of SuHx-treated

Figure 4 *(continued)*
rats was determined by morphometric analysis of pulmonary vessels following Elastica van Giesson staining (n=6–8 lungs per group). Scale bar: 20 μm. e, f) Immunofluorescent staining for e) Ki-67 (green) and f) CD68 (white) was performed in small pulmonary arteries from vehicle- and 6-MP-treated rats. SMA (red) and nuclei (DAPI; blue) were co-stained with Ki-67 or CD68. Quantification of fluorescence is shown in the bar graph next to the images (images representative of n=6–8 lungs per group). g) Mean cardiomyocyte CSA was assessed in the right ventricle from vehicle- and 6-MP-treated rats following haematoxylin and eosin staining. Scale bar: 20 μm. Quantification of CSA is shown in the bar graph next to the images (n=6–8 lungs per group). h) Picrosirius red staining was performed to assess fibrosis in the right ventricle from vehicle- and 6-MP treated rats. Scale bar: 80 μm. Quantification of fibrosis is shown in the bar graph next to the images (n=6–8 lungs per group). *: $p<0.05$. The t-test was used for comparisons between two groups. Data are presented as mean±sem.

6-MP treatment reverses the development of PH, restores BMP-signalling and increases Nur77 *in vivo*

Before starting 6-MP treatment during disease progression, we first determined the expression levels of Nur77 in the SuHx model, and observed that the expression of Nur77 is increased at initiation of the disease while its expression decreases when disease progresses from week 6 onwards (Supplementary Fig. 3). However, in MCT rats Nur77 levels remained elevated until the usual day of end-experiments: day 21 (data not shown). [25] Therefore, to assess the therapeutic potential of 6-MP in PH, we treated SuHx rats with two doses of 6-MP (1 mg/kg/day and 7.5 mg/kg/day) from day 28 days after the induction of PH. The therapeutic dose of 6-MP (7.5 mg/kg/day) significantly decreased RVSP, Ea, and Eed, but not Ees/Ea (Fig. 5A), while the sub-clinical dose of 6-MP used in the prevention trial (1 mg/kg/day) only significantly decreased Eed, but had no effect on the other parameters (Fig. 5A). The therapeutic dose of 6-MP markedly improved RV function (increase in SV), reduced RV hypertrophy (decrease in RVWT, RVEDD and Fulton index), and suppressed remodelling of the lung vasculature (Fig 5B-D). However, no significant effect of the therapeutic dose of 6-MP was observed on TAPSE, but the sub-clinical dose of 6-MP exhibited an increase in SV and a modest decrease in RVWT and RVEDD (Fig. 5B). Similarly as in the prevention study, the therapeutic dose of 6-MP decreased cell proliferation (number of Ki67 positive cells) (Fig. 5E), RV hypertrophy (cross sectional area) (Fig. 5F), and RV fibrosis (picro sirius staining) (Fig. 5G). In addition, we found that 6-MP significantly increased RV capillary density when compared to the vehicle treated animals (Supplementary Fig. 4). Importantly, we found no evidence of 6-MP affecting blood cell composition or systemic blood pressure (Supplementary Fig. 5A-C; data not shown), but did improve the survival rate of the SuHx rats (Supplementary Fig. 5D).

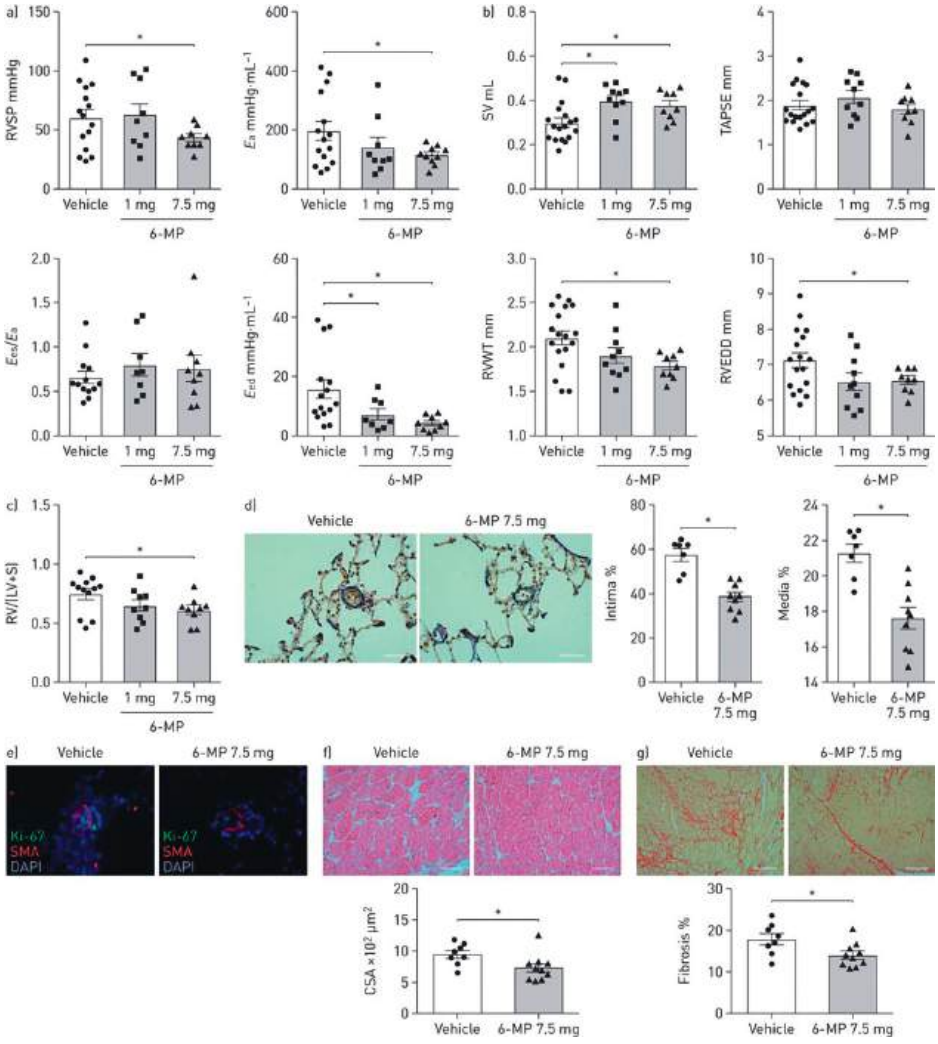

Figure 5. 6-Mercaptopurine (6-MP) reverses pulmonary vascular remodelling and pulmonary hypertension (PH) in Sugen/hypoxia (SuHx)-induced PH in rats.

RVSP: right ventricular systolic pressure; Ea: arterial elastance; Ees: end-systolic elastance; Eed: end-diastolic elastance; SV: stroke volume; TAPSE: tricuspid annular plane systolic excursion; RVWT: right ventricular wall thickness; RVEDD: right ventricular end-diastolic diameter; RV: right ventricle; LV: left ventricle; S: septum; SMA: α-smooth muscle actin; DAPI: 4′,6-diamidino-2-phenylindole; CSA: cross-sectional area. a) Two concentrations (1 and 7.5 mg·kg−1·day−1) of 6-MP were administered in the drinking water from day 42 to day 70 to SuHx rats after randomisation. Echocardiography, followed by physiological measurements, was carried out at the day of termination (day 70). RVSP (top left), Ea (top right), Ees/Ea (bottom left) and Eed (bottom right) are shown for the indicated groups of rats (n=14 rats for vehicle or n=9 for 6-MP 1 mg·kg−1·day−1 or n=9 for 6-MP 7.5 mg·kg−1·day−1 per group). b) SV (top left), TAPSE (top right), RVWT (bottom left) and RVEDD (bottom right) are shown for the indicated groups (n=9–14 rats per group). c) Right ventricular hypertrophy was measured, as defined by the Fulton index (weight of RV/(LV+S)) (n=9–14 rats per group). d) The neointima to media ratio of pulmonary arteries

Figure 5 *(continued)*
(<90 μm in diameter) from lung sections of SuHx-treated rats was determined by morphometric analysis of pulmonary vessels following Elastica van Giesson staining (n=9–14 rats per group). Scale bar: 20 μm. e) Immunofluorescent staining for Ki-67 (green) was performed in small pulmonary arteries from vehicle- and 6-MP-treated rats. SMA (red) and nuclei (DAPI; blue) were co-stained with Ki-67 (images representative of n=9–14 lungs per group). f) Mean cardiomyocyte CSA was assessed in the RV from vehicle- and 6-MP-treated rats. Scale bar: 20 μm. Quantification of CSA is shown in the bar graph next to the images (n=9–14 rats per group). g) Picrosirius red staining was performed to assess the fibrosis in the RV from vehicle- and 6-MP-treated rats. Scale bar: 80 μm. Quantification of fibrosis is shown in the bar graph next to the images (n=9–14 rats per group). *: $p<0.05$. The t-test was used for comparisons between two groups. Multiple comparisons were assessed by one-way ANOVA followed by Bonferroni's post hoc test. Data are presented as mean±sem.

We next examined the effect of 6-MP treatment on BMP signalling in the lungs of the SuHx rats. In the prevention study, we found that 6-MP increased the expression levels of BMPR2, pSmad1/5/8 and Id3 as demonstrated by immunofluorescent analysis (Fig. 6A-C). Furthermore, 6-MP treatment significantly increased the expression levels of Nur77 in the vessel wall (Fig. 6D). However, no effect of 6-MP on Nur77 in total lung tissue was found as shown by western blot analysis (Supplementary Fig. 6). Consistent with the above findings, therapeutic dose of 6-MP was able to increase the protein levels of BMPR2, pSmad1/5/8, Id1, and Id3 in the reversal study (Fig. 6E-F, Supplementary Fig. 7A). However, no significant effect of 6-MP on phospho-ERK1/2 or apoptosis was observed (Supplementary Fig. 7B-C). Immunofluorescent analysis showed that 6-MP increased the expression levels of Nur77 in the vessel wall (Fig. 6G) while a modest increase was observed in total lung lysates (Fig. 6E-F). Taken together, 6-MP augmented BMP signaling in vivo, at least partly, via Nur77. We summarized our findings in Figure 6H.

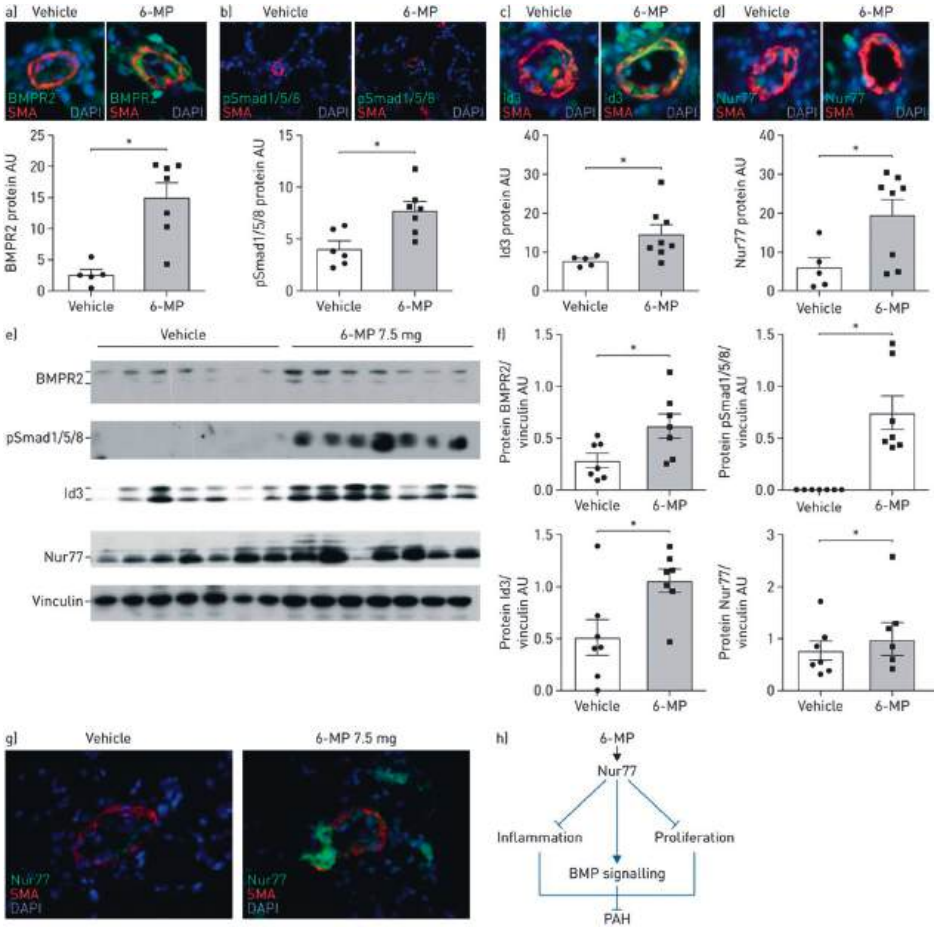

Figure 6. 6-Mercaptopurine (6-MP) enhances Nur77 expression and amplifies bone morphogenetic protein (BMP) signalling *in vivo*.

BMPR2: BMP receptor 2; SMA: α-smooth muscle actin; DAPI: 4′,6-diamidino-2-phenylindole; pSmad1/5/8: phosphorylated Smad1/5/8; AU: arbitrary units; PAH: pulmonary arterial hypertension. a–d) Immunofluorescent staining for a) BMPR2 (green), b) pSmad1/5/8 (green), c) Id3 (green) and d) Nur77 (green) was performed in small pulmonary arteries from vehicle- and 6-MP-treated rats from the prevention study. SMA (red) defines smooth muscle cells and DAPI (blue) was used to counterstain nuclei (n=6–8 lungs per group). e) Western blots showing BMPR2, pSmad1/5/8, Id3 and Nur77 with vinculin as a loading control in total lung lysates from the Sugen/hypoxia rats treated with vehicle and 6-MP (7.5 mg·kg−1·day−1) (n=7 lungs per group). f) Relative densitometric analyses of the Western blots showing BMPR2, pSmad1/5/8, Id3 and Nur77 (n=7 lungs per group). g) Immunofluorescent staining for Nur77 (green) was performed in small pulmonary arteries from vehicle- and 6-MP (7.5 mg·kg−1·day−1)-treated rats. SMA (red) and nuclei (DAPI; blue) were co-stained with Nur77 (n=8 lungs per group). *: $p<0.05$. The t-test was used for comparisons between two groups. Multiple comparisons were assessed by one-way ANOVA followed by Bonferroni's post hoc test. Data are presented as mean±sem. h) Proposed mechanism of Nur77 6-MP in the reversal of PAH. 6-MP increases the transcriptional activity of Nur77 which 1) inhibits inflammation through blocking the NF-κB pathway, 2) blocks proliferation through inhibition of cell cycle proteins and 3) enhances BMP signalling via activation of the

Figure 6 *(continued)*
BMPR2-pSmad1/5/8–Id1/3 axis by enhancing BMPR2 expression. Abnormal proliferation and excessive inflammation with impaired BMP signalling leads to initiation and progression of PAH. Activation of Nur77 via clinically approved small-molecule activators such as the Nur77 agonist 6-MP reverses these aberrant changes and attenuates PAH.

DISCUSSION

The present study demonstrates that down-regulation of Nur77 in the pulmonary vasculature is involved in the pathogenesis of PAH and that activation of Nur77 by 6-MP could be a novel therapeutic option to reverse the abnormal vascular remodelling and RV hypertrophy in PAH. This concept (Fig. 6H) is based on our findings that (i) Nur77 expression is down-regulated in both pulmonary MVECs and lungs of iPAH and HPAH patients; (ii) Absence of Nur77 leads to EC dysfunction and PA-SMC proliferation; (iii) Nur77 suppresses inflammation through inhibition of the NFκB pathway; (iv) pharmacological activation or gain of function of Nur77 inhibits MVEC dysfunction and potently augments BMP/SMAD signalling in MVECs and lungs in vitro and in vivo. Finally, we demonstrated that (v) pharmacological activation of Nur77 attenuates abnormal vascular remodelling and improves RV function in vivo.

Expression of Nur77 has been implicated in several vascular diseases, including atherosclerosis, cardiac hypertrophy, and coronary restenosis [20-28], where Nur77 inhibits proliferation of endothelial cells, smooth muscle cells, pericytes and fibroblasts, while at the same time suppressing inflammation [23, 28, 35, 43]. Proliferation and inflammation are key features of pulmonary vascular remodelling in PAH [13-17]. Several known triggers of PAH such as DNA damage, inflammation, hypoxia, TGFβ signalling, histone acetylation, and disturbed flow have been shown to regulate Nur77 expression and activity in a cell-and context-dependent manner [30, 46-48]. Indeed, in the present study we found that inhibition of HDACs increased Nur77 expression in PAH MVECs (Supplementary Fig. 1F). In addition, post-translational modifications such as phosphorylation and ubiquitination were also shown to regulate Nur77 expression/activity. Indeed, a number of kinases have been shown to phosphorylate and/or interact with Nur77 directly to modulate its activity [22]. Nur77 agonist, 6-MP increases the activity of Nur77 and its family members Nurr1 and NOR-1 via direct modulation of the activation function-1 (AF-1) which is located within the amino terminal-regulatory (A/B) domain of Nur77. Interestingly, this increase in activity of Nur77 by 6-MP doesn't require

the ligand binding domain (LBD) of Nur77. It has also been demonstrated that 6-MP can modulate the activity of the Nur77 coactivator TRAP220 which directly interacts with the AF-1 domain of Nur77 *in vivo* [49]. Therefore, 6-MP can regulate the expression and activity of Nur77 via direct modulation of the AF-1 domain and/or activation of its coactivator TRAP220 in a cell-and context dependent manner. However, as it is beyond the scope of this study, this has not been investigated in the current study.

A key mechanism by which Nur77 and its agonist 6-MP inhibit cell proliferation is through attenuation of CyclinD1, a known target gene of Nur77 [25, 33, 50]. Indeed, we demonstrated that restoration of Nur77 in PAH MVECs reduced CyclinD1 expression and cellular proliferation. While the role of Nur77 was never before studied in relevant cell populations from patients with PAH, two recent studies demonstrated that Nur77 exhibits anti-proliferative effects in rat PA-SMCs via STAT3/Pim-1/NFAT pathway and human PA-SMCs via the Axin2-beta-catenin signaling pathway [28, 29]. Consistent with this, in the present study we also found that 6-MP directly decreases proliferation of healthy human PASMCs (Supplementary Fig. 1E). The communication between ECs and SMCs plays an essential role in the pathogenesis of PAH. In our study, we found that Nur77 is a key player at the interplay between these cells since the secretome of the diseased PA-ECs stimulates PA-SMC growth. In addition to effects on the EC and SMC proliferation, Nur77 and its activator 6-MP are known to inhibit the NFκB pathway, thereby reducing the production of several cytokines [21, 24, 27]. Here, we confirm that 6-MP decreases the secretion of inflammatory cytokines in pulmonary MVECs and also in serum and lung tissue of the 6-MP treated SuHx rats.

While the effects of Nur77 on vascular proliferation and inflammation were possibly exerted through interaction with multiple pathways, we provide first evidence that at least some of this effect in PAH is through control of the BMPR2 gene. Germline mutations in BMPR2 is the strongest known genetic risk factor associated with PAH; about 40% of all subjects carrying mutations resulting in haplo-insufficiency will ultimately develop HPAH [4, 16, 32, 44, 45]. Even in iPAH patients both BMPR2 and BMP signalling are reduced [4, 6]. Loss of BMPR2 has been linked to increased inflammation and proliferation of pulmonary ECs, and it has been suggested that restoring BMP signalling might be beneficial for the treatment of PAH patients [18, 19]. Indeed, enhanced BMP signalling by BMP9 treatment reduced the development of PAH in animal models [37]. Previously, Nur77 was shown to modulate TGFβ signalling in a cell- and context-dependent manner [30, 31]. Our data provides the first in vitro and

in vivo evidence that Nur77 controls BMP signalling as well. Our findings imply that Nur77, via the BMPR2-Smad-Id1 axis, may significantly promote EC function in HPAH and iPAH. Therefore, activation of Nur77 can serve as a novel therapeutic approach for HPAH and other PAH patients with impaired BMP signalling.

Whether using a prevention or reversal strategy, oral administration of 6-MP markedly reduced RVSP and improved RV function in the SuHx PH rat model. The hemodynamic effects of 6-MP were associated with markedly reduced proliferation and inflammation and reversed abnormal vascular remodelling. Crucially, the beneficial effect of 6-MP was associated with normalization of Nur77 expression and BMP signalling. Taking into account the observed beneficial effect of 6-MP in SuHx rats in this short treatment period, prolonged treatment with 6-MP may even result in a stronger reversal of PAH. Importantly, we observed no immunosuppression at the dose given in the 6-MP treated animals in both the prevention and reversal study. Although no side effects were observed in these preclinical models and 6-MP is already used in several clinical conditions in patients [21, 32, 35], future research should focus on testing 6-MP in combination with other PAH drugs as well as the development of lung-specific delivery methods [46] to achieve efficient pulmonary efficacy at low drug concentrations.

Despite recent advances in PAH research, there is still no cure for this deadly disease. EC dysfunction is a crucial element in the initiation and pathogenesis of PAH and our data provide evidence that Nur77 is a novel positive regulator of pulmonary MVEC function and thereby inhibits adverse vascular remodelling in PAH. Specifically, Nur77 exhibits significant anti-proliferative and anti-inflammatory effects and augments BMP signalling in vitro and in vivo. In conclusion, 6-MP displays beneficial effects in vitro and in vivo, and this well-known drug provides an innovative treatment opportunity for patients suffering from the so far untreatable disease PAH.

ACKNOWLEDGMENTS

We thank Martijn Rabelink for providing shRNAs targeting Nur77.

SUPPORT STATEMENT

We acknowledge support from the Netherlands CardioVascular Research Initiative: the Dutch Heart Foundation, Dutch Federation of University Medical Centers, the Netherlands Organization for Health Research and Development, and the Royal Netherlands Academy of Sciences Grant 2012-08 awarded to the Phaedra consortium (http://www.phaedraresearch.nl). We also acknowledge support for KK by the Grants4Targets (Bayer AG) grant number-2016-03-1554 and by the Dutch Lung Foundation (Longfonds) grant number-5.2.17.198J0.

DISCLOSURES

None

REFERENCES

1. Tuder RM, Archer SL, Dorfmuller P, Erzurum SC, Guignabert C, Michelakis E, Rabinovitch M, Schermuly R, Stenmark KR, Morrell NW. Relevant issues in the pathology and pathobiology of pulmonary hypertension. *Journal of the American College of Cardiology* 2013: 62(25 Suppl): D4-12.
2. D'Alonzo GE, Barst RJ, Ayres SM, Bergofsky EH, Brundage BH, Detre KM, Fishman AP, Goldring RM, Groves BM, Kernis JT, et al. Survival in patients with primary pulmonary hypertension. Results from a national prospective registry. *Annals of internal medicine* 1991: 115(5): 343-349.
3. Galie N, Humbert M, Vachiery JL, Gibbs S, Lang I, Torbicki A, Simonneau G, Peacock A, Vonk Noordegraaf A, Beghetti M, Ghofrani A, Gomez Sanchez MA, Hansmann G, Klepetko W, Lancellotti P, Matucci M, McDonagh T, Pierard LA, Trindade PT, Zompatori M, Hoeper M, Aboyans V, Vaz Carneiro A, Achenbach S, Agewall S, Allanore Y, Asteggiano R, Paolo Badano L, Albert Barbera J, Bouvaist H, Bueno H, Byrne RA, Carerj S, Castro G, Erol C, Falk V, Funck-Brentano C, Gorenflo M, Granton J, Iung B, Kiely DG, Kirchhof P, Kjellstrom B, Landmesser U, Lekakis J, Lionis C, Lip GY, Orfanos SE, Park MH, Piepoli MF, Ponikowski P, Revel MP, Rigau D, Rosenkranz S, Voller H, Luis Zamorano J. 2015 ESC/ERS Guidelines for the diagnosis and treatment of pulmonary hypertension: The Joint Task Force for the Diagnosis and Treatment of Pulmonary Hypertension of the European Society of Cardiology (ESC) and the European Respiratory Society (ERS): Endorsed by: Association for European Paediatric and Congenital Cardiology (AEPC), International Society for Heart and Lung Transplantation (ISHLT). *Eur Heart J* 2016: 37(1): 67-119.
4. Morrell NW, Adnot S, Archer SL, Dupuis J, Jones PL, MacLean MR, McMurtry IF, Stenmark KR, Thistlethwaite PA, Weissmann N, Yuan JX, Weir EK. Cellular and molecular basis of pulmonary arterial hypertension. *Journal of the American College of Cardiology* 2009: 54(1 Suppl): S20-31.
5. Yang J, Davies RJ, Southwood M, Long L, Yang X, Sobolewski A, Upton PD, Trembath RC, Morrell NW. Mutations in bone morphogenetic protein type II receptor cause dysregulation of Id gene expression in pulmonary artery smooth muscle cells: implications for familial pulmonary arterial hypertension. *Circulation research* 2008: 102(10): 1212-1221.
6. Atkinson C, Stewart S, Upton PD, Machado R, Thomson JR, Trembath RC, Morrell NW. Primary pulmonary hypertension is associated with reduced pulmonary vascular expression of type II bone morphogenetic protein receptor. *Circulation* 2002: 105(14): 1672-1678.
7. Voelkel NF, Gomez-Arroyo J, Abbate A, Bogaard HJ, Nicolls MR. Pathobiology of pulmonary arterial hypertension and right ventricular failure. *Eur Respir J* 2012: 40(6): 1555-1565.
8. Perros F, Bonnet S. Bone morphogenetic protein receptor type II and inflammation are bringing old concepts into the new pulmonary arterial hypertension world. *American journal of respiratory and critical care medicine* 2015: 192(7): 777-779.
9. Alastalo TP, Li M, Perez Vde J, Pham D, Sawada H, Wang JK, Koskenvuo M, Wang L, Freeman BA, Chang HY, Rabinovitch M. Disruption of PPARgamma/beta-catenin-mediated regulation of apelin impairs BMP-induced mouse and human pulmonary arterial EC survival. *The Journal of clinical investigation* 2011: 121(9): 3735-3746.

10. Hong KH, Lee YJ, Lee E, Park SO, Han C, Beppu H, Li E, Raizada MK, Bloch KD, Oh SP. Genetic ablation of the BMPR2 gene in pulmonary endothelium is sufficient to predispose to pulmonary arterial hypertension. *Circulation* 2008: 118(7): 722-730.
11. Yuan K, Shao NY, Hennigs JK, Discipulo M, Orcholski ME, Shamskhou E, Richter A, Hu X, Wu JC, de Jesus Perez VA. Increased Pyruvate Dehydrogenase Kinase 4 Expression in Lung Pericytes Is Associated with Reduced Endothelial-Pericyte Interactions and Small Vessel Loss in Pulmonary Arterial Hypertension. *The American journal of pathology* 2016: 186(9): 2500-2514.
12. Zhang H, Wang D, Li M, Plecita-Hlavata L, D'Alessandro A, Tauber J, Riddle S, Kumar S, Flockton AR, McKeon BA, Frid MG, Reisz JA, Caruso P, El Kasmi KC, Jezek P, Morrell NW, Hu CJ, Stenmark KR. The Metabolic and Proliferative State of Vascular Adventitial Fibroblasts in Pulmonary Hypertension is Regulated through a MiR-124/PTBP1/PKM Axis. *Circulation* 2017.
13. Le Hiress M, Tu L, Ricard N, Phan C, Thuillet R, Fadel E, Dorfmuller P, Montani D, de Man F, Humbert M, Huertas A, Guignabert C. Proinflammatory Signature of the Dysfunctional Endothelium in Pulmonary Hypertension. Role of the Macrophage Migration Inhibitory Factor/CD74 Complex. *American journal of respiratory and critical care medicine* 2015: 192(8): 983-997.
14. Toshner M, Voswinckel R, Southwood M, Al-Lamki R, Howard LS, Marchesan D, Yang J, Suntharalingam J, Soon E, Exley A, Stewart S, Hecker M, Zhu Z, Gehling U, Seeger W, Pepke-Zaba J, Morrell NW. Evidence of dysfunction of endothelial progenitors in pulmonary arterial hypertension. *American journal of respiratory and critical care medicine* 2009: 180(8): 780-787.
15. Savai R, Pullamsetti SS, Kolbe J, Bieniek E, Voswinckel R, Fink L, Scheed A, Ritter C, Dahal BK, Vater A, Klussmann S, Ghofrani HA, Weissmann N, Klepetko W, Banat GA, Seeger W, Grimminger F, Schermuly RT. Immune and inflammatory cell involvement in the pathology of idiopathic pulmonary arterial hypertension. *American journal of respiratory and critical care medicine* 2012: 186(9): 897-908.
16. Voelkel NF, Tamosiuniene R, Nicolls MR. Challenges and opportunities in treating inflammation associated with pulmonary hypertension. *Expert review of cardiovascular therapy* 2016: 14(8): 939-951.
17. Meloche J, Renard S, Provencher S, Bonnet S. Anti-inflammatory and immunosuppressive agents in PAH. *Handbook of experimental pharmacology* 2013: 218: 437-476.
18. Majka S, Hagen M, Blackwell T, Harral J, Johnson JA, Gendron R, Paradis H, Crona D, Loyd JE, Nozik-Grayck E, Stenmark KR, West J. Physiologic and molecular consequences of endothelial Bmpr2 mutation. *Respiratory research* 2011: 12: 84.
19. Xiong J. BMPR2 spruces up the endothelium in pulmonary hypertension. *Protein & cell* 2015: 6(10): 703-708.
20. Kurakula K, Hamers AA, de Waard V, de Vries CJ. Nuclear Receptors in atherosclerosis: a superfamily with many 'Goodfellas'. *Molecular and cellular endocrinology* 2013: 368(1-2): 71-84.
21. Kurakula K, Hamers AA, van Loenen P, de Vries CJ. 6-Mercaptopurine reduces cytokine and Muc5ac expression involving inhibition of NFkappaB activation in airway epithelial cells. *Respiratory research* 2015: 16: 73.
22. Kurakula K, Koenis DS, van Tiel CM, de Vries CJ. NR4A nuclear receptors are orphans but not lonesome. *Biochimica et biophysica acta* 2014: 1843(11): 2543-2555.

23. Kurakula K, van der Wal E, Geerts D, van Tiel CM, de Vries CJ. FHL2 protein is a novel co-repressor of nuclear receptor Nur77. *The Journal of biological chemistry* 2011: 286(52): 44336-44343.
24. Kurakula K, Vos M, Logiantara A, Roelofs JJ, Nieuwenhuis MA, Koppelman GH, Postma DS, van Rijt LS, de Vries CJ. Nuclear Receptor Nur77 Attenuates Airway Inflammation in Mice by Suppressing NF-kappaB Activity in Lung Epithelial Cells. *Journal of immunology (Baltimore, Md : 1950)* 2015: 195(4): 1388-1398.
25. Medzikovic L, Schumacher CA, Verkerk AO, van Deel ED, Wolswinkel R, van der Made I, Bleeker N, Cakici D, van den Hoogenhof MM, Meggouh F, Creemers EE, Remme CA, Baartscheer A, de Winter RJ, de Vries CJ, Arkenbout EK, de Waard V. Orphan nuclear receptor Nur77 affects cardiomyocyte calcium homeostasis and adverse cardiac remodelling. *Scientific reports* 2015: 5: 15404.
26. Qin Q, Chen M, Yi B, You X, Yang P, Sun J. Orphan nuclear receptor Nur77 is a novel negative regulator of endothelin-1 expression in vascular endothelial cells. *Journal of molecular and cellular cardiology* 2014: 77: 20-28.
27. You B, Jiang YY, Chen S, Yan G, Sun J. The orphan nuclear receptor Nur77 suppresses endothelial cell activation through induction of IkappaBalpha expression. *Circulation research* 2009: 104(6): 742-749.
28. Nie X, Tan J, Dai Y, Mao W, Chen Y, Qin G, Li G, Shen C, Zhao J, Chen J. Nur77 downregulation triggers pulmonary artery smooth muscle cell proliferation and migration in mice with hypoxic pulmonary hypertension via the Axin2-beta-catenin signaling pathway. *Vascular pharmacology* 2016: 87: 230-241.
29. Liu Y, Zhang J, Yi B, Chen M, Qi J, Yin Y, Lu X, Jasmin JF, Sun J. Nur77 suppresses pulmonary artery smooth muscle cell proliferation through inhibition of the STAT3/Pim-1/NFAT pathway. *American journal of respiratory cell and molecular biology* 2014: 50(2): 379-388.
30. Palumbo-Zerr K, Zerr P, Distler A, Fliehr J, Mancuso R, Huang J, Mielenz D, Tomcik M, Furnrohr BG, Scholtysek C, Dees C, Beyer C, Kronke G, Metzger D, Distler O, Schett G, Distler JH. Orphan nuclear receptor NR4A1 regulates transforming growth factor-beta signaling and fibrosis. *Nature medicine* 2015: 21(2): 150-158.
31. Zhou F, Drabsch Y, Dekker TJ, de Vinuesa AG, Li Y, Hawinkels LJ, Sheppard KA, Goumans MJ, Luwor RB, de Vries CJ, Mesker WE, Tollenaar RA, Devilee P, Lu CX, Zhu H, Zhang L, Dijke PT. Nuclear receptor NR4A1 promotes breast cancer invasion and metastasis by activating TGF-beta signalling. *Nature communications* 2014: 5: 3388.
32. Domenech E, Nos P, Papo M, Lopez-San Roman A, Garcia-Planella E, Gassull MA. 6-mercaptopurine in patients with inflammatory bowel disease and previous digestive intolerance of azathioprine. *Scandinavian journal of gastroenterology* 2005: 40(1): 52-55.
33. Marinkovic G, Kroon J, Hoogenboezem M, Hoeben KA, Ruiter MS, Kurakula K, Otermin Rubio I, Vos M, de Vries CJ, van Buul JD, de Waard V. Inhibition of GTPase Rac1 in endothelium by 6-mercaptopurine results in immunosuppression in nonimmune cells: new target for an old drug. *Journal of immunology (Baltimore, Md : 1950)* 2014: 192(9): 4370-4378.

34. Weigel G, Griesmacher A, DeAbreu RA, Wolner E, Mueller MM. Azathioprine and 6-mercaptopurine alter the nucleotide balance in endothelial cells. *Thrombosis research* 1999: 94(2): 87-94.
35. Pires NM, Pols TW, de Vries MR, van Tiel CM, Bonta PI, Vos M, Arkenbout EK, Pannekoek H, Jukema JW, Quax PH, de Vries CJ. Activation of nuclear receptor Nur77 by 6-mercaptopurine protects against neointima formation. *Circulation* 2007: 115(4): 493-500.
36. Szulcek R, Happe CM, Rol N, Fontijn RD, Dickhoff C, Hartemink KJ, Grunberg K, Tu L, Timens W, Nossent GD, Paul MA, Leyen TA, Horrevoets AJ, de Man FS, Guignabert C, Yu PB, Vonk-Noordegraaf A, van Nieuw Amerongen GP, Bogaard HJ. Delayed Microvascular Shear Adaptation in Pulmonary Arterial Hypertension. Role of Platelet Endothelial Cell Adhesion Molecule-1 Cleavage. *American journal of respiratory and critical care medicine* 2016: 193(12): 1410-1420.
37. Long L, Ormiston ML, Yang X, Southwood M, Graf S, Machado RD, Mueller M, Kinzel B, Yung LM, Wilkinson JM, Moore SD, Drake KM, Aldred MA, Yu PB, Upton PD, Morrell NW. Selective enhancement of endothelial BMPR-II with BMP9 reverses pulmonary arterial hypertension. *Nature medicine* 2015: 21(7): 777-785.
38. da Silva Goncalves Bos D, Van Der Bruggen CE, Kurakula K, Sun XQ, Casali KR, Casali AG, Rol N, Szulcek R, Dos Remedios C, Guignabert C, Tu L, Dorfmuller P, Humbert M, Wijnker PJM, Kuster DWD, van der Velden J, Goumans MJ, Bogaard HJ, Vonk-Noordegraaf A, de Man FS, Handoko ML. Contribution of Impaired Parasympathetic Activity to Right Ventricular Dysfunction and Pulmonary Vascular Remodeling in Pulmonary Arterial Hypertension. *Circulation* 2017.
39. de Raaf MA, Kroeze Y, Middelman A, de Man FS, de Jong H, Vonk-Noordegraaf A, de Korte C, Voelkel NF, Homberg J, Bogaard HJ. Serotonin transporter is not required for the development of severe pulmonary hypertension in the Sugen hypoxia rat model. *Am J Physiol Lung Cell Mol Physiol* 2015: 309(10): L1164-1173.
40. Korchynskyi O, ten Dijke P. Identification and functional characterization of distinct critically important bone morphogenetic protein-specific response elements in the Id1 promoter. *The Journal of biological chemistry* 2002: 277(7): 4883-4891.
41. Zhan Y, Du X, Chen H, Liu J, Zhao B, Huang D, Li G, Xu Q, Zhang M, Weimer BC, Chen D, Cheng Z, Zhang L, Li Q, Li S, Zheng Z, Song S, Huang Y, Ye Z, Su W, Lin SC, Shen Y, Wu Q. Cytosporone B is an agonist for nuclear orphan receptor Nur77. *Nature chemical biology* 2008: 4(9): 548-556.
42. Taraseviciene-Stewart L, Kasahara Y, Alger L, Hirth P, Mc Mahon G, Waltenberger J, Voelkel NF, Tuder RM. Inhibition of the VEGF receptor 2 combined with chronic hypoxia causes cell death-dependent pulmonary endothelial cell proliferation and severe pulmonary hypertension. *FASEB journal : official publication of the Federation of American Societies for Experimental Biology* 2001: 15(2): 427-438.
43. Huo Y, Yi B, Chen M, Wang N, Chen P, Guo C, Sun J. Induction of Nur77 by hyperoside inhibits vascular smooth muscle cell proliferation and neointimal formation. *Biochemical pharmacology* 2014: 92(4): 590-598.

44. Deng Z, Morse JH, Slager SL, Cuervo N, Moore KJ, Venetos G, Kalachikov S, Cayanis E, Fischer SG, Barst RJ, Hodge SE, Knowles JA. Familial primary pulmonary hypertension (gene PPH1) is caused by mutations in the bone morphogenetic protein receptor-II gene. *American journal of human genetics* 2000: 67(3): 737-744.
45. van der Bruggen CE, Happe CM, Dorfmuller P, Trip P, Spruijt OA, Rol N, Hoevenaars FP, Houweling AC, Girerd B, Marcus JT, Mercier O, Humbert M, Handoko ML, van der Velden J, Vonk Noordegraaf A, Bogaard HJ, Goumans MJ, de Man FS. Bone Morphogenetic Protein Receptor Type 2 Mutation in Pulmonary Arterial Hypertension: A View on the Right Ventricle. *Circulation* 2016: 133(18): 1747-1760.
46. Yin Y, Wu X, Yang Z, Zhao J, Wang X, Zhang Q, Yuan M, Xie L, Liu H, He Q. The potential efficacy of R8-modified paclitaxel-loaded liposomes on pulmonary arterial hypertension. *Pharmaceutical research* 2013: 30(8): 2050-2062.

SUPPLEMENTAL FIGURES

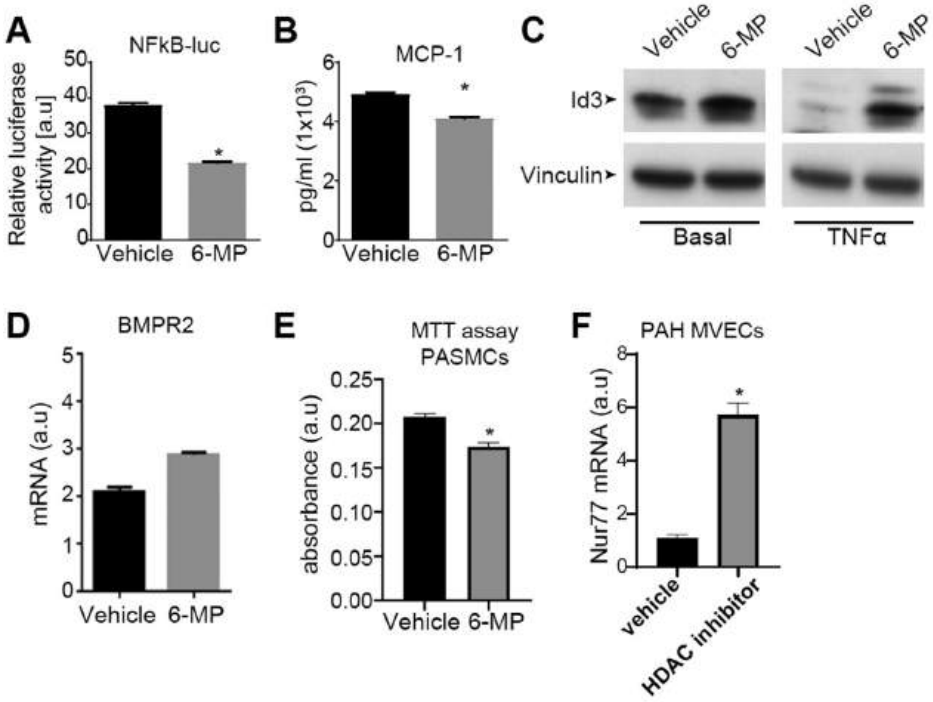

Supplement Figure 1: 6-MP decreases inflammation and enhances BMP signaling.
(A) NFKB-luciferase activity in HEK293T cells was measured following treatment with 6-MP (10 μM) and stimulation with TNFα (50 ng/mL) for 6 h (n=3). (B) ELISA for MCP-1 was performed in supernatants from MVECs following treatment with 6-MP (10 μM) and stimulation with TNFα (50 ng/mL) for 6 h (n=3). (C) Representative western blots showing Id3 relative to vinculin as loading control under basal and TNFα (50 ng/mL) stimulation and TNFα (50 ng/mL) and 6-MP (10 μM) treatment for 6 h. (D) qRT-PCR was performed to assess mRNA expression of BMPR2 following treatment with 6-MP (10 μM) for 6 h (n=3). (E) MTT assays were performed to assess proliferation of healthy human PASMCs following treatment with 6-MP for 24 h (n=3). (F) HDAC inhibition significantly increased mRNA levels of Nur77 after treatment of PAH MVECs with HDAC inhibitor Quisinostat (5 μM) for 16 h (n=3). *p<0.05. Student's t-tests were used for comparisons between two groups. Error bars, mean ± SEM.

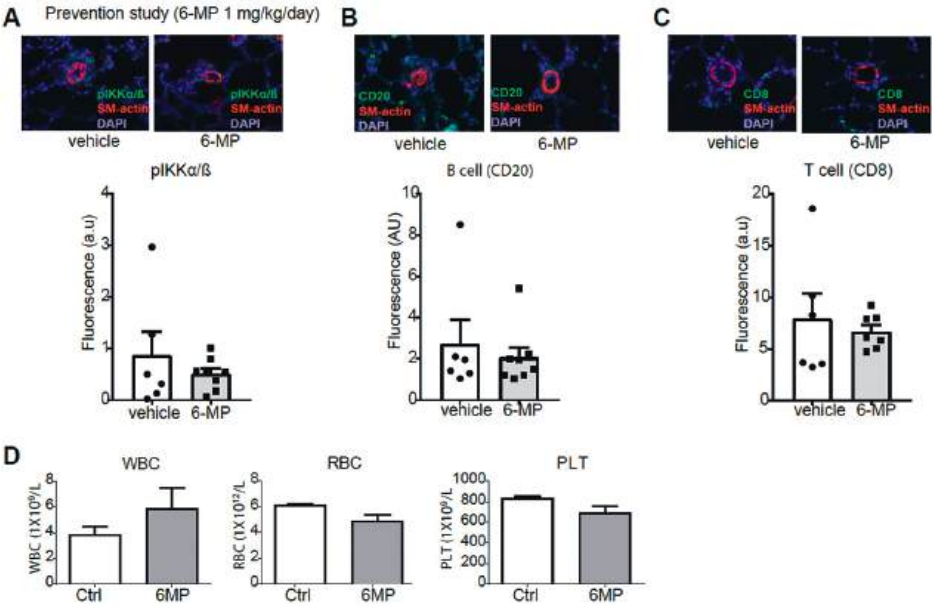

Supplement Figure 2: 6-MP prevents inflammation and does not change blood cell composition in the prevention study.

(A-C) Immunofluorescent staining for pIKKα/β (green) (A), CD20 (green) (B) and CD8 (green) (C) in small pulmonary arteries from vehicle and 6-MP treated rats. SM-actin (red) and nuclei (DAPI) were co-stained with pIKKα/β, or CD20 or CD8. Quantification of the fluorescence is shown next to the images. The images are representative of n = 6-8 lungs per group. (D) White-blood cells, red-blood cells and platelets were counted using coulter counter after terminating the rats in the prevention study. *p<0.05. Student's t-tests were used for comparisons between two groups. Error bars, mean ± SEM.

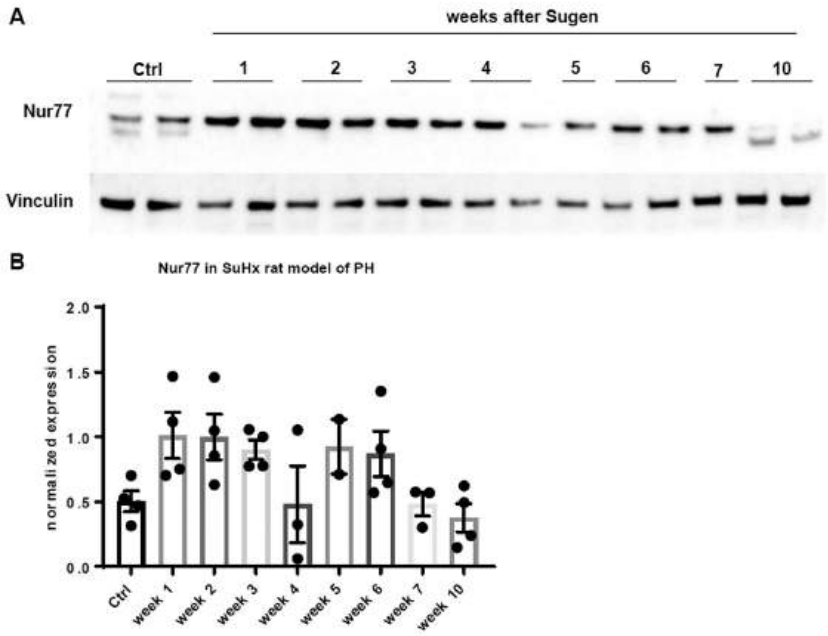

Supplement Figure 3: Nur77 expression levels during disease progression in SuHx rat model of PH. (A-B) Representative western blot (A) and relative densitometry analyses of western blot (B) of Nur77 lung tissue from the SuHx rat model at different time points. Vinculin served as a loading control and used for normalization.

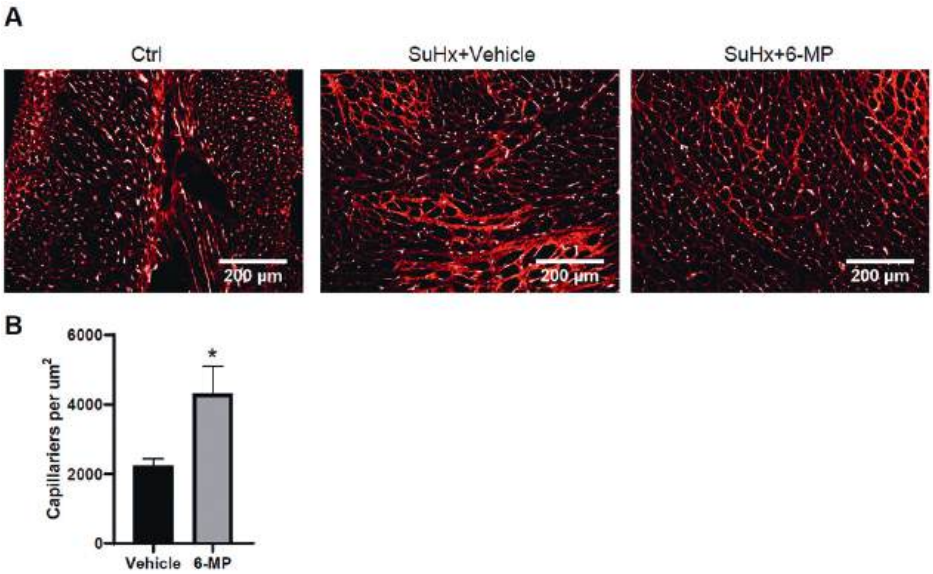

Supplement Figure 4: 6-mp enhances RV capillary density in SuHx model of PH in the reversal study. (A) Representative immunofluorescence photomicrographs of PECAM-a (white) and Wheat Germ Agglutinin (WGA, red) in the RV of control, SuHx and 6-MP treated animals (reversal study; n=5-6 per group). (B) Number of PECAM-a positive capillaries were quantified using Image J software.

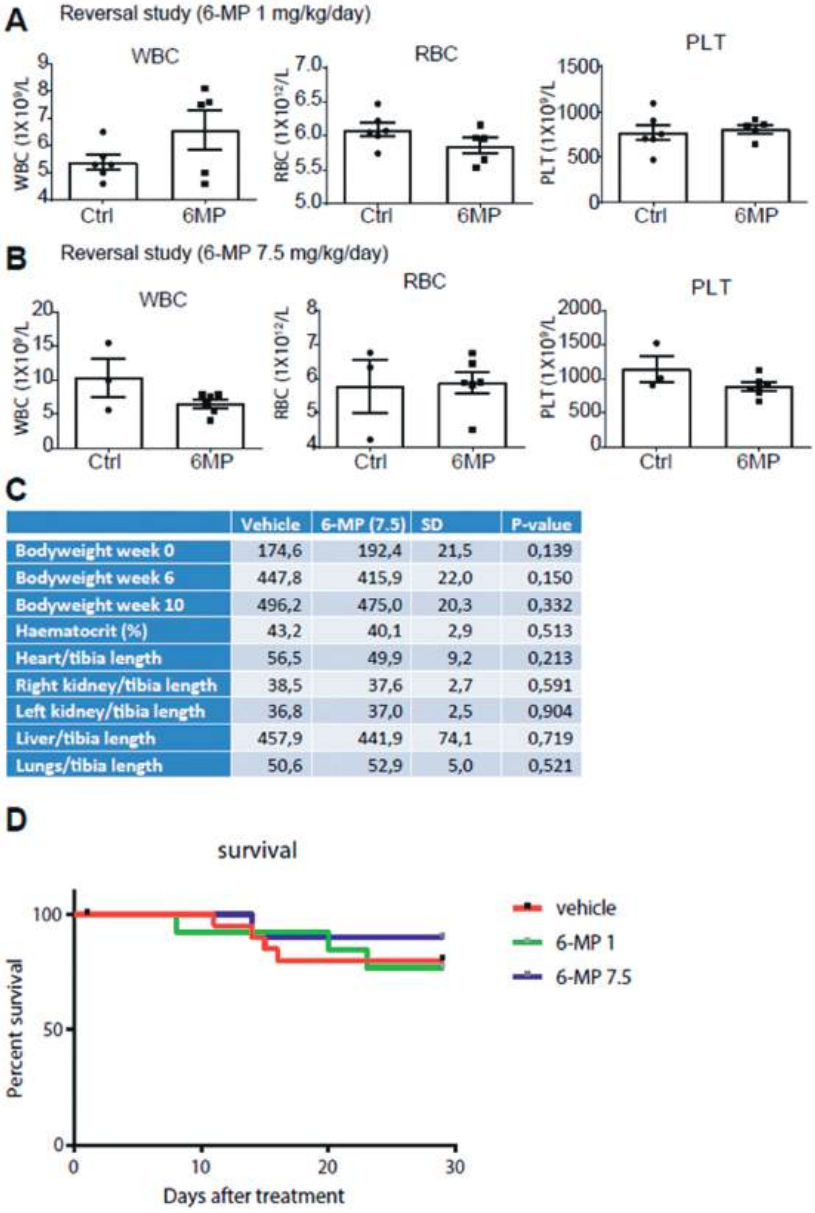

	Vehicle	6-MP (7.5)	SD	P-value
Bodyweight week 0	174,6	192,4	21,5	0,139
Bodyweight week 6	447,8	415,9	22,0	0,150
Bodyweight week 10	496,2	475,0	20,3	0,332
Haematocrit (%)	43,2	40,1	2,9	0,513
Heart/tibia length	56,5	49,9	9,2	0,213
Right kidney/tibia length	38,5	37,6	2,7	0,591
Left kidney/tibia length	36,8	37,0	2,5	0,904
Liver/tibia length	457,9	441,9	74,1	0,719
Lungs/tibia length	50,6	52,9	5,0	0,521

Supplementary Figure 5: 6-MP does not effect on blood cell composition, and improves survival in the reversal study *in vivo*.

(A-B) White-blood cells, red-blood cells and platelets were counted using coulter counter after terminating the rats in both the 6-MP 1 mg/kg/day (A) and 7.5 mg/kg/day (B) reversal study. (C) Autopsy data from the 6-MP 7.5 mg/kg/day reversal study. (D) Therapeutic dose of 6-MP (7.5 mg/kg/day) improved the survival of experimentally induced PH rats. *p<0.05. Student's t-tests were used for comparisons between two groups. Multiple comparisons were assessed by one-way ANOVA, followed by Bonferroni post-hoc test. Error bars, mean ± s.e.m.

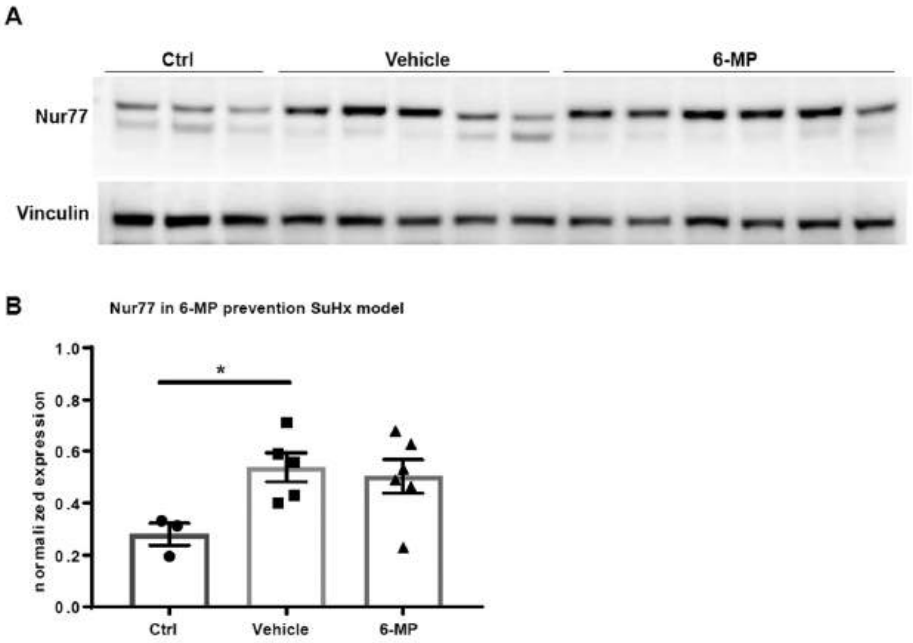

Supplementary Figure 6: The expression levels of Nur77 in the SuHx rat model of angioproliferative PH.

A-B) Representative western blot (A) and relative densitometric analyses of western blot (B) of Nur77 in total lung lysates form control, vehicle and 6-MP prevention study was performed (time point 6 weeks). Vinculin served as a loading control and used for normalization.

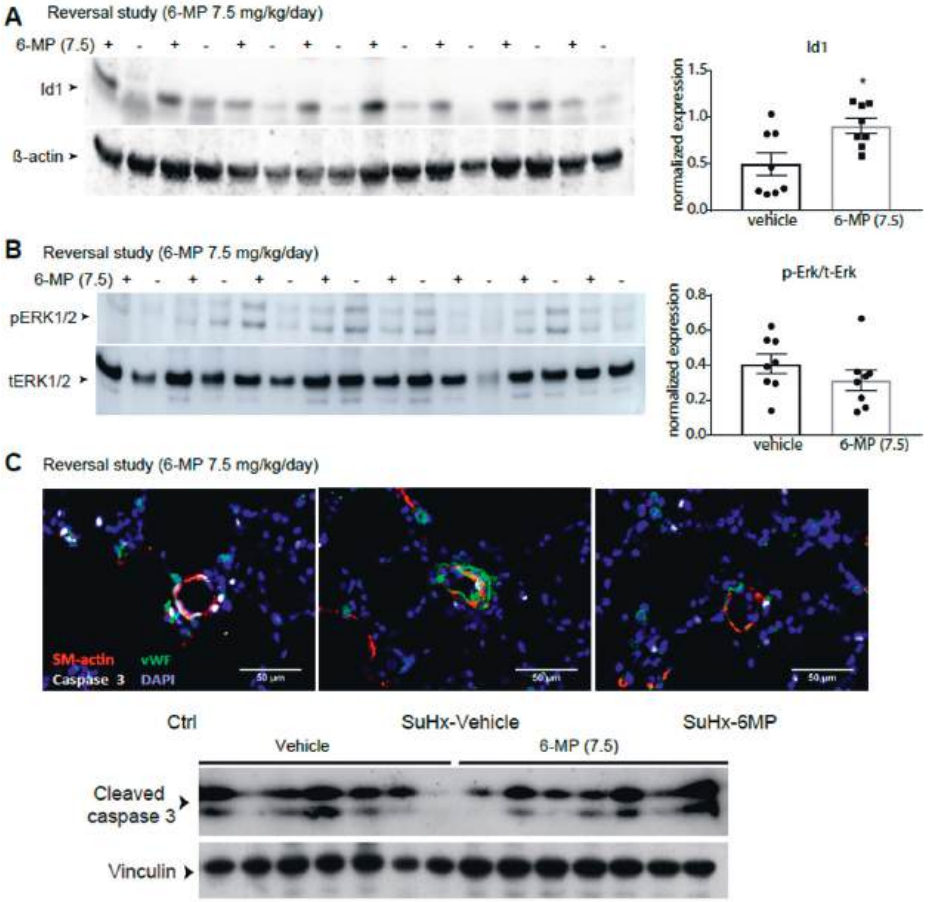

Supplementary Figure 7: 6-MP enhances Id1 expression, but has no significant effect on pERK1/2 and caspase activation.

A-B) Western blots of lung lysates from therapeutic dose of 6-MP reversal study. Relative densitometric analyses showing Id1 **(A)** and pERK1/2 **(B)** relative to β-actin and total ERK1/2, respectively (n=8). *p<0.05. Multiple comparisons were assessed by one-way ANOVA, followed by Bonferroni post-hoc test. Error bars, mean ± s.e.m. **(C)** Representative immunofluorescence photomicrographs of Caspase 3 (white), α-smooth muscle actin (SM-actin, red), and Von Willebrand factor (vWF, green) in the lungs from 6-MP reversal study. DAPI (blue) (upper panel). Western blots of lung lysates from therapeutic dose of 6-MP reversal study for cleaved caspase 3 (lower panel).

SUPPLEMENTAL MATERIAL AND METHODS

Human lung samples and cell culture

Control lung tissues and pulmonary arteries were obtained from patients undergoing surgery for lung carcinoma (control). Samples were obtained distant from the malignant lesion and were dissected by a pathologist. Lung tissues and pulmonary arteries were also obtained from iPAH and HPAH-patients undergoing lung transplantation. Lung sample collection was approved by the local ethics committees and written informed consent was obtained. Isolation and culturing of human pulmonary microvascular endothelial cells (MVECs) from lungs of control and PAH patients was described previously [1]. PA-SMCs were isolated and cultured from control donors and described elsewhere [2]. Briefly, SMCs were isolated using the explant technique and used at passage 6 to 8 and were characterized by SM α-actin expression showing uniform fibrillar staining. MVECs from 6 control subjects, 6 iPAH subjects, and 6 HPAH subjects were studied. HEK293T cells were cultured in Dulbecco's modified Eagle's medium (DMEM) with 20 mM glucose, supplemented with 10% serum and penicillin-streptomycin (Invitrogen).

Plasmids and chemicals

Nur77 over-expression plasmids, luciferase reporter constructs: BMP response element (BRE)-luc, CyclinD1-luc, NurRE-luc and NFκB-luc have been described before [3-6]. TNFα and BMP9 were purchased from Peprotech and R&D systems, respectively.

Western blot

Cell lysates were prepared with NP-40 lysis buffer and western blotting was performed as described before [6]. Briefly, cell lysates were resolved by SDS-PAGE, and transferred to polyvinylidene difluoride (PVDF) membranes (Millipore). Blots were blocked with 5% nonfat milk in PBS with 0.1% Tween 20 (PBST) and then developed with diluted antibodies for pSmad1 (1:1000 dilution; pS1 antibody [7]), Nur77 (1:1000 dilution; Abcam), and vinculin (1:1000 dilution; H300; Santa Cruz) at 4°C overnight, followed by horseradish peroxidase-conjugated anti-mouse or anti-rabbit (GE Healthcare) secondary antibodies using an ECL system (Fisher Scientific). Lung tissue of the rats was homogenized in radioimmunoprecipitation assay (RIPA) buffer containing phosphatase and protease inhibitors (Sigma-Aldrich). The protein concentration was quantified by the Pierce 660 nm

protein assay kit (Thermo Scientific). 20 µg protein was used to detect the expression of BMPR2 (1:1000; MA5-15827, Thermo Fisher), phospho-smad1/5/8 (1:1000; 13820, cell signaling) and Id1 (1:500; sc-488, Santa Cruz), and vinculin as loading control (1:1000 dilution; H300; Santa Cruz) at 4°C overnight, followed by appropriate secondary antibody incubation.

Transient transfection and luciferase assays

HEK293T cells were transiently transfected with indicated luciferase reporter plasmids and Nur77 using PEI transfection reagent (Polysciences), following the recommendations of the manufacturer. Primary MVECs were transfected using TransfeX reagent (ATCC) as per the instructions of the manufacturer. β-galactosidase plasmid was co-transfected as an internal control. 48 hours after transfection, the cells were harvested and lysed for measuring the luciferase activity using luciferase reporter assay system from Promega by a Perkin Elmer luminometer Victor3 1420. The amount of plasmid DNA in each well was equalized with an empty vector when necessary and each experiment (in duplicate) was repeated at least three times.

Quantitative Real Time-PCR (qRT-PCR)

Total RNA extraction was performed using NucleoSpin RNA II (Machery Nagel, Düren). cDNA synthesis was performed with iScript (Bio-Rad), followed by real-time PCR using the SYBR Green (Bio-Rad) and a Bio-Rad CFX Connect device. Primers used for real-time PCR are detailed in supplementary table 1. GAPDH served as a control for the amount of cDNA present in each sample. Data were analyzed using the comparative difference in cycle number (ΔCT) method according to the manufacturer's instructions.

Lenti-viral transduction

Recombinant lentiviral particles of overexpression of Nur77 and short hairpin RNAs (shRNAs) targeting Nur77 were produced, concentrated, and titrated as described previously [4]. Five different human shRNAs that target different regions in the Nur77 mRNA were tested and two shRNAs were chosen for generation of lentiviruses based on the efficiency of the knockdown. Lentiviral infection in cultured MVECs was performed as described previously [4]. Transduction efficiency was determined by immunofluorescence, qRT-PCR and western blot.

Cell viability and proliferation assays

3-(4,5-dimethyl-2-thiazolyl)-2,5-diphenyl-2H-tetrazolium bromide (MTT) assays were performed as described previously [3]. Briefly, cells were seeded in a 96-well plate at a density of 3×103 cells/well and incubated overnight. Cells were made quiescent by incubation in medium without FCS for 6 h and then incubated overnight with FCS (10% [vol/vol]) for 24 h. After the incubation, cells were incubated with 10 µl of MTT reagent (5 mg/ml) for 3 h at 37°C. 100 µl of isopropanol was added to each well and incubated for 15 min. Colorimetric analysis was performed with an enzyme-linked immunosorbent assay (ELISA) plate reader. Cells were also counted using an automated cell counter (Biorad). Each experiment (in quadruplicate) was repeated at least three times.

SuHx rat model of pulmonary hypertension (PH)

Male Sprague-Dawley rats (bodymass ≈150-220 gr; Charles River) were used throughout the experiment. Rats were housed in standard conditions and food and water was available ad libitum. SU5416+Hypoxia (SuHx)-mediated PH was induced according to previously published protocols [8, 9]. Briefly, rats were subjected to a single injection of SU5416 (25 mg/kg, Tocris Bioscience) followed by a 4-week transient exposure to 10% hypoxia and 2 week normoxic re-exposure. In the prevention study, rats received 6-MP (1 mg/kg/day) in drinking water from day 0 to day 42. In the reversal study, after randomization (treatment vs vehicle), animals were divided into two groups receiving 6-MP (1 mg/kg/day or 7.5 mg/kg/day, Sigma–Aldrich) or vehicle (DMSO) in the drinking water from day 42 to day 70. Echocardiography was performed before and after the treatment to study cardiac function. At the end of the experiment (day 42 or day 70) rats were anaesthetized for hemodynamic assessment via RV catheterization, after which rats were exsanguinated. Both lung and cardiac tissues were separated for further analysis. All experiments were approved by an independent local animal ethic committee of the Free university medical center, Amsterdam

(study number VU-FYS 13-01A4), and were carried out in compliance with guidelines issued by the Dutch government.

Echocardiography

All animals underwent echocardiographic assessments (Prosound SSD-4000 and UST-5542) as published previously [9], to measure RV wall thickness (RVWT), RV end diastolic diameter (RVEDD), tricuspid annular plane systolic excursion (TAPSE), stroke

volume (SV), heart rate (HR), cardiac output (CO), pulmonary artery acceleration time (PAAT), and cycle length (cl) before and after the treatment, respectively.

Hemodynamic evaluation and RV hypertrophy

Animals were anaesthetized for open-chest RV catheterization (AD Instruments and Millar Instruments) as previously described [8]. RV systolic pressure (RVSP) was determined from steady state measurement, as well as RV afterload (Ea-Arterial elastance). Pressure-volume loops after vena-cava occlusion were obtained and used to derive end-systolic elastance (Ees), and end-diastolic elastance (Eed). Arterial ventricular coupling was calculated as Ees/Ea.

Morphometry of heart and lungs

To assess the extent of RV hypertrophy, the heart was removed and the RV free wall was separated from the left ventricle (LV) and ventricular septum. Wet weights of the RV, free LV and septum were determined separately, and the ratio of RV weight to LV plus septum weight (RV/[LV+S]) was calculated for RV hypertrophy. At the end of experiment, lungs were inflated with an 1% solution of low-melt-agarose and fixed in formalin (overnight) and embedded in paraffin. To determine the pulmonary vascular remodelling, paraffin embedded 5-µm-thick lung sections were stained with Elastica van Giesson to measure the relative wall thickness of pulmonary arterioles (PA), as well as the intimal and medial wall thickness separately, as described previously [8, 9]. The relative wall thickness of PA was calculated as: PA wall thickness = 2* medial wall thickness / outer diameter *100%. For further analysis of RV dimensions, 5-µm-thick sections of frozen cardiac tissues (transversally cut) were stained with haematoxylin and eosin, and a mean cardiomyocyte cross-sectional area (CSA) was assessed. Moreover, picrosirius red staining was used to assess the degree of fibrosis in cardiac cryosections. Level of fibrosis was expressed as the percentage of tissue area positive for collagen compared to total area.

Immunofluorescence microscopy

Human and rat lung tissues were fixed and stained as previously described [10]. Briefly, paraffin sections were deparaffinized and rehydrated. Sections were boiled for 40 min in Vector® Antigen Unmasking Solution (Vector) using a pressure cooker. After blocking with 1% BSA in 0.1% Tween-PBS, sections were incubated overnight at 4°C with primary antibodies directed against Nur77 (1:50; sc-5569, Santa Cruz), Von Willebrand factor (1:1000, Abcam), and alpha smooth muscle actin (1:5000; Sigma). All sections were

mounted with ProLong® Gold antifade reagent (Invitrogen) containing DAPI. For the analyses of pulmonary vascular proliferation, 5-µm-thick lung paraffin sections were incubated at 40C overnight with primary Ki67 antibody (1:100; AB9260, EMD Millipore). To determine the pulmonary vascular inflammation, the lung sections were incubated at 40C overnight with primary CD68 (1:1000; ab31630, Abcam), CD20 (1:1000; sc-7735, Santa Cruz) and CD8-antibodies (1:500; ab33786, Abcam) to detect macrophages, B cells and cytotoxic T cells, respectively. Moreover, to analyze the effect of 6-MP on Nur77 and BMP signalling, the following antibodies were used: Nur77 (1:50; sc-5569, Santa Cruz), BMPR2 (1:25; PA5-11863, Thermo Fisher), p-smad1/5/8 (1:2000; 13820, Cell signalling), Cleaved caspase 3 (1:400; 9661; Cell signaling) and Id3 (1:400; sc-490, Santa Cruz). DAPI was used to counterstain the nuclei.

Statistical analysis

Statistical analyses were performed using Graphpad Prism 7 for Windows (GraphPad Software). Student's t-tests were used for comparisons between two groups. Multiple comparisons were assessed by one-way ANOVA, followed by Bonferroni post-hoc test. p-values < 0.05 were considered significant. All statistical tests used two-sided tests of significance. Data are presented as mean ± SEM.

Supplementary Table 1: Human primer sequences for qRT-PCR

Gene	Primers
IL-6	Fw: CCCACACAGACAGCCACTCA
	Rv: CCGTCGAGGATGTACCGAAT
RANTES	Fw: CGCTGTCATCCTCATTGCTA
	Rv: TGTACTCCCGAACCCATTTC
TNF-α	Fw: AGGACACCATGAGCACTGAAAG
	Rv: AGGAGAGGCTGAGGAACAAG
IL-1β	Fw: TGGCAGAAAGGGAACAGAAAGG
	Rv: GTGAGTAGGAGAGGTGAGAGAGG
Nur77	Fw: GTTCTCGGAGGTCATCCGCAAG
	Rv: GCAGGGACCTTGAGAAGGCCA
BMPR2	Fw: AACTGTTGGSGCTGATTGGC
	Rv: CGGTTTGCAAAGGAAAACAC
Id1	Fw: CTGCTCTACGACATGAACGG
	Rv: GAAGGTCCCTGATGTAGTCGAT
Id3	Fw: CACCTCCAGAACGCAGGTGCTG
	Rv: AGGGCGAAGTTGGGGCCCAT
GAPDH	Fw: AGCCACATCGCTCAGACAC
	Rv: GCCCAATACGACCAAATCC

REFERENCES

1. Szulcek R, Happe CM, Rol N, Fontijn RD, Dickhoff C, Hartemink KJ, Grunberg K, Tu L, Timens W, Nossent GD, Paul MA, Leyen TA, Horrevoets AJ, de Man FS, Guignabert C, Yu PB, Vonk-Noordegraaf A, van Nieuw Amerongen GP, Bogaard HJ. Delayed Microvascular Shear Adaptation in Pulmonary Arterial Hypertension. Role of Platelet Endothelial Cell Adhesion Molecule-1 Cleavage. American journal of respiratory and critical care medicine 2016: 193(12): 1410-1420.
2. Long L, Ormiston ML, Yang X, Southwood M, Graf S, Machado RD, Mueller M, Kinzel B, Yung LM, Wilkinson JM, Moore SD, Drake KM, Aldred MA, Yu PB, Upton PD, Morrell NW. Selective enhancement of endothelial BMPR-II with BMP9 reverses pulmonary arterial hypertension. Nature medicine 2015: 21(7): 777-785.
3. Kurakula K, Hamers AA, van Loenen P, de Vries CJ. 6-Mercaptopurine reduces cytokine and Muc5ac expression involving inhibition of NFkappaB activation in airway epithelial cells. Respiratory research 2015: 16: 73.
4. Kurakula K, van der Wal E, Geerts D, van Tiel CM, de Vries CJ. FHL2 protein is a novel co-repressor of nuclear receptor Nur77. The Journal of biological chemistry 2011: 286(52): 44336-44343.
5. Korchynskyi O, ten Dijke P. Identification and functional characterization of distinct critically important bone morphogenetic protein-specific response elements in the Id1 promoter. The Journal of biological chemistry 2002: 277(7): 4883-4891.
6. Kurakula K, Vos M, Otermin Rubio I, Marinkovic G, Buettner R, Heukamp LC, Stap J, de Waard V, van Tiel CM, de Vries CJ. The LIM-only protein FHL2 reduces vascular lesion formation involving inhibition of proliferation and migration of smooth muscle cells. PloS one 2014: 9(4): e94931.
7. Persson U, Izumi H, Souchelnytskyi S, Itoh S, Grimsby S, Engstrom U, Heldin CH, Funa K, ten Dijke P. The L45 loop in type I receptors for TGF-beta family members is a critical determinant in specifying Smad isoform activation. FEBS letters 1998: 434(1-2): 83-87.
8. da Silva Goncalves Bos D, Van Der Bruggen CE, Kurakula K, Sun XQ, Casali KR, Casali AG, Rol N, Szulcek R, Dos Remedios C, Guignabert C, Tu L, Dorfmuller P, Humbert M, Wijnker PJM, Kuster DWD, van der Velden J, Goumans MJ, Bogaard HJ, Vonk-Noordegraaf A, de Man FS, Handoko ML. Contribution of Impaired Parasympathetic Activity to Right Ventricular Dysfunction and Pulmonary Vascular Remodeling in Pulmonary Arterial Hypertension. Circulation 2017.
9. de Raaf MA, Kroeze Y, Middelman A, de Man FS, de Jong H, Vonk-Noordegraaf A, de Korte C, Voelkel NF, Homberg J, Bogaard HJ. Serotonin transporter is not required for the development of severe pulmonary hypertension in the Sugen hypoxia rat model. Am J Physiol Lung Cell Mol Physiol 2015: 309(10): L1164-1173.
10. Duim SN, Kurakula K, Goumans MJ, Kruithof BP. Cardiac endothelial cells express Wilms' tumor-1: Wt1 expression in the developing, adult and infarcted heart. Journal of molecular and cellular cardiology 2015: 81: 127-135.

CHAPTER 4

MnTBAP reverses pulmonary vascular remodeling and improves cardiac function in experimental pulmonary arterial hypertension

Maria Catalina Gomez-Puerto [1,†], Xiao-Qing Sun [2,†], Ingrid Schalij [2], Mar Orriols [1], Xiaoke Pan [2], Robert Szulcek [2], Marie-José Goumans [1], Harm-Jan Bogaard [2,*], Qian Zhou [3,‡] and Peter ten Dijke [1,‡]

[1] Dept. of Cell and Chemical Biology and Oncode Institute, Leiden University Medical Center, 2300 RC, Leiden, The Netherlands; M.C.Gomez_Puerto@lumc.nl (M.C.G.-P.); marorriols@gmail.com (M.O.); M.J.T.H.Goumans@lumc.nl (M.-J.G.); P.ten_Dijke@lumc.nl (P.t.D.)

[2] Dept. of Pulmonary Medicine, Amsterdam Cardiovascular Sciences, Amsterdam UMC, Vrije Universiteit Amsterdam, 1081 HZ, Amsterdam, The Netherlands; x.sun@amsterdamumc.nl (X.-Q.S.); i.schalij@amsterdamumc.nl (I.S.); x.pan@amsterdamumc.nl (X.P.); r.szulcek@amsterdamumc.nl (R.S.)

[3] Dept. of Cardiology and Angiology I, Heart Center Freiburg University, Faculty of Medicine, University of Freiburg, 79106, Freiburg, Germany

***** Correspondence: HJ.Bogaard@amsterdamumc.nl; Tel./Fax: +31-20-44-4328

† M.C.G.-P. and X.-Q.S. contributed equally to this work.

‡ Q.Z. and P.T.-D. contributed equally to this work.

Int J Mol Sci. 2020 Jun 10;21(11):4130.

ABSTRACT

Pulmonary arterial hypertension (PAH) is a life-threatening disease characterized by obstructed pulmonary vasculatures. Current therapies for PAH are limited and only alleviate symptoms. Reduced levels of BMPR2 are associated with PAH pathophysiology. Moreover, reactive oxygen species, inflammation and autophagy have been shown to be hallmarks in PAH. We previously demonstrated that MnTBAP, a synthetic metalloporphyrin with antioxidant and anti-inflammatory activity, inhibits the turn-over of BMPR2 in human umbilical vein endothelial cells. Therefore, we hypothesized that MnTBAP might be used to treat PAH. Human pulmonary artery endothelial cells (PAECs), as well as pulmonary microvascular endothelial (MVECs) and smooth muscle cells (MVSMCs) from PAH patients, were treated with MnTBAP. In vivo, either saline or MnTBAP was given to PAH rats induced by Sugen 5416 and hypoxia (SuHx). On PAECs, MnTBAP was found to increase BMPR2 protein levels by blocking autophagy. Moreover, MnTBAP increased BMPR2 levels in pulmonary MVECs and MVSMCs isolated from PAH patients. In SuHx rats, MnTBAP reduced right ventricular (RV) afterload by reversing pulmonary vascular remodeling, including both intima and media layers. Furthermore, MnTBAP improved RV function and reversed RV dilation in SuHx rats. Taken together, these data highlight the importance of MnTBAP as a potential therapeutic treatment for PAH.

Keywords: autophagy; BMPR2; MnTBAP; pulmonary arterial hypertension (PAH); human pulmonary arterial endothelial cells (PAECs); inflammation

1. INTRODUCTION

Pulmonary arterial hypertension (PAH) is a life-threatening disease characterized by obstructed pulmonary vasculature due to deregulated proliferation, migration and survival of pulmonary vascular cells (i.e., smooth muscle cells (SMCs) and endothelial cells (ECs)) for which the underlying mechanisms are not well understood [1]. Patients suffering from PAH have an increase in mean pulmonary arterial pressure leading to right ventricular (RV) failure [2]. Currently, no curative treatment is available and despite the efforts therapeutic options for PAH are limited and only alleviate symptoms [3-5]. Although rare, the disease occurs most frequently at a young age often even in childhood [6], and females have a three-fold increase in developing PAH [7]. Upon diagnosis, the average life expectancy of PAH patients is approximately 7–10 years and only lung transplantation offers any survival potential, which is not a long term solution as treatment [8].

There are different etiologies for PAH, including hereditary PAH (hPAH) and idiopathic PAH (iPAH). While both forms are clinically indistinguishable, the underlying etiology is different. hPAH is associated with inheritable genetic defects. Heterozygous germline mutations in *BMPR2,* a gene encoding the bone morphogenetic protein (BMP) type 2 receptor, are the most common causal factors in hPAH [9]. Interestingly, in both hPAH and iPAH, a reduction in BMPR2 expression in ECs has been reported [10-12]. Besides, since not all individuals carrying mutations in *BMPR2* will develop PAH, environmental factors including hypoxia and inflammation may provide local triggers for the disease [13-17].

Rescuing BMPR2 expression, function or signaling represents a promising treatment for PAH patients [18-20]. Manganese (III) tetrakis (4-benzoic acid) porphyrin (MnTBAP), a synthetic metalloporphyrin with antioxidant [21-23] and anti-inflammatory [23-26] effects, has been shown to inhibit the turn-over of BMPR2 in human umbilical vein endothelial cells (HUVECs) [25]. Moreover, MnTBAP offers beneficial effects in bleomycin-induced pulmonary fibrosis [27], carrageenan-induced pleurisy [28], lung contusion [26], renal fibrosis [29] and renal injury [24, 30].

We and others have reported that endogenous BMPR2 is degraded through the lysosome in primary human pulmonary artery endothelial (PAECs) and smooth muscle cells (PASMCs) and that autophagy activation contributes to BMPR2 degradation [12, 19, 31, 32]. In the present study, we show that partly by blocking autophagy, MnTBAP increases

BMPR2 levels in pulmonary microvascular endothelial cells (MVECs) isolated from iPAH patients. Furthermore, for the first time, we demonstrate that MnTBAP reverses experimental PAH and improves cardiac function. Taken together, these data highlight the importance of MnTBAP as a potential therapeutic treatment for PAH.

2. MATERIALS AND METHODS

2.1. Antibodies and Reagents

The following anti-human antibodies were used: mouse anti-BMPR2 (612292, recognizing the cytoplasmic domain) from BD Biosciences (Vianen, The Netherlands), mouse anti-MAP1LC3B (5F10, 0231-100, recognizing the N terminus of MAP1LC3B) from Nanotools (Teningen, Germany) and mouse anti-SQSTM1 (sc-28359, recognizing the C terminus of SQSTM1) from Santa Cruz (Heidelberg, Germany). Rabbit anti-α/β-Tubulin (#2148) was from cell signaling (Leiden, The Netherlands) and mouse anti-glyceraldehyde-3-phosphate dehydrogenase (GAPDH) (MAB374) was from Millipore (Amsterdam-Zuidoost, The Netherlands). Rabbit (W4011) and mouse (W4021) horseradish peroxidase conjugated secondary antibodies were from Promega (Leiden, The Netherlands). Bafilomycin A_1 (BafA1; B1793), cycloheximide (CHX; **01810**) were obtained from Sigma Aldrich (St. Louis, MO, USA). Manganese (III) tetrakis (4-benzoic acid) porphyrin (MnTBAP; 475870) was from Merck (Calbiochem). Tumor necrosis factor alpha (TNF-α; 300-01A) was obtained from PeproTech (London, UK).

2.2. Cell Culture

Human pulmonary artery endothelial cells (PAECs) were purchased from Lonza (CC-2530, Basel, Switzerland) and were used between passages 4 and 8. Cells were maintained in Endothelial Cell Basal Medium 2 (Promo Cell, Heidelberg, Germany, C-22211), supplemented with ECGM-2 SupplementPack (Promo Cell, Heidelberg, Germany, C-39211) containing 0.02 mL/mL FCS, 5 ng/mL hEGF, 0, 2 g/mL hydrocortisone, 10 ng/mL hbFGF, 20 ng/mL insulin-like growth factor (R^3-IGF-1), 0.5 ng/mL VEGF, 1 µg/mL Ascorbic Acid and 22.5 µg/mL heparin.

Primary human pulmonary microvascular endothelial and smooth muscle cells (MVECs and MVSMCs) were obtained from end-stage PAH patients and healthy tissues of lobectomy donors, as described before [48]. The tissue harvest and MVEC/MVSMC isolations were approved by the local ethics committees at the Amsterdam

UMC (Amsterdam, The Netherlands) and written informed consent was obtained. MVECs were cultured in complete ECM medium supplemented with 1% pen/strep, 1% endothelial cell growth supplement, and 5% FCS (ScienceCell, Uden, The Netherlands). MVSMC were cultured in Dulbecco's Modified Eagle Medium: F12 (Lonza, Basel, Switzerland, BE04-687F/U1) supplemented with 1% pen/strep and 10% FBS (ScienceCell, Uden, The Netherlands). Cell lines were routinely tested for mycoplasma contamination and only used if negative.

2.3. Western Blot Analysis

Western blot analysis was performed using standard techniques. In brief, cells were lysed in Laemmli buffer (0.12 M Tris HCl, pH 6.8, 4% SDS, 20% glycerol, 35 mM β-mercaptoethanol) and boiled for 5 min. Protein concentrations were measured using DC protein assay (Bio-Rad, 5000116). Equal amounts of total lysate were analyzed by sodium dodecyl sulfate polyacrylamide gel electrophoresis (SDS-PAGE). Proteins were transferred to polyvinylidene difluoride membrane (Millipore, Amsterdam-Zuidoost, The Netherlands, IPFL00010). Membranes were blocked with 5% non-fatty milk and incubated with the appropriate antibodies according to the manufacturer's instructions. Membranes were then washed, incubated with appropriate peroxidase-conjugated secondary antibodies and developed by ECL (Bio-Rad, 1705061).

2.4. Quantitative Real-Time PCR

Total RNA was isolated using a NucleoSpin RNA kit (Macherey Nagel, Duren, Germany, 740955) according to manufacturer's protocol. Total RNA was isolated using a NucleoSpin RNA kit (Macherey Nagel, Duren, Germany, 740955) according to manufacturer's protocol. RNA was reverse transcribed using RevertAid RT Reverse Transcription Kit (ThermoFisher Scientific, Landmeer, The Netherlands, K1691). Generated cDNA was amplified with primer pairs for the indicated gene, using the CFX Connect Real-Time PCR Detection System (Bio-Rad). GAPDH was used as housekeeping gene. Quantification was performed relative to the levels of the GAPDH and normalised to control conditions. The data analysis was performed using the $2^{-\Delta\Delta Ct}$ method1. Primer sequences: *BMPR2* forward AACTGTTGGAGCTGATTGGC reverse CGGTTTGCAAAGGAAAACAC. *GAPDH* forward AGCCACATCGCTCAGACAC reverse GCCCAATACGACCAAATCC.

2.5. Flow Cytometry Analysis

PAECs were treated with HCQ (20 μM) and MnTBAP (50 μM). Cells were then trypsinized and incubated in Endothelial Cell Basal Medium 2 (Promo Cell, Heidelberg, Germany,

C-22211), supplemented with ECGM-2 SupplementPack (Promo Cell, Heidelberg, Germany, C-39211) with Cyto-ID Autophagy Detection dye (Enzo Life Sciences, Brussels, Belgium, ENZ-51031-0050) at a dilution of 1:500 for 25 min at 37 °C. Subsequently, cells were washed and analyzed by flow cytometry. All data were analyzed using FlowJo software.

2.6. Experimental Pulmonary Arterial Hypertension

All experiments with animals were approved by an independent local animal ethic committee at Amsterdam UMC (Amsterdam, The Netherlands, study number 129-RUG18-02), and were carried out in compliance with guidelines issued by the Dutch government.

2.7. SuHx Rat Model of Pulmonary Hypertension and MnTBAP Treatment

Male Sprague-Dawley rats (n = 24; 170–210 g; Charles River, Sulzfeld, Germany) were used throughout the experiment. Rats were housed in standard conditions and food and water was available ad libitum. SU5416+Hypoxia (SuHx)-mediated PAH protocol was induced as described previously [37, 49]. Briefly, rats were subjected a single injection of SU5416 ((25 mg/kg, 3037, Tocris Bioscience, Bristol, UK) followed by a 4-week transient exposure to 10% hypoxia (Biospherix Ltd., New York, NY, USA) maintained by a nitrogen generator (Avilo, Dirksland, The Netherlands) and re-exposed to normoxia for 6 weeks. Animals were randomized at week 6 receiving either saline (SuHx) or MnTBAP 10 mg/kg (MnTBAP) by intraperitoneal injection 3 times per week for 4 weeks. This dose and frequency of MnTBAP administration were according to previous reports in mice [29]. Due to loss of rats, hemodynamic data was collected from 6 rats in SuHx group and 7 rats in MnTBAP group. As control, data of healthy male Sprague-Dawley rats were taken from a previous published study of our group as (ctrl, n = 7) [37].

2.8. Hemodynamic Measurements

Echocardiography (Prosound SSD-4000 and UST-5542; Aloka, Tokyo, Japan) was performed at the beginning and the end of the treatment to measure the cardiac function, including SV, heart rate, PAAT, cl, TAPSE, RV wall thickness and RVEDD. PAAT/cl% was used to estimate RVSP, and TPR was calculated as mean pulmonary artery pressure/cardiac output.

At the end of the experiment, rats were anaesthetized with 4% isoflurane for hemodynamic assessment via open-chest RV catheterization (Millar Instruments, Houston, TX, USA). RVSP was determined from steady state measurement, as well as Ea. Pressure–volume loops after vena-cava occlusion were obtained and used to

measure Ees and Eed. RV–arterial coupling was calculated as Ees/Ea. One out of 13 rats with hemodynamic measurement was detected to have much higher Ea than the rest. Under the circumstance that Ea is normally distributed in historical database, the Dixon outlier test was applied and it revealed that this rat—in contrast to all other individuals of the MnTBAP treated group—was characterized as a significant outlier. Based on a previous literature [50], this rat was excluded from all statistical evaluations. Analysis of echocardiography and pressure–volume loops was done blinded.

2.9. Morphometry of the Pulmonary Vasculatures

After RV catheterization, animals were exsanguinated. Lungs were collected and inflated with an 1% solution of low-melt-agarose and fixed in formalin and embedded in paraffin. To determine the pulmonary vascular remodeling, paraffin embedded 5-µm-thick lung sections were stained with Elastica van Giesson. Small pulmonary arteries were divided into three classes, based on external diameters: 0–30, 30–60 and 60–100 µm [49]. Occluded pulmonary arteries with an external diameter between 0–100 µm were counted. Media and intima wall thickness of pulmonary vasculatures classified by the external diameters, were measured and recorded separately as described previously [49], and as described in supplement Figure 2. Morphometry analysis of the pulmonary vasculatures was done blinded.

2.9.1. Immunofluorescence Staining

Rat lungs were collected and inflated with an 1% solution of low-melt-agarose and fixed in formalin and embedded in paraffin. Five micrometer-thick lung paraffin sections were deparaffinized and rehydrated. Sections were boiled for 40 min in Vector® Antigen Unmasking Solution (Vector, Burlingame, USA) using a pressure cooker. After blocking with goat serum 10% (ThermoFisher Scientific, Massachusetts, USA), sections were incubated overnight at 4 °C with primary antibodies directed against 8-OHdG (1:150; bs-1278R, Bioss Antibodies, Woburn, MA, USA), co-stained with von Willebrand factor (1:1000; ab8822, Abcam, Cambridge, UK), and alpha smooth muscle actin (1:1000; Sigma-Aldrich, St. Louis, MO, USA). All sections were mounted with ProLong® Gold antifade reagent (Invitrogen, Massachusetts, USA) containing DAPI.

2.9.2. Immunofluorescence Quantification

Images were acquired on a Marianas digital imaging microscopy workstation (Intelligent Imaging Innovations (3i), Denver, CO, USA). SlideBook imaging analysis software (SlideBook 6, 3i) was used to semi-automatically quantify the images.

Pulmonary vascular 8-OHdG mean relative fluorescence intensity was semi-automatically quantified and measured over twenty vessels.

2.10. Statistical Analysis

Statistical analysis was performed using Prism for Windows (GraphPad 8 software). Normality of data was checked with Kolmogorov-Smirnov test and either log-transformation or non-parametric test was performed if data was not normally distributed. Unpaired two-sided student's test was used to calculate statistical differences between two groups. The survival estimates were performed by log rank (Mantel-Cox) test between SuHx rats with/without MnTBAP treatment. Multiple comparisons were assessed by one-way ANOVA, followed by Bonferroni's post-hoc test. Two-way ANOVA for repeated measurements followed by Bonferroni post-hoc test was used to compare parameters collected from echocardiography. A p-value of <0.05 was considered statistically significant. Data presented as mean ± SD.

3. RESULTS

3.1. MnTBAP Increases BMPR2 Levels In Vitro by Inhibiting Autophagy

To investigate whether MnTBAP treatment increases BMPR2 protein levels in the context of PAH, primary human PAECs were treated with MnTBAP and the lysosomal inhibitor bafilomycin A1 (BafA1) as a positive control. As expected, BMPR2 levels were significantly increased after BafA1 treatment [12] (Figure 1A). Consistent with our previous findings [25], MnTBAP treatment resulted in a dose-dependent increase of BMPR2 protein levels in PAECs (Figure 1A or B). No significant differences on *BMPR2* mRNA levels were observed after MnTBAP treatment, indicating no changes at the transcriptional level (Figure 1C).

In addition, PAECs treated with MnTBAP in the presence of the protein synthesis inhibitor cycloheximide (CHX) show an increase in BMPR2, suggesting that MnTBAP mechanism of action does not depend on protein translation (Figure 2A). Since BMPR2 is degraded through the lysosomal pathway in an autophagy related fashion, we investigated whether MnTBAP could modulate autophagy. The levels of the autophagy markers microtubule associated protein 1 light chain 3 beta-II (MAP1LC3B-II) and sequestosome 1 (SQSTM1) were measured by western blotting analysis. Interestingly, both MAP1LC3B-II and SQSTM1 protein levels augmented after MnTBAP treatment

(Figure 2B). An increase in MAP1LC3B-II or SQSTM1 could be interpreted as an increase in autophagic flux or as a decrease in functional autophagy due to a block in autophagosome degradation. To elucidate whether changes in MAP1LC3B-II and SQSTM1 correspond to an increase or a block in autophagic flux, PAECs were treated with MnTBAP in combination with BafA1 to prevent lysosomal degradation and block the fusion of autophagosomes with lysosomes. PAECs treated with MnTBAP alone show similar MAP1LC3B-II and SQSTM1 levels when compared to cells treated with MnTBAP and BafA1 (Figure 2B). To validate our findings, autophagy changes were measured by flow cytometry using Cyto-ID, a dye selectively labelling autophagic vacuoles (Figure 2C). PAECs treated with MnTBAP alone or MnTBAP in combination with hydroxychloroquine (HCQ) (an inhibitor of lysosomal function acting in a comparable way to BafA1) showed an equal accumulation of autophagic vacuoles (Figure 2C). Taken together, these results indicate that MnTBAP impairs functional autophagy *in vitro*.

3.2. MnTBAP Increases the Levels of BMPR2 in Pulmonary MVECs and MVSMCs Isolated from iPAH Patients

Besides heterozygous mutations in the BMPR2 gene, inflammation has been identified as a crucial factor in the pathogenesis of PAH [13,15]. In particular, the pro-inflammatory cytokine tumor necrosis factor alpha (TNF-α) has been shown to reduce BMPR2 transcription in PAECs and PASMCs [13]. To elucidate whether MnTBAP could increase BMPR2 levels in the presence of inflammation, PAECs were treated with TNF-α and MnTBAP. As expected, a decrease in BMPR2 protein levels was observed after TNF-α treatment (Figure 3A). Interestingly, in the presence of TNF-α and MnTBAP, BMPR2 protein levels were rescued when compared to TNF-α alone (Figure 3A). To further investigate whether MnTBAP could be a potential treatment for PAH, MVECs isolated from iPAH patients were treated with the compound. As reported before [12], the upper band of BMPR2, which corresponds to the fully glycosylated mature form of the receptor [33,34], was not observed in any iPAH MVECs compared with control MVECs (Figure 3B). Importantly, an increase in BMPR2 levels after MnTBAP treatment was detected in both control MVECs and iPAH MVECs (Figure 3B). Consistent changes in pSMAD1/5 protein levels were not observed after MnTBAP treatment.

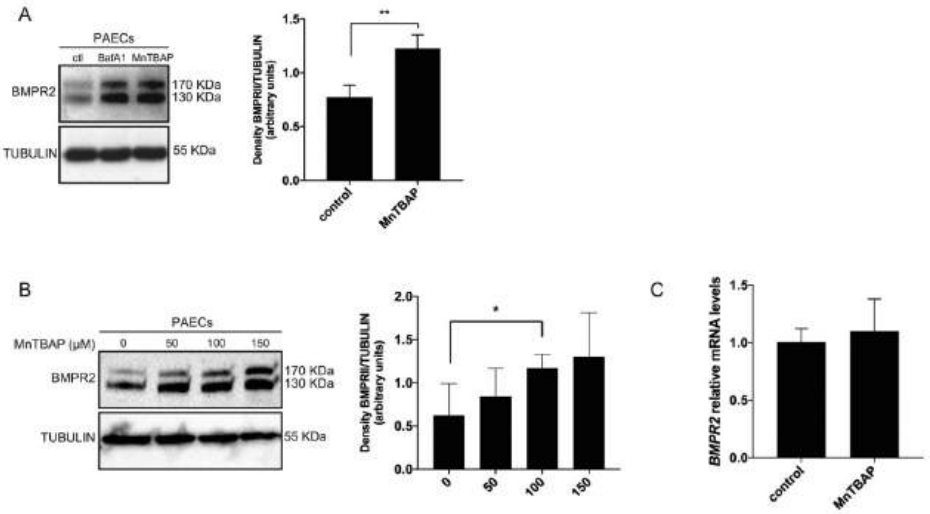

Figure 1. MnTBAP increases BMPR2 at the post-transcriptional level.
(A) pulmonary artery endothelial cells (PAECs) were treated with MnTBAP (50 μM) and BafA1 (20 nM) for 16 h. Left panel: BMPR2 protein expression was analyzed by western blot. BMPR2 protein levels increased after treatment. Tubulin is used as a loading control. Representative results of at least 3 independent experiments are shown. Right panel: Quantification of BMPR2 protein levels normalized for tubulin. (B) PAECs were treated with 50 μM, 100 μM and 150 μM of MnTBAP for 16 h. BMPR2 levels increased in a dose dependent manner. (C) BMPR2 mRNA expression analyzed by qRT-PCR remains constant after PAECs were treated with MnTBAP (50 μM). Data presented as mean ± SD. * $p < 0.05$, ** $p < 0.01$.

The close interaction between SMCs and ECs is important for vessel formation and maintenance, and was shown to be involved in PAH pathogenesis [35,36]. Therefore, we investigated whether MnTBAP could also upregulate BMPR2 levels in microvascular MVSMCs from iPAH patients. An increase in BMPR2 levels was observed in MnTBAP treated iPAH MVSMCs by western blotting analysis (Figure 3C). A block in autophagy after MnTBAP treatment was confirmed by measuring MAP1LC3B-II through western blotting analysis (Figure 3C).

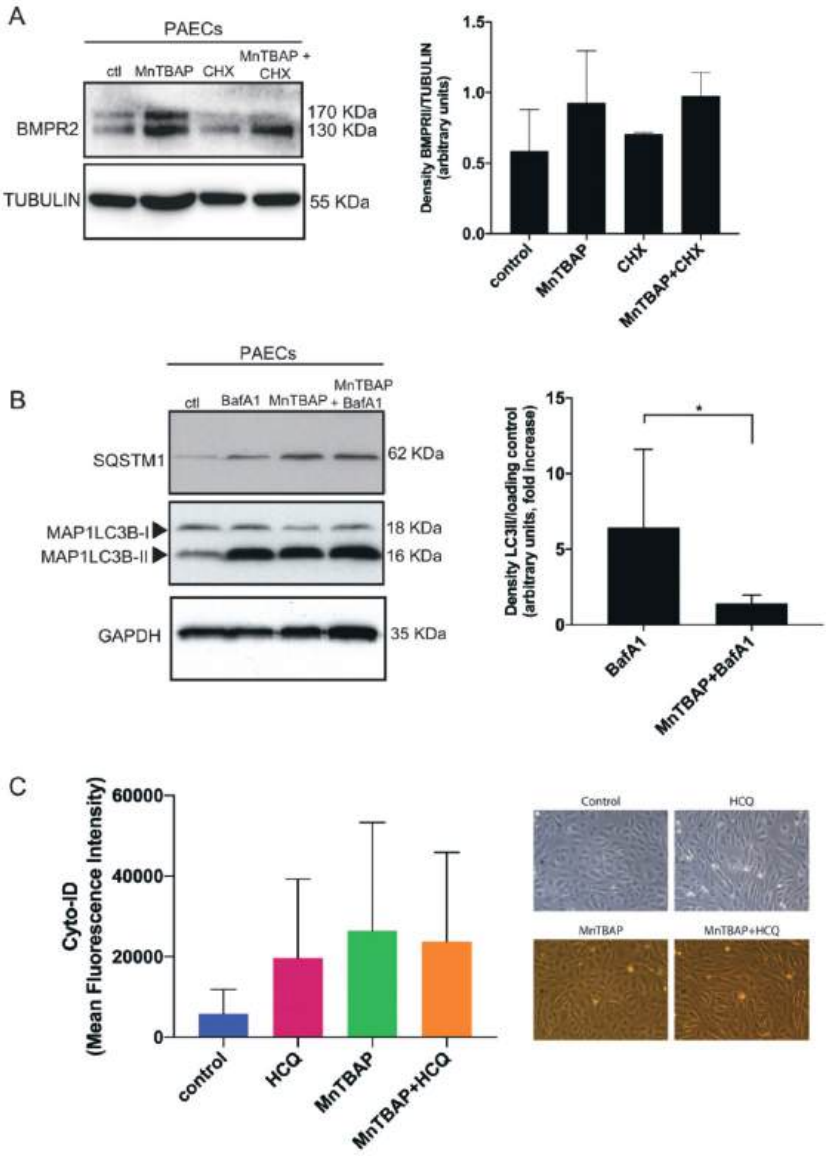

Figure 2. MnTBAP inhibits BMPR2 degradation by blocking autophagy.

(**A**) MnTBAP restores inhibitory effects of cyclohexamide (CHX) on BMPR2 protein expression. PAECs were treated with MnTBAP (50 μM) for 16 h, cycloheximide for 2 h and the combination. BMPR2 protein expression was analyzed by western blot. Tubulin is used as a loading control. Representative results of at least 3 independent experiments are shown. (**B**) PAECs were treated with MnTBAP (50 μM) in the presence or absence of BafA1 (20 nM) for 16 h and lysed directly after the treatment. Left panel: MAP1LC3B-II protein levels were analyzed by western blot. Glyceraldehyde-3-phosphate dehydrogenase (GAPDH) is used as a loading control. Representative results of at least 3 independent experiments are shown. Right panel: Western blot quantification of MAP1LC3B-II normalized for the loading control. The data are presented as fold increases relative to cells treated with BafA1. (**C**) Left panel: Flow cytometry-

Figure 2 *(continued)*
based analysis of the quantification of autophagic vesicle content in PAECs by means of the Cyto-I D dye. Cells treated with MnTBAP (50 μM) for 16 h with and without hydroxychloroquine (HCQ) (20 μM) and analyzed directly after the treatment. Right panel: Representative light microscopy images of PAECs treated for 16 h with MnTBAP (50 μM), HCQ (20 μM) and the combination, to show the status of the cells after MnTBAP treatment. Upper panels, bright field images; lower panels, fluorescent images. Magnification: ×20. Data presented as mean ± SD. * $p < 0.05$.

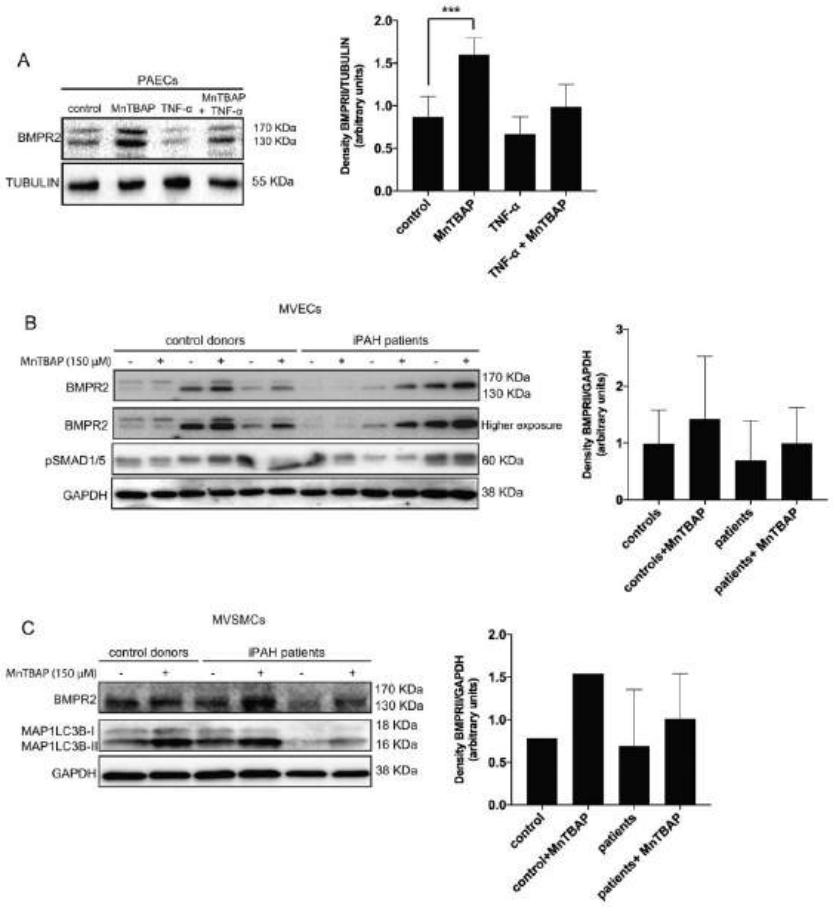

Figure 3. MnTBAP restores the levels of BMPR2 in pulmonary microvascular endothelial cells (MVECs) and microvascular smooth muscle cells (MVSMCs) isolated from idiopathic pulmonary arterial hypertension (iPAH) patients.
(A) hPAECs were treated with MnTBAP (150 μM) for 16 h and TNF-α (10 ng/mL) for 2 h. Left panel: BMPR2 protein expression was analyzed by western blot. Tubulin is used as a loading control. Representative results of at least 3 independent experiments are shown. Right panel: Quantification of BMPR2 protein levels. (B and C) Pulmonary MVECs and MVSMCs isolated from iPAH patients were treated with MnTBAP (150 μM) for 24 h. Left panel: BMPR2, pSMAD1/5 and MAP1LC3B-II protein expression was analyzed by western blot. GAPDH is used as a loading control. Representative results of at least 3 independent experiments are shown. Right panel: Quantification of BMPR2 protein levels. Data presented as mean ± SD. *** $p < 0.001$.

2.3. MnTBAP Reduced RV Afterload in Experimental PAH

To assess the therapeutic effect of MnTBAP in vivo, we treated SuHx rats with MnTBAP from week 6 to week 10 after induction of PAH. No significant difference in survival was found between the vehicle group and MnTBAP treated group (Figure 4A). Rats exposed to the SuHx protocol showed signs of severe PAH at week 6 as confirmed by echocardiography [37]. As shown by pressure–volume analysis, 4 weeks treatment with MnTBAP significantly reduced RV afterload in SuHx-induced PAH rats, as revealed by reduced arterial elastance (Ea) at week 10 (Figure 4B). Consistently, the echocardiography analysis revealed that total pulmonary resistance (TPR) was significantly reduced by MnTBAP treatment from week 6 to week 10 (Figure 4C). Meanwhile, right ventricular systolic pressure (RVSP) as well as pulmonary artery acceleration time normalized to cycle length (PAAT/cl%) remained unchanged by the treatment (Figure 4B,C).

Moreover, MnTBAP treatment reduced RV diastolic stiffness at week 10 as revealed by reduced end diastolic elastance (Eed) (Figure 4D), while RV contractility and RV-arterial coupling were unaffected as shown by end systolic elastance (Ees) and Ees/Ea, respectively (Figure 4E). Accordingly, the echocardiography analysis shows that MnTBAP treatment improved stroke volume (SV) and tricuspid annular plane systolic excursion (TAPSE) from week 6 to week 10 (Figure 4F). In addition, MnTBAP partly reversed RV remodeling as shown by reduced RV end diastolic diameter (RVEDD) (Figure 4G).

To further elucidate the origin of the reduced RV afterload, we performed histology on the lungs to measure pulmonary vascular remodeling (Figure 5A). MnTBAP treatment reversed pulmonary vascular remodeling, as shown by a significantly reduced number of occluded vessels after the treatment (Figure 5B). Representative images of open, partly remodelled and an occluded vessel are shown in Supplementary Figure S1. Further quantification of remodeling showed that MnTBAP reduced intima remodeling in all pulmonary vessels sized up to 100 μm (Figure 5C), and reduced media remodeling in pulmonary vessels between 60–100 μm (Figure 5D). Details on pulmonary vascular remodeling quantification can be found in Supplementary Figure S2.

Since MnTBAP is a synthetic metalloporphyrin with antioxidant effect, we examined the effect of MnTBAP on oxidative stress. Immunofluorescence staining with anti-8-Oxo-2′-deoxyguanosine (8-OHdG) revealed that MnTBAP treatment reduced oxidative stress in the pulmonary vasculature (Figure 5E,F).

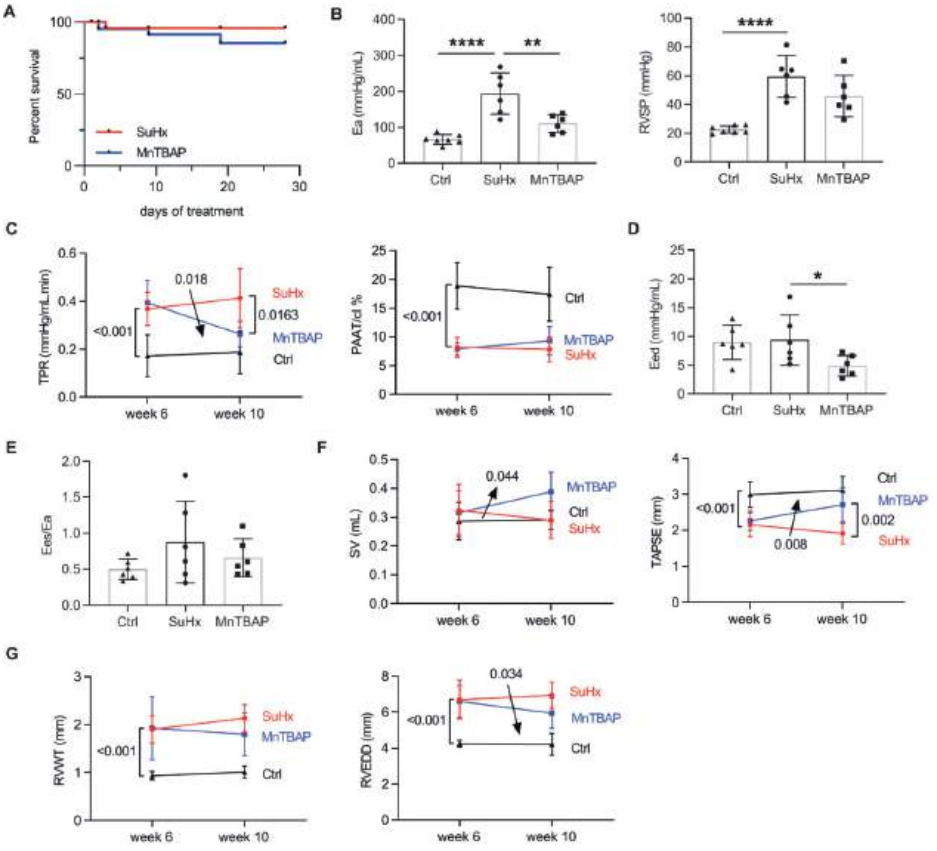

Figure 4. MnTBAP reduces right ventricular (RV) afterload and improves cardiac function in SuHx-induced PAH in rats.

(A) MnTBAP treatment did not affect survival in PAH rats. (B) Pressure–volume loop analysis shows that MnTBAP treatment reduced RV afterload (Ea) at week 10, with remained RVSP. (C) Echocardiography analysis shows that MnTBAP delayed the progression of TPR from week 6 to week 10, and reduced TPR at week 10, while PAAT/cl% was not affected. (D,E) Pressure–volume loop analysis shows that MnTBAP reduced RV stiffness (Eed) at week 10, with remained RV-arterial coupling (Ees/Ea). (F,G) MnTBAP treatment delayed progression towards RV failure as shown by echocardiography at week 6 and week 10, with decreased RVEDD, and improved SV and TAPSE. Arrows represent significant interaction of the two-way ANOVA. Data presented as mean ± SD. * $p < 0.05$, ** $p < 0.01$, **** $p < 0.0001$ versus SuHx. Ea = arterial elastance, RVSP = right ventricular systolic pressure, TPR = total pulmonary resistance, PAAT = pulmonary artery acceleration time, cl = cycle length, Eed = end diastolic elastance, Ees = end systolic elastance, SV = stroke volume, TAPSE = tricuspid annular plane systolic excursion, RVWT = right ventricular wall thickness, RVEDD = right ventricular end diastolic diameter. MnTBAP reduced pulmonary vascular remodeling and oxidative stress in experimental PAH.

The effect of MnTBAP on RV afterload and vascular remodeling was related to a block in autophagy (Figure 1 and Figure 3C). Vessels from MnTBAP-treated SuHx rats showed a trend of reduced MAP1LC3B expression (Figure S3). Quantification was done including both ECs and SMCs. However, western blots from lung homogenates did not show any changes in MAP1LC3B (data not shown). We could speculate that not all cells in the lung respond to MnTBAP in the same way and therefore changes in MAP1LC3B could be masked.

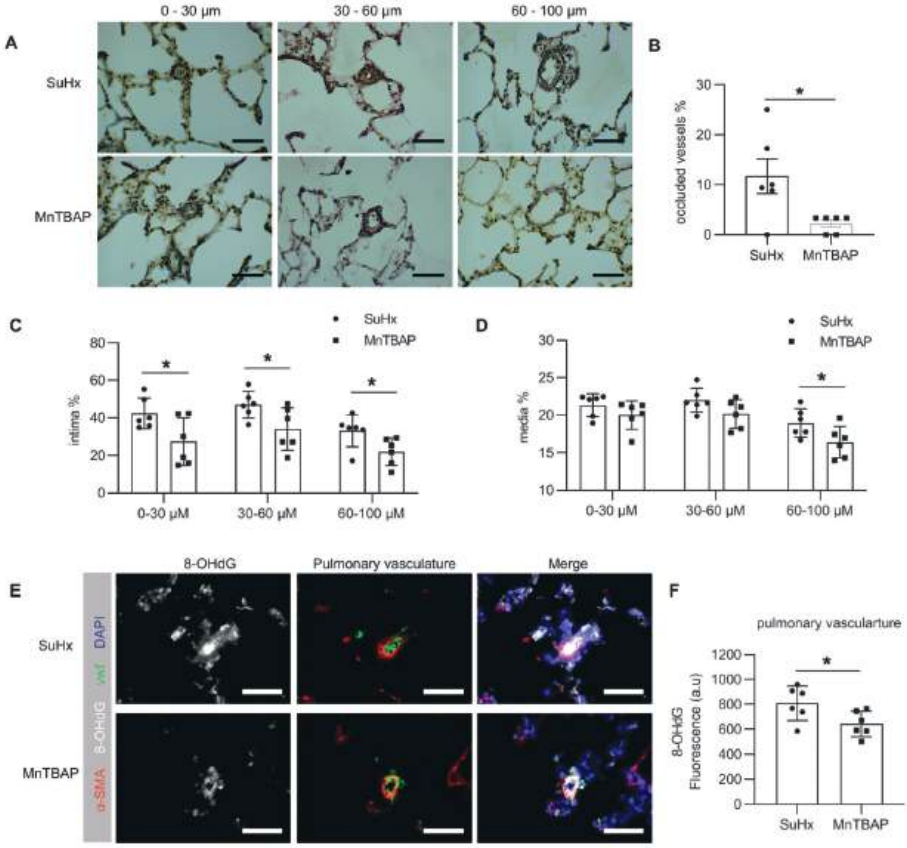

Figure 5. MnTBAP reduces pulmonary vascular remodeling and oxidative damage in SuHx-induced PAH in rats.

(A) Representative images of the pulmonary vasculatures by Elastica van Giesson staining. Scale bar: 50 µm. (B) Quantification of occluded vessels in SuHx and MnTBAP-treated rats. (C) Quantification of intima remodeling ratio in pulmonary vasculatures between 0–30, 30–60 and 60–100 µm, respectively. (D) Quantification of media remodeling ratio in pulmonary vasculatures between 0–30, 30–60 and 60–100 µm, respectively. (E) Representative images of 8-OHdG immunofluorescence staining in the lungs. Scale bar: 50 µm. α-SM (red), vwF (green) and DAPI (blue) were co-stained with 8-OHdG (white). (F) Quantification of 8-OHdG intensity shows that MnTBAP reduced 8-OHdG within the pulmonary vasculatures. * $p < 0.05$. Data presented as mean ± SD. 8-OHdG: 8-Oxo-2′-deoxyguanosine, α-SM: alpha smooth muscle actin, vwF: von Willebrand factor.

4. DISCUSSION

In the present study, we demonstrated for the first time that MnTBAP can increase BMPR2 levels in PAECs and pulmonary MVECs and MVSMCs isolated from iPAH patients, partly by inhibiting autophagy. Moreover, our experimental data in vivo indicate that MnTBAP treatment may be a promising therapy to reverse pulmonary vascular remodeling and benefit the RV.

PAH is a life-threatening disease for which no curative treatment is available. Since reduced BMPR2 is associated with PAH pathophysiology, restoring BMPR2 levels seems to be a suitable and promising alternative to effectively treat PAH patients. Indeed, increasing BMPR2 levels via adenoviral gene transfer into ECs of lungs was found to reverse hypoxic induced PH in rats [38]. In the present study, we demonstrated for the first time that MnTBAP increases BMPR2 levels in PAECs and pulmonary MVECs and MVSMCs isolated from iPAH patients. We have shown that even in the presence of CHX, MnTBAP increases BMPR2 levels in PAECs. This goes in line with our previous findings, where pre-treatment of HUVECs with MnTBAP for 16 h prior to addition of CHX increased BMPR2 stability [25]. In summary, our data suggest that MnTBAP modulates BMPR2 degradation and underlines the role of such compound as a favorable PAH treatment.

We recently demonstrated that BMPR2 is degraded through the lysosomal pathway in an autophagy-related fashion in PAECs [12], therefore we hypothesized that MnTBAP influences BMPR2 levels possibly through the regulation of autophagy. As expected, our results suggest that MnTBAP impairs functional autophagy in vitro; the exact mechanism of how MnTBAP works has yet to be elucidated. Furthermore, the possibility that MnTBAP increases BMPR2 levels by decreasing inflammation cannot be excluded, as inflammation has been shown to reduce BMPR2 levels [13,15] and to trigger autophagy [39,40].

As a cell-permeable superoxide dismutase mimetic, MnTBAP has been found to show beneficial effects in multiple disease models related to oxidative damages, including bleomycin-induced pulmonary fibrosis [27], carrageenan-induced pleurisy [28], lung contusion [26], renal fibrosis [29] and renal injury [24,30]. More interestingly, a previous study revealed that MnTBAP treatment regressed PH in Fawn hooded rats (FHR) by acting on PAMSCs [41]. Considering the previous and based on the positive findings of MnTBAP on BMPR2 in vitro, SuHx-induced PAH rats were treated with MnTBAP.

Unlike FHR which spontaneously develops PH characterized by medial hypertrophy of the vessels [42], SuHx-induced PAH rats has been shown to be a reliable animal model replicating the characteristics of PAH, including occlusions of small-to-mild-sized pulmonary vasculatures, and the virtual unresponsiveness to current PAH treatments [43]. By pressure–volume loop and echocardiography analysis, we found that MnTBAP partly reverse established PAH in SuHx rats, as shown by reduced Ea and TPR. Further analysis by histology on the lungs revealed that MnTBAP reversed pulmonary vascular remodeling, in both the intima and media layers. This is consistent with the increase of BMPR2 levels after ECs and SMCs are treated with MnTBAP in vitro. Moreover, our finding on reduced media layer thickness is consist with a previous study, which showed that MnTBAP reduced media layer thickness in FHR by reducing hypoxia-inducible factor-1α and restoring voltage-gated potassium channels in FHR PAMSCs [41]. Based on the effects of MnTBAP on BMPR2, autophagy, oxidative stress and inflammation, as well as the interactions between these stimuli, MnTBAP treatment may reverse pulmonary vascular remodeling via multiple mechanisms.

In addition, it has to be noted that the survival of PAH patients is determined by the RV function [44,45]. Therefore, it is crucial that the compounds used to treat pulmonary vasculatures are beneficial or at least non-toxic to the heart. In a congestive heart failure model, MnTBAP treatment significantly ameliorated the symptoms by reducing oxidative stress [46]. However, the effects of MnTBAP on the RV have never been studied before. Importantly, we found for the first time that MnTBAP treatment is beneficial to the RV as shown by reduced RV stiffness, improved SV and TAPSE, and reversed RV dilation. The observed effects on the RV could be mediated by the anti-oxidation and anti-inflammation effect of MnTBAP, as oxidative stress and inflammation are largely increased in SuHx RV [37,47]. Or the beneficial effect on the RV are indirectly due to reduction of the RV afterload.

However, this study is limited by including only one animal model, thus it is unclear whether MnTBAP has direct beneficial effects on the RV, or benefits the RV indirectly due to reduction of the RV afterload. Besides the anti-oxidation and anti-inflammation effects, MnTBAP may also benefit the RV by modulating BMPR2 levels, particularly in ECs of the RV. Further studies using, e.g., pulmonary artery banding models could help to better understand the role MnTBAP on the RV. Moreover, it has to be noted that the observed effects of MnTBAP in vivo might be partly independent from the observed effects in vitro. Further studies to check BMPR2 and LC3B-II levels in PAEC

and PASMCs from MnTBAP treated rats would be helpful to better understand the observed effects in the pulmonary vasculatures in vivo. Besides, a group of healthy control rats with MnTBAP treatment would be helpful to better understand the role of MnTBAP on healthy ECs and PASMCs. Although MnTBAP has not been approved to be used in humans, yet, we did not observe any adverse effect by MnTBAP in SuHx rats.

5. CONCLUSION

We demonstrated for the first time that MnTBAP modulates BMPR2 degradation in ECs and SMCs of PAH patients, partly by inhibiting autophagy. Moreover, our in vivo data revealed that MnTBAP treatment can partly reverse RV afterload and pulmonary vascular remodeling in established experimental PAH. Importantly, it is beneficial to the RV by reducing RV afterload. Collectively, MnTBAP may be a promising intervention for PAH.

ACKNOWLEDGEMENTS

The research was supported by the Netherlands CardioVascular Research Initiative: the Dutch Heart Foundation, Dutch Federation of University Medical Centers, the Netherlands Organization for Health Research and Development, and the Royal Netherlands Academy of Sciences (CVON-PHAEDRA) and Cancer Genomics Center Netherlands (to PTD). MCGP, XQS, MO, RS and XP were supported by CVON-PHAEDRA. HJB was supported by research grants from Actelion, GSK and Ferrer (Therabel).

FUNDING

This research was funded by the Netherlands CardioVascular Research Initiative: the Dutch Heart Foundation, Dutch Federation of University Medical Centres, the Netherlands Organisation for Health Research and Development, and the Royal Netherlands Academy of Sciences. Grant number CVON-2012-08 PHAEDRA, CVON-2018-29 PHAEDRA-IMPACT.

CONFLICTS OF INTEREST

The authors declare no conflict of interest.

REFERENCES

1 Guignabert C, Tu L, Hiress M Le, et al. Pathogenesis of pulmonary arterial hypertension: lessons from cancer. Eur Respir Rev 2013; 22: 543-551

2 Rosenkranz S. Pulmonary hypertension 2015: current definitions, terminology, and novel treatment options. Clin Res Cardiol 2015; 104: 197-207

3 Wilkins MR, Aman J, Harbaum L, et al. Recent advances in pulmonary arterial hypertension. F1000Research 2018; 7

4 McGoon MD, Benza RL, Escribano-Subias P, et al. Pulmonary arterial hypertension: Epidemiology and registries. In Journal of the American College of Cardiology. Vol 62. , 2013; D51-D59.

5 Provencher S, Archer SL, Ramirez FD, et al. Standards and Methodological Rigor in Pulmonary Arterial Hypertension Preclinical and Translational Research. Circ Res 2018; 122: 1021-1032

6 Ivy D. Pulmonary Hypertension in Children. Cardiol Clin 2016; 34: 451-472

7 White RJ. Estrogen: Friend or Foe in Pulmonary Hypertension? Am J Respir Crit Care Med 2016; 193: 1084-1086

8 Lan N, Massam B, Kulkarni S, et al. Pulmonary Arterial Hypertension: Pathophysiology and Treatment. Diseases 2018; 6: 38

9 Machado RD, Southgate L, Eichstaedt CA, et al. Pulmonary Arterial Hypertension: A Current Perspective on Established and Emerging Molecular Genetic Defects. Hum Mutat 2015; 36: 1113-1127

10 Lavoie JR, Ormiston ML, Perez-Iratxeta C, et al. Proteomic analysis implicates translationally controlled tumor protein as a novel mediator of occlusive vascular remodeling in pulmonary arterial hypertension. Circulation 2014; 129: 2125-2135

11 Andruska A, Spiekerkoetter E. Consequences of BMPR2 Deficiency in the Pulmonary Vasculature and Beyond: Contributions to Pulmonary Arterial Hypertension. Int J Mol Sci 2018; 19

12 Gomez-Puerto MC, van Zuijen I, Huang CJZ, et al. Autophagy contributes to BMP type 2 receptor degradation and development of pulmonary arterial hypertension. J Pathol July 2019

13 Hurst LA, Dunmore BJ, Long L, et al. TNFα drives pulmonary arterial hypertension by suppressing the BMP type-II receptor and altering NOTCH signalling. Nat Commun 2017; 8: 14079

14 Machado RD, Eickelberg O, Elliott CG, et al. Genetics and Genomics of Pulmonary Arterial Hypertension. J Am Coll Cardiol 2009; 54: S32-S42

15 Rabinovitch M, Guignabert C, Humbert M, et al. Inflammation and immunity in the pathogenesis of pulmonary arterial hypertension. Circ Res 2014; 115: 165-175

16 Groth A, Vrugt B, Brock M, et al. Inflammatory cytokines in pulmonary hypertension. Respir Res 2014; 15: 47

17 Soon E, Holmes AM, Treacy CM, et al. Elevated Levels of Inflammatory Cytokines Predict Survival in Idiopathic and Familial Pulmonary Arterial Hypertension. Circulation 2010; 122: 920-927

18 Orriols M, Gomez-Puerto MC, ten Dijke P. Erratum to: BMP type II receptor as a therapeutic target in pulmonary arterial hypertension. Cell Mol Life Sci 2017; 74: 2997-2997

19 Dunmore BJ, Drake KM, Upton PD, et al. The lysosomal inhibitor, chloroquine, increases cell surface BMPR-II levels and restores BMP9 signalling in endothelial cells harbouring BMPR-II mutations. Hum Mol Genet 2013; 22: 3667-3679
20 Spiekerkoetter E, Tian X, Cai J, et al. FK506 activates BMPR2, rescues endothelial dysfunction, and reverses pulmonary hypertension. J Clin Invest 2013; 123: 3600-3613
21 Tumurkhuu G, Koide N, Dagvadorj J, et al. MnTBAP, a synthetic metalloporphyrin, inhibits production of tumor necrosis factor-Î± in lipopolysaccharide-stimulated RAW 264.7 macrophages cells via inhibiting oxidative stress-mediating p38 and SAPK/JNK signaling. FEMS Immunol Med Microbiol 2007; 49: 304-311
22 Quan M, Cai C, Valencia G, et al. MnTBAP or Catalase Is More Protective against Oxidative Stress in Human Retinal Endothelial Cells Exposed to Intermittent Hypoxia than Their Co-Administration (EUK-134). React Oxyg Species 2017; 3: 47-65
23 Batinić-Haberle I, Cuzzocrea S, Rebouças JS, et al. Pure MnTBAP selectively scavenges peroxynitrite over superoxide: Comparison of pure and commercial MnTBAP samples to MnTE-2-PyP in two models of oxidative stress injury, an SOD-specific Escherichia coli model and carrageenan-induced pleurisy. Free Radic Biol Med 2009; 46: 192-201
24 Bi X, Wang J, Liu Y, et al. MnTBAP treatment ameliorates aldosterone-induced renal injury by regulating mitochondrial dysfunction and NLRP3 inflammasome signalling. Am J Transl Res 2018; 10: 3504
25 Zhou Q, Einert M, Schmitt H, et al. MnTBAP increases BMPR-II expression in endothelial cells and attenuates vascular inflammation. Vascul Pharmacol 2016; 84: 67-73
26 Suresh M V., Yu B, Lakshminrusimha S, et al. The protective role of MnTBAP in oxidant-mediated injury and inflammation in a rat model of lung contusion. Surgery 2013; 154: 980-990
27 Venkatadri R, Iyer AK V., Ramesh V, et al. MnTBAP Inhibits Bleomycin-Induced Pulmonary Fibrosis by Regulating VEGF and Wnt Signaling. J Cell Physiol 2017; 232: 506-516
28 Cuzzocrea S, Zingarelli B, Costantino G, et al. Beneficial effects of Mn(III)tetrakis (4-benzoic acid) porphyrin (MnTBAP), a superoxide dismutase mimetic, in carrageenan-induced pleurisy. Free Radic Biol Med 1999; 26: 25-33
29 Yu J, Mao S, Zhang Y, et al. MnTBAP Therapy Attenuates Renal Fibrosis in Mice with 5/6 Nephrectomy. Oxid Med Cell Longev 2016; 2016: 1-10
30 Zahmatkesh M, Kadkhodaee M, Moosavi SMS, et al. Beneficial effects of MnTBAP, a broad-spectrum reactive species scavenger, in rat renal ischemia/reperfusion injury. Clin Exp Nephrol 2005; 9: 212-218
31 Dunmore BJ, Drake KM, Upton PD, et al. The Lysosomal Inhibitor, Chloroquine, Increases Cell Surface BMPR-II Levels and Restores BMP9 Signalling in Endothelial Cells Harbouring BMPR-II Mutations. Hum Mol Genet 2013; 22: 3667-3679
32 Long L, Yang X, Southwood M, et al. Chloroquine Prevents Progression of Experimental Pulmonary Hypertension via Inhibition of Autophagy and Lysosomal Bone Morphogenetic Protein Type II Receptor Degradation. Circ Res 2013; 112: 1159-1170
33 Durrington HJ, Upton PD, Hoer S, et al. Identification of a Lysosomal Pathway Regulating Degradation of the Bone Morphogenetic Protein Receptor Type II. J Biol Chem 2010; 285: 37641-37649
34 Lowery JW, Amich JM, Andonian A, et al. N-linked glycosylation of the bone morphogenetic protein receptor type 2 (BMPR2) enhances ligand binding. Cell Mol Life Sci 2014; 71: 3165-3172

35 John A, Kizhakkedath P, Al-Gazali L, et al. Defective cellular trafficking of the bone morphogenetic protein receptor type II by mutations underlying familial pulmonary arterial hypertension. Gene 2015; 561: 148-156
36 Lilly B. We Have Contact: Endothelial Cell-Smooth Muscle Cell Interactions. Physiology 2014; 29: 234-241
37 Christman BW, McPherson CD, Newman JH, et al. An Imbalance between the Excretion of Thromboxane and Prostacyclin Metabolites in Pulmonary Hypertension. N Engl J Med 1992; 327: 70-75
38 Reynolds AM, Xia W, Holmes MD, et al. Bone morphogenetic protein type 2 receptor gene therapy attenuates hypoxic pulmonary hypertension. Am J Physiol Lung Cell Mol Physiol 2007; 292: L1182-L1192
39 Bertin S, Samson M, Pons C, et al. Comparative Proteomics Study Reveals That Bacterial CpG Motifs Induce Tumor Cell Autophagy in Vitro and in Vivo. Mol Cell Proteomics 2008, 7: 2311-2322
40 Xu Y, Jagannath C, Liu XD, et al. Toll-like Receptor 4 Is a Sensor for Autophagy Associated With Innate Immunity. Immunity 2007; 27: 135-144
41 Archer SL, Marsboom G, Kim GH, et al. Epigenetic attenuation of mitochondrial superoxide dismutase 2 in pulmonary arterial hypertension: a basis for excessive cell proliferation and a new therapeutic target. Circulation 2010; 121: 2661-2671
42 Sato K, Webb S, Tucker A, et al. Factors influencing the idiopathic development of pulmonary hypertension in the fawn hooded rat. Am Rev Respir Dis 1992; 145: 793–797
43 Bonnet S, Provencher S, Guignabert C, et al. Translating research into improved patient care in pulmonary arterial hypertension. Am J Respir Crit Care Med 2017; 195: 583-595
44 Mauritz GJ, Kind T, Marcus JT, et al. Progressive changes in right ventricular geometric shortening and long-term survival in pulmonary arterial hypertension. Chest 2012; 141: 935-943
45 Sandoval J, Bauerle O, Palomar A, et al. Survival in primary pulmonary hypertension: Validation of a prognostic equation. Circulation 1994; 89: 1733-1744
46 Nojiri H, Shimizu T, Funakoshi M, et al. Oxidative Stress Causes Heart Failure with Impaired Mitochondrial Respiration. J Biol Chem 2006; 281: 33789-33801
47 Bogaard HJ, Natarajan R, Henderson SC, et al. Chronic pulmonary artery pressure elevation is insufficient to explain right heart failure. Circulation 2009; 120: 1951-1960
48 Da Silva Gonçalves Bós D, Van Der Bruggen CEE, Kurakula K, et al. Contribution of impaired parasympathetic activity to right ventricular dysfunction and pulmonary vascular remodeling in pulmonary arterial hypertension. Circulation 2018; 137: 910-924
49 Szulcek R, Happé CM, Rol N, et al. Delayed Microvascular Shear Adaptation in Pulmonary Arterial Hypertension. Role of Platelet Endothelial Cell Adhesion Molecule-1 Cleavage. Am J Respir Crit Care Med 2016; 193: 1410-1420
50 de Raaf MA, Kroeze Y, Middelman A, et al. Serotonin transporter is not required for the development of severe pulmonary hypertension in the Sugen hypoxia rat model. Am J Physiol Cell Mol Physiol 2015; 309: L1164-L1173
51 Yu J, Mao S, Zhang Y, et al. MnTBAP Therapy Attenuates Renal Fibrosis in Mice with 5/6 Nephrectomy. Oxid Med Cell Longev 2016; 2016: 7496930.
52 Stiedl O, Spiess J. Effect of Tone-Dependent Fear Conditioning on Heart Rate and Behavior of C57BL/6N Mic. Behav Neurosci 1997; 111: 703-711

SUPPLEMENT MATERIALS

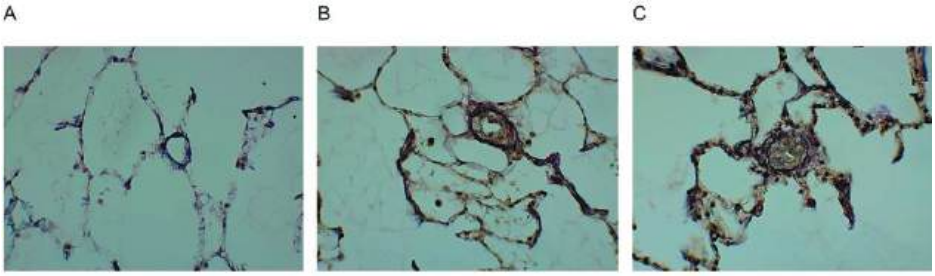

Supplemental Figure 1. Representative images of pulmonary vasculatures.
Representative images of an open vessel (A), a partly remodelled vessel (B) and an occluded vessel (C).

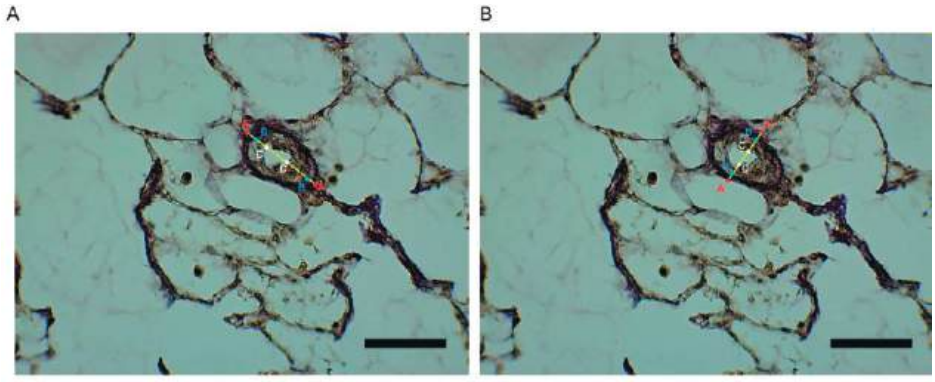

Supplemental Figure 2. Quantification of pulmonary vascular remodelling.

Intima layer thickness % = [length (BB) – length (CC)] / length (AA)

Media layer thickness % = [length (AA) – length (BB)] / length (AA)

Minimally 20 transversally pulmonary arterioles cut, with an outer diameter between 0 and 30 µm, 30 and 60 µm, 60 and 100 µm, randomly distributed over the lungs, were measured. Every vessel was measured two times as shown by (A) and (B), and the average value was calculated. Scale bar: 50 µm.

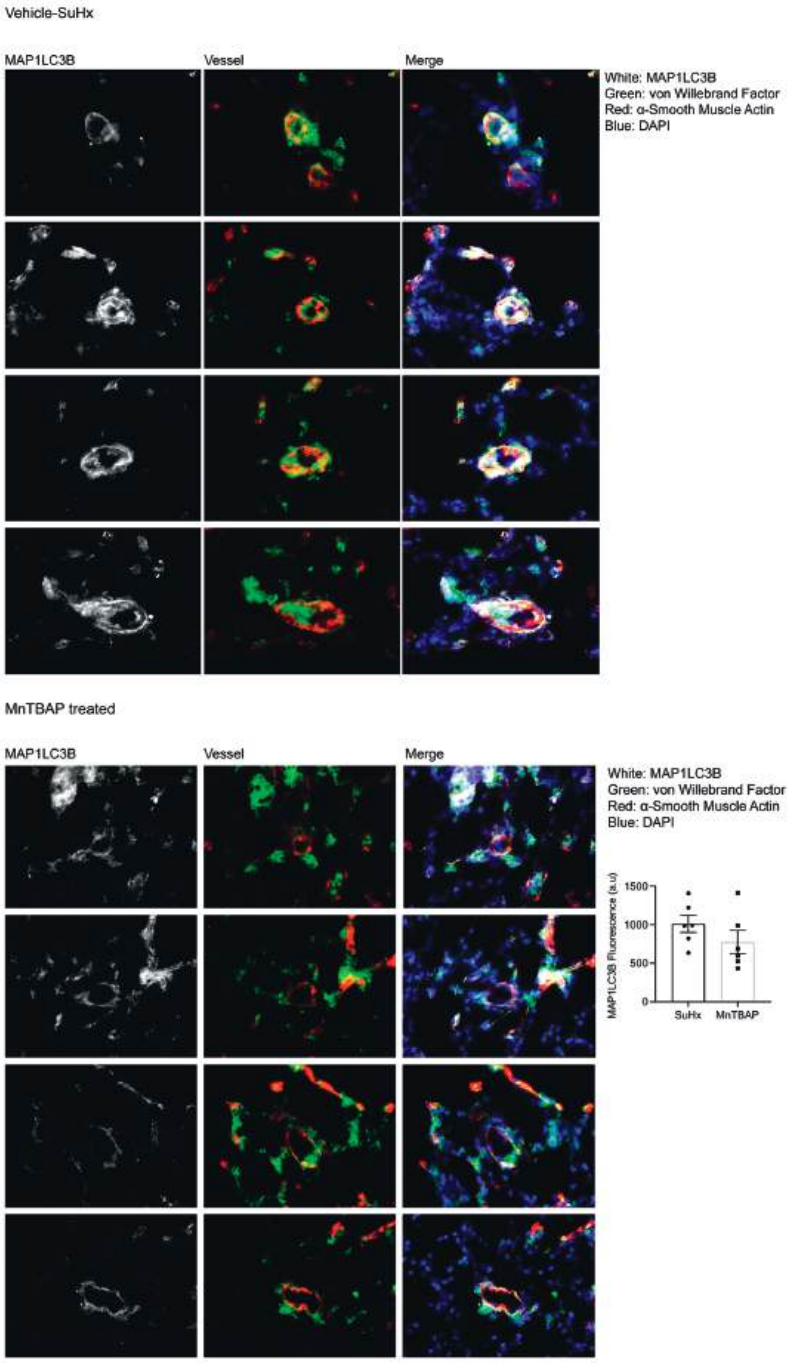

Supplemental Figure 3. MAP1LC3B expression in pulmonary vasculatures.
Immunofluorescence staining of MAP1LC3B in vehicle-SuHx group (A) and MnTBAP treatment group (B). White: MAP1LC3B, green: von Willebrand factor, red: alpha smooth muscle actin, blue: DAPI. (C) Quantification of MAP1LC3B intensity in pulmonary vasculatures. Vessels from MnTBAP-treated SuHx rats showed a trend of reduced MAP1LC3B.

Part III

Novel treatment targeting growth factors and histone acetylation

CHAPTER 5

Nintedanib improves cardiac fibrosis but leaves pulmonary vascular remodelling unaltered in experimental pulmonary hypertension

Nina Rol[1,2]*, Michiel A. de Raaf[1,2]*, Xiaoqing Sun[1], Vincent P. Kuiper[1], Denielli da Silva Gonçalves Bos[1,2], Chris Happé[1,2], Kondababu Kurakula[3], Chris Dickhoff[4,5], Raphael Thuillet[6,7], Ly Tu[6,7], Christophe Guignabert[6,7], Ingrid Schalij[1,2], Xiaoke Pan[1,2], Franziska E. Herrmann[8], Geerten P. van Nieuw Amerongen[2], Pieter Koolwijk[2], Anton Vonk-Noordegraaf[1] , Frances S. de Man[1,2], Lutz Wollin[8], Marie-José Goumans[3], Robert Szulcek[1,2], Harm J. Bogaard[1]

*** Both authors contributed equally to this publication**

[1] Department of Pulmonology, VU University Medical Center, Amsterdam, The Netherlands. [2]Department of Physiology, Institute for Cardiovascular Research, VU University Medical Center, Amsterdam, The Netherlands. [3] Department of Molecular Cell Biology and Cancer Genomics Centre Netherlands, Leiden University Medical Center, Leiden, The Netherlands. [4] Department of Cardio-Thoracic Surgery, VU University Medical Center, Amsterdam, The Netherlands. [5] Department of Surgery, VU University Medical Center, Amsterdam, The Netherlands. [6] INSERM UMR_S999, Le Plessis-Robinson, France. [7] Université Paris-Sud, Université Paris-Saclay, Le Kremlin Bicêtre, France. [8] Boehringer Ingelheim, Respiratory Diseases Research, Biberach, Germany.

Cardiovasc Res. 2019 Feb 1;115(2):432-439.

ABSTRACT

Aims

Pulmonary arterial hypertension (PAH) is associated with increased levels of circulating growth factors and corresponding receptors such as platelet derived growth factor, fibroblast growth factor and vascular endothelial growth factor. Nintedanib, a tyrosine kinase inhibitor targeting primarily these receptors, is approved for the treatment of patients with idiopathic pulmonary fibrosis. Our objective was to examine the effect of nintedanib on proliferation of human pulmonary microvascular endothelial cells (MVEC) and assess its effects in rats with advanced experimental pulmonary hypertension (PH).

Methods and results

Proliferation was assessed in control and PAH MVEC exposed to nintedanib. PH was induced in rats by subcutaneous injection of Sugen (SU5416) and subsequent exposure to 10% hypoxia for 4 weeks (SuHx model). Four weeks after re-exposure to normoxia, nintedanib was administered once daily for 3 weeks. Effects of the treatment were assessed with echocardiography, right heart catheterization, and histological analysis of the heart and lungs. Changes in extracellular matrix production was assessed in human cardiac fibroblasts stimulated with nintedanib. Decreased proliferation with nintedanib was observed in control MVEC, but not in PAH patient derived MVEC. Nintedanib treatment did not affect right ventricular (RV) systolic pressure or total pulmonary resistance index in SuHx rats and had no effects on pulmonary vascular remodelling. However, despite unaltered pressure overload, the right ventricle showed less dilatation and decreased fibrosis, hypertrophy, and collagen type III with nintedanib treatment. This could be explained by less fibronectin production by cardiac fibroblasts exposed to nintedanib.

Conclusion

Nintedanib inhibits proliferation of pulmonary MVECs from controls, but not from PAH patients. While in rats with experimental PH nintedanib has no effects on the pulmonary vascular pathology, it has favourable effects on RV remodelling.

KEYWORDS

Pulmonary arterial hypertension, tyrosine kinase inhibitor, endothelial cell, vascular remodeling, cardiac fibrosis

INTRODUCTION

Pulmonary arterial hypertension (PAH) is a devastating condition of increased pulmonary vascular resistance attributed to vasoconstriction and vascular remodelling such as intimal thickening, medial hyperplasia, and muscularization of the small pulmonary arteries. Right ventricular (RV) hypertrophy, fibrosis and dilatation lead to heart failure and death in PAH patients. Dysregulated signalling by growth factors including platelet derived growth factor (PDGF), fibroblast growth factor (FGF), vascular endothelial growth factor (VEGF), and transforming growth factor-β (TGF-β) contribute to remodelling in PAH in both the pulmonary vasculature and the heart.[1–5] Until now, treatment success of vasodilating therapy is limited as it does not reverse the vascular alterations. Interest has shifted to therapies targeting growth factor receptors to mitigate or even reverse vascular remodelling.[6–8]

Circulating PDGF and its receptors are up-regulated in endothelial cells (EC) and smooth muscle cells in PAH patients and contribute to RV fibrosis.[5,9,10] Although imatinib, primarily a PDGF receptor antagonist, had positive results in animal models, clinical studies showed mixed results with some haemodynamic improvement, unchanged exercise capacity, and serious side-effects.[11,12] Perhaps one explanation for persistent pulmonary vascular remodelling after imatinib treatment is ongoing deregulated signalling through the VEGF and FGF receptors.[13] Production of basal FGF by EC is increased in idiopathic PAH (iPAH) patients and also serum levels are elevated.[14–16] Likewise, VEGF, together with its receptor, is abundantly expressed in ECs of plexiform lesions and circulating VEGF is also increased in PAH.[10,17–19] On the other hand, inhibition of the VEGF receptor (combined with hypoxia, as in the SuHx model) can also be used to induce pulmonary hypertension (PH) in animal models and reflects intimal remodelling as observed in human disease. The paradoxal effects of blocking the VEGF receptor as a potential treatment and a possible inducer in PAH is still an enigma.[17]

Nintedanib is a tyrosine kinase inhibitor (TKI) that has been approved for the treatment of idiopathic pulmonary fibrosis (IPF). Nintedanib targets primarily PDGF-, FGF-, and VEGF-mediated proliferation in pulmonary fibroblasts, and possibly TGF-β-mediated transformation to myofibroblasts.[20–22] Experimentally and clinically nintedanib has been proven to attenuate lung fibrosis, while reports of development of PH are lacking.[23,24] The anti-proliferative properties of nintedanib have a potential beneficial

effect on pulmonary vascular remodelling by reversing the associated PH in patients with IPF. Nintedanib might even have the potential of being a new treatment option for Group 1 PH. In contrast, given the fact that TKIs with inhibiting properties on the VEGF receptor are associated with the development of clinical (dasatinib) and experimental (SU5416) PH,[6,25] it could also be postulated that nintedanib triggers the development of PAH or worsens IPF associated PH.

We hypothesized that the inhibitive properties of nintedanib on proliferation could have favourable effects on PH by reducing vascular remodelling. Therefore, we studied the functional effect of nintedanib in primary pulmonary microvascular endothelial cells (MVEC) and in the SuHx rat model in an advanced stage of PH.

MATERIAL AND METHODS

Reagents

The ethanesulfonate of nintedanib (Methyl (3Z)-3-{[(4-{methyl[(4-methylpiperazin-1-yl)acetyl]amino}phenyl)amino](phenyl)methylidene}-2-oxo-2,3-dihydro-1H-indole-6-carboxylate) (Boehringer Ingelheim Pharma, Biberach, Germany) was dissolved in deionized water. For use in animal models, nintedanib was administered at a dose of 41.5 mg/kg (50.0 mg/kg with ethanesulfonate) once daily by oral gavage for 21 days, at a safe dose level based on the available results of 28-day or 90-day repeated dose toxicity studies (according to ICH guidelines).

Cell culture

Cell isolation and culture were performed as previously described. [26] In brief, control pulmonary MVEC were isolated from patients that underwent lobectomy for suspected or proven lung malignancy. PAH MVEC were isolated from lung tissue obtained during lung transplantation. Patient characteristics are reported in table 1. The study was reviewed by the Institutional Review Board (IRB) of the VU University Medical Center (Amsterdam, the Netherlands) and decided that consent was not necessary because of use of rest material. The study was performed conform the declaration of Helsinki regarding ethical priniciples for medical research involving human subjects. Endothelial cell isolation and culture of the smallest pulmonary vessels was performed as previously described. Purity of cell isolations was confirmed by immunofluorescent staining. [26, 27] The cells were stimulated with $VEGF_{165}$ (25 ng/ml, ReliaTech GmbH,

Wolfenbuttel, Germany) for 20 minutes to induce phosphorylation of Erk1/2 (pErk1/2) and lysed for western blot analysis.

Human cardiac fibroblasts were cultured in DMEM with 10% FCS. When confluent, medium was changed to DMEM with 1% FCS and supplemented with or not with 1 μM Nintedanib for 24 hours.

Table 1 – Patient characteristics

Donor	mPAP (mmHg)	Etiology	Gender	Age (yr)
1	43	iPAH	F	42
2	89	iPAH	F	22
3	85	iPAH	M	21
4	94	iPAH	F	30

iPAH = idiopathic pulmonary arterial hypertension; mPAP = mean pulmonary artery pressure.

Proliferation

The effect of nintedanib on the proliferation rate of MVEC was measured by 5-ethynyl-2'-deoxyuridine (EdU) thymidine analogue incorporation (Click-It EdU Alexa Fluor 488 Imaging Kit, C10337, Invitrogen, Carlsbad, CA, USA). Cells were seeded at a density of $7x10^3$ cells/cm^2 and attached overnight. MVEC were pre-incubated with nintedanib (0.3 μM) in presence of 1% human serum albumin for two hours and stimulated with $VEGF_{165}$ (25 ng/ml, ReliaTech GmbH, Wolfenbuttel, Germany) and EdU nucleotides were added. After 24 hours cells were fixed and protocol was performed according to the manufacturer's instructions. Per condition 5 pictures were taken at a magnification of 20x by an Axiovert 200 Marianas inverted wide-field fluorescence microscope (Carl Zeiss Microscopy, Jena, Germany) and the number of proliferating nuclei was counted.

Extracelular matrix production

To study the influence of nintedanib on matrix production in the heart, cardiac fibroblasts treated with nintedanib (1μM) for 24 hours in DMEM with 1% FCS were lysed in RIPA supplemented with protease inhibitors. Fibronection, as a measure of fibrosis, was determined by Western blot. Membranes were incubated with α-Fibronectin antibody (Sigma F7387) and α-Vinculin as loading control (Sigma V9131).

Animal model

This study was approved by the local Animal Welfare committee (VU-Fys 13-14) and performed conform the guidelines from directive 2010/63/EU of the European Parliament on the protection of animals us for scientific purposes. Progressive pressure-overload in conjunction with angioproliferative pulmonary vascular remodeling was induced by the combined exposure to SU5416 and hypoxia, as previously characterized by our group.[28] Male Sprague-Dawley rats weighing 200 g received a single subcutaneous injection of SU5416 (25 mg/kg, Tocris) and were exposed to a simulated altitude of 5000 meters in a nitrogen dilution chamber for 4 weeks; thereafter the animals were kept at the sea level for another 7 weeks. Twelve animals were treated with nintedanib for 3 weeks, starting in week 8, at an advanced stage of PH in the SuHx model. Dose calculation was adjusted to the individual body weights twice weekly and administred by oral gavage (50 mg/kg). Clinical signs and body weights were measured daily. Experimental protocol is depicted in Figure 2A.

Echocardiography and hemodynamics

On the day of necropsy, animals were anesthetized (isoflurane; 4.0/2.5% induction/maintenance; 1:1 O2/air mix) followed by an injection of buprenorphine analgesia (0.1 mg/kg). After intubation, echocardiography was performed using a ProSound system (Prosound SSD-4000) equipped with a 13-Mhz linear transducer (UST-5542, Aloka, Tokyo, Japan), as described previously.[28] Hemodynamic measurements were performed with a 4.5-mm Millar conductance catheter, which was inserted in the right ventricular outflow tract to acquire the right ventricular systolic pressure (RVSP), used for total pulmonary resistance index calculations (TPRI). Pressure-volume loop analyses were performed as described previously.[29] Animals were killed via exsanguination and organs were weighed and processed for analysis. End experiments were performed unblinded, following experiments were performed blinded to treatment group.

Histology and immunofluorescent staining

Tissues were fixed in formalin, embedded in paraffin and 4 µm thick sections were prepared for histology and immunofluorescent staining. Lung tissue was stained with Elastica van Gieson and scanned (3DHISTECH, Budapest, Hungary). Averaged media and intima wall thickness were measured as described previously.[29, 30]

Total collagen content of the right ventricle (RV) was assessed by picrosirius red staining. Distinction between collagen type I (Southern Biotech, 1310-01, 1:100) and

type III (Southern Biotech1330-01, 1:100) was made with immunofluorescent staining. Therefore, slides were fixed in acetone at 4°C, permeabilized with 0.2% Triton, and blocked with 1% BSA. Slides were incubated overnight with primary antibodies for collagen type I and III with co-staining for PECAM-1 (Santa Cruz, sc-1506-R). Alexa Fluor conjugated secondary species-specific secondary antibodies (dilution 1:250) were added and slides were covered with Prolong Gold Antifade Reagent with DAPI (Thermo Fisher Scientific, P36931). Three pictures of the right ventricle were taken with an Axiovert 200 Marianas inverted wide-field fluorescence microscope (Carl Zeiss Microscopy) at 10X magnification. Area of collagen was measured around transversally cut cardiomyocytes, excluding regions around vessels, using ImageJ.

Western blot

For Western blot analysis MVEC and RV lysates were processed as described by Szulcek, *et al*.[26] Membranes were blocked in 5% BSA (Sigma-Aldrich) in Tris-buffered saline (pH=7.6) with 0.1% tween for 1 hour at room temperature, membranes were incubated overnight at 4^0C with primary antibodies: phosphor-p44/42 MAPK (Cell Signaling, 9106S, 1:1000), p44/42 MAPK (Cell Signaling, 9102S, 1:1000) and β-actin (Sigma-Aldrich, A3854, 1:50 000). After 1 hour incubation with horseradish peroxidase (HRP) conjugated species-specific secondary antibodies (Dako, 1:1000 for cell lysates, 1:5000 for RV lysates) blots were visualized with chemiluminiscence with the LAS-3000 (Fujifilm, Tokyo, Japan). Phosphorylated protein was normalized to total protein and β-actin was used as loading control.

RT-PCR

RNA was isolated from rat RV tissue (1 μg of total RNA). cDNA generation was performed using iScript cDNA synthesis kit (Bio-Rad, #170-8891). For PCR reactions FAST SYBR Green Master Mix (Thermo Fisher Scientific, 4385612). With a cDNA pool of all samples best annealing temperatures and standard curve were optimized for the following primers: collagen I, collagen III, connective tissue growth factor (CTGF), osteopontin-1, and brain natriuretic peptide (BNP) (sequences shown in table 2).

Statistics

Statistical analysis was performed using Graphpad Prism 6.0. Differences between two groups was assessed with paired (*in vitro*) and unpaired (*in vivo*) t-tests (parametric) or Mann-Whitney tests (nonparametric). Multiple comparisons were tested by one-way or two-way ANOVA, followed by the suitable post-hoc tests for between-group

differences. Data are reported as mean ± SEM. RT-PCR data are shown as Log 2 fold change, statistical analysis was performed on Log 2 fold change.

Table 2 - Primer sequences used for RT-PCR

Connective tissue growth factor (CTGF)	Forward	5'-CTGTTCCAAGACCTGTGGGAT-3'
	Reverse	5'-TTTTGCCCTTCTTAATGTTCT-3'
Collagen I	Forward	5'- GAACGGAGATGATGGGGAAG-3'
	Reverse	5'- CCAAACCACTGAAACCTCTG-3'
Collagen III	Forward	5'- AGTGGCCATAATGGGGAACG-3'
	Reverse	5'- ATGAATTGGGATGCAACTAC -3'
BNP	Forward	5'- GCTGCTTTGGGCAGAAGATAGA -3'
	Reverse	5'- GCCAGGAGGTCTTCCTAAAACA -3'
Osteopontin-1	Forward	5'- CCCATCTCAGAAGCAGAATCTT -3'
	Reverse	5'- GTCATGGCTTTCATTGGAGTTG -3'
18S	Forward	5'-GCAATAACAGGTCTGTGATGCC-3'
	Reverse	5'-CACGAATGGGGTTCAACG-3'

RESULTS

Nintedanib inhibits VEGF induced proliferation of pulmonary MVEC

To assess the minimal effective dose of nintedanib, we examined the inhibitory effects of different concentrations of nintedanib on the phosphorylation of Erk1/2 upon VEGF stimulation, a downstream target involved in VEGF driven proliferation of endothelial cells.[31] Nintedanib inhibited VEGF-induced pErk1/2 in control MVECs in a concentration-dependent manner ($p = 0.005$) (Figure 1 A-B). At 0.3 μM, a concentration not resulting in morphological changes,[20] pErk1/2 levels were similar to non-stimulated conditions ($p = 0.02$). This concentration was used for all subsequent experiments.VEGF-induced proliferation of control MVECs, assessed by EdU incorporation, was reduced by nintedanib ($p = 0.02$) (Figure 1 C). While nintedanib inhibited VEGF stimulated ERK1/2 phosphorylation in PAH MVEC, it had no significant effect on the proliferation of PAH patients derived MVEC ($p = 0.15$) (Figure 1 A-C).

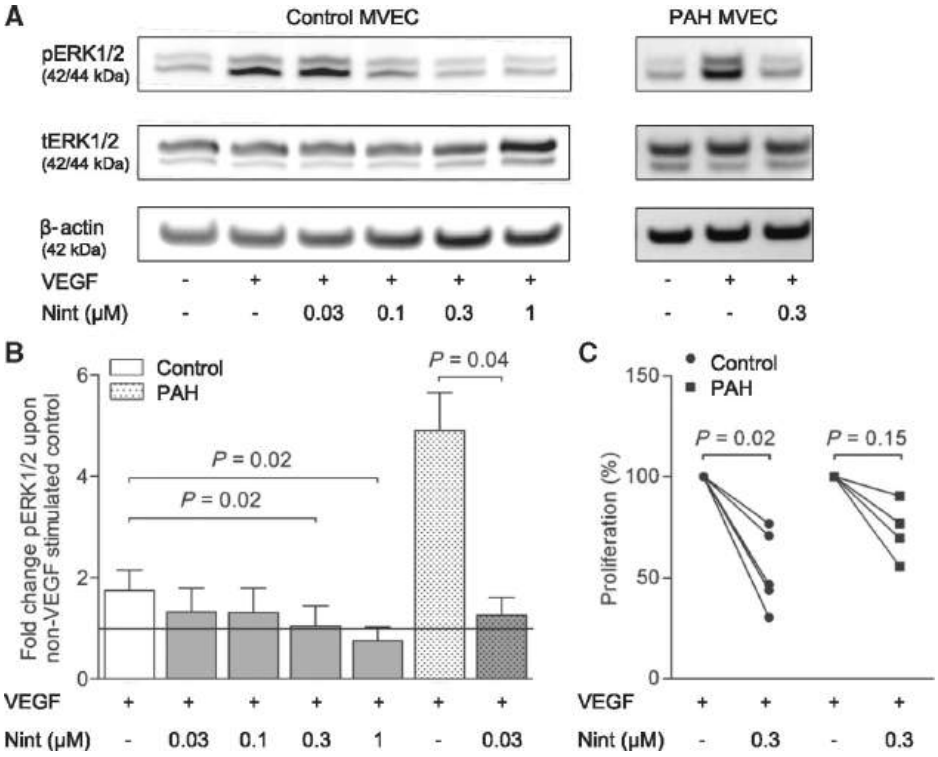

Figure 1 - Nintedanib attenuates VEGF induced proliferation of microvascular endothelial cells
Human primary microvascular endothelial cells (MVEC) were incubated with nintedanib at the concentrations indicated and stimulated with vascular endothelial growth factor (VEGF). Phosphorylated Erk1/2 (pErk1/2), total ERK1/2 (tErk1/2), and β-actin were quantified by Western blot. A representative blot is shown in (A). The densitometric quantification of the ratio pErk1/2 / tErk1/2 (control n = 5, PAH n = 4) depicted as fold increase upon non-stimulated MVEC is depicted in (B). One-way ANOVA was used to determine statistical significance. MVEC proliferation after VEGF stimulation in combination with pretreatment with or without 0.3 μM nintedanib was assessed with EdU staining (control n = 5, PAH n =4), ratio paired t-test was performed (C).

Nintedanib does not affect pulmonary vascular remodeling

To assess *in vivo* effects, we treated SuHx rats for three weeks with nintedanib starting in week 8. RV end diastolic diameter (RVEDD) was decreased after nintedanib treatment ($p = 0.002$), with a trend towards less RV stiffness (Eed, $p = 0.07$) and an increased pulmonary artery acceleration time corrected for cycle length (PAAT/cl, $p = 0.07$) (Table 3). However, right ventricular end systolic pressure, total pulmonary resistance index, stroke volume index and tricuspid annular plan systolic excursion (TAPSE) were not different between vehicle and nintedanib treated rats (Table 3). Heart weight and Fulton

index (RV/(LV ± S) were not different between vehicle and nintedanib treated animals (Table 3). Hematocrit was decreased in nintedanib treated animals (p = 0.03). Our histological analysis in the lung, intimal and medial wall thickness was not different between vehicle and nintedanib treated animals (Figure 2 B).

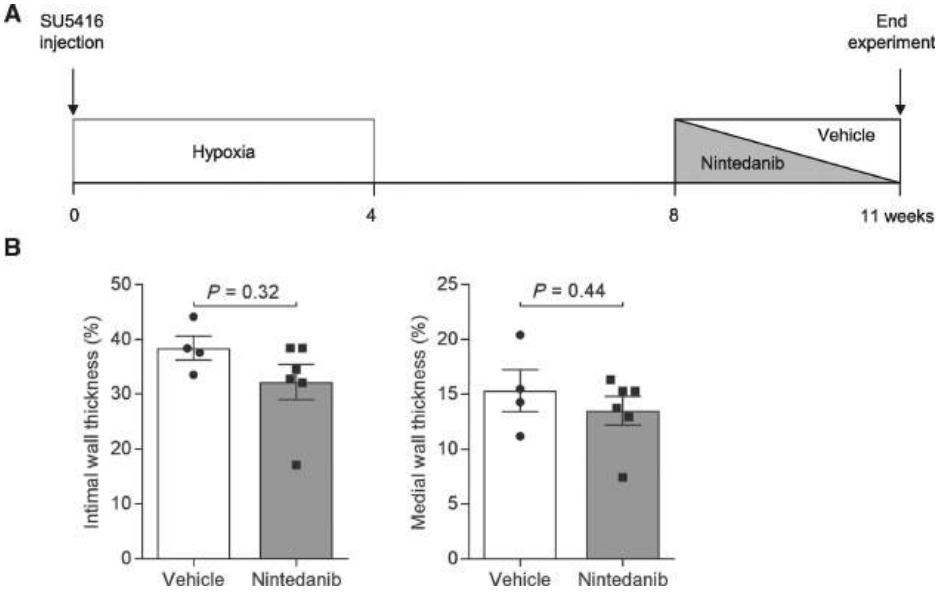

Figure 2 - Nintedanib did not reduce pulmonary vascular remodeling in experimental PH
Pulmonary hypertension was induced in rats (vehicle n = 4, nintedanib n = 6) by SU5416 injection in combination with 4 weeks hypoxia (10% O2). At week eight, when advanced pulmonary lesions are formed, rats were treated with vehicle or nintedanib (50 mg/kg) for 3 weeks (A). Intimal and medial wall thickness of the pulmonary vasculature was not changed. A total of 19–50 vessels per rat were measured. Data shown as mean ± SEM (B).

Nintedanib improves RV adaptation in SuHx rats

Cardiac fibrosis, detected by increasing RV diastolic stiffness, is suggested to contribute to right ventricular failure in PAH patients. [32, 33] Because the antifibrotic effect of nintedanib on the heart is still unknown, we assessed whether nintedanib treatment would result in less RV fibrosis. In the animal model total collagen was measured with picrosirius red staining. We observed a decrease of total collagen in the RV of nintedanib treated rats (Figure 3 B). To assess collagen deposition, we quantified collagen I and III in the RV by RT-PCR and immunofluorescent staining. Collagen I was significantly lowered at mRNA level. Less collagen III was observed with immunofluorescent staining, without affecting the collagen I/III ratio (Figure 3 A,

C, D). To explore the TGF-β mediated anti-fibrotic properties of nintedanib on the RV of pulmonary hypertensive rats, we quantified connective tissue growth factor mRNA levels in the RV-tissue. Connective tissue growth factor was not inhibited by nintedanib treatment (Figure 3 A).

Table 3 – Characteristics of vehicle and nintedanib treated SuHx rats

	SuHx + vehicle (n = 12)	SuHx + Nintedanib (n = 9)	p-value
Terminal body weight (g)	466 ± 20.2	423 ± 16.5	0.12
RVSP (mmHg)	61.6 ± 7.4	66.8 ± 4.6	0.39
dP/dt max (mmHg/s)	2600 ± 336	2970 ± 294	0.42
SVI (mL/cm2)	0.44 ± 0.05	0.52 ± 0.05	0.28
TPRI (mmHg/mL/min/m^2)	0.94 ± 0.24	0.73 ± 0.07	0.59
Eed	15.7 ± 3.4	8.3 ± 1.3	0.07
TAPSE (mm)	1.9 ± 0.1	2.0 ± 0.1	0.78
RVEDD (mm)	7.2 ± 0.2	6.4 ± 0.1	0.002
PAAT/cl (%)	7.4 ± 0.6	8.5 ± 0.3	0.07
Hematocrit (%)	44.3 ± 0.8	40.0 ± 1.5	0.03
Heart weight (g)	2.3 ± 0.1	2.2 ± 0.1	0.53
Fulton index (RV/(LV+S))	0.60 ± 0.05	0.66 ± 0.04	0.36

Overview of body weight, catheterization, echocardiographic, and ex vivo measurements comparing SuHx rats after 3weeks of treatment with vehicle or nintedanib. For parametric data unpaired t-test was used, for non-parametric data Mann–Whitney U-test was performed. Data shown as mean±SEM. (vehicle n=9, nintedanib n=12.)

dP/dt, delta pressure/delta time; Eed, end-diastolic elastance; LV, left ventricle; PAAT/cl, pulmonary artery acceleration time divided by the cycle length; RV, right ventricle; RVEDD, right ventricular end diastolic diameter; RVSP, right ventricular systolic pressure; RVWT, right ventricular wall thickness; S, septum; SVI, stroke volume index; TPRI, total pulmonary resistance index; TAPSE, tricuspid annular plane systolic excursion.

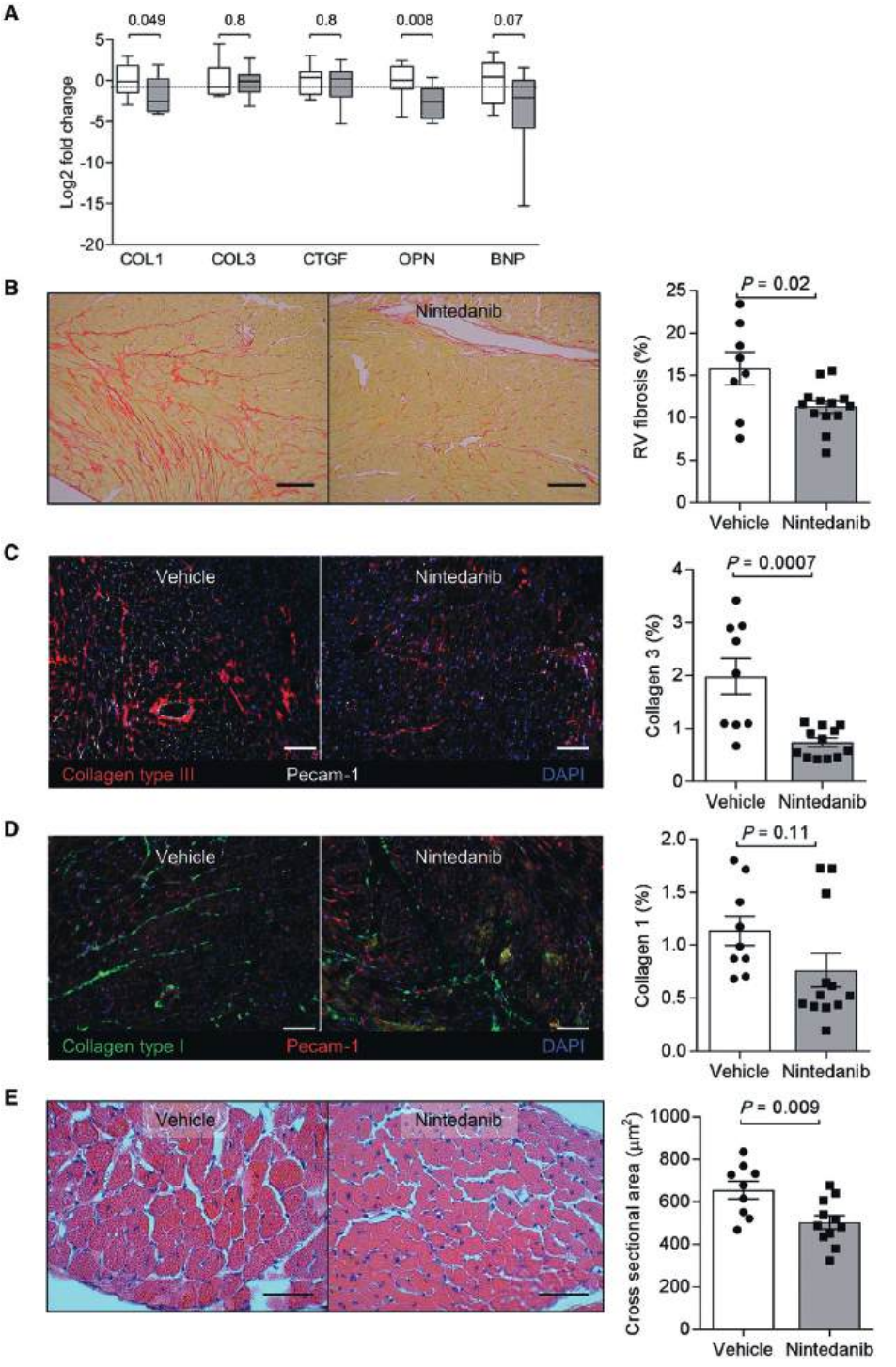
A
0.049
0.8
0.8
0.008
0.07
Log2 fold change
COL1
COL3
CTGF
OPN
BNP
B
Nintedanib
P = 0.02
RV fibrosis (%)
Vehicle
Nintedanib
C
Vehicle
Nintedanib
Collagen type III
Pecam-1
DAPI
P = 0.0007
Collagen 3 (%)
D
Vehicle
Nintedanib
Collagen type I
Pecam-1
DAPI
P = 0.11
Collagen 1 (%)
E
Vehicle
Nintedanib
P = 0.009
Cross sectional area (µm²)

Figure 3 - Nintedanib inhibits cardiac fibrosis, osteopontin-1 and hypertrophy in experimental PH
In the right ventricle nintedanib (vehicle n = 9 white bars, nintedanib n = 12 grey bars) treatment showed a significant four-fold decrease in collagen type I and osteopontin-1 transcriptional levels. Data shown as mean values, bars represent min to max (A). Nintedanib treated rats showed a significant (P = 0.02) decrease in picrosirius red staining in the right ventricle. Scale bar indicates 150 µm (B). Immunofluorescent staining for collagen type III proved a significant decrease (P < 0.001) in the nintedanib group. Scale bar indicates 100 µm (C). Collagen level type I was unchanged (three pictures of the RV per animal). Scale bar indicates 100 µm (D). Less hypertrophy of the right ventricle was observed (P = 0.009). Scale bar indicates 150 µm (E). For parametric data unpaired t-test was used, for non-parametric data Mann–Whitney U-test was performed. Data shown as mean ± SEM (B–E). Vehicle n = 9, nintedanib n = 12 (A–E).

Cardiomyocyte hypertrophy, another contributor to RV diastolic stiffness, was also decreased in the nintedanib group, compared to vehicle (p = 0.0007) (Figure 3 E). Osteopontin-1 and BNP, prognostic markers in heart failure, were decreased after treatment with nintedanib (p = 0.008 and p = 0.07, respectively) (Figure 3 A).

Cardiac fibroblasts treated with nintedanib showed decreased fibronectin production, indicating a role for nintedanib in decreased fibrosis in the heart (Figure 4).

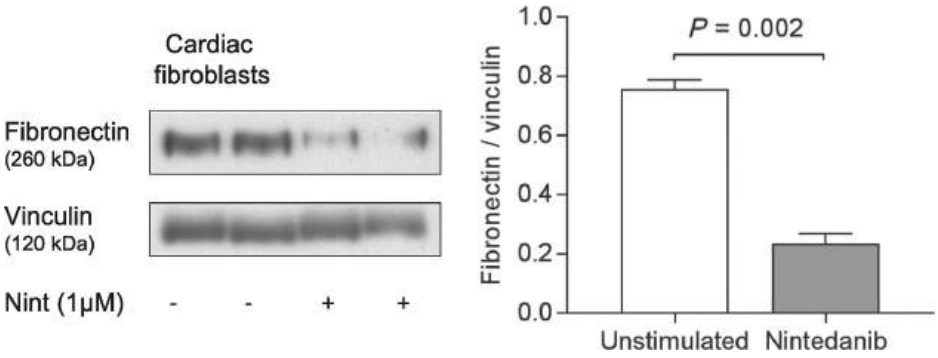

Figure 4 – Effect of nintedanib on fibronectin in cardiac fibroblasts.
Two human cardiac fibroblast cell lines were treated with nintedanib (1 µM, 24 h) and the effect of this compound on fibronectin production was determined. Representative western blot of two experiments is shown. Vinculin was used as a loading control for quantification by western blot. Densitometric quantification of the blots showed that fibronectin, a measure of fibrosis, was significantly reduced by nintedanib (P = 0.002). Paired t-test was performed (n = 4). Data shown as mean ± SEM.

DISCUSSION

We have shown in our study that nintedanib inhibits proliferation of primary pulmonary microvascular endothelial cells from normal subjects, but not from PAH patients. In rats with experimentally induced PH, nintedanib treatment did not result in a reversal of pulmonary vascular remodeling, but did improve RV adaptation. Nintedanib improved RV contractility, decreased RV dilatation and reduced RV hypertrophy and collagen content.

A recent publication showed that inhibition of pErk1/2 by nintedanib regulated proliferation of macrovascular endothelial cells of the lung indicating therapeutic potential for the treatment of PAH.[34] In line with this study, we demonstrated the inhibitory effects of nintedanib on pErk1/2 and proliferation rate in control MVEC. Nintedanib showed a heterogeneous effect in the PAH donor group and could thereby not significantly reduce proliferation in patient endothelial cells. This could explain the lack of effect on pulmonary vascular remodeling observed in our *in vivo* experiment. While acute vasodilating effects of TKIs have been reported, we did not observe reductions in pulmonary or systemic pressures.[35, 36]

Paradoxically, TKI drugs that interfere with growth factor receptor signaling can also trigger endothelial proliferation and the development of pulmonary vascular remodeling and PAH.[6] A series of case reports described PAH induced by dasatinib[6, 8] and it was suggested that Src kinase inhibition played a causative rol[6]. Experimentally, the TKI Sugen causes endothelial apoptosis, an effect which has been explained by inhibition of the VEGF receptor and observations that the healthy lung endothelium is dependent on the presence of VEGF for its survival.[37] Upon exposure to a second hit, such as hypoxia[38] or a high shear stress[39, 40], the initial phase of apoptosis is followed by uncontrolled endothelial proliferation. In the rat model, Sugen is administered only once at the beginning of the protocol, and at the time of progressive lung vascular remodeling Sugen is no longer present. Therefore, lung vascular remodeling in the later stages of the Sugen hypoxia model, which closely resembles remodeling in human PAH, could be partly dependent on intact VEGF-R signaling, thus providing the rationale for our study. The fact that Nintedanib did not reverse remodeling, suggests that intimal proliferation in the remodeled Sugen hypoxia lung has to a certain degree become independent from growth factor receptor signaling. The same seems to be true for microvascular endothelial cells from PAH patients.

Despite suggestions that TKIs may provide a beneficial therapy in PAH, there is also concern that these drugs may have cardiotoxic effects. Previously, we reported no negative effects on capillary density and right ventricular pressure adaptation in rats after pulmonary artery banding treated with BIBF1000, a close structural analogue to nintedanib.[41] Even though decreased VEGF signaling is linked to capillary rarefaction in the heart and thereby to RV heart failure[42], we found no loss in capillaries but decreased dilatation, fibrosis and hypertrophy in the right ventricle of nintedanib treated rats. Other parameters potentially indicating worsening of right ventricular dysfunction, such as decreased TAPSE or cardiac index, were unchanged.[43] Our data suggest that nintedanib prevented RV fibrosis by direct inhibition of cardiac fibroblasts, leading to a decreased production of fibronectin.

In conclusion we found beneficial effects of nintedanib on control pulmonary endothelium *in vitro* and favorable effects on the right ventricle in rats with PH. A clinical trial might confirm that nintedanib may safely be administered to IPF patients with associated PH and might confirm or refute the absence of changes in pulmonary vascular remodeling by nintedanib in our rat model of PH.

ACKNOWLEDGMENTS

We would like to acknowledge M. H. van Wijhe (VU University Medical Center) for his input to this study and M.A. Paul (VU University Medical Center) and K.J. Hartemink (Antoni van Leeuwenhoek Hospital) for their contribution to tissue collection.

CONFLICT OF INTEREST

None declared

FUNDING

This work was financially supported by Boehringer Ingelheim. We acknowledge the support from the Netherlands CardioVascular Research Initiative; the Dutch Heart Foundation, Dutch Federation of University Medical Centres, the Netherlands Organisation for Health Research and Development and the Royal Netherlands Academy of Sciences. Grant number: 2012-08.

REFERENCES

1. Hassoun PM, Mouthon L, Barbera JA, Eddahibi S, Flores SC, Grimminger F, Jones PL, Maitland ML, Michelakis ED, Morrell NW, Newman JH, Rabinovitch M, Schermuly R, Stenmark KR, Voelkel NF, Yuan JX, Humbert M. Inflammation, growth factors, and pulmonary vascular remodeling. *J Am Coll Cardiol* 2009;**54**:S10-S19.
2. Voelkel NF, Gomez-Arroyo J, Abbate A, Bogaard HJ, Nicolls MR. Pathobiology of pulmonary arterial hypertension and right ventricular failure. *Eur Respir J* 2012;**40**:1555-1565.
3. Godinas L, Guignabert C, Seferian A, Perros F, Bergot E, Sibille Y, Humbert M, Montani D. Tyrosine kinase inhibitors in pulmonary arterial hypertension: a double-edge sword? *Semin Respir Crit Care Med* 2013;**34**:714-724.
4. Guignabert C, Tu L, Girerd B, Ricard N, Huertas A, Montani D, Humbert M. New molecular targets of pulmonary vascular remodeling in pulmonary arterial hypertension: importance of endothelial communication. *Chest* 2015;**147**:529-537.
5. Gomez-Arroyo J, Sakagami M, Syed AA, Farkas L, Van TB, Kraskauskas D, Mizuno S, Abbate A, Bogaard HJ, Byron PR, Voelkel NF. Iloprost reverses established fibrosis in experimental right ventricular failure. *Eur Respir J* 2015;**45**:449-462.
6. Montani D, Bergot E, Gunther S, Savale L, Bergeron A, Bourdin A, Bouvaist H, Canuet M, Pison C, Macro M, Poubeau P, Girerd B, Natali D, Guignabert C, Perros F, O'Callaghan DS, Jais X, Tubert-Bitter P, Zalcman G, Sitbon O, Simonneau G, Humbert M. Pulmonary arterial hypertension in patients treated by dasatinib. *Circulation* 2012;**125**:2128-2137.
7. Guignabert C, Phan C, Seferian A, Huertas A, Tu L, Thuillet R, Sattler C, Le Hiress M, Tamura Y, Jutant EM, Chaumais MC, Bouchet S, Maneglier B, Molimard M, Rousselot P, Sitbon O, Simonneau G, Montani D, Humbert M. Dasatinib induces lung vascular toxicity and predisposes to pulmonary hypertension. *J Clin Invest* 2016;**126**:3207-3218.
8. Weatherald J, Chaumais MC, Savale L, Jais X, Seferian A, Canuet M, Bouvaist H, Magro P, Bergeron A, Guignabert C, Sitbon O, Simonneau G, Humbert M, Montani D. Long-term outcomes of dasatinib-induced pulmonary arterial hypertension: a population-based study. *Eur Respir J* 2017;**50**.
9. Perros F, Montani D, Dorfmuller P, Durand-Gasselin I, Tcherakian C, Le PJ, Mazmanian M, Fadel E, Mussot S, Mercier O, Herve P, Emilie D, Eddahibi S, Simonneau G, Souza R, Humbert M. Platelet-derived growth factor expression and function in idiopathic pulmonary arterial hypertension. *Am J Respir Crit Care Med* 2008;**178**:81-88.
10. Selimovic N, Bergh CH, Andersson B, Sakiniene E, Carlsten H, Rundqvist B. Growth factors and interleukin-6 across the lung circulation in pulmonary hypertension. *Eur Respir J* 2009;**34**:662-668.
11. Schermuly RT, Dony E, Ghofrani HA, Pullamsetti S, Savai R, Roth M, Sydykov A, Lai YJ, Weissmann N, Seeger W, Grimminger F. Reversal of experimental pulmonary hypertension by PDGF inhibition. *J Clin Invest* 2005;**115**:2811-2821.
12. Ghofrani HA, Seeger W, Grimminger F. Imatinib for the treatment of pulmonary arterial hypertension. *N Engl J Med* 2005;**353**:1412-1413.

13. Casanovas O, Hicklin DJ, Bergers G, Hanahan D. Drug resistance by evasion of antiangiogenic targeting of VEGF signaling in late-stage pancreatic islet tumors. *Cancer Cell* 2005;**8**:299-309.
14. Benisty JI, McLaughlin VV, Landzberg MJ, Rich JD, Newburger JW, Rich S, Folkman J. Elevated basic fibroblast growth factor levels in patients with pulmonary arterial hypertension. *Chest* 2004;**126**:1255-1261.
15. Tu L, Dewachter L, Gore B, Fadel E, Dartevelle P, Simonneau G, Humbert M, Eddahibi S, Guignabert C. Autocrine fibroblast growth factor-2 signaling contributes to altered endothelial phenotype in pulmonary hypertension. *Am J Respir Cell Mol Biol* 2011;**45**:311-322.
16. Izikki M, Guignabert C, Fadel E, Humbert M, Tu L, Zadigue P, Dartevelle P, Simonneau G, Adnot S, Maitre B, Raffestin B, Eddahibi S. Endothelial-derived FGF2 contributes to the progression of pulmonary hypertension in humans and rodents. *J Clin Invest* 2009;**119**:512-523.
17. Voelkel NF, Gomez-Arroyo J. The role of vascular endothelial growth factor in pulmonary arterial hypertension. The angiogenesis paradox. *Am J Respir Cell Mol Biol* 2014;**51**:474-484.
18. Voelkel NF, Vandivier RW, Tuder RM. Vascular endothelial growth factor in the lung. *Am J Physiol Lung Cell Mol Physiol* 2006;**290**:L209-L221.
19. Kumpers P, Nickel N, Lukasz A, Golpon H, Westerkamp V, Olsson KM, Jonigk D, Maegel L, Bockmeyer CL, David S, Hoeper MM. Circulating angiopoietins in idiopathic pulmonary arterial hypertension. *Eur Heart J* 2010;**31**:2291-2300.
20. Wollin L, Wex E, Pautsch A, Schnapp G, Hostettler KE, Stowasser S, Kolb M. Mode of action of nintedanib in the treatment of idiopathic pulmonary fibrosis. *Eur Respir J* 2015;**45**:1434-1445.
21. Inomata M, Nishioka Y, Azuma A. Nintedanib: evidence for its therapeutic potential in idiopathic pulmonary fibrosis. *Core Evid* 2015;**10**:89-98.
22. Wollin L, Maillet I, Quesniaux V, Holweg A, Ryffel B. Antifibrotic and anti-inflammatory activity of the tyrosine kinase inhibitor nintedanib in experimental models of lung fibrosis. *J Pharmacol Exp Ther* 2014;**349**:209-220.
23. Chaudhary NI, Roth GJ, Hilberg F, Muller-Quernheim J, Prasse A, Zissel G, Schnapp A, Park JE. Inhibition of PDGF, VEGF and FGF signalling attenuates fibrosis. *Eur Respir J* 2007;**29**:976-985.
24. Richeldi L, Cottin V, du Bois RM, Selman M, Kimura T, Bailes Z, Schlenker-Herceg R, Stowasser S, Brown KK. Nintedanib in patients with idiopathic pulmonary fibrosis: Combined evidence from the TOMORROW and INPULSIS((R)) trials. *Respir Med* 2016;**113**:74-79.
25. Nicolls MR, Mizuno S, Taraseviciene-Stewart L, Farkas L, Drake JI, Al HA, Gomez-Arroyo JG, Voelkel NF, Bogaard HJ. New models of pulmonary hypertension based on VEGF receptor blockade-induced endothelial cell apoptosis. *Pulm Circ* 2012;**2**:434-442.
26. Szulcek R, Happe CM, Rol N, Fontijn RD, Dickhoff C, Hartemink KJ, Grunberg K, Tu L, Timens W, Nossent GD, Paul MA, Leyen TA, Horrevoets AJ, de Man FS, Guignabert C, Yu PB, Vonk-Noordegraaf A, van Nieuw Amerongen GP, Bogaard HJ. Delayed Microvascular Shear-adaptation in Pulmonary Arterial Hypertension: Role of PECAM-1 Cleavage. *Am J Respir Crit Care Med* 2016.
27. van der Heijden M, van Nieuw Amerongen GP, van BJ, Paul MA, Groeneveld AB, van Hinsbergh VW. Opposing effects of the angiopoietins on the thrombin-induced permeability of human pulmonary microvascular endothelial cells. *PLoS One* 2011;**6**:e23448.

28. de Raaf MA, Schalij I, Gomez-Arroyo J, Rol N, Happe C, de Man FS, Vonk-Noordegraaf A, Westerhof N, Voelkel NF, Bogaard HJ. SuHx rat model: partly reversible pulmonary hypertension and progressive intima obstruction. *Eur Respir J* 2014;**44**:160-168.
29. D. DSGB. Contribution of impaired parasympathetic activity to right ventricular dysfunction and pulmonary vascular remodeling in pulmonary arterial hypertension. In press.
30. Okada K, Tanaka Y, Bernstein M, Zhang W, Patterson GA, Botney MD. Pulmonary hemodynamics modify the rat pulmonary artery response to injury. A neointimal model of pulmonary hypertension. *Am J Pathol* 1997;**151**:1019-1025.
31. Meadows KN, Bryant P, Vincent PA, Pumiglia KM. Activated Ras induces a proangiogenic phenotype in primary endothelial cells. *Oncogene* 2004;**23**:192-200.
32. Bogaard HJ, Abe K, Vonk NA, Voelkel NF. The right ventricle under pressure: cellular and molecular mechanisms of right-heart failure in pulmonary hypertension. *Chest* 2009;**135**:794-804.
33. Rain S, Handoko ML, Trip P, Gan CT, Westerhof N, Stienen GJ, Paulus WJ, Ottenheijm CA, Marcus JT, Dorfmuller P, Guignabert C, Humbert M, Macdonald P, Dos Remedios C, Postmus PE, Saripalli C, Hidalgo CG, Granzier HL, Vonk-Noordegraaf A, van der Velden J, de Man FS. Right ventricular diastolic impairment in patients with pulmonary arterial hypertension. *Circulation* 2013;**128**:2016-2025, 2011-2010.
34. Awad KS, Elinoff JM, Wang S, Gairhe S, Ferreyra GA, Cai R, Sun J, Solomon MA, Danner RL. Raf/ERK drives the proliferative and invasive phenotype of BMPR2-silenced pulmonary artery endothelial cells. *Am J Physiol Lung Cell Mol Physiol* 2016;**310**:L187-L201.
35. Abe K, Toba M, Alzoubi A, Koubsky K, Ito M, Ota H, Gairhe S, Gerthoffer WT, Fagan KA, McMurtry IF, Oka M. Tyrosine kinase inhibitors are potent acute pulmonary vasodilators in rats. *Am J Respir Cell Mol Biol* 2011;**45**:804-808.
36. Pankey EA, Thammasiboon S, Lasker GF, Baber S, Lasky JA, Kadowitz PJ. Imatinib attenuates monocrotaline pulmonary hypertension and has potent vasodilator activity in pulmonary and systemic vascular beds in the rat. *Am J Physiol Heart Circ Physiol* 2013;**305**:H1288-H1296.
37. Lahm T, Crisostomo PR, Markel TA, Wang M, Lillemoe KD, Meldrum DR. The critical role of vascular endothelial growth factor in pulmonary vascular remodeling after lung injury. *Shock* 2007;**28**:4-14.
38. Taraseviciene-Stewart L, Kasahara Y, Alger L, Hirth P, Mc MG, Waltenberger J, Voelkel NF, Tuder RM. Inhibition of the VEGF receptor 2 combined with chronic hypoxia causes cell death-dependent pulmonary endothelial cell proliferation and severe pulmonary hypertension. *FASEB J* 2001;**15**:427-438.
39. Sakao S, Taraseviciene-Stewart L, Lee JD, Wood K, Cool CD, Voelkel NF. Initial apoptosis is followed by increased proliferation of apoptosis-resistant endothelial cells. *FASEB J* 2005;**19**:1178-1180.
40. Happe CM, de Raaf MA, Rol N, Schalij I, Vonk-Noordegraaf A, Westerhof N, Voelkel NF, de Man FS, Bogaard HJ. Pneumonectomy combined with SU5416 induces severe pulmonary hypertension in rats. *Am J Physiol Lung Cell Mol Physiol* 2016:ajplung.
41. de Raaf MA. Tyrosine Kinase Inhibitor BIBF1000 does not hamper right ventricular pressure adaptation in rats. *Am J Physiol Heart Circ Physiol* 2016.

42. Bogaard HJ, Natarajan R, Henderson SC, Long CS, Kraskauskas D, Smithson L, Ockaili R, McCord JM, Voelkel NF. Chronic pulmonary artery pressure elevation is insufficient to explain right heart failure. *Circulation* 2009;**120**:1951-1960.
43. Bogaard HJ, Mizuno S, Hussaini AA, Toldo S, Abbate A, Kraskauskas D, Kasper M, Natarajan R, Voelkel NF. Suppression of histone deacetylases worsens right ventricular dysfunction after pulmonary artery banding in rats. *Am J Respir Crit Care Med* 2011;**183**:1402-1410.

CHAPTER 6

Histone deacetylase inhibition with quisinostat reduces pulmonary vascular remodeling in experimentally induced PAH by inhibiting proliferation and inflammation

Xiao-Qing Sun[1], Quint A J Hagdorn[2], Diederik E Van der Feen[2], Eva L Peters[1], Ingrid Schalij[1], Peter ten Dijke[3], Frances S de Man[1], Rolf M F Berger[2], Marie-José Goumans[3], Harm Jan Bogaard[1], Kondababu Kurakula[3]

[1]Department of Pulmonary Medicine, Amsterdam Cardiovascular Sciences, Amsterdam UMC, Vrije Universiteit Amsterdam, Amsterdam, The Netherlands. [2]Center for Congenital Heart Diseases, University Medical Center Groningen, University of Groningen, the Netherlands. [3]Deptartment of Cell and Chemical Biology, Leiden University Medical Center, Leiden, the Netherlands.

(in preparation)

ABSTRACT:

Introduction: Histone deacetylases (HDACs) expression and activity are increased in pulmonary arterial hypertension (PAH). Although inhibiting HDACs has been promoted as a treatment for PAH, results from preclinical studies using first generation inhibitors were equivocal and raised concerns regarding safety. Quisinostat is a "second generation" HDAC inhibitor, which is highly potent against class I and II HDACs and elicits a prolonged pharmacodynamics response. Quisinostat was well tolerated in a phase I trial in patients with solid tumor. Collectively, we hypothesized that quisinostat may treat experimental PAH.

Objective: To determine the effect of quisinostat on vascular remodeling and right ventricular (RV) function in experimentally induced PAH.

Methods: HDAC1 expression was measured in lungs and microvascular endothelial cells (MVECs) from PAH patients. HDAC activity, proliferation and inflammation were measured after quisinostat treatment of PAH MVECs. Chronic quisinostat treatment was tested in three experimental rat models for PAH: the Sugen + hypoxia (SuHx) model, the Monocrotaline shunt flow (MF) model and pulmonary artery banding (PAB).

Results: We found that HDAC1 expression is increased in lungs and MVECs from PAH patients. Inhibition of HDAC activity by quisinostat strongly decreased proliferation and inflammation in MVECs. In addition, conditioned medium from quisinostat treated PAH MVECs inhibited the growth of healthy smooth muscle cells. *In vivo,* quisinostat treatment reduced RV systolic pressure, RV afterload and total pulmonary resistance in SuHx rats. Further tissue analysis by histology revealed that quisinostat reduced pulmonary vascular remodeling in both SuHx and MF rat models by reducing the intima layer thickness. Meanwhile, quisinostat had no independent effect on RV function or RV remodeling as shown by treatment of PAB rats. Consistent with the findings on PAH MVECs, quisinostat treatment reduced proliferation and perivascular inflammation in the lungs of PAH rat models.

Conclusions- Quisinostat can partly reverse RV afterload and pulmonary vascular remodeling in established experimental PAH, and may be a promising intervention for PAH.

Key Words: pulmonary arterial hypertension, histone deacetylases, vascular remodeling, endothelial cell, proliferation, inflammation

INTRODUCTION

Pulmonary arterial hypertension (PAH) is a progressive disorder in which endothelial dysfunction and vascular remodeling obstruct small pulmonary arteries, resulting in a marked and sustained elevation of pulmonary artery pressure, and eventually right ventricular (RV) failure and death [1]. The abnormal pulmonary vascular remodeling is characterized by a hyperproliferative, apoptosis-resistant and inflammatory phenotype of pulmonary arterial endothelial cells (PAECs) and smooth muscle cells (PASMCs) [2-5]. Current PAH therapies have little effect on vascular remodeling and therefore result in only a modest reduction in pulmonary pressure. Due to the limited improvement in morbidity and mortality [6], there continues to be an urgent need to identify new molecular targets that can safely and efficiently reverse vascular remodeling in PAH patients.

Emerging evidence has demonstrated the important role of epigenetics in the pathogenesis of PAH [7, 8]. Epigenetics is defined as all heritable changes in gene expression that are not related to changes in the underlying DNA sequence, e.g. histone modification, DNA methylation and microRNAs [8]. Post-translational histone modifications, such as acetylation of lysine residues on the N-terminal tails of histones, modulates chromatin structure and accessibility by altering DNA-histone interactions [9]. Among the two enzyme families regulating histone acetylation, histone deacetylases (HDACs) contain a highly conserved deacetylase domain and are responsible for the removal of acetyl groups [10]. HDACs regulates several key cellular processes like proliferation, apoptosis and inflammation, and are implicated in several cardiovascular diseases such as atherosclerosis, coronary restenosis, and cardiac hypertrophy [11-14]. Abnormal HDAC expression and activity has also been reported to play a role in PAH, with increased expression of HDAC1, 2, 4, 5, 6 and 8 in lung homogenates [15, 16], in the pulmonary artery (PA) [15], in PAECs [17, 18], in PASMCs [17] and in PA adventitial fibroblasts (PAAFs) [15].

Small-molecule HDAC inhibitors have shown promising therapeutic benefits in experimentally induced PAH and RV hypertrophy, including the broad spectrum HDAC inhibitor (vorinostat), class I HDAC inhibitors (valproic acid, sodium butyrate, apicidin, mocetinostat, entinostat) and the HDAC6 inhibitor tubastatin A [19]. Unfortunately, other studies, including those from our lab, showed far less promising effects of broad spectrum inhibitors: the class I and II HDAC inhibitor trichostatin A (TSA) did not reverse pulmonary vascular remodeling in the sugen hypoxia (SuHx) rat model of PAH

and caused deterioration of cardiac function in rats with RV pressure overload as a result of PA banding (PAB) [20, 21]. Therefore, the effects of HDAC inhibitors in PAH patients remain unpredictable. To date, new generation of HDAC inhibitors have been developed that may effectively inhibit the disease causing increased in HDAC activity in the PAH lung while exhibiting minimal or no systemic and cardiac toxic effects. Quisinostat (JNJ-26481585) is a novel second-generation HDAC inhibitor, with a boosted pharmacodynamic response and enhanced efficacy at nanomolar concentrations in several tumor models [22, 23]. Quisinostat has been used in phase II trials studying the treatment of solid tumors, lymphoma and hematological malignancies [24, 25]. More importantly, compared to the traditionally used HDAC inhibitors, quisinostat shows a more potent inhibition on HDAC1 and a more potent anti-proliferative effect in various human cancer cell lines [22]. Therefore, we hypothesized that quisinostat may have therapeutic benefit in PAH.

Here, we show that inhibition of HDAC activity by quisinostat decreases *in vitro* proliferation and inflammation of pulmonary MVECs derived from patients with PAH. Chronic oral administration of quisinostat reversed abnormal vascular remodeling in lungs of the SuHx rat model and in the monocrotaline shunt flow (MF). Importantly, quisinostat did not compromise RV function after PAB. Taken together, our data suggest that HDACs inhibition by quisinostat may become a novel therapeutic option in PAH.

METHODS

See supplementary material for detailed methods.

Human lung samples and cell culture

Collection of lung specimens was approved by the local ethical committee and written informed consent from patients was obtained. Human pulmonary MVECs and PASMCs were isolated and cultured from idiopathic PAH patients and control lung explant tissue as previously described [26]. Cells between passage 5 and 8 were used for experiments.

Cell count analysis and proliferation assays

MVECs were pretreated with vehicle or quisinostat (1 μM) for 48h and the number of cells was counted using a TC20™ Automated Cell Counter (Bio-Rad). MVECs or PASMCs

were pretreated with vehicle or quisinostat (1 or 5 μM) for 24h and Cell viability (MTT) assays were performed as described previously [26].

Determination of PASMC growth in cultured medium of MVECs

PAH MVECs were pretreated with vehicle or quisinostat (1 μM) for 24 h. Conditioned medium from these cells was added to serum starved control PASMCs and incubated for 48 hours after which the number of cells were counted using TC20™ Automated Cell Counter (Bio-Rad). Of note, the half-life of quisinostat is 2 hours.

Quisinostat treatment in the SuHx PAH rat model

The SuHx PAH model was induced according to previously published protocol [26]. Briefly, adult male Sprague-Dawley rats were subjected to a single subcutaneous injection of SU5416 (25 mg/kg) followed by a 4-week transient exposure to 10% hypoxia and 4 weeks of normoxic re-exposure. After randomization, animals were divided into two groups receiving 5 mg/kg quisinostat (SuHx+Q, n = 9) or vehicle (5% DMSO; SuHx, n = 9) in drinking water from week 6 to week 10. At the end of the experiment, rats were anaesthetized for hemodynamic assessment via echocardiography and RV catheterization, after which rats were exsanguinated. All measurements and analyses were done in a blinded manner. See supplementary material for more details.

Quisinostat treatment in the MF PAH rat model

The MF rat PAH model was induced as described previously [27]. Briefly, adult male Lewis rats were subjected to a single subcutaneous injection of 60 mg/kg monocrotaline (MCT) followed by aorto-caval shunt surgery at day 7, which approximately doubles pulmonary blood flow. MF induces neomuscularization and medial hypertrophy from day 7 to 14, neointimal lesions from day 14 to 21 and RV failure from day 21 to 28. Rats were randomly assigned to 3 groups: 1) MF rats sacrificed at day 21 (MF21) as a baseline group; 2) treatment with vehicle (5% DMSO in drinking water) from day 21 to 35 (MF35 Veh); 3) treatment from day 21 to 35 with 5 mg/kg quisinostat (MF35 Q). At the end of the experiment, rats were anaesthetized for hemodynamic assessment via echocardiography and RV catheterization, after which rats were exsanguinated. All measurements and analyses were done in a blinded manner. See supplementary material for more details.

Quisinostat treatment in the PAB induced RV pressure load rat model

To assess direct myocardial effects of quisinostat, isolated RV pressure load was created in 16 adult male Wistar rats by main pulmonary artery banding (PAB) surgery as described previously, with a tight constriction at the size of an 18G needle [27]. At day 28, Rats were randomly assigned to 1) treatment with vehicle (5% DMSO in drinking water) from day 28 to 56 (PAB), or 2) treatment with 5 mg/kg quisinostat from day 28 to 56 (PAB+Q). Before sacrifice, all rats underwent hemodynamic evaluation by echocardiography, after which lungs and hearts were collected for histopathologic evaluation.

Fulton index measurement

To assess the extent of RV hypertrophy, the RV free wall was separated from the left ventricle (LV) and ventricular septum. Wet weights of the RV, free LV and septum were determined separately, and the ratio of RV weight to LV plus interventricular septum weight (Fulton index: RV/[LV+S]) was calculated for RV hypertrophy.

Statistical analysis

Statistical analyses were performed using the GraphPad Prism software for windows, version 8.0. Normality of data was checked and either log-transformation or non-parametric test was performed if data was not normally distributed. Unpaired student's t-tests were used for comparisons between two groups. Multiple comparisons were assessed by one-way ANOVA, followed by Bonferroni's post-hoc test. Two-way ANOVA for repeated measurements followed by Sidak's post-hoc was used for repeated data of echocardiography analysis. Kruskal-wallis test followed by Dunn's multiple comparison test was used for data that was not normally distributed. A value of $P < 0.05$ was considered significant. All statistical tests used two-sided tests of significance. Data are presented as mean ± SEM.

RESULTS

HDAC1 is increased in PAH and quisinostat reduces HDAC1 activity in PAH MVECs

Because HDAC1 has a key role in the uncontrolled proliferation of cancer cells [14, 28], we measured its expression level in lung lysates from PAH patients. General patient characteristics and hemodynamics are presented in (Table 1). As shown by western blot analysis, the protein expression of HDAC1 in lung lysates of PAH patients was significantly increased (Fig.1A). Consistently, we found a trend of increased HDAC1

protein expression in primary lung MVECs from PAH patients (Fig. 1B). PAH MVECs treated with quisinostat for 24 hours significantly reduced HDAC1 activity in a dose dependent manner, as shown by reduced GJA1 and Cyclin D1 (Fig.1D, E), while there was not differences in HDAC1 mRNA levels (Fig.1C).

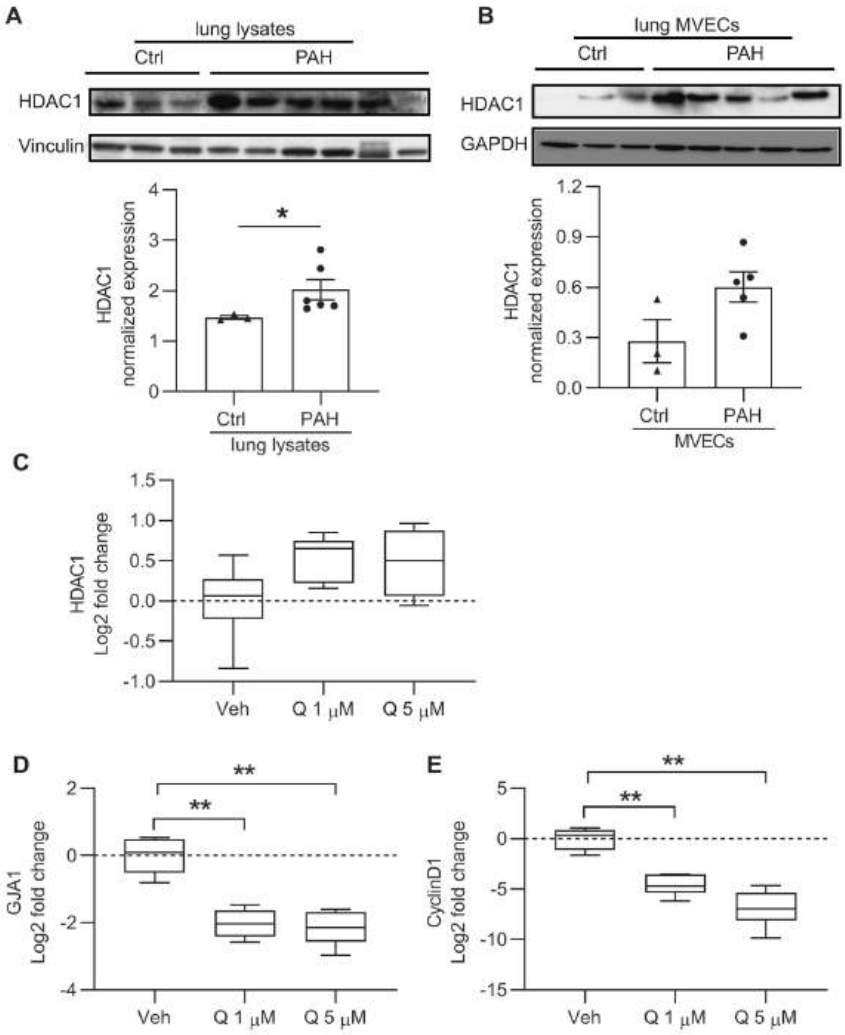

Figure 1. HDAC1 expression is increased in PAH and quisinostat reduces HDAC1 activity in microvascular ECs.

(A, B) HDAC1 western blot images and quantification on lung lysates (A) and lung MVECs (B) of ctrl donors and PAH patients. **(C-E)** qRT-PCR was performed to assess mRNA expression of HDAC1 (C), GJA1 (D) and Cyclin D1 (E) following treatment with DMSO or quisinostat 1 or 5 μM in PAH MVECs for 24 hours. *p<0.05, **p<0.01. Error bars in (A, B): mean ± s.e.m. Error bars in (C-E): min to max. Ctrl: control; Veh: vehicle; Q: quisinostat.

Quisinostat treatment reduced RV afterload and pulmonary vascular remodeling in experimentally induced PAH rats

To assess therapeutic efficacy and safety of HDAC inhibition by quisinostat, we employed two experimental models of PAH (the SuHx and MF rat model) and one model of isolated RV pressure overload (PAB). While protein expression of HDAC1 was unaltered in whole lung lysates from SuHx rats, its activity was increased, as shown by a reduced level of acetylated α-tubulin (Fig. 2A-C). Four weeks of treatment with quisinostat reduced HDAC activity in the SuHx pulmonary vasculature (Fig. 2D, E). Since body weight at the end of the study was lower in quisinostat treated rats, we used body surface area (BSA) to index all hemodynamic parameters where applicable. As shown by pressure-volume loop analysis, quisinostat reduced RV systolic pressure (RVSP) and arterial elastance (Ea) index in SuHx rats (Fig. 2F). Consistently, as revealed by echocardiography analysis, quisinostat reduced PAAT/cl% and total pulmonary resistance index (TPRI) (Fig. 2G). To elucidate the origin of the reduced RV afterload, we further measured pulmonary vascular remodeling and found that quisinostat reduced the percentage of occluded vessels (Fig. 2H, I). Quisinostat reversed vascular remodeling in the intima layer, but not the media layer (Fig. 2J). In MF induced PAH rats, two weeks of treatment with quisinostat did not affect RV afterload, as revealed by unchanged RVSP, PAAT/cl% and TPRI (Fig. 3A, B). However, histology analysis showed that quisinostat treatment reduced the intima layer thickness and not the media layer thickness, consistent with findings in the SuHx lung (Fig. 3C, D).

Quisinostat has no direct effects on the RV in experimental PAH models

Previous studies indicated that HDAC inhibitors may compromise RV adaptation to pressure overload [21]. Here, using pressure-volume analysis, we observed no changes in RV function in SuHx rats after quisinostat treatment. RV stiffness, RV relaxation, RV contractility and RV coupling were all unchanged (Supplement Fig. 1A, B). Likewise, no changes in SVI or TAPSE were seen by echocardiography (Supplement Fig. 1C). Further measurements of RV remodeling by echocardiography revealed that quisinostat did not delay the progression of RV dilation or reverse RV hypertrophy, as shown by unaltered RVEDD index and RVWT index, respectively (Supplement Fig. 1D). The findings were further confirmed by a constant Fulton index and an unchanged RV CSA (Supplement Fig. 1E, F). In MF induced PAH, quisinostat did not affect cardiac function, as shown by an unchanged CI and TAPSE (Supplement Fig. 1G) and no change in RV hypertrophy (unchanged Fulton index, Supplement Fig. 1H).

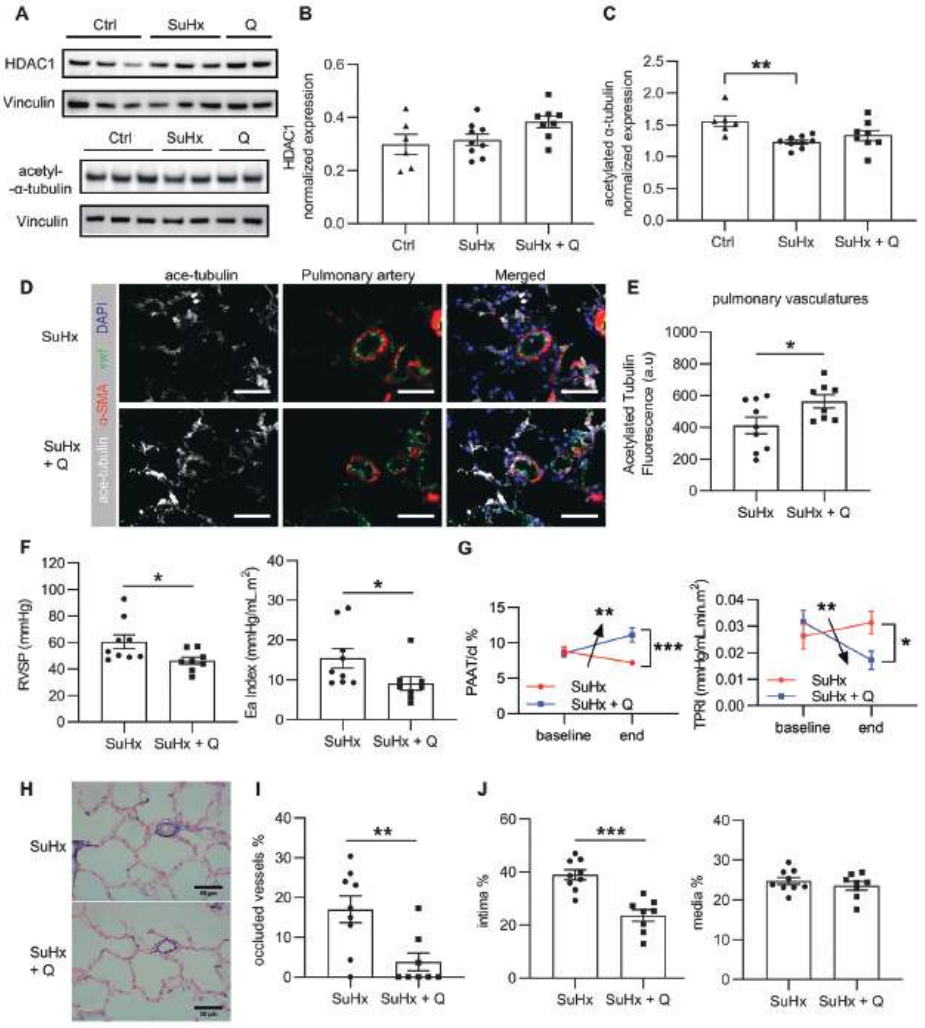

Figure 2. Quisinostat treatment reduced RV afterload and pulmonary vascular remodeling in SuHx rat model.

(A) Representative images of western blot on lung lysates of ctrl, SuHx and quisinostat treated rats. **(B, C)** Western blot quantification reveals that HDAC1 is not changed while acetylated α-tubulin is decreased in lungs of SuHx rats. **(D)** Representative images of immunofluorescence staining on lungs of SuHx rats. White: acetylated α-tubulin, red: α-smooth muscle actin, green: von Willebrand factor, blue: DAPI. **(E)** Quantification of acetylated α-tubulin in pulmonary vasculatures of SuHx and quisinostat treated rats. **(F)** RVSP and Ea index were reduced in SuHx rats by quisinostat, as revealed by pressure-volume loop analysis. **(G)** PAAT/cl% and TPRI were reduced in SuHx rats by quisinostat, as revealed by echocardiography analysis. **(H)** Representative images of EvG staining on lungs of SuHx rats. **(I, J)** Quantification of EvG staining shows that quisinostat reduced occluded vessels and intima layer thickness in SuHx rats. Scale bar = 50 μm. *p<0.05, **p<0.01, ***p<0.001. Data shown as mean ± s.e.m.

To further investigate the direct effects on the RV of HDAC inhibition by quisinostat, we treated PAB rats with quisinostat. Six weeks of quisinostat treatment of PAB rats did not change RV function, as revealed by unchanged CI, TAPSE and RV stroke work (Fig. 3E). Further measurement of RV remodeling revealed no difference in RV hypertrophy (unchanged Fulton index) (Fig. 3F) and constant RV CSA (Fig. 3G, H). Quisinostat did not affect cardiac fibrosis as shown by Masson's trichrome staining in the RV and LV (Fig. 3H).

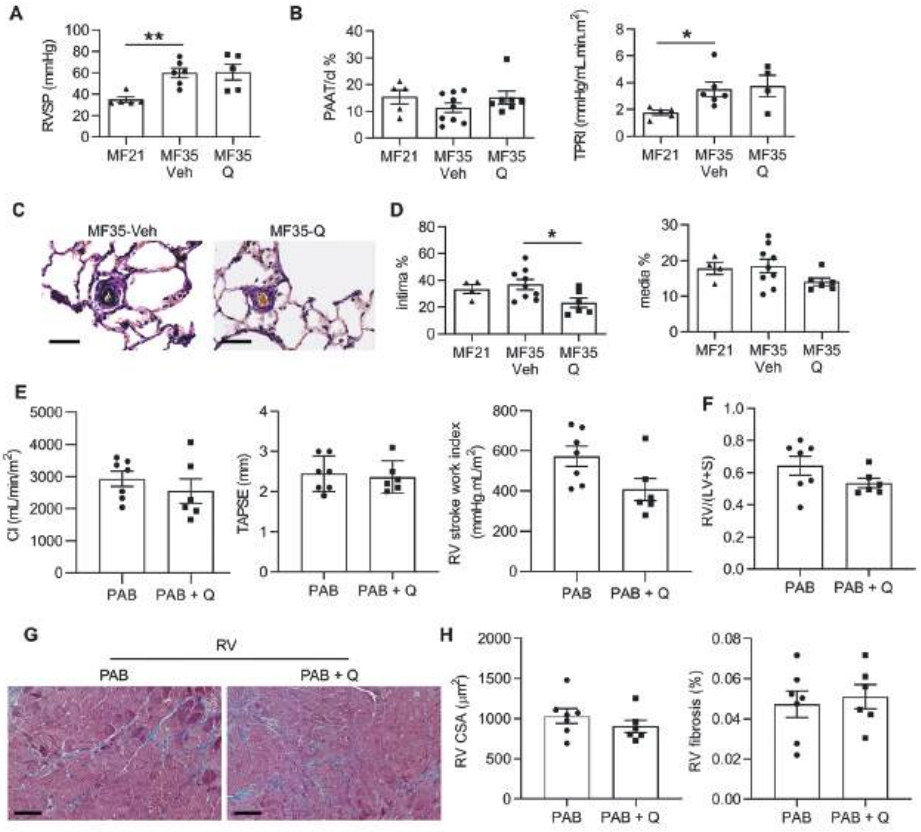

Figure 3. Quisinostat treatment reduced pulmonary vascular remodeling in MCT-flow rat model while had no effect on PAB rat model.

(A) In MCT-flow rats, RVSP was not changed by quisinostat, as revealed by right heart catheterization. **(B)** PAAT/cl% and TPRI were unchanged in MCT-flow rats by quisinostat, as revealed by echocardiography analysis. **(C)** Representative images of EvG staining on lungs of MCT-flow rats. Scale bar = 50 µm. **(D)** Quantification of EvG staining shows that quisinostat reduced intima layer thickness in MCT-flow rats. **(E)** In PAB rats, quisinostat treatment did not affect RV function as shown by echocardiography. **(F)** Fulton index in PAB rats as shown by RV/(LV+S). **(G)** Representative images of Masson's trichrome staining on the RV. Scale bar = 100 µm. **(H)** Quantification of CSA and fibrosis in the RV. *p<0.05. Data shown as mean ± s.e.m.

Quisinostat reduced proliferation in PAH MVECs and PAH animal models

To further elucidate the effects on pulmonary vascular remodeling in the two PAH models, we examined the effect of quisinostat on proliferation and apoptosis. Quisinostat reduced the proliferation of cultured pulmonary MVECs from control and PAH patients alike (Fig. 4A, B), which is consistent with the reduced intima layer thickness observed in the PAH rat models. An MTT assay confirmed that quisinostat reduced proliferation of PAH MVECs in a dose dependent manner (Fig. 4C). Moreover, despite unaltered media layer thickness observed in vivo, the conditioned medium from PAH MVECs treated with quisinostat was found to reduce proliferation in PASMCs (Fig. 4D).

Consistent with the anti-proliferative effect observed in vitro, chronic treatment with quisinostat reduced PCNA immunofluorescence staining of the pulmonary vasculature in SuHx rats (Fig. 4E, F). Quisinostat treatment did not change the degree of apoptosis in either PAH animal model, as shown by unchanged cleaved caspase-3 immunofluorescence staining and western blot (Supplement Fig. 2A-E).

Quisinostat reduced inflammation in PAH MVECs and PAH animal models

HDAC inhibitors exert anti-inflammatory actions in multiple diseases, via effects on monocytes and macrophages, as well as by inhibiting pro-inflammatory cytokines, chemokines and nitric oxide [29]. In order to elucidate the anti-inflammatory effects of quisinostat in PAH, we measured inflammatory responses of PAH MVECs following TNF-α stimulation. As shown by qRT-PCR, quisinostat significantly reduced the level of pro-inflammatory cytokines and chemokines in PAH MVECs, including TNF-α, IL-6, MCP-1 and CCL5 (Fig. 5A-D). Moreover, quisinostat reduced inflammatory cell adhesion to PAH MVECs, as shown by decreased gene expression of VCAM1 and ICAM1 (Fig. 5E, F). Consistent with the anti-inflammatory effects in PAH MVECs, chronic treatment with quisinostat reduced perivascular inflammation in the lungs from SuHx rats, as revealed by quantification of CD45 immunofluorescence staining (Fig. 5G, H).

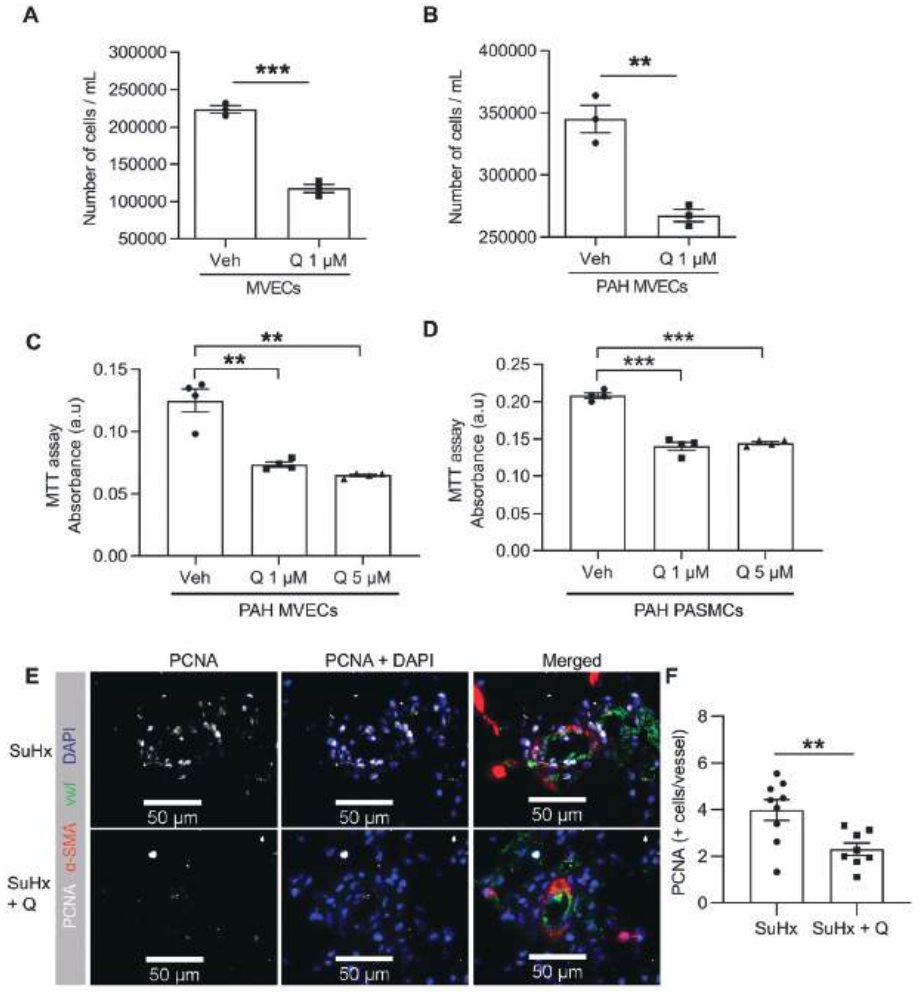

Figure 4. Quisinostat reduces proliferation in PAH MVECs and PAH rat model.
(A, B) Quisinostat reduced proliferation in ctrl MVECs (A) and PAH MVECs (B) as shown by decreased number of cells compared to vehicle group with DMSO after 48 h. **(C)** MTT assays were performed to assess PAH MVEC proliferation following treatment with quisinostat 1 or 5 µM for 24h. **(D)** Assessment of serum starved PASMC proliferation following incubation with conditioned medium from PAH MVECs with DMSO, quisinostat 1 µM or 5 µM. **(E)** Representative images of PCNA immunofluorescence staining on lung slides of SuHx rats with or without quisinostat treatment. White: PCNA, red: α-smooth muscle actin, green: von Willebrand factor, blue: DAPI. Scale bar = 50 µm. **(F)** Quantification of PCNA positive cells reveals that quisinostat reduced pulmonary vascular proliferation in SuHx rats. **p<0.01, ***p<0.001. Data shown as mean ± s.e.m.

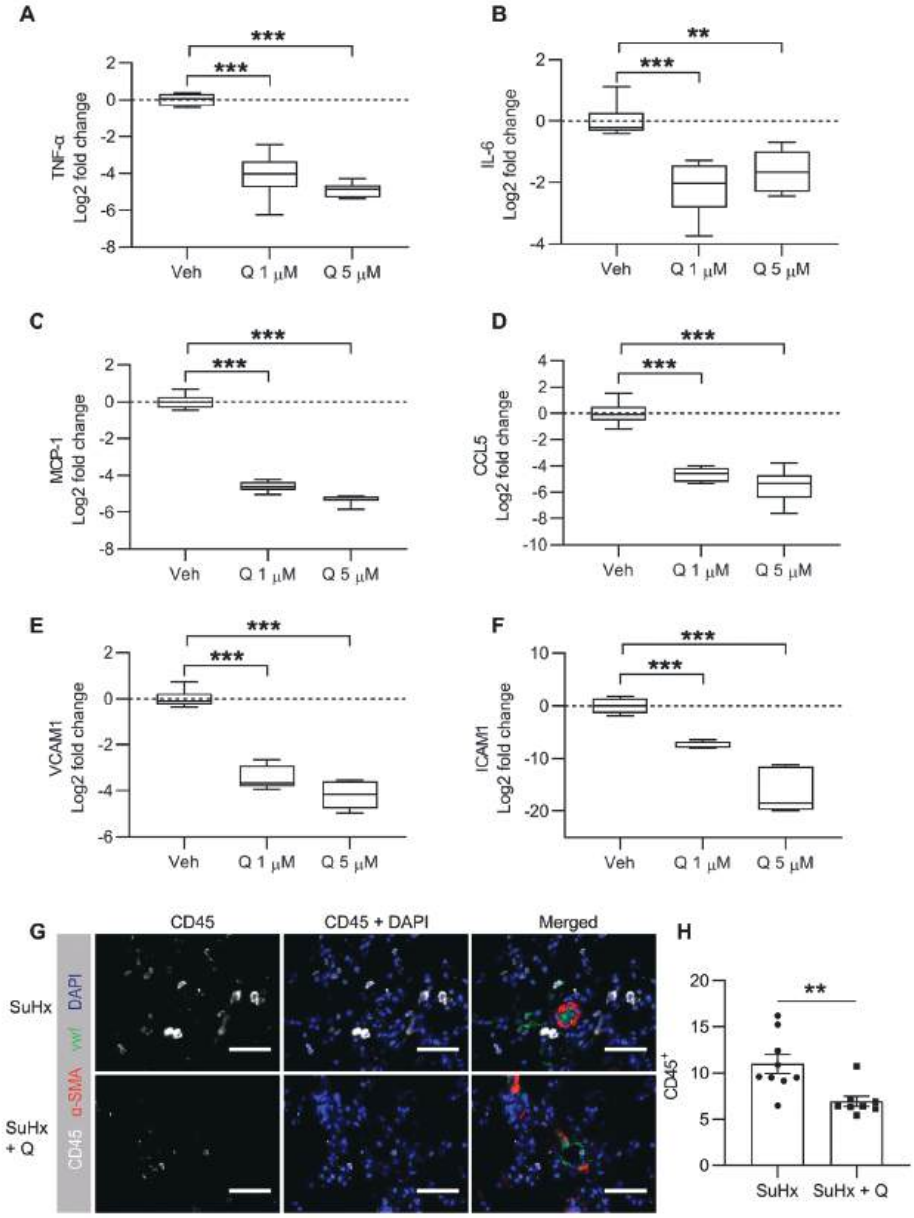

Figure 5. Quisinostat reduces inflammation in PAH MVECs and PAH rat model.
(A-F) qRT-PCR was performed to assess RNA expression of TNF-α (A), IL-6 (B), MCP-1 (C), CCL5 (D), VCAM1 (E) and ICAM1 (F) following treatment with DMSO or quisinostat in TNF-α stimulated PAH MVECs. **(G)** Representative images of CD45 immunofluorescence staining on lung slides of SuHx rats with or without quisinostat treatment. White: CD45, red: α-smooth muscle actin, green: von Willebrand factor, blue: DAPI. Scale bar = 50 μm. **(H)** Quantification of CD45 positive cells around the vessels reveals that quisinostat reduced perivascular inflammation in lungs of SuHx rats. **p<0.01, ***p<0.001. Error bars in (A-F): min to max. Data shown as mean ± s.e.m (H).

Quisinostat did not normalize BMP/TGF-β signaling in PAH MVECs or PAH rat model

As HDACs are known to regulate the BMP and TGF-β signaling pathways in multiple types of cells [30], we hypothesized that quisinostat may benefit PAH via affecting the BMP/TGF-β signaling pathway. However, we did not find increased BMPR2 in PAH MVECs after quisinostat treatment (Supplement Fig. 3A). In the SuHx rat model, the BMPR2 receptor as well as downstream signaling was unaltered after quisinostat treatment, as shown by western blot of whole lung lysates and immunofluorescence staining of the pulmonary vasculature (Supplement Fig. 3B-F). Although quisinostat reduced mRNA expression of the TGF-β target gene PAI-1 in PAH MVECs in a dose dependent manner (Supplement Fig. 4A), no reduction in PAI-1 protein was seen in the lungs from SuHx rats (Supplement Fig. 4B). P-smad 2/3 levels were unaltered after quisinostat treatment (Supplement Fig. 4C-E).

Table 3. PAH related HDACs and inflammation

HDAC class		PAH patient	PAH animal	Inflammatory cells	Cytokines
HDAC I	HDAC1	↑	↑	T-cell activation	TNF-α, IL-6, MCP-1, CCL5
	HDAC2	↑	↑	Macrophage activation	IL-6, MCP-1
	HDAC3		↑	Macrophage activation; monocyte adhesion	IL-1β, VACM-1, MCP-1
	HDAC8	↑			IL-1β
HDAC IIa	HDAC4	↑	↑	Macrophage activation; monocyte adhesion	VCAM-1
	HDAC5	↑	↑	Macrophage activation, differentiation and proliferation; monocyte adhesion	TNF-α
	HDAC7				
	HDAC9				
HDAC IIb	HDAC6	↑	↑	T-cell activation; macrophage activation	TNF-α, IL-1β, IL-6
	HDAC10				
HDAC III	Sirtuins				
HDAC IV	HDAC11				

DISCUSSION

The current study demonstrates for the first time that the second-generation HDAC inhibitor quisinostat inhibits proliferation and inflammation of primary vascular cells from PAH patients and reverses pulmonary vascular remodeling in experimentally induced PAH. Moreover, our data indicate that quisinostat has no adverse effects on RV function or RV remodeling. Therefore, quisinostat could be a novel promising therapeutic option for PAH.

Increased HDACs in PAH and the inhibition effect of quisinostat

HDACs play a pivotal role in cell survival, proliferation and various other key processes, and dysregulated activity of HDACs is implicated in multiple diseases [31, 32]. In mammals, there are four major classes of HDACs, as shown in Table 1 [31]. In PAH, multiple studies have demonstrated increased HDAC expression in pulmonary tissues from PAH patients and animals with experimentally induced PAH (Table 3), including human lung homogenates (HDAC1, HDAC4, HDAC5, HDAC8) [15, 16], PA (HDAC1 and 8) [15], PAH-PAECs (HDAC4 and HDAC5) [18], PAAFs (HDAC1, 2 and 8) [15], and PAAFs from chronically hypoxic calves (HDAC1, HDAC2 and HDAC3) [33], increased mRNA and protein level of HDACs 3, 4 and 5 in isolated PA in MCT PAH rats [34], up-regulated HDAC6 in lungs, distal PAs, and isolated PASMCs and PAECs from PAH patients and animal models (MCT and SuHx) [17]. Class I HDAC activity seems particularly relevant for the development of PAH, particularly HDAC1 which plays a key role in the uncontrolled proliferation of cancer cells [14, 28]. More interestingly, HDAC1 has been recently found to induce proliferation in various non-cancer cells, such as cardiac fibroblasts, pancreatic beta cells, as well as PASMCs [35-38]. In the current study, we measured HDAC1 expression in lungs and MVECs of PAH patients. Consistent with previous studies, we found that the protein expression of HDAC1 was increased in lung tissues from PAH patients. Moreover, we showed for the first time a moderately increased HDAC1 expression in primary lung MVECs from PAH patients. HDAC1 protein expression was unchanged in the SuHx rat lung, which might differ with the human situation by the fact that human samples were from patients with end-stage PAH, while the SuHx rat model represents an earlier stage of PAH. Despite unchanged HDAC1 expression, HDACs activity was increased in lung tissues of SuHx rat, as shown by decreased acetyl-α-tubulin levels.

Quisinostat treatment in experimentally induced PAH

HDAC inhibitors are small molecules designed to block dysregulated HDAC activity by binding to the active enzymatic sites in multiple HDACs [39, 40]. Several HDAC inhibitors have been approved for the treatment of some types of cancer, because of their ability to inhibit proliferation and induce apoptosis. However, the efficacy of most current HDAC inhibitors is limited due to their suboptimal potency for class I HDACs and transient pharmacodynamic responses. The novel HDAC inhibitor quisinostat was identified to improve the effects on proliferation and apoptosis. As a second generation oral inhibitor, quisinostat shows a broad spectrum of inhibition toward both class I (HDAC1-3, 8) and class II (HDAC4-6) HDAC family members, with a prolonged pharmacodynamic response *in vivo* [22]. Compared to the commonly used HDAC inhibitors, quisinostat shows a more potent inhibition on PAH related HDACs which are found to be aberrant in PAH. Quisinostat has the highest potency against HDAC1, which is 20-fold more potent than R306465 and 530-fold more potent than vorinostat *in vitro* [22]. In agreement with previous studies, our results show that quisinostat reduces the activity of HDAC1 and HDACs overall in MVECs in a dose dependent manner, as shown by deceased gene expression levels of GJA1 and Cyclin D1, respectively, which have been shown to be the downstream targets [41, 42]. Moreover, chronic treatment with quisinostat reduces the activity of HDACs *in vivo* as shown by increased acetylated tubulin in pulmonary vasculatures.

Therapeutic benefits of HDACs inhibitors were suggested in PAH animal models, particularly when applying valproic acid, vorinostat and MC1568 [16, 18, 43]. However, TSA is also reported to have no effect on SuHx rats and that the drug could even induce cardiac functional deterioration in PAB rats [20, 21]. We hypothesized that quisinostat could have superior efficacy in PAH, based on a superior inhibition on PAH related HDACs and a prolonged pharmacodynamic response. Indeed, we found that quisinostat treatment for four weeks partly reversed established PAH in SuHx rats, particularly through affecting intima layer thickness. Moreover, two weeks of quisinostat treatment reduced intima layer remodeling in MF rats, while hemodynamics was not improved, suggesting a limited role of intima remodeling in this PAH model. Together these data demonstrate that the beneficial effects of quisinostat treatment on intima layer remodeling are not PAH model specific.

Based on the observation of reduced pulmonary vascular remodeling *in vivo*, we further investigated the effects of quisinostat on proliferation and apoptosis. A previous study

shows that quisinostat exhibited a more potent anti-proliferative effect in various human cancer cell lines than several other commonly used HDAC inhibitors [22]. Consistent with the potent anti-proliferative effect in cancer cells, we showed that quisinostat had a profound effect on proliferation of primary lung MVECs from PAH patients and non-PAH donors, and also that quisinostat reduced the number of proliferating cells in the pulmonary vasculature *in vivo*. While apoptosis was reported previously, no effect on apoptosis was observed in the current study.

Quisinostat treatment and inflammation

Data from PAH animal models and PAH patients suggest that inflammation contributes to the development of PAH [44]. Recently, an anti-inflammatory characteristic of HDAC inhibitors was revealed, by affecting monocytes and macrophages, as well as inhibiting pro-inflammatory cytokines, chemokines and nitric oxide [29]. Several HDAC inhibitors have been shown to reverse inflammatory diseases, including experimentally induced colitis, arthritis, and LPS-induced septic shock [45]. However, the same HDAC inhibitors were also found to have no effects on inflammation in some other diseases [45]. The divergent effects of HDAC inhibitors on inflammation suggest that the role of each individual HDAC in inflammatory diseases could be variant [45].

The anti-inflammatory effects of HDAC inhibitors in PAH have barely been studied before. The aberrant HDACs (1-6) found in PAH have been shown to regulate inflammation via activation of macrophage and T-cell, and regulation of multiple cytokines including TNF-α, IL-6, MCP-1, CCL5 and VCAM1 [45]. Even though valproic acid can reduce inflammation in an MCT rat model as a prevention intervention, the therapeutic effects of HDAC inhibitors on inflammation and the establishment of PAH is unknown. Compared to the commonly used HDAC inhibitors such as vorinostat, quisinostat has much more inhibition potency against these inflammation related HDACs [22]. In current study, we found that quisinostat can reduce inflammatory responses in PAH ECs, as shown by the large reduction in cytokines and chemokines. This is consistent with the targeted cytokines of HDAC1-6. Moreover, quisinostat can reduce perivascular inflammation in PAH animal models, which reveals quisinostat as a promising anti-inflammatory therapy for PAH.

Quisinostat treatment on the RV

In PAH, survival is determined by the condition of the RV rather than the degree of pulmonary vascular resistance [46]. Therefore, it is important for drugs used in the

treatment of PAH to be beneficial or at least non-toxic to the RV. Previous studies discovered that HDACs are involved in cardiac hypertrophy and a variety of heart diseases, such as arrhythmia, left heart failure, acute coronary syndromes and cardiac hypertrophy [11, 47-49]. Furthermore, a previous study shows that treatment with HDAC inhibitors TSA can induce a functional deterioration in PAB rat model, which was associated with the development of fibrosis and capillary rarefaction in the RV [21]. Therefore, even though HDAC inhibitors might be beneficial to PAH by reducing pulmonary vascular remodeling, they may also worsen the adaptive processes in the heart.

In the current study, despite a reduction of RV afterload in SuHx rats after quisinostat treatment, cardiac function and RV remodeling were not improved accordingly. We therefore tested quisinostat on PAB rat model to investigate the direct effect on the RV. Unlike the beneficial findings on left heart failure or the detrimental effects on PAB rats, here we did not observe any direct effects of quisinostat on the RV. The different observation between quisinostat and TSA could be due to their different potency towards various HDACs. Though lack of direct comparison, quisinostat was shown to have distinct HDAC isotype specificity compared to vorinostat, which is an analog of TSA [50, 51]. Quisinostat exhibited a higher potency against HDAC1, 2 and 4 than vorinostat, while a much lower potency against HDAC6 [22]. While HDAC2 and 4 are found to regulate cardiac hypertrophy [52], HDAC6 can inhibit apoptosis by inducing Suvivin deacetylation [53, 54]. Inhibition of HDAC6 was found to benefit experimental PAH by inducing apoptosis in PAH-PASMCs [17]. However, the independent effects of HDAC6 inhibition on the RV, especially on the apoptosis of RV capillaries, is unknown. Therefore, we speculate that the strong potency of TSA against HDAC6 might explain the capillary rarefaction found in the RV.

Quisinostat as a new therapeutic option for PAH

It has to be noted that although beneficial, the effects of quisinostat are still limited, giving it a lower priority as a promising treatment, when compared to some other novel therapies tested in PAH. With the same PAH animal models, a previous study from our group showed that RVX208, an inhibitor of bromodomain-containing protein 4, not only reduced pulmonary vascular resistance and remodeling, but also had independent beneficial effects on cardiac function and RV remodeling, which were not observed after quisinostat treatment [27]. Therefore, although current study excluded the doubt of cardiac detrimental effects of quisinostat, the establishment of clinical trials with HDAC inhibitors in PAH patients lacks priority compared to other novel therapies.

CONCLUSION

In conclusion, the expression of HDAC1 is increased in the lung of PAH patients and HDAC activity is increased in the PAH vasculature of rats with experimentally induced PAH. Treatment with the second-generation HDAC inhibitor quisinostat can reduce proliferation and inflammatory response in PAH MVECs, and partly reverse pulmonary vascular remodeling in preclinical PAH models by reducing pulmonary vascular proliferation and inflammation. Importantly, it has no adverse effect on cardiac function. Therefore, quisinostat may provide a safe novel therapeutic option by inhibiting HDACs in PAH.

DISCLOSURES

None

ACKNOWLEDGEMENTS

Michel Weij and Annemieke van Oosten of the University Medical Center Groningen are acknowledged for performing the aortocaval shunt surgery and hemodynamic measurements. Xiaoke Pan of the VU Medical Center in Amsterdam is acknowledged for optimizing the human microvascular endothelial cell culture.

REFERENCES

1. Rubin LJ. Primary pulmonary hypertension. N Engl J Med 1997;336:111-7.
2. Morrell NW, Adnot S, Archer SL, Dupuis J, Jones PL, MacLean MR, et al. Cellular and molecular basis of pulmonary arterial hypertension. J Am Coll Cardiol. 2009;54(1 Suppl):S20-31. Epub 2009/07/09. doi: 10.1016/j.jacc.2009.04.018. PubMed PMID: 19555855; PubMed Central PMCID: PMCPMC2790324.
3. Voelkel NF, Gomez-Arroyo J, Abbate A, Bogaard HJ, Nicolls MR. Pathobiology of pulmonary arterial hypertension and right ventricular failure. Eur Respir J. 2012;40(6):1555-65. Epub 2012/06/30. doi: 10.1183/09031936.00046612. PubMed PMID: 22743666; PubMed Central PMCID: PMCPMC4019748.
4. Le Hiress M, Tu L, Ricard N, Phan C, Thuillet R, Fadel E, et al. Proinflammatory Signature of the Dysfunctional Endothelium in Pulmonary Hypertension. Role of the Macrophage Migration Inhibitory Factor/CD74 Complex. Am J Respir Crit Care Med. 2015;192(8):983-97. Epub 2015/07/24. doi: 10.1164/rccm.201402-0322OC. PubMed PMID: 26203495.
5. Savai R, Pullamsetti SS, Kolbe J, Bieniek E, Voswinckel R, Fink L, et al. Immune and inflammatory cell involvement in the pathology of idiopathic pulmonary arterial hypertension. Am J Respir Crit Care Med. 2012;186(9):897-908. Epub 2012/09/08. doi: 10.1164/rccm.201202-0335OC. PubMed PMID: 22955318.
6. Lajoie AC, Lauziere G, Lega JC, Lacasse Y, Martin S, Simard S, et al. Combination therapy versus monotherapy for pulmonary arterial hypertension: a meta-analysis. Lancet Respir Med. 2016;4(4):291-305. Epub 2016/03/05. doi: 10.1016/S2213-2600(16)00027-8. PubMed PMID: 26935844.
7. Kim JD, Lee A, Choi J, Park Y, Kang H, Chang W, et al. Epigenetic modulation as a therapeutic approach for pulmonary arterial hypertension. Exp Mol Med. 2015;47:e175. Epub 2015/08/01. doi: 10.1038/emm.2015.45. PubMed PMID: 26228095; PubMed Central PMCID: PMCPMC4525299.
8. Saco TV, Parthasarathy PT, Cho Y, Lockey RF, Kolliputi N. Role of epigenetics in pulmonary hypertension. Am J Physiol Cell Physiol. 2014;306(12):C1101-5. Epub 2014/04/11. doi: 10.1152/ajpcell.00314.2013. PubMed PMID: 24717578; PubMed Central PMCID: PMCPMC4060002.
9. Lalonde ME, Cheng X, Cote J. Histone target selection within chromatin: an exemplary case of teamwork. Gene Dev. 2014;28(10):1029-41. doi: 10.1101/gad.236331.113. PubMed PMID: WOS:000336497800001.
10. Peserico A, Simone C. Physical and functional HAT/HDAC interplay regulates protein acetylation balance. J Biomed Biotechnol. 2011;2011(1110-7251 (Electronic)):371832. Epub 2010/12/15. doi: 10.1155/2011/371832. PubMed PMID: 21151613; PubMed Central PMCID: PMCPMC2997516.
11. Kong Y, Tannous P, Lu G, Berenji K, Rothermel BA, Olson EN, et al. Suppression of class I and II histone deacetylases blunts pressure-overload cardiac hypertrophy. Circulation. 2006;113(22):2579-88. Epub 2006/06/01. doi: 10.1161/CIRCULATIONAHA.106.625467. PubMed PMID: 16735673; PubMed Central PMCID: PMCPMC4105979.

12. McKinsey TA. Therapeutic potential for HDAC inhibitors in the heart. Annu Rev Pharmacol Toxicol. 2012;52:303-19. Epub 2011/09/29. doi: 10.1146/annurev-pharmtox-010611-134712. PubMed PMID: 21942627.
13. Gatla HR, Muniraj N, Thevkar P, Yavvari S, Sukhavasi S, Makena MR. Regulation of Chemokines and Cytokines by Histone Deacetylases and an Update on Histone Decetylase Inhibitors in Human Diseases. Int J Mol Sci. 2019;20(5). Epub 2019/03/08. doi: 10.3390/ijms20051110. PubMed PMID: 30841513; PubMed Central PMCID: PMCPMC6429312.
14. Glaser KB, Li JL, Staver MJ, Wei RQ, Albert DH, Davidsen SK. Role of Class I and Class II histone deacetylases in carcinoma cells using siRNA. Biochem Bioph Res Co. 2003;310(2):529-36. doi: 10.1016/j.bbrc.2003.09.043. PubMed PMID: WOS:000185904300041.
15. Chelladurai P, Dabral S, Basineni SR, Chen CN, Schmoranzer M, Bender N, et al. Isoform-specific characterization of class I histone deacetylases and their therapeutic modulation in pulmonary hypertension. Sci Rep. 2020;10(1):12864. Epub 2020/08/01. doi: 10.1038/s41598-020-69737-x. PubMed PMID: 32733053; PubMed Central PMCID: PMCPMC7393135.
16. Zhao L, Chen CN, Hajji N, Oliver E, Cotroneo E, Wharton J, et al. Histone deacetylation inhibition in pulmonary hypertension: therapeutic potential of valproic acid and suberoylanilide hydroxamic acid. Circulation. 2012;126(4):455-67. Epub 2012/06/20. doi: 10.1161/CIRCULATIONAHA.112.103176. PubMed PMID: 22711276; PubMed Central PMCID: PMCPMC3799888.
17. Boucherat O, Chabot S, Paulin R, Trinh I, Bourgeois A, Potus F, et al. HDAC6: A Novel Histone Deacetylase Implicated in Pulmonary Arterial Hypertension. Sci Rep. 2017;7(1):4546. Epub 2017/07/05. doi: 10.1038/s41598-017-04874-4. PubMed PMID: 28674407; PubMed Central PMCID: PMCPMC5495763.
18. Kim J, Hwangbo C, Hu X, Kang Y, Papangeli I, Mehrotra D, et al. Restoration of impaired endothelial myocyte enhancer factor 2 function rescues pulmonary arterial hypertension. Circulation. 2015;131(2):190-9. Epub 2014/10/23. doi: 10.1161/CIRCULATIONAHA.114.013339. PubMed PMID: 25336633; PubMed Central PMCID: PMCPMC4293354.
19. Chelladurai P, Seeger W, Pullamsetti SS. Epigenetic mechanisms in pulmonary arterial hypertension: the need for global perspectives. Eur Respir Rev. 2016;25(140):135-40. Epub 2016/06/02. doi: 10.1183/16000617.0036-2016. PubMed PMID: 27246590.
20. De Raaf MA, Hussaini AA, Gomez-Arroyo J, Kraskaukas D, Farkas D, Happe C, et al. Histone deacetylase inhibition with trichostatin A does not reverse severe angioproliferative pulmonary hypertension in rats (2013 Grover Conference series). Pulm Circ. 2014;4(2):237-43. Epub 2014/07/10. doi: 10.1086/675986. PubMed PMID: 25006442; PubMed Central PMCID: PMCPMC4070779.
21. Bogaard HJ, Mizuno S, Hussaini AA, Toldo S, Abbate A, Kraskauskas D, et al. Suppression of histone deacetylases worsens right ventricular dysfunction after pulmonary artery banding in rats. Am J Respir Crit Care Med. 2011;183(10):1402-10. Epub 2011/02/08. doi: 10.1164/rccm.201007-1106OC. PubMed PMID: 21297075.
22. Arts J, King P, Marien A, Floren W, Belien A, Janssen L, et al. JNJ-26481585, a novel "second-generation" oral histone deacetylase inhibitor, shows broad-spectrum preclinical antitumoral activity. Clin Cancer Res. 2009;15(22):6841-51. Epub 2009/10/29. doi: 10.1158/1078-0432.CCR-09-0547. PubMed PMID: 19861438.

23. Venugopal B, Baird R, Kristeleit RS, Plummer R, Cowan R, Stewart A, et al. A phase I study of quisinostat (JNJ-26481585), an oral hydroxamate histone deacetylase inhibitor with evidence of target modulation and antitumor activity, in patients with advanced solid tumors. Clin Cancer Res. 2013;19(15):4262-72. Epub 2013/06/07. doi: 10.1158/1078-0432.CCR-13-0312. PubMed PMID: 23741066.
24. Zhong L, Zhou S, Tong R, Shi J, Bai L, Zhu Y, et al. Preclinical assessment of histone deacetylase inhibitor quisinostat as a therapeutic agent against esophageal squamous cell carcinoma. Invest New Drugs. 2019;37(4):616-24. Epub 2018/09/01. doi: 10.1007/s10637-018-0651-4. PubMed PMID: 30168013.
25. Bao L, Diao H, Dong N, Su X, Wang B, Mo Q, et al. Histone deacetylase inhibitor induces cell apoptosis and cycle arrest in lung cancer cells via mitochondrial injury and p53 up-acetylation. Cell Biol Toxicol. 2016;32(6):469-82. Epub 2016/07/18. doi: 10.1007/s10565-016-9347-8. PubMed PMID: 27423454; PubMed Central PMCID: PMCPMC5099365.
26. Kurakula K, Sun XQ, Happe C, da Silva Goncalves Bos D, Szulcek R, Schalij I, et al. Prevention of progression of pulmonary hypertension by the Nur77 agonist 6-mercaptopurine: role of BMP signalling. Eur Respir J. 2019;54(3). Epub 2019/07/06. doi: 10.1183/13993003.02400-2018. PubMed PMID: 31273046.
27. Van der Feen DE, Kurakula K, Tremblay E, Boucherat O, Bossers GPL, Szulcek R, et al. Multicenter Preclinical Validation of BET Inhibition for the Treatment of Pulmonary Arterial Hypertension. Am J Respir Crit Care Med. 2019;200(7):910-20. Epub 2019/05/03. doi: 10.1164/rccm.201812-2275OC. PubMed PMID: 31042405.
28. Cao LL, Song X, Pei L, Liu L, Wang H, Jia M. Histone deacetylase HDAC1 expression correlates with the progression and prognosis of lung cancer: A meta-analysis. Medicine (Baltimore). 2017;96(31):e7663. Epub 2017/08/03. doi: 10.1097/MD.0000000000007663. PubMed PMID: 28767587; PubMed Central PMCID: PMCPMC5626141.
29. Mohammadi A, Sharifi A, Pourpaknia R, Mohammadian S, Sahebkar A. Manipulating macrophage polarization and function using classical HDAC inhibitors: Implications for autoimmunity and inflammation. Crit Rev Oncol Hematol. 2018;128:1-18. Epub 2018/07/01. doi: 10.1016/j.critrevonc.2018.05.009. PubMed PMID: 29958625.
30. Scholl C, Weibetamuller K, Holenya P, Shaked-Rabi M, Tucker KL, Wolfl S. Distinct and overlapping gene regulatory networks in BMP- and HDAC-controlled cell fate determination in the embryonic forebrain. BMC Genomics. 2012;13:298. Epub 2012/07/04. doi: 10.1186/1471-2164-13-298. PubMed PMID: 22748179; PubMed Central PMCID: PMCPMC3460768.
31. Gallinari P, Di Marco S, Jones P, Pallaoro M, Steinkuhler C. HDACs, histone deacetylation and gene transcription: from molecular biology to cancer therapeutics. Cell Res. 2007;17(3):195-211. Epub 2007/02/28. doi: 10.1038/sj.cr.7310149. PubMed PMID: 17325692.
32. Haberland M, Montgomery RL, Olson EN. The many roles of histone deacetylases in development and physiology: implications for disease and therapy. Nat Rev Genet. 2009;10(1):32-42. Epub 2008/12/10. doi: 10.1038/nrg2485. PubMed PMID: 19065135; PubMed Central PMCID: PMCPMC3215088.

33. Li M, Riddle SR, Frid MG, El Kasmi KC, McKinsey TA, Sokol RJ, et al. Emergence of fibroblasts with a proinflammatory epigenetically altered phenotype in severe hypoxic pulmonary hypertension. J Immunol. 2011;187(5):2711-22. Epub 2011/08/05. doi: 10.4049/jimmunol.1100479. PubMed PMID: 21813768; PubMed Central PMCID: PMCPMC3159707.
34. Chen F, Li X, Aquadro E, Haigh S, Zhou J, Stepp DW, et al. Inhibition of histone deacetylase reduces transcription of NADPH oxidases and ROS production and ameliorates pulmonary arterial hypertension. Free Radic Biol Med. 2016;99:167-78. Epub 2016/10/23. doi: 10.1016/j.freeradbiomed.2016.08.003. PubMed PMID: 27498117; PubMed Central PMCID: PMCPMC5240036.
35. Yang Q, Dahl MJ, Albertine KH, Ramchandran R, Sun M, Raj JU. Role of histone deacetylases in regulation of phenotype of ovine newborn pulmonary arterial smooth muscle cells. Cell Prolif. 2013;46(6):654-64. Epub 2014/01/28. doi: 10.1111/cpr.12076. PubMed PMID: 24460719; PubMed Central PMCID: PMCPMC3904681.
36. Galletti M, Cantoni S, Zambelli F, Valente S, Palazzini M, Manes A, et al. Dissecting histone deacetylase role in pulmonary arterial smooth muscle cell proliferation and migration. Biochem Pharmacol. 2014;91(2):181-90. Epub 2014/07/27. doi: 10.1016/j.bcp.2014.07.011. PubMed PMID: 25063234.
37. Draney C, Austin MC, Leifer AH, Smith CJ, Kener KB, Aitken TJ, et al. HDAC1 overexpression enhances beta-cell proliferation by down-regulating Cdkn1b/p27. Biochem J. 2018;475(24):3997-4010. Epub 2018/10/17. doi: 10.1042/BCJ20180465. PubMed PMID: 30322885.
38. Lin C, Wei D, Xin D, Pan J, Huang M. Ellagic acid inhibits proliferation and migration of cardiac fibroblasts by down-regulating expression of HDAC1. J Toxicol Sci. 2019;44(6):425-33. Epub 2019/06/07. doi: 10.2131/jts.44.425. PubMed PMID: 31168029.
39. Dokmanovic M, Clarke C, Marks PA. Histone deacetylase inhibitors: overview and perspectives. Mol Cancer Res. 2007;5(10):981-9. Epub 2007/10/24. doi: 10.1158/1541-7786.MCR-07-0324. PubMed PMID: 17951399.
40. Zhang L, Zhang J, Jiang Q, Zhang L, Song W. Zinc binding groups for histone deacetylase inhibitors. J Enzyme Inhib Med Chem. 2018;33(1):714-21. Epub 2018/04/05. doi: 10.1080/14756366.2017.1417274. PubMed PMID: 29616828; PubMed Central PMCID: PMCPMC6009916.
41. Hu J, Colburn NH. Histone deacetylase inhibition down-regulates cyclin D1 transcription by inhibiting nuclear factor-kappaB/p65 DNA binding. Mol Cancer Res. 2005;3(2):100-9. Epub 2005/03/10. doi: 10.1158/1541-7786.MCR-04-0070. PubMed PMID: 15755876.
42. Zupkovitz G, Tischler J, Posch M, Sadzak I, Ramsauer K, Egger G, et al. Negative and positive regulation of gene expression by mouse histone deacetylase 1. Mol Cell Biol. 2006;26(21):7913-28. Epub 2006/08/31. doi: 10.1128/MCB.01220-06. PubMed PMID: 16940178; PubMed Central PMCID: PMCPMC1636735.
43. Lan B, Hayama E, Kawaguchi N, Furutani Y, Nakanishi T. Therapeutic efficacy of valproic acid in a combined monocrotaline and chronic hypoxia rat model of severe pulmonary hypertension. PLoS One. 2015;10(1):e0117211. Epub 2015/01/30. doi: 10.1371/journal.pone.0117211. PubMed PMID: 25629315; PubMed Central PMCID: PMCPMC4309681.

44. Groth A, Vrugt B, Brock M, Speich R, Ulrich S, Huber LC. Inflammatory cytokines in pulmonary hypertension. Respir Res. 2014;15:47. Epub 2014/04/18. doi: 10.1186/1465-9921-15-47. PubMed PMID: 24739042; PubMed Central PMCID: PMCPMC4002553.
45. Cantley MD, Haynes DR. Epigenetic regulation of inflammation: progressing from broad acting histone deacetylase (HDAC) inhibitors to targeting specific HDACs. Inflammopharmacology. 2013;21(4):301-7. Epub 2013/01/24. doi: 10.1007/s10787-012-0166-0. PubMed PMID: 23341163.
46. Mauritz GJ, Kind T, Marcus JT, Bogaard HJ, van de Veerdonk M, Postmus PE, et al. Progressive changes in right ventricular geometric shortening and long-term survival in pulmonary arterial hypertension. Chest. 2012;141(4):935-43. Epub 2011/10/01. doi: 10.1378/chest.10-3277. PubMed PMID: 21960697.
47. Liu F, Levin MD, Petrenko NB, Lu MM, Wang T, Yuan LJ, et al. Histone-deacetylase inhibition reverses atrial arrhythmia inducibility and fibrosis in cardiac hypertrophy independent of angiotensin. J Mol Cell Cardiol. 2008;45(6):715-23. Epub 2008/10/18. doi: 10.1016/j.yjmcc.2008.08.015. PubMed PMID: 18926829; PubMed Central PMCID: PMCPMC2630487.
48. Zhao TC, Cheng G, Zhang LX, Tseng YT, Padbury JF. Inhibition of histone deacetylases triggers pharmacologic preconditioning effects against myocardial ischemic injury. Cardiovasc Res. 2007;76(3):473-81. Epub 2007/09/22. doi: 10.1016/j.cardiores.2007.08.010. PubMed PMID: 17884027.
49. Wang Y, Chen P, Wang L, Zhao J, Zhong Z, Wang Y, et al. Inhibition of Histone Deacetylases Prevents Cardiac Remodeling After Myocardial Infarction by Restoring Autophagosome Processing in Cardiac Fibroblasts. Cell Physiol Biochem. 2018;49(5):1999-2011. Epub 2018/09/21. doi: 10.1159/000493672. PubMed PMID: 30235443.
50. Hebbel RP, Vercellotti GM, Pace BS, Solovey AN, Kollander R, Abanonu CF, et al. The HDAC inhibitors trichostatin A and suberoylanilide hydroxamic acid exhibit multiple modalities of benefit for the vascular pathobiology of sickle transgenic mice. Blood. 2010;115(12):2483-90. Epub 2010/01/08. doi: 10.1182/blood-2009-02-204990. PubMed PMID: 20053759; PubMed Central PMCID: PMCPMC2845902.
51. Li W, Sun Z. Mechanism of Action for HDAC Inhibitors-Insights from Omics Approaches. Int J Mol Sci. 2019;20(7). Epub 2019/04/04. doi: 10.3390/ijms20071616. PubMed PMID: 30939743; PubMed Central PMCID: PMCPMC6480157.
52. Kee HJ, Kook H. Roles and targets of class I and IIa histone deacetylases in cardiac hypertrophy. J Biomed Biotechnol. 2011;2011:928326. Epub 2010/12/15. doi: 10.1155/2011/928326. PubMed PMID: 21151616; PubMed Central PMCID: PMCPMC2997602.
53. Matthias P, Yoshida M, Khochbin S. HDAC6 a new cellular stress surveillance factor. Cell cycle (Georgetown, Tex). 2008;7(1):7-10. Epub 2008/01/17. doi: 10.4161/cc.7.1.5186. PubMed PMID: 18196966.
54. Riolo MT, Cooper ZA, Holloway MP, Cheng Y, Bianchi C, Yakirevich E, et al. Histone deacetylase 6 (HDAC6) deacetylates survivin for its nuclear export in breast cancer. The Journal of biological chemistry. 2012;287(14):10885-93. Epub 2012/02/16. doi: 10.1074/jbc.M111.308791. PubMed PMID: 22334690; PubMed Central PMCID: PMCPMC3322878.

SUPPLEMENTAL FIGURES

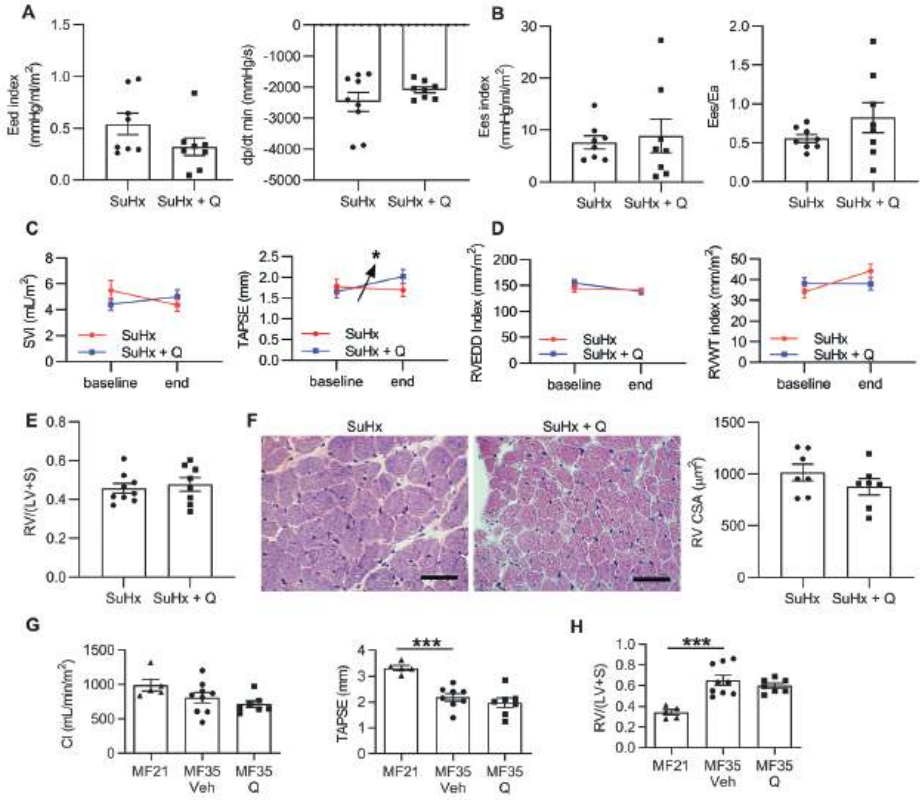

Supplement Figure 1. Quisinostat treatment has no effect on the RV of PAH rat models.
(A, B) In SuHx rat model, quisinostat treatment did not change RV stiffness (Eed index), RV relaxation (dp/dt min) (A), RV contractility (Ees index) or RV coupling (Ees/Ea) (B) as revealed by pressure-volume loop analysis. **(C, D)** Quisinostat did not change cardiac function (C) or RV remodeling (D) in SuHx rats as shown by echocardiography. **(E, F)** Quisinostat did not change RV hypertrophy in SuHx rats as shown by Fulton index (E) and RV CSA (F). Scale bar = 50 µm. **(G)** In MCT-flow rats, quisinostat did not change cardiac function as shown by echocardiography analysis. **(H)** Fulton index of MCT-flow rats after quisinostat treatment. *p<0.05. Data shown as mean ± s.e.m.

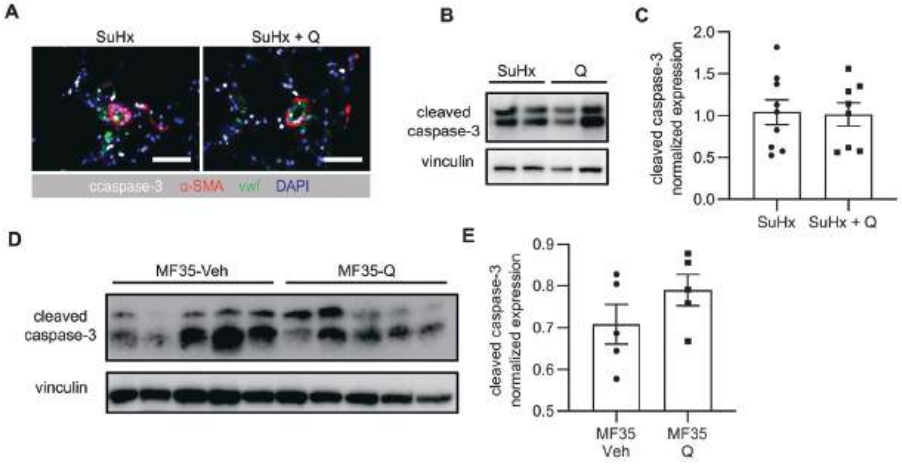

Supplement Figure 2. Quisinostat treatment has no effect on apoptosis in lungs of PAH rat models. **(A)** Representative images of cleaved caspase-3 immunofluorescence staining on lung slides of SuHx rats with or without quisinostat treatment. White: cleaved caspase-3, red: α-smooth muscle actin, green: von Willebrand factor, blue: DAPI. Scale bar = 50 μm. **(B)** Representative images of cleaved caspase-3 western blot on lung lysates of SuHx rats. **(C)** Quantification of cleaved caspase-3 western blot on lung lysates of SuHx rats. **(D)** Representative images of cleaved caspase-3 western blot on lung lysates of MCT-flow rats. **(E)** Quantification of cleaved caspase-3 western blot on lung lysates of MCT-flow rats. Data shown as mean ± s.e.m.

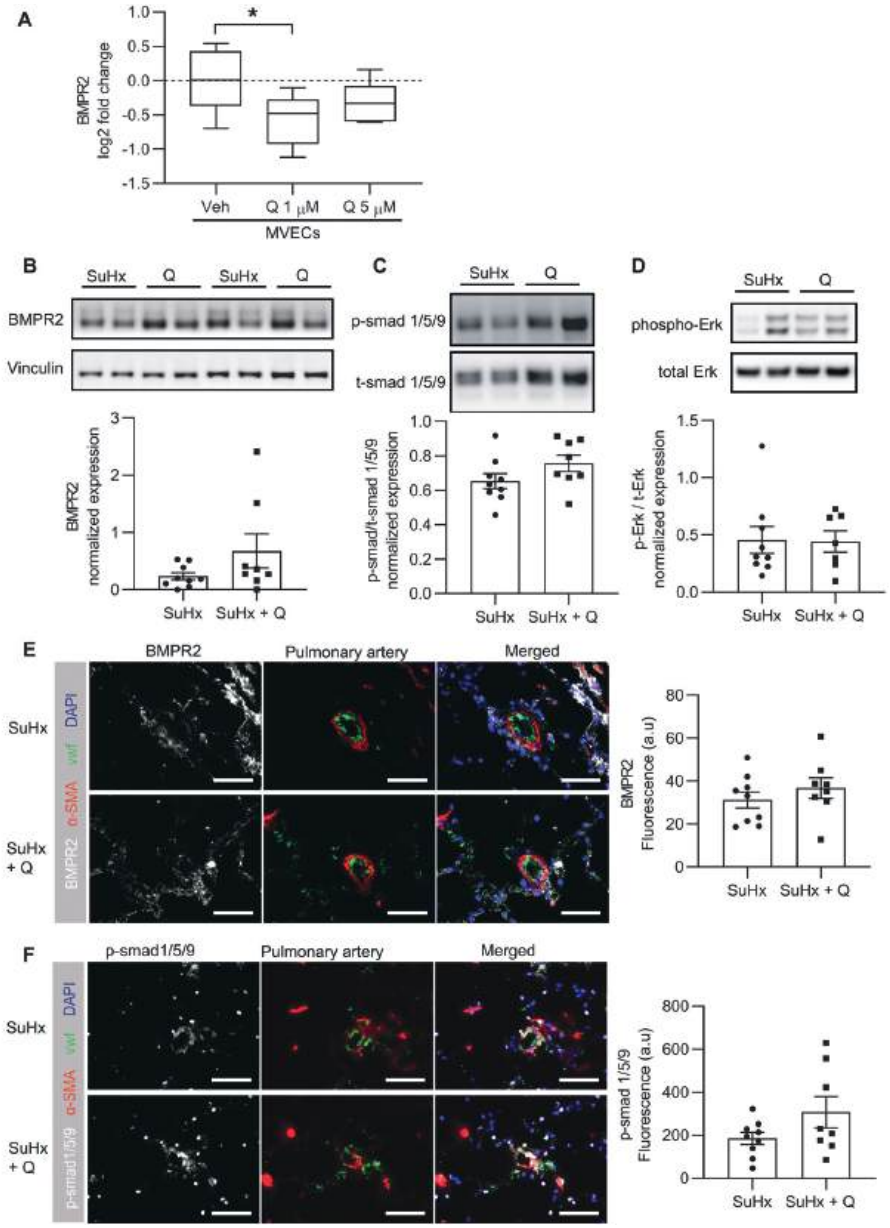

Supplement Figure 3. Quisinostat treatment has no effect on BMPR2 signaling in PAH MVECs and PAH rat model.

(A) qRT-PCR was performed to assess RNA expression of BMPR2 following treatment with DMSO or quisinostat in BMP9 stimulated MVECs. **(B-D)** Western blot of BMPR2 (B), p-smad1/5/9 (C) and phosphor-Erk (D) on lung tissues of SuHx rats following treatment with DMSO or quisinostat. **(E, F)** Immunofluorescence staining of BMPR2 (E) and p-smad1/5/9 (F) on lung slides of SuHx rats with or without quisinostat treatment. White: BMPR2 (E) or p-smad1/5/9 (F), red: α-smooth muscle actin, green: von Willebrand factor, blue: DAPI. Scale bar = 50 μm. Error bars in (A): mean ± s.e.m. Data shown as mean ± s.e.m (B-F).

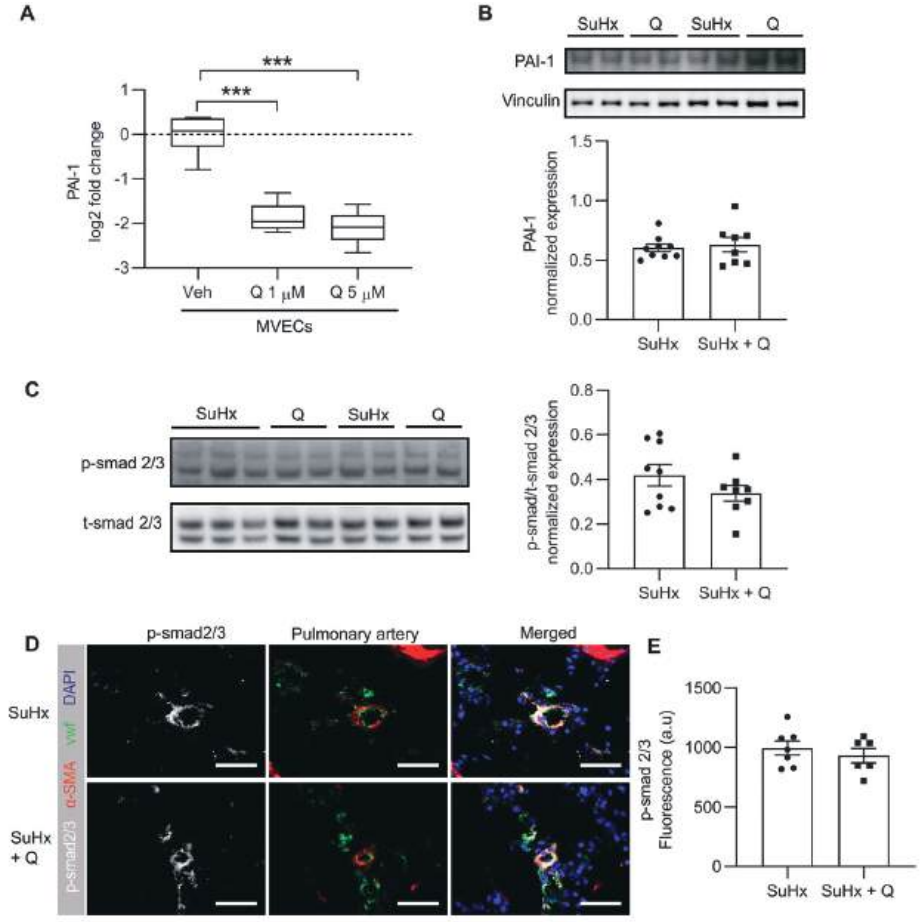

Supplement Figure 4. Quisinostat treatment reduces TGF-β signaling in PAH MVECs and PAH rat model.

(A) qRT-PCR was performed to assess RNA expression of PAI-1 following treatment with DMSO or quisinostat in PAH MVECs. **(B)** Western blot of PAI-1 on lung lysates of SuHx rats. **(C)** Western blot of p-smad 2/3 on lung lysates of SuHx rats. **(D)** Representative images of p-smad 2/3 immunofluorescence staining on lung slides of SuHx rats with or without quisinostat treatment. White: p-smad 2/3, red: α-smooth muscle actin, green: von Willebrand factor, blue: DAPI. Scale bar = 50 μm. **(E)** Quantification of p-smad 2/3 fluorescence in pulmonary vasculatures. *p<0.05. Error bars in (A): mean ± s.e.m. Data shown as mean ± s.e.m (C, E).

SUPPLEMENT METHODS

Cell culture and tissue sections

Collection of lung specimens was approved by the local ethical committee and written informed consent from patients was obtained. Human pulmonary artery microvascular endothelial cells (MVECs), as well as smooth muscle cells (PASMCs) were isolated and cultured from idiopathic PAH patients and control lung explant tissue as previously described [1]. Cells between passage 5 and 8 were used for experiments.

Quantitative Real Time-PCR (qRT-PCR)

Total RNA from cultured cells was isolated using NucleoSpin RNA II isolation kit (Machery Nagel, Düren) following the manufacturer's instructions. All the cDNA was synthesized with the iScript cDNA kit (Bio-Rad) following the manufacturer's instructions. RT-qPCR was performed with SYBR Green Supermix (Bio-Rad) using specific primers on CFX Real-Time PCR detection System (Bio-Rad). qPCR results were analyzed using the delta delta Ct method. GAPDH was used as an internal control for the amount of cDNA present in each sample.

Protein expression by western blot on cells and rat tissues

Whole cell lysates, lung and right ventricle (RV) tissue of the rats was homogenized in radioimmunoprecipitation assay buffer containing phosphatase and protease inhibitors (Sigma-Aldrich). The protein concentration was quantified by the Pierce 660 nm protein assay kit (ThermoFisher Scientific, Rockford, IL, USA), and western blot was performed as described [1]. Briefly, equal amount of protein was loaded on SDS-PAGE and transferred to polyyvinylidene difluoride (PVDF) membraines (Millipore). Blots were blocked by 5% non-fat milk or 5% bovine serum albumin (BSA) for 1 hour at room temperature (RT), and incubated with primary antibody at 4°C overnight, to detect the expression of histone deacytylase 1 (HDAC1) (1:500; NB100-56340; Novus Biologicals, Abingdon, UK), acetylated tubulin (1:1000; T6793, Sigma-Aldrich, St.Louis, MO, USA), cleaved caspase-3 (1:1000; #9611; cell signaling Technology Inc. Beverly, MA, USA), p-smad 2/3 (1:1000; sc-11769; Santa Cruz Biotechnology, Dallas, TX, USA), t-smad 2/3 (1:1000; 8685; Cell Signaling Technology Inc. Beverly, MA, USA), BMPR2 (1:500; 612292; BD Biosciences, Vianen, The Netherlands), p-smad 1/5/9 (1:1000; 13820; cell signaling Technology Inc. Beverly, MA, USA) and t-smad 1/5/9 (1:500; sc-6031-R, Santa Cruz Biotechnology, Dallas, TX, USA). It was followed by appropriate secondary antibody incubation. The protein expression was quantified with Image J, and protein

amount was normalized by vinculin (1:500; sc-5573; Santa Cruz Biotechnology, Dallas, TX, USA) as loading control.

Cell viability assays

Cell viability was determined by 3-(4,5-dimethyl-2-thiazolyl)-2,5-diphenyl-2H-tetrazolium bromide (MTT) assays and were performed as described previously[1] Briefly, cells were seeded in a 96-well plate at a density of 3×103 cells/well in ECM medium (Sciencell, Catalog#1001) and incubated overnight. Cells were made synchronized by incubation in medium without FCS for 6 h and then incubated overnight with FCS (10% [vol/vol]) and vehicle or quisinostat (1 μM) for 24 h. After the incubation time, 10 μL of MTT reagent (5 mg/ml) was added to the cells for 3 h at 37°C. 100 μL of isopropanol was added to each well and incubated for 15 min at RT. Colorimetric analysis was performed with a spectrophotometer. Each experiment (in quadruplicate) was repeated at least three times.

Cell count analysis

MVECs were pretreated with vehicle or quisinostat (1 μM) for 48h and the number of cells was counted using a TC20™ Automated Cell Counter (Bio-Rad).

Determination of PASMC growth in cultured medium of MVECs

PAH MVECs were pretreated with vehicle or quisinostat (1 μM) for 24 h. Conditioned medium from these cells was added to control PASMCs and incubated for 48 hours after which the number of cells were counted using TC20™ Automated Cell Counter (Bio-Rad). Of note, the half-life of Quisinostat is 2 hours.

Experimental animal approval

All animal experiments were approved by the Dutch Central Ethical Committee for Animal Experiments. Experiments with SU5416 + Hypoxia (SuHx), monocrotaline + shunt flow (MF) and pulmonary artery banding (PAB) rats were approved by an independent local animal ethic committee at the University Medical Center Groningen (Groningen, the Netherlands, study numbers AVD105002015129 and AVD105002015134). All animal experiments were performed based on published standards for translational research in PAH [1, 2].

Quisinostat treatment in SuHx rat PAH model

Male Sprague-Dawley rats (n = 18, 140-180 g, Envigo, Horst, the Netherlands) were used throughout the experiment. Rats were housed in standard conditions, with available food

and water. SuHx PAH rat model was induced according to published protocol [1]. Rats were subjected to a single subcutaneous injection of SU5416 (25 mg/kg, 3037, Tocris Bioscience, Bristol, UK), and followed by a 4-week exposure to 10% hypoxia (Biospherix Ltd, New York, NY, USA) maintained by a nitrogen generator (Avilo, Dirksland, the Netherlands) and 4 weeks of normoxic re-exposure. After randomization, animals were divided into two groups receiving 5 mg/kg quisinostat (SuHx+Q, n = 9) or vehicle (SuHx, n = 9, 5% DMSO) in drinking water from week 6 to week 10. At the end of the experiment, rats were anaesthetized for hemodynamic assessment including echocardiography and RV catheterization. After the measurements, rats were exsanguinated, lung and cardiac tissues were collected for further analysis. All measurements and analyses were done in a blinded manner.

Hemodynamic Measurements in SuHx PAH rat model

At the beginning and the end of the treatment, echocardiography (Prosound SSD-4000 and UST-5542; Aloka, Tokyo, Japan) was performed to measure cardiac function. At the end of the experiment, rats were anaesthetized with 4% isoflurane, and hemodynamic data were collected by open-chest RV catheterization (Millar Instruments, Houston, TX). RV systolic pressure was determined from measurement at steady state, as well as arterial elastance (Ea). Pressure-volume loops following vena-cava occlusion were collected and used to measure end systolic elastance (Ees) and end diastolic elastance. RV-arterial coupling was further calculated as Ees/Ea.

Quisinostat treatment in MCT + Shunt flow PAH rat model

25 Wistar male rats (±200g; Charles River, Fr) were kept in standard conditions, with available food and water. MF PAH rat model was induced by a subcutaneous injection of MCT (60 mg/kg, Sigma) at day 0, followed by aorto-caval shunt surgery at day 7, which approximately doubles pulmonary blood flow. MF can induce neomuscularization and medial layer remodeling from day 7 to 14, intima layer remodeling from day 14 to day 21, and RV failure from day 21 to 28. Rats were randomized into 3 groups: 1) MF rats sacrificed at day 21 (MF21) as baseline group; 2) treatment with vehicle (5% DMSO in drinking water) from day 21, and sacrificed at day 35 (MF35 Veh); 3) treatment with 5 mg/kg Quisinostat in drinking water from day 21, and sacrificed at day 35 (MF35 Q). Echocardiography was also performed before the treatment(at day 21) to determine baseline cardiac function. At the end of the study, before sacrifice the animals, rats were anesthetized and subjected to hemodynamic evaluation by echocardiography and right heart catheterization. Lung and heart tissues were collected for further analysis. All measurements and analyses were done in a blinded manner.

Quisinostat treatment in the PAB rat RV pressure load model

In models of PAH, it is difficult to dissect whether effects of therapy on the RV result from a direct therapeutic effect on RV myocardium, or an indirect effect caused by modulated afterload. Therefore, to assess direct myocardial effects of quisinostat in this setting, isolated RV pressure load was created in 16 adult male Wistar rats (±200 g, Charles River, Fr) by PAB surgery at day 0, by a tight constriction with 18G needle. One rat died within the first hour after surgery. PAB gradient was assessed by means of echocardiography at day 14. One rat was excluded due to a non-significant degree of pressure load, defined as a minimum systolic PAB gradient of 40 mmHg on echocardiography at day 14. All other rats showed to be subjected to effective RV pressure load. Rats were grouped into two groups with equal mean PAB gradient. Rats were randomized into 2 groups: 1) treatment with vehicle (5% DMSO in drinking water) from day 28 to 56 (PAB), or 2) treatment with 5 mg/kg quisinostat in drinking water from day 28 to 56. At the end of the study, rats were anesthetized and subjected to hemodynamic evaluation by echocardiography. Lung and heart tissues were collected. All measurements and analyses were done in a blinded manner.

Measurement of RV hypertrophy

To assess the extent of RV hypertrophy, the RV free wall was separated from the left ventricle (LV) and ventricular septum. Wet weights of LV plus septum, and the RV were collected separately, after which the ratio of RV weight to LV plus interventricular septum weight (Fulton index: RV/[LV+IVS]) was calculated. For further analysis of RV hypertrophy, 5-µm-thick paraffin sections of RV tissues were stained with haematoxylin and eosin, after which the mean myocardial cross-sectional area was assessed.

Quantification of pulmonary vascular remodeling

Paraffin-embedded lung sections of 5 µm were stained following the Elastica-Van Gieson protocol, and images were collected under 400 x magnification (Hamamatsu nanoviewer, Japan). 40 vessels (diameter < 100 µm) per sample were analyzed with Image J as previously described [1].

Measurement of RV fibrosis

To measure RV fibrosis, paraffin-embedded RV sections 5 µm were stained according to the Masson protocol, after which the images were collected under 400x magnification (Hamamatsu nanoviewer, Japan). The percentage of fibrosis was calculated by using the positive pixel count algorithm (V9) on image scope V12.3.

Immunofluorescence staining

Cryosections of lung issues were sectioned at 5μm, blocked with 1% BSA in PBS, and incubated overnight with primary anti-acetylated tubulin (1:1000; T6793, Sigma-Aldrich, St.Louis, MO, USA), cleaved-caspase 3 (1:400; #9661, Cell Signaling Technology Inc. Beverly, MA, USA), PCNA (1:100; sc-7907, Santa Cruz Biotechnology, Dallas, TX, USA), CD45 (1:50; sc-53045, Santa Cruz Biotechnology, Dallas, TX, USA), BMPR2 (1:200; MA5-15827, ThermoFisher Scientific, Rockford, IL, USA), p-smad 1/5/9 (1:800; #13820, Cell Signaling Technology Inc. Beverly, MA, USA) and p-smad 2/3 (1:50; sc-11769, Santa Cruz Biotechnology, Dallas, TX, USA) followed by appropriate secondary antibody (Invitrogen, MA, USA) for 1 hour. Sections were also incubated with α-smooth muscle actin-Cy3 (α-SMA, 1:100, C6198, Sigma-Aldrich, St.Louis, MO, USA) and von willebrand factor-FITC (vwF, 1:100; ab8822, Abcam, Cambridge, UK). Counter staining was performed using 4'6-diamidino-2-phenylindole (DAPI, H-1200, Vector Labs).

Image collection and quantification are performed as described in our previous study [1]. Briefly, the images were collected using a ZEISS Axiovert 200M Marianas inverted microscope at x400 and a digital microscope software (Slidebook 6, Intelligent imaging innovations). Captured images were adjusted and merged using Abobe Illustrator (AI, version 23.03). For evaluating protein expressions, fluorescent intensity of each vesseleach molecule was measured within the area co-stained with α-SMA and vwF at high power field (x400) and the data was corrected for the vascular lumen area assessed with FIJI software [1]. More than 20 vessels per section were measured.

Statistical analysis

Statistical analyses were performed with the GraphPad Prism software for windows, version 8.0. Normality of data was checked. Log-transformation or non-parametric test was applied if data was not normally distributed. Unpaired student's t-tests were used for comparisons between two groups. Multiple comparisons were used by one-way ANOVA, followed by Bonferroni's post-hoc test. For repeated measurements of echocardiography analysis, two-way ANOVA was applied followed by Sidak's post-hoc. Kruskal-wallis test followed by Dunn's multiple comparison test was used for data that was not normally distributed. A value of $P < 0.05$ was considered significant. All statistical tests used two-sided tests of significance. All data are presented as mean ± SEM.

REFERENCES

1. Kurakula K, Sun XQ, Happe C, da Silva Goncalves Bos D, Szulcek R, Schalij I, et al. Prevention of progression of pulmonary hypertension by the Nur77 agonist 6-mercaptopurine: role of BMP signalling. Eur Respir J. 2019;54(3). Epub 2019/07/06. doi: 10.1183/13993003.02400-2018. PubMed PMID: 31273046.
2. Van der Feen DE, Kurakula K, Tremblay E, Boucherat O, Bossers GPL, Szulcek R, et al. Multicenter Preclinical Validation of BET Inhibition for the Treatment of Pulmonary Arterial Hypertension. Am J Respir Crit Care Med. 2019;200(7):910-20. Epub 2019/05/03. doi: 10.1164/rccm.201812-2275OC. PubMed PMID: 31042405.

Part IV

Treatment and the right ventricle

CHAPTER 7

Role of cardiac inflammation in right ventricular failure

Xiao-Qing Sun[1], Antonio Abbate[2], Harm-Jan Bogaard[1]

[1]Department of Pulmonology, VU University Medical Center/Institute for Cardiovascular Research, Amsterdam, The Netherlands.
[2]Department of Medicine, Virginia Commonwealth University, Richmond, VA, USA.

Cardiovasc Res. 2017 Oct 1;113(12):1441-1452

ABSTRACT

Right ventricular failure (RVF) is the main determinant of mortality in patients with pulmonary arterial hypertension (PAH). Although the exact pathophysiology underlying RVF remains unclear, inflammation may play an important role, as it does in left heart failure. Perivascular pulmonary artery and systemic inflammation is relatively well studied and known to contribute to the initiation and maintenance of the pulmonary vascular insult in PAH. However, less attention has been paid to the role of cardiac inflammation in RVF and PAH. Consistent with many other types of heart failure, cardiac inflammation, triggered by systemic and local stressors, has been shown in RVF patients as well as in RVF animal models. RV inflammation likely contributes to impaired RV contractility, maladaptive remodeling and a vicious circle between RV and pulmonary vascular injury. Although the potential to improve RV function through anti-inflammatory therapy has not been tested, this approach has been applied clinically in left ventricular failure patients, with variable success. Because inflammation plays a dual role in the development of both pulmonary vascular pathology and RVF, anti-inflammatory therapies may have a potential double benefit in patients with PAH and associated RVF.

KEYWORDS

Inflammation, right ventricular failure, pulmonary arterial hypertension

ABBREVIATIONS

AECA	anti-endothelial cell antibody
CCL	C-C motif chemokine ligand
CINC	cytokine-induced neutrophil chemoattractant
CO	cardiac output
CXCL	C-X-C motif ligand
CXCR	C-X-C motif receptor
CX3CL	C-X3-C motif ligand
Ea	arterial elastance
EC	endothelial cell
Ees	end systolic elastance
Fn14	fibroblast growth factor-inducible 14
HF	heart failure
HFpEF	heart failure with preserved ejection fraction
HFrEF	heart failure with reduced ejection fraction
HLA-DR	human leukocyte antigen-antigen D related
ICAM	intercellular adhesion molecule
IL	interleukin
IPAH	idiopathic pulmonary arterial hypertension
LVF	left ventricular failure
MCT	monocrotaline
miR	microRNA
MMP	matrix metalloproteinase
NF-κB	nuclear factor-κB
NOS	nitric oxide synthase
NYHA	New York Heart Association
PAB	pulmonary artery banding
PAH	pulmonary arterial hypertension
PE	pulmonary embolism
PH	pulmonary hypertension
ROS	reactive oxygen species
RVF	right ventricular failure
SERCA	sarcoplasmic/endoplasmic reticulum calcium ATPase
SLRP	small leucine-rich proteoglycan
SSc	systemic sclerosis
sST2	soluble suppression of tumorigenicity 2
SuHx	SU5416 plus hypoxia
TAC	transverse aortic constriction
TNF	tumor necrosis factor
TNFR	tumor necrosis factor receptor
TWEAK	TNF-like weak inducer of apoptosis
VCAM	vascular cell adhesion molecule

1. INTRODUCTION

Pulmonary arterial hypertension (PAH) is a fatal disease characterized by pulmonary vascular remodeling and a chronic and frequently progressive increase in right ventricle (RV) afterload, eventually leading to RV failure (RVF) and premature death. Although the initial insult in PAH involves the pulmonary vasculature, RVF is the most important determinant of mortality in patients with PAH.[1] Many questions, however, regarding the mechanisms underlying RVF remain unclear.

In recent years, multiple studies have focused on the evidence of inflammation in PAH, and highlighted the role of inflammation in the initiation and maintenance of pulmonary vascular remodeling.[2-4] Accumulation of perivascular inflammatory cells as well as systemic overabundance of pro-inflammatory cytokines and chemokines have been observed in clinical and experimental PAH, and have been proposed to contribute to the process of pulmonary vascular remodeling.[2, 3, 5, 6] However, compared to the pulmonary vasculature, the role of inflammation in the transition from RV adaptation to failure is less well known. Intriguingly, evidence of RV inflammation has been found in patients with acute pulmonary embolism (PE) related RVF and in patients with HIV and systemic sclerosis associated PAH (SSc-PAH).[7-9] Moreover, cardiac inflammation has been demonstrated in several experimental RVF models, with increased infiltration of inflammatory cells and expression of multiple cytokines and chemokines, which are related to the progression of RVF.[10, 11]

Evidence of inflammatory responses in the heart of patients with many types of cardiovascular diseases other than PAH has been accumulating for decades.[12-14] Inflammation is considered a *double-edged sword*, as it stimulates the immune response to microbial infection while it may also lead to further injuries in noninfectious conditions, such as cardiovascular diseases.[12] The "Cytokine Hypothesis" is regarded as one of the basic mechanisms for the development of heart failure (HF), and states that a cardiac event triggers systemic activation of pro-inflammatory cytokines, which in turn accelerate the progression of HF.[15] Indeed, increased levels of circulating inflammatory cytokines have been found associated with the New York Heart Association (NYHA) functional class in HF patients.[16]

The aim of this review is to provide an overview of available evidence of inflammation in RV and to discuss the potential role of inflammation in the pathogenesis and progression of RVF.

2. VICIOUS CIRCLE BETWEEN RV INFLAMMATION AND RVF

Currently, it is unclear to what extent inflammation contributes to the development or progression of RVF. It is possible that inflammation is key to the transition from RV adaptation to failure, but RV inflammation could also be a mere bystander and a simple consequence of the primary processes involved in RVF. Based on available evidence, we propose a key role of inflammation and neurohormonal signaling in the vicious circle of pulmonary vascular remodeling and RVF. (Figure 1)

2.1 Potential Inflammatory triggers in RVF: wall stress, ischemia, systemic inflammation and neurohormonal activation

Due to the multifactorial nature of PAH, it is difficult to pinpoint an initial trigger of RV inflammation. We propose that both local stressors and systemic influences could promote a "pro-inflammatory environment" in the overloaded RV. Potential local triggers of cardiac inflammation include mechanical stress and ischemia, while systemic influences likely consist of increased circulating levels of proinflammatory cytokines and activated immune cells and neurohormonal activation.

Both *in vitro* and *in vivo* studies have suggested that mechanical stress can directly initiate cardiac inflammation through the local production of reactive oxygen species (ROS) and secondary activation of nuclear factor-κB (NF-κB).[17-19] 10 minutes of mechanical stretch in adult feline cardiomyocytes can induce myocardial overexpression of pro-inflammatory cytokines such as tumor necrosis factor-α (TNF-α), which is followed by leukocyte infiltration.[17] *In vivo*, aortic banding can increase the level of TNF-α, interleukin-6 (IL-6), C-C motif chemokine ligand 2 (CCL2), CCL3 and inflammatory cell accumulation in the left ventricle (LV).[20] In the rat model of experimental pulmonary hypertension (PH) induced by monocrotaline (MCT), RV inflammation was not found in stable PH but in progressive PH, the latter being associated with a larger RV end-diastolic diameter indicating a higher RV wall stress. In addition, exercise was observed to increase RV inflammation in progressive PH, which is related to increased RV wall stress during episodes of activity, also suggesting

that high RV wall stress might be an explanation for RV inflammation.[21] These studies are not entirely conclusive, however, because of the direct pro-inflammatory properties of MCT administration.[22, 23]

In addition to mechanical stress, ischemia is another known trigger of the expression of inflammatory cytokines in the heart.[24-27] Although the normal RV is less susceptible to infarction,[28] the pressure overloaded RV is more susceptible to ischemia than the pressure overloaded LV, because of a diminished RV coronary flow reserve, a greater systolic-diastolic coronary flow ratio, and an impaired angiogenic response to increased afterload.[29] Therefore, RV ischemia due to a decrease in capillary density and right coronary artery perfusion impairment may explain the findings of RV inflammation in experimental PH[30, 31] as well as in SScPAH patients, who are known to have functional abnormalities of the small coronary arteries.[32]

Spill-over of pulmonary vascular inflammation into the systemic circulation may lead to increased serum levels of inflammatory cytokines in PAH, which are not only biomarkers that can be used for risk stratification of PAH patients,[33] but may also directly affect RV function. Inflammatory cells may be activated in the lung and subsequently invade the RV. However, because only few inflammatory cells can be observed infiltrating the RV from iPAH patients (alike experimental RVF models (Table 1)), it is doubtful whether systemic inflammation plays a role in RV inflammatory responses. It is more likely that local stresses together with neurohormonal overdrive play crucial roles in this process.

Increased activity of neurohormonal system, particularly the renin-angiotensin-aldosterone system and the neuro-adrenergic system,[34, 35] is a second systemic aspect of PAH well capable of triggering inflammation both in the pulmonary vasculature and in the heart.[36, 37] During HF development, increased activity of the sympathetic nervous system contributes to increased cardiac inflammation, including upregulated expression of TNF-α and IL-1b.[38] Treatment with the selective β-blocker bisoprolol improved cardiac function as well as reduced RV inflammation in experimental PH rats.[39] Both Angiotensin II (Ang II) and cytokines are promotors of endothelin-1 (ET-1) expression,[40-43] and ET-1 can increase the expression of cardiac pro-inflammatory cytokines and neurohormonal activation.[44-46] Moreover, cardiac inducible nitric oxide synthase (iNOS) expression can be increased by cytokines such as TNF-α and IL-1, which causes further calcium and mitochondrial dysfunction, as well as additional

disruption of the neuro-adrenergic system.[47-49] Altogether, while cardiac inflammation may contribute to the progression of RVF, the failing heart will further promote sympathetic overdrive, creating a vicious circle between RV inflammation, and RVF and pulmonary vascular remodeling. (Figure. 1)

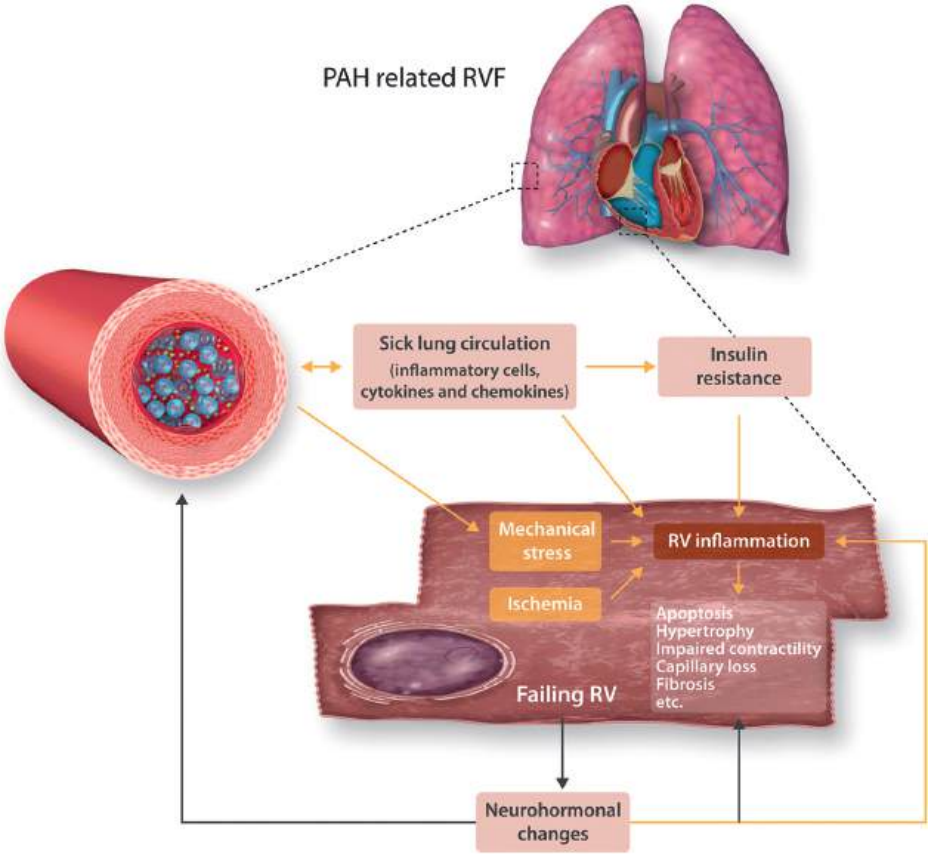

FIGURE 1. The role of inflammation in the vicious circle between pulmonary vascular remodeling and right ventricular failure.
In PAH, perivascular inflammation plays a role in pulmonary vascular remodeling, which leads to increased RV mechanical stress, ischemia, and increased inflammation in systemic circulation, triggering RV inflammation. Increased activity of neurohormonal system is also a trigger of RV inflammation. While RV inflammation may lead to the progression of RVF, the failing heart will further increase neurohormonal activity, which promotes pulmonary vascular remodeling. Altogether, a vicious circle is formed between RV inflammation, RVF and pulmonary vascular remodeling. PAH pulmonary arterial hypertension, RVF right ventricular failure

Table 1 Cardiac inflammation in the failing RV

		RV inflammation
PAH-RVF	iPAH	trend of increased lymphocyte and neutrophil infiltration
	HIV-PAH	lymphocyte and macrophage infiltration, EC expression of VCAM-1, ICAM-1, E-selectin and HLA-DR
	SSc-PAH	lymphocyte, neutrophil and macrophage infiltration
experimental RVF	MCT rat	leukocyte and neutrophil infiltration, increased TNF-α, TWEAK, IL-1β and IL-6
	PAB mice or rat	lymphocyte and macrophage infiltration, increased chemokines CCL2, CCL5, CXCL6, CXCL10, CX3CL1 and CXCL16
	shunt piglet	increased TNF-α, IL-1α, IL-1β and ICAM-1
	SuHx rat	trend of increased IL-6 and CCL-2
	ovariectomized SuHx rat	increased IL-6 and CCL-2

iPAH, idiopathic pulmonary arterial hypertension; SSc, systemic sclerosis; MCT, monocrotaline; PAB, pulmonary artery banding; SuHx, SU5416 plus hypoxia; EC, endothelial cell; VCAM-1, vascular cell adhesion molecule-1; ICAM-1, intercellular adhesion molecule; HLA-DR, human leukocyte antigen-antigen D related; TNF, tumor necrosis factor; TWEAK, TNF-like weak inducer of apoptosis; IL, interleukin; CCL, C-C motif chemokine ligand; CXCL, C-X-C motif ligand; CX3CL, C-X3-C motif ligand.

2.2 Evidence of cardiac inflammation in RVF

2.2.1 Inflammatory cell recruitment into the failing RV

Presence of multiple leukocytes, cytokines and chemokines has been studied in the failing RV. A recent study of biventricular biopsies from 15 patients with HIV-associated PAH found lymphocytic myocarditis in 12 patients, microvasculitis in 3 of these patients, and increased endothelial cell (EC) adhesion molecules in all 15 patients, including vascular cell adhesion molecule-1 (VCAM-1), intercellular adhesion molecule-1 (ICAM-1), E-selectin and human leukocyte antigen-antigen D related (HLA-DR).[50] Also the study of heart tissues from SSc-PAH patients revealed inflammation in RV tissues. SSc is a disease with a multifaceted pathology, characterized by an enhanced inflammatory status, vasculopathy and excessive fibrosis in skin and internal organs. PAH induced RVF is the leading cause of death in SSc patients.[51] Compared to idiopathic PAH (IPAH) patients, SSc-PAH patients have a worse RV function and prognosis, even though the pulmonary vascular resistance is similar.[52, 53] By analyzing the heart tissues from 5 SSc-PAH patients, Overbeek *et al.* found significantly more leukocytes in the RV tissues compared with normal controls as well as compared with the RV from IPAH

patients, including increased number of lymphocytes, macrophages and neutrophilic granulocytes, suggesting that inflammation may contribute to a worse RV function in SSc-PAH patients.[9] In contrast, the authors found no significant inflammatory cell infiltration increase in RV tissues from 9 patients who died from IPAH compared to control, though there is a tendency towards increased neutrophils and lymphocytes.[9] This finding was confirmed by Begieneman *et al.* who compared the number of lymphocytes, macrophages and neutrophilic granulocytes in RV tissues between 11 patients who died of IPAH compared to controls.[7]

Studies on RV inflammation in PAH are limited by a small sample size and by the fact that only RV tissues from patients with end-stage disease were available. It is possible that inflammation is no longer present or active in end-stage RVF, but heavily involved in the transition from RV adaptation to failure. In addition, even though the quantity of inflammatory cells is low in the RV from IPAH patients, their functional effects may still be important on the progression of the disease (Figure. 2).

2.2.2 Experimental RVF: inflammatory cell influx and altered expression of cytokines

Important evidence that inflammation does play a role in the progression of RV failure comes from studies of experimental RVF. Several animal models have been used to investigate the pathogenesis of PH and PH-induced RVF, such as MCT induced PH, pulmonary artery banding (PAB), angioproliferative disease due to blockade of vascular endothelial growth factor receptor antibody blocker (SU5416) plus chronic hypoxia (SuHx) and systemic to pulmonary shunt models.[54-56] Though it is clear that there is no perfect experimental model of human PAH currently available, these models have provided valuable contributions to the understanding of PAH.

MCT: MCT is a plant-derived alkaloid that induces pulmonary EC injury and perivascular inflammation.[54] A single subcutaneous injection of 40 mg/kg MCT induces stable PH with a preserved cardiac output (CO) in rats after 2 weeks, while 60 mg/kg MCT induces progressive PH developing RVF.[21] Multiple studies have shown that RV inflammation is increased in progressive MCT induced PH, including leukocyte infiltration,[21, 39] neutrophil activation,[10, 57] increased expression of pro-inflammatory cytokines including TNF-α,[10, 57-61] TNF-like weak inducer of apoptosis (TWEAK),[59] IL-1β[60] and IL-6.[62] Moreover, inflammatory activation in the RV of MCT rats is characterized by a specific time course, showing an early increase which peaks at the stage of RV dilation, and continues into the RVF stage.[10, 62] Among the pro-inflammatory cytokine

pathways, TNF superfamily signaling appears to be involved in the pathogenesis of RVF via the non-canonical NF-κB pathway, with increasing expression of NF-κB subunits p100/p52 and Rel-B.[59] On the other hand, no inflammatory changes have been found in stable MCT induced PH.[21, 63] Collectively, these data suggest a possible association between RV inflammatory activation and early stages of RVF.

PAB: Mice develop RVF one week after the PAB operation. Several chemokines have been found upregulated in the RV in this model, including CCL2, CCL5, C-X-C motif ligand 6 (CXCL6), CXCL10, C-X3-C motif ligand 1 (CX3CL1) and CXCL16. Among these chemokines, CXCL16, CX3CL1 and CCL5 may play a role in RV remodeling via enhancing small leucine-rich proteoglycans (SLRPs).[64] Meanwhile, leukocyte infiltration was also increased in the RV, including both $CD4^+$ and $CD8^+$ T cells, while no chemokine or leukocytes increase was found in the LV.[64] The expression of TWEAK receptor fibroblast growth factor-inducible 14 (Fn14) is also increased in the RV from PAB mice.[65] TWEAK belongs to the TNF superfamily and TWEAK levels are inversely correlated with the severity of PAH in patients.[66] In another chronic PAB-induced RVF model in rats, elevated expression of activated NF-κB and increased numbers of CD68-positive macrophages were found in RV tissues. Chronic treatment with the NF-κB inhibitor pyrrolidinedithiocarbamate reversed RV inflammation and fibrosis, as well as improved RV function after PAB.[67]

Aortic-pulmonary shunt: Aortic-pulmonary shunting in growing piglets is a recognized model of congenital left-to-right shunt-induced PH.[11] While the piglets develop PH with preserved RV function with three months of shunting, more prolonged shunting can induce pronounced RVF, with elevated serum TNF-α levels and increased cardiac expression of pro-inflammatory cytokines.[11] The expressions of IL-1α and IL-1β were increased in both the RV and LV of shunted piglets, while TNF-α and ICAM-2 expressions were only increased in the RV. No changes were found in IL-6, IL-10, IL-19, IL-33, suppression of tumorigenicity 2 (ST2), ICAM-1, VCAM-1 or signal transducer and activator of transcription 3.[11, 68] The fact that expressions of cytokines are increased in the LV may indicate the progression towards global HF. In addition, a negative correlation was found between RV ICAM-2 gene expression and RV-pulmonary artery coupling as shown by end systolic elastance/arterial elastance (Ees/Ea).[68]

Others: In SuHx induced PAH rats, the gene expression of IL-6 and CCL-2 in RV tissues had a tendency to be up-regulated, but differences are not significant.[69] However,

female ovariectomized SuHx rats were found to develop severe RV dysfunction and significantly up-regulated gene expression of IL-6 and CCL-2 in the RV.[69] In a tetralogy of Fallot model by transvalvular patch inducing RV tract enlargement together with PAB in piglets, even though RVF was established with significant fibrosis and myocardial hypertrophy, cardiac inflammation was not observed.[70]

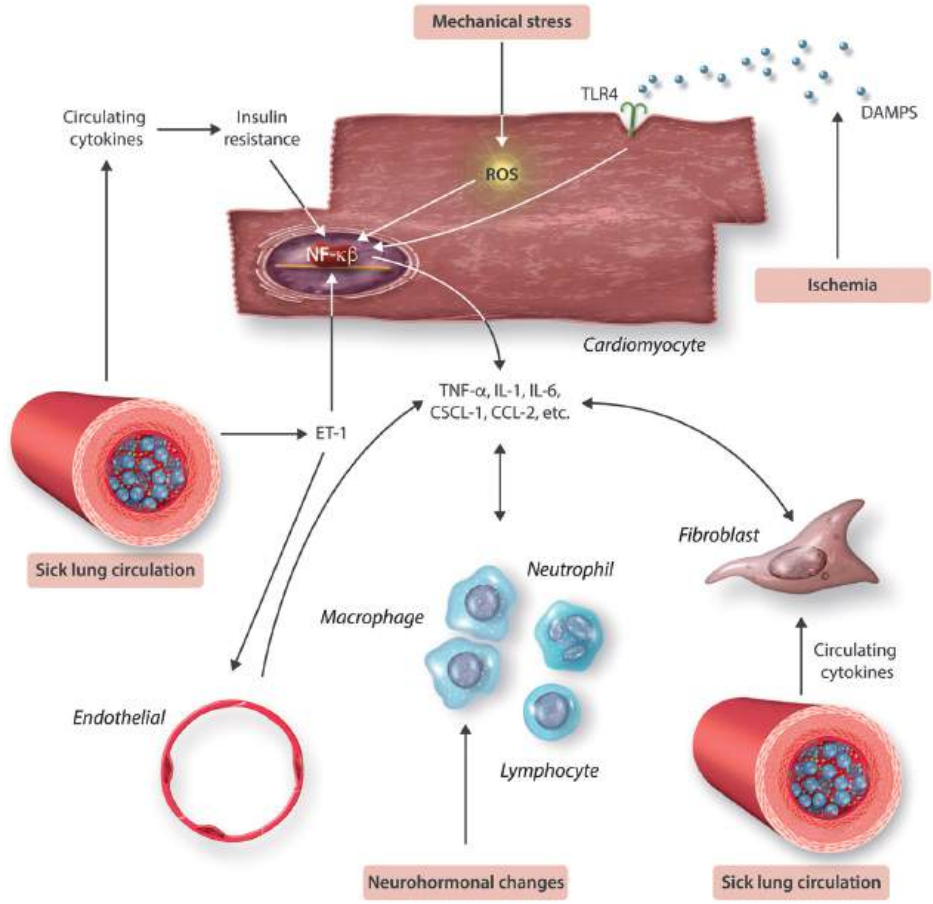

FIGURE 2. Recruitment of inflammatory cells into the failing right ventricle
Recruiment of inflammatory cells into the failing RV is attributed to the direct effect of neurohormonal changes and increased cytokines production. Neurohormonal overdrive can directly promote cardiac macrophage recruitment. Circulating cytokines generated within a "sick lung" circulation contribute to cardiac insulin resistance, which induces NF-KB activation in cardiomyocytes. Mechanical stress can induce NF-KB activation in cardiomyocytes by producing ROS. Ischemia can stimulate cardiomyocytes to release DAMPs, which activate NF-KB through binding to TLR4. The activation of NF-KB in cardiomyocytes leads to the expression of a wide range of pro-inflammatory cytokines that

FIGURE 2 *(continued)*
promote the recruitment of inflammatory cells into the RV. In addition, increased ET-1 from the lung contributes to cytokine production of both cardiomyocytes and ECs. The cytokines TNF-α and IL-1 may induce fibroblast production of other pro-inflammatory cytokines and chemokines, which further increase the recruitment of inflammatory cells into the RV. TLR4, Toll-like receptor 4; DAMPs, damage-associated molecular patterns.

2.2.2 Cardiac inflammation in RVF related to other diseases

The presence of acute RVF following PE is a strong predictor of poor clinical outcome.[71-73] Iwadate *et al.* found an increased number of macrophages in RV tissues from 16 out of 20 patients who had died of PE.[8, 74] By analyzing the heart tissues from 22 patients with PE, Begieneman *et al.* found aggregates of lymphocytes, macrophages and neutrophilic granulocytes coinciding with areas of myocytolysis in both the RV and LV, indicating the presence of myocarditis and endocarditis in these patients.[7]

In a rat model of PE induced by microspheres injection via the right jugular vein, massive accumulation of neutrophils and monocyte/macrophage was found in the RV, as well as increased chemokine expression, including CCL2, cytokine-induced neutrophil chemoattractant-1 (CINC-1), CINC-2, CXCL2 and CCL3.[75] Moreover, suppression of the inflammatory response by the anti-inflammatory agent ketorolac sodium improved survival in this PE model, while antibodies targeted at neutrophil or chemoattractants, such as polymorphonuclear leukocytes and CINC-1, reduced neutrophil accumulation and activity, limited RV damage and prevented RVF.[75-77]

RVF due to a pulmonary hypertensive crisis can be experimentally reproduced in animals by transient PAB.[78] In a dog model with 90-minute PAB, persistent RVF was found to be associated with increased RV expression of TNF-α, IL-1β, IL-6, IL-6/IL-10 ratio, CCL2, VCAM-1, neutrophil and macrophage infiltration, as well as decreased IL-10 and IL-33.[78, 79] After establishment of RVF in pigs after 2 hours of PAB, microarray analysis showed that 9 inflammation related genes were up-regulated in RV tissues, including IL-6, IL-8, pentraxin 3, CCL2, CXCL6 and CXCL2.[80] RVF is the leading cause of early death after cardiac transplantation, and RV inflammation was found significantly increased in experimental brain death-induced RVF, including IL-1β, IL-6, IL-10, TNF-α, ICAM-1, ICAM-2 and VCAM-1, whereas IL-33 expression was decreased.[81] By analyzing 26 donor RV biopsies, TNF-α expression was found to be a predictor for the development of RVF in patients early after transplantation.[82]

2.3 How inflammation could contribute to the development of RVF

2.3.1 Inflammation and contractility

Both inflammatory cells and cytokines can impair myocardial contractility. It has been recognized that several leukocytes, notably neutrophils and macrophages, can directly impair *in vitro* myocardial contractility via multiple mechanisms.[83-85] When neutrophils are exposed to formulated peptides of bacterial origins, α4 integrin can mediate an oxidant induced Neutrophils can cause a reduction in contractility of co-cultured cardiomyocytes under the stimulation of formulated peptides of bacterial origins,[83, 85] while macrophages can decrease myocardial contractility by binding to ICAM-1.[86] These effects have also been confirmed *in vivo,* for example as leukocyte dependent decreased contractility in animal models of left ventricular failure (LVF).[87, 88] In transverse aortic constriction (TAC) mice model, impaired LV contractility has been found to be associated with T cell infiltration, while LV contractility is preserved in T cell deficient mice and anti-CD3 pre-treated mice.[89, 90]

Among the pro-inflammatory cytokines, TNF-α contributes to contractile dysfunction by inducing β-adrenergic receptor uncoupling, ROS formation and iNOS expression, and by decreasing contractile proteins in cardiomyocytes.[91, 92] A study in rats showed that circulating concentrations of TNF-α similar to HF patients are sufficient to cause persistent negative inotropic effects and are reversible after stopping TNF-α infusion.[91] In a recent study with MCT induced PH rats, TNF-α overexpression in RV was significantly correlated with the downregulation of sarcoplasmic/endoplasmic reticulum calcium ATPase (SERCA) 2a expression and overexpression of phospholamban, which contributes to calcium overload.[58] Moreover, microRNA 208 (miR208) inhibition together with increased TNF-α as a "second hit" was found to contribute to the transition from compensated RV hypertrophy to RVF, with decreased CO and RV contractility.[93]

Various studies have revealed a link between IL-1b and impaired contractility, mainly due to L-type calcium channel inhibition and β-adrenergic receptor desensitization.[94, 95] In addition, IL-1b can increase NO activity by increasing iNOS expression, which can further disrupt calcium channels, β-adrenergic receptor signaling and mitochondrial function, contributing to impaired contractility.[48, 49, 96] IL-1b also changes the expression of the calcium handling proteins phospholamban and SERCA in cardiomyocytes.[97]

The effects of IL-6 on myocardial contractility are well documented both *in vitro* and *in vivo*. IL-6 not only has a direct inotropic effect on isolated papillary muscle and reduces SERCA in isolated cardiomyocytes,[98] but also reduces the expression of α-myosin heavy chain, β-myosin heavy chain and cardiac actin.[91] *In vivo*, subcutaneous administration of IL-6 to rats can lead to a dose-dependent deterioration of cardiac contractility.[99]

In contrast, IL-33/ST2 signaling may have a cardioprotective role via the fibroblast-cardiomyocyte paracrine system.[100] In the heart, IL-33 is synthesized by cardiac fibroblasts while its receptors ST2L and soluble ST2 (sST2) are both biomechanically induced in cardiomyocytes.[100, 101] In the failing RV of dogs subjected to transient PAB, the expression of IL-33 was decreased and a correlation was found between Ees/Ea ratio and RV gene expression of IL-33, suggesting a protective role of IL-33 in RV contractility.[78] Intriguingly, patients with HF show elevated sST2 especially in the presence of PH and RV dysfunction, and sST2 levels carry a strong prognostic value.[102, 103] Moreover, serum sST2 is increased in PAH patients, and its level is strictly related to the degree of RV dilatation and systolic dysfunction.[104] In the recent RELAX trial, performed in 174 patients with HF with preserved ejection fraction (HFpEF), no associations were found between sST2 levels and LV function, but higher sST2 levels were significantly associated with higher RV systolic pressure and impaired RV contractility.[105] Based on the cardioprotective role of IL-33/ST2 pathway, it is likely that sST2 binds to IL-33, decreasing its tissue availability and thus blocking cardioprotective effects through ST2L.

2.3.2 Inflammation and myocardial hypertrophy, apoptosis and fibrosis

Pro-inflammatory cytokines and leukocytes contribute to heart remodeling by inducing myocardial hypertrophy, apoptosis and fibrosis. Several studies have revealed the effect of macrophages to induce cardiac hypertrophy in HF models through various mechanisms, involving miR55 and activating transcription factor 3.[106, 107] By inducing the re-expression of fetal genes and downregulating the calcium homeostasis genes, IL-1β can cause hypertrophy of neonatal rat cardiomyocytes *in vitro*.[108] IL-6 family signaling induces gene expression in the cardiomyocytes that is associated with pathological hypertrophy.[109] TNF-α can induce myocardial hypertrophy *in vitro*,[110, 111] as well as induce LV hypertrophy and dilation *in vivo*.[112] In addition, TWEAK and its receptor Fn14 are involved in pathological cardiac hypertrophy and promote myocardial hypertrophy *in vitro*.[113] Transgenic overexpression of full length-TWEAK in mice resulted in dilated cardiomyopathy with myocardial hypertrophy.[114] In PAB induced RVF mice, Fn14 deletion attenuated RV hypertrophy.[113]

TNF-α can trigger apoptosis in many cell types, including cardiomyocytes.[115, 116] This effect was not only demonstrated *in vitro*, but also in dogs with LVF.[92] Moreover, TNF-α can increase cardiac fibrosis through activating MMP and downregulating tissue inhibitor of MMP in a ROS dependent way.[117-119] *In vivo*, TNF-knockout mice with aortic banding showed attenuated apoptosis, hypertrophy and fibrosis, with improved cardiac function.[20] TNF-α increases the expression of other inflammatory cytokines such as IL-1 and IL-6, thus further impairing cardiac function.[20] However, it has to be mentioned that TNF-α has a more complex role in cardiac remodeling and function. Further research on selective TNF-receptor (TNFR) knock out mice indicates that the effects of TNF on inflammatory and ventricular remodeling are receptor specific. TNFR1 exacerbates the inflammatory response, myocardial hypertrophy, apoptosis and fibrosis, whereas TNFR2 ameliorates these events.[120] Finally, TWEAK/Fn14 has also been found to be implicated in processes of cardiac fibrosis.[114, 121] In PAB induced RVF mice, Fn14 deletion reduced RV fibrosis.[65] While multiple studies on fibrosis of the pressure-overloaded myocardium have focused on the role of macrophages as driving cell type,[122, 123] recent studies have revealed a crucial role of lymphocytes in cardiac remodeling. In TAC induced LVF mice, LV fibrosis can be prevented in mice deficient in mature $CD4^+$ T cells, although cardiac hypertrophy can still be observed.[90] Further studies using the TAC model revealed markedly decreased LV hypertrophy and fibrosis in T cell deficient mice or anti-CD3 antibody treated wild-type mice.[89] In addition, a study using the AngII infusion model of hypertensive cardiac remodeling revealed a crucial role of $CD8^+$ cells in perivascular and interstitial fibrosis via recruitment and activation of macrophages.[124]

Chemokines such as CXCL16 and CCL5 contribute to RV fibrosis after PAB by modulating the expression of SLRP in cardiac fibroblasts, which are known as fibrosis regulators.[64] Besides, the cardiomyocytes-macrophages cross talk mediated by the interferon Y-CXCL10-CXCR 3 axis also contributes to cardiac fibrosis.[125]

In contrast, as a potent immunomodulatory that inhibits various pro-inflammatory cytokines,[126] adeno viral expression of IL-10 protects against MCT induced PH in rats with decreased pulmonary vascular remodeling and RV hypertrophy.[127] Aerobic exercise at an early stage has cardioprotective effects in MCT induced PH rats, partly by decreasing TNF-α/IL-10 ratio.[61] IL-33 was found to reduce AngII and phenylephrine induced hypertrophy of cardiomyocytes *in vitro*.[100] Targeted deletion of ST2 in mice led to marked hypertrophy and fibrosis following pressure overload, while treatment of WT

mice with purified recombinant IL-33 protected the myocardium but not in $ST^{-/-}$ mice, revealing IL-33/ST2 signaling as a crucial cardioprotective fibroblast-cardiomyocyte paracrine system.[100]

Cardiac fibroblasts play important roles as sensors and amplifiers of signals from immune cells and cardiomyocytes, by secretion of cytokines, growth factors and chemokines.[128] Both TNF-α and IL-1 can increase fibroblast migration and induce fibroblast production of other pro-inflammatory cytokines (e.g., IL-6) and chemokines (e.g., CXCL-1, -2, -5, -8).[129, 130] While TNF-α can increase cardiac fibroblast proliferation, IL-1 was shown to inhibit it.[131-133] In addition, IL-1 can activate the expression of transforming growth factor β (TGF-β), which is the major profibrotic cytokine that induces differentiation of fibroblasts into myofibroblasts and the generation of extracellular matrix proteins.[134, 135] In addition, macrophages play an important role in the differentiation of fibroblast into myofibroblasts via expression of TGF-β.[136, 137]

2.3.3 Capillary rarefaction

Capillary rarefaction is an additional cause of RV ischemia besides decreased coronary perfusion. Capillary rarefaction has been found in the RV from SuHx and MCT rats, but not in the RV of rats subjected to pulmonary artery banding.[30, 138, 139] Capillary rarefaction may also occur in PAH patients, particularly in patients with ssc-PAH.[138] It has been recognized that impaired angiogenesis and microvascular EC injury contribute to capillary rarefaction, in particular downregulation of VEGF signaling and microRNA 126.[140]

Anti-endothelial cell antibodies (AECAs) have been detected in the serum of patients with IPAH or with SSc-PAH or with SSc without PAH.[141, 142] The identified target antigens include lamin A/C, tubulin β-chain and vinculin, which are implicated in cell morphology, metabolism and protein folding in various cell types.[143] Indeed, ACEAs have been found to activate EC and induce EC apoptosis and therefore play a role in the pathogenesis of EC damage and vasculitis.[144-146] IgG from ACEA-positive PAH patients has been found to induce inflammatory response on EC.[147]

Even though there is no direct evidence indicating the role of AECAs on RV capillary density, their presence in PAH patient serum suggests a potential role. Indeed in SSc patients, a correlation was found between the detection of ACEAs and the development

of severe digital ischemia and PAH.[148] However, the role of AECAs on RV capillary rarefaction during PAH needs to be further studied.

2.3.4 Immunometabolism

Pro-inflammatory cytokines have been found to promote systemic insulin resistance and contribute to cardiac insulin resistance.[149-151] Moreover, exposure of fatty acids or high glucose can induce NF-KB activation in cardiomyocytes, which in turn increases the production of pro-inflammatory cytokines.[152, 153] In metabolic cardiomyopathy, inflammation and insulin resistance in adipose tissue induce systemic inflammation and insulin resistance, leading to inflammatory cell infiltration in the heart, thereby contributing to adverse cardiac remodeling.[154-156]

Multiple preclinical studies have suggested a role of insulin resistance in the pathogenesis of PAH.[157-159] Indeed, patients with PH and diabetes have higher right atrial pressure, as well as lower RV stroke volume and an increase in RV fibrosis, compared to patients with PAH alone.[160-162] In addition, a recent clinical study revealed that iPAH patients have glucose intolerance and an impaired ability to produce insulin following a glucose challenge. Pancreatic beta-cell dysfunction in iPAH is associated with circulating CXCL-10.[163]

Altogether, the vicious cycle between inflammatory responses and metabolic dysregulation may play a role in linking systemic inflammation and inflammation in RV. However, the link between inflammation, metabolic dysregulation and RV dysfunction in PAH needs to be further studied.

Table 2 Contribution of inflammation to the development of RVF

major inflammtory elements in RVF		major cardiac effects
leukocytes	macrophages	impair contractility, induce hypertrophy, apoptosis and fibrosis
	neutrophils	impair contractility
	T lymphocytes	induce fibrosis
pro-inflammatory cytokines	TNF-α	impairs contractility, induces hypertrophy, apoptosis and fibrosis
	IL-1β and IL-6	impair contractility, induce hypertrophy
	TWEAK	induces hypertrophy and fibrosis
chemokines	CCL5 and CXCL16	induce fibrosis

3. ANTI-INFLAMMATORY THERAPIES

The biological effects of pro-inflammatory cytokines can be antagonized by so-called "biological response modifiers", which bind and/or neutralize soluble cytokines such as IL-1β and TNF-α. Although none of these anti-inflammatory therapies have been approved for clinical use to treat left HF, several therapies have been explored in phase II-III clinical trials.

3.1 IL-1 blockade in HF

IL-1 is a major pro-inflammatory cytokine and in the complex processes involved in innate immune responses IL-1 acts as a "gatekeeper of inflammation".[164] IL-1 has been found to contribute to pulmonary arterial remodeling in PAH.[4] IL-1β is the main circulating form of IL-1, responsible for systemic effects.[14] Among HF patients, a correlation has been found between declining functional class and increasing levels of IL-1β.[165] Similarly in PAH patients, IL-1β serum levels are also increased and these levels correlate with a worse outcome.[33]

Several clinical trials were conducted to assess the effects of IL-1 blockade with anakinra on HF patients. In AIR-HF trial on 7 patients with HF with reduced EF (HFrEF), anakinra treatment for 14 days reduced the plasma concentrations of IL-1β, C-reactive protein and IL-6, as well as improved aerobic exercise capacity.[166] In the D-HART pilot trial with 12 HFpEF patients, anakinra treatment for 14 days also reduced the systemic inflammatory response and led to a significant improvement in aerobic exercise capacity.[167] A more recent pilot trial of anakinra on acute decompensated HF (ADHF study [NCT02173548]) with 30 HFrEF patients showed reduced systemic inflammatory responses and no adverse clinical events.[168] Another study in 60 patients with recently decompensated HFrEF (RED-HART study [NCT01936909]) treatment with anakinra for 12 weeks resulted in areduction of systemic inflammation, improvement in peak aerobic capacity and a trend toward reduce hospital readmission for HF at 6 months.[169, 170]

3.2 TNF-a blockade

TNF-α has been recognized as a part of the innate immune system response to different forms of stress, which can be initiated independently from a specific antigen and use pattern recognition receptors. TNF-α stimulates NF-κB and increases the expression of genes required to control infection and injury.[92] In HF patients, TNF-α has been shown to be paradoxically increased in serum and the elevated level of serum TNF-α correlates

with high mortality.[171] In PAH patients, elevated levels of serum TNF-α have also been found, even though no correlation was found between TNF-α levels and survival.[33]

While TNF antagonism was beneficial in experimental HF models,[92, 172] randomized trials of anti-TNF therapy in human HF failed to show benefit. In the ATTACH trial for patients with NYHA class III-IV, anti-TNF therapy with infliximab did not improve HF and infliximab in high dosage was associated with worsening of the clinical status.[173] The TNF antagonist etanercept had short-term beneficial effects in small early studies, but larger multicenter trials in NYHA classes II-IV HF patients failed to demonstrate a benefit on mortality or hospitalization.[174, 175] Additionally, it was also recognized that treatment with the available TNF-α antagonists may involve significant toxicity, e.g. stabilization of circulating TNF-α (etanercept), and induction of lysis of cells expressing transmembrane TNF-α (infliximab).[176, 177] Hence, TNF-a is not a viable therapeutic target in HF.

3.3 other anti-inflammatory therapies

Cytokines can promote ET-1 expression, which mediates a variety of processes including vasoconstriction, fibrosis, hypertrophy and neurohormonal activation, and ET-1 promotes inflammatory responses in the heart.[40, 44-46] An anti-inflammatory action has been attributed to the dual endothelin receptor antagonist bosentan in PAH.[178] However, clinical trials using bosentan in HF have suggested no overall benefit.[179] The direct effect of bosentan on the RV in PAH continues to be debated. A double-blind controlled trial in PAH patients with WHO functional class III demonstrated that bosentan failed to improve RV ejection fraction.[180] One explanation is that ET-1 has positive inotropic effects on the myocardium and may preserve RV contractility in RV hypertrophy; as such, ET antagonists may potentially lead to RV dysfunction in some PAH patients.

The ACE2-angiotensin-(1-7)-Mas axis is a potential new target for the treatment of PAH and heart failure.[181] Ang 1-7 can decrease myocardial levels of pro-inflammatory cytokines including TNF-α and IL-6, thus reducing cardiac inflammation.[182, 183] Ang 1-7 treatment has cardioprotective effects in experimental models of non-ischemic and ischemic cardiomyopathy.[182-185] The serum level of Ang-(1-7) was found to be decreased in patients with congenital heart disease related PAH.[186] Ang-(1-7) administration had beneficial pulmonary effects in the MCT induced PH model, without adverse effects on systemic blood pressure.[187] The effect of Ang-(1-7) on RVF needs to be further studied.

4. CONCLUSION

Triggered by systemic as well as local stresses, PAH and right heart failure are associated with inflammatory activation. Inflammatory cell influx commonly exists in the failing RV from patients with SSc associated and HIV associated PAH patients. While a limited number of studies on RV tissues from end-stage idiopathic PAH patients showed little evidence of inflammatory activation in the RV, existing human and experimental data suggest a role for inflammation in the early response to severe pressure overload and in the transition from RV adaptation to failure. All forms of PAH are associated with increased circulating levels of cytokines that are known to have the potential to interfere with cardiac contractility and remodeling. Preclinical studies on cardiac inflammation all suggest that inflammation is key in the vicious circle that exists between RV and pulmonary arterial remodelling. The benefits from anti-inflammatory therapies on LVF are still unclear, and the negative outcome of some clinical trials over the last years has raised doubt on the role of inflammation in HF. However, compared to LVF, anti-inflammatory therapies may be more successful when applied in PAH related RVF, since inflammation plays a dual role in the pathogenesis of both pulmonary artery remodeling and RVF.

Acknowledgement:
We acknowledge the support from the Netherlands CardioVascular Research Initiative; the Dutch Heart Foundation, Dutch Federation of University Medical Centres, the Netherlands Organisation for Health Research and Development and the Royal Netherlands Academy of Sciences".

REFERENCES

1. van Wolferen SA, Marcus JT, Boonstra A, Marques KM, Bronzwaer JG, Spreeuwenberg MD, Postmus PE, Vonk-Noordegraaf A. Prognostic value of right ventricular mass, volume, and function in idiopathic pulmonary arterial hypertension. *Eur Heart J* 2007;**28**:1250-1257.
2. Angelini DJ, Su Q, Yamaji-Kegan K, Fan C, Teng X, Hassoun PM, Yang SC, Champion HC, Tuder RM, Johns RA. Resistin-like molecule-beta in scleroderma-associated pulmonary hypertension. *Am J Respir Cell Mol Biol* 2009;**41**:553-561.
3. Perros F, Dorfmuller P, Montani D, Hammad H, Waelput W, Girerd B, Raymond N, Mercier O, Mussot S, Cohen-Kaminsky S, Humbert M, Lambrecht BN. Pulmonary lymphoid neogenesis in idiopathic pulmonary arterial hypertension. *Am J Respir Crit Care Med* 2012;**185**:311-321.
4. Parpaleix A, Amsellem V, Houssaini A, Abid S, Breau M, Marcos E, Sawaki D, Delcroix M, Quarck R, Maillard A, Couillin I, Ryffel B, Adnot S. Role of interleukin-1 receptor 1/MyD88 signalling in the development and progression of pulmonary hypertension. *Eur Respir J* 2016;**48**:470-483.
5. Rabinovitch M, Guignabert C, Humbert M, Nicolls MR. Inflammation and immunity in the pathogenesis of pulmonary arterial hypertension. *Circ Res* 2014;**115**:165-175.
6. Voelkel NF, Tamosiuniene R, Nicolls MR. Challenges and opportunities in treating inflammation associated with pulmonary hypertension. *Expert Rev Cardiovasc Ther* 2016;**14**:939-951.
7. Begieneman MP, van de Goot FR, van der Bilt IA, Vonk Noordegraaf A, Spreeuwenberg MD, Paulus WJ, van Hinsbergh VW, Visser FC, Niessen HW. Pulmonary embolism causes endomyocarditis in the human heart. *Heart* 2008;**94**:450-456.
8. Iwadate K, Doi M, Tanno K, Katsumura S, Ito H, Sato K, Yonemura I, Ito Y. Right ventricular damage due to pulmonary embolism: examination of the number of infiltrating macrophages. *Forensic Sci Int* 2003;**134**:147-153.
9. Overbeek MJ, Mouchaers KT, Niessen HM, Hadi AM, Kupreishvili K, Boonstra A, Voskuyl AE, Belien JA, Smit EF, Dijkmans BC, Vonk-Noordegraaf A, Grunberg K. Characteristics of interstitial fibrosis and inflammatory cell infiltration in right ventricles of systemic sclerosis-associated pulmonary arterial hypertension. *Int J Rheumatol* 2010;**2010**.
10. Campian ME, Hardziyenka M, de Bruin K, van Eck-Smit BL, de Bakker JM, Verberne HJ, Tan HL. Early inflammatory response during the development of right ventricular heart failure in a rat model. *Eur J Heart Fail* 2010;**12**:653-658.
11. Rondelet B, Dewachter C, Kerbaul F, Kang X, Fesler P, Brimioulle S, Naeije R, Dewachter L. Prolonged overcirculation-induced pulmonary arterial hypertension as a cause of right ventricular failure. *Eur Heart J* 2012;**33**:1017-1026.
12. Frangogiannis NG. The inflammatory response in myocardial injury, repair, and remodelling. *Nat Rev Cardiol* 2014;**11**:255-265.
13. Mann DL. Inflammatory mediators and the failing heart: past, present, and the foreseeable future. *Circ Res* 2002;**91**:988-998.
14. Van Tassell BW, Raleigh JM, Abbate A. Targeting interleukin-1 in heart failure and inflammatory heart disease. *Curr Heart Fail Rep* 2015;**12**:33-41.

15. Seta Y, Shan K, Bozkurt B, Oral H, Mann DL. Basic mechanisms in heart failure: the cytokine hypothesis. *J Card Fail* 1996;**2**:243-249.
16. Testa M, Yeh M, Lee P, Fanelli R, Loperfido F, Berman JW, LeJemtel TH. Circulating levels of cytokines and their endogenous modulators in patients with mild to severe congestive heart failure due to coronary artery disease or hypertension. *J Am Coll Cardiol* 1996;**28**:964-971.
17. Kapadia SR, Oral H, Lee J, Nakano M, Taffet GE, Mann DL. Hemodynamic regulation of tumor necrosis factor-alpha gene and protein expression in adult feline myocardium. *Circ Res* 1997;**81**:187-195.
18. Shioi T, Matsumori A, Kihara Y, Inoko M, Ono K, Iwanaga Y, Yamada T, Iwasaki A, Matsushima K, Sasayama S. Increased expression of interleukin-1 beta and monocyte chemotactic and activating factor/monocyte chemoattractant protein-1 in the hypertrophied and failing heart with pressure overload. *Circ Res* 1997;**81**:664-671.
19. Li N, Karin M. Is NF-kappaB the sensor of oxidative stress? *FASEB J* 1999;**13**:1137-1143.
20. Sun M, Chen M, Dawood F, Zurawska U, Li JY, Parker T, Kassiri Z, Kirshenbaum LA, Arnold M, Khokha R, Liu PP. Tumor necrosis factor-alpha mediates cardiac remodeling and ventricular dysfunction after pressure overload state. *Circulation* 2007;**115**:1398-1407.
21. Handoko ML, de Man FS, Happe CM, Schalij I, Musters RJ, Westerhof N, Postmus PE, Paulus WJ, van der Laarse WJ, Vonk-Noordegraaf A. Opposite effects of training in rats with stable and progressive pulmonary hypertension. *Circulation* 2009;**120**:42-49.
22. Wilson DW, Segall HJ, Pan LC, Lame MW, Estep JE, Morin D. Mechanisms and pathology of monocrotaline pulmonary toxicity. *Crit Rev Toxicol* 1992;**22**:307-325.
23. Akhavein F, St-Michel EJ, Seifert E, Rohlicek CV. Decreased left ventricular function, myocarditis, and coronary arteriolar medial thickening following monocrotaline administration in adult rats. *J Appl Physiol (1985)* 2007;**103**:287-295.
24. Zhu M, Goetsch SC, Wang Z, Luo R, Hill JA, Schneider J, Morris SM, Jr., Liu ZP. FoxO4 promotes early inflammatory response upon myocardial infarction via endothelial Arg1. *Circ Res* 2015;**117**:967-977.
25. Frangogiannis NG. The immune system and cardiac repair. *Pharmacol Res* 2008;**58**:88-111.
26. Adams V, Linke A, Wisloff U, Doring C, Erbs S, Krankel N, Witt CC, Labeit S, Muller-Werdan U, Schuler G, Hambrecht R. Myocardial expression of Murf-1 and MAFbx after induction of chronic heart failure: Effect on myocardial contractility. *Cardiovasc Res* 2007;**73**:120-129.
27. Lin L, Kim SC, Wang Y, Gupta S, Davis B, Simon SI, Torre-Amione G, Knowlton AA. HSP60 in heart failure: abnormal distribution and role in cardiac myocyte apoptosis. *Am J Physiol Heart Circ Physiol* 2007;**293**:H2238-2247.
28. Dell'Italia LJ, Lembo NJ, Starling MR, Crawford MH, Simmons RS, Lasher JC, Blumhardt R, Lancaster J, O'Rourke RA. Hemodynamically important right ventricular infarction: follow-up evaluation of right ventricular systolic function at rest and during exercise with radionuclide ventriculography and respiratory gas exchange. *Circulation* 1987;**75**:996-1003.
29. Ohuchi H, Beighley PE, Dong Y, Zamir M, Ritman EL. Microvascular development in porcine right and left ventricular walls. *Pediatr Res* 2007;**61**:676-680.

30. Bogaard HJ, Natarajan R, Henderson SC, Long CS, Kraskauskas D, Smithson L, Ockaili R, McCord JM, Voelkel NF. Chronic pulmonary artery pressure elevation is insufficient to explain right heart failure. *Circulation* 2009;**120**:1951-1960.
31. Ryan JJ, Huston J, Kutty S, Hatton ND, Bowman L, Tian L, Herr JE, Johri AM, Archer SL. Right ventricular adaptation and failure in pulmonary arterial hypertension. *Can J Cardiol* 2015;**31**:391-406.
32. Montisci R, Vacca A, Garau P, Colonna P, Ruscazio M, Passiu G, Iliceto S, Mathieu A. Detection of early impairment of coronary flow reserve in patients with systemic sclerosis. *Ann Rheum Dis* 2003;**62**:890-893.
33. Soon E, Holmes AM, Treacy CM, Doughty NJ, Southgate L, Machado RD, Trembath RC, Jennings S, Barker L, Nicklin P, Walker C, Budd DC, Pepke-Zaba J, Morrell NW. Elevated levels of inflammatory cytokines predict survival in idiopathic and familial pulmonary arterial hypertension. *Circulation* 2010;**122**:920-927.
34. Wensel R, Jilek C, Dorr M, Francis DP, Stadler H, Lange T, Blumberg F, Opitz C, Pfeifer M, Ewert R. Impaired cardiac autonomic control relates to disease severity in pulmonary hypertension. *Eur Respir J* 2009;**34**:895-901.
35. Ciarka A, Doan V, Velez-Roa S, Naeije R, van de Borne P. Prognostic significance of sympathetic nervous system activation in pulmonary arterial hypertension. *Am J Respir Crit Care Med* 2010;**181**:1269-1275.
36. Murray DR, Prabhu SD, Chandrasekar B. Chronic beta-adrenergic stimulation induces myocardial proinflammatory cytokine expression. *Circulation* 2000;**101**:2338-2341.
37. Kalra D, Sivasubramanian N, Mann DL. Angiotensin II induces tumor necrosis factor biosynthesis in the adult mammalian heart through a protein kinase C-dependent pathway. *Circulation* 2002;**105**:2198-2205.
38. Prabhu SD, Chandrasekar B, Murray DR, Freeman GL. beta-adrenergic blockade in developing heart failure: effects on myocardial inflammatory cytokines, nitric oxide, and remodeling. *Circulation* 2000;**101**:2103-2109.
39. de Man FS, Handoko ML, van Ballegoij JJ, Schalij I, Bogaards SJ, Postmus PE, van der Velden J, Westerhof N, Paulus WJ, Vonk-Noordegraaf A. Bisoprolol delays progression towards right heart failure in experimental pulmonary hypertension. *Circ Heart Fail* 2012;**5**:97-105.
40. Seccia TM, Belloni AS, Kreutz R, Paul M, Nussdorfer GG, Pessina AC, Rossi GP. Cardiac fibrosis occurs early and involves endothelin and AT-1 receptors in hypertension due to endogenous angiotensin II. *Journal of the American College of Cardiology* 2003;**41**:666-673.
41. Galie N. The endothelin system in pulmonary arterial hypertension. *Cardiovascular Research* 2004;**61**:227-237.
42. Yoshizumi M, Kurihara H, Morita T, Yamashita T, Oh-hashi Y, Sugiyama T, Takaku F, Yanagisawa M, Masaki T, Yazaki Y. Interleukin 1 increases the production of endothelin-1 by cultured endothelial cells. *Biochem Biophys Res Commun* 1990;**166**:324-329.
43. Corder R, Carrier M, Khan N, Klemm P, Vane JR. Cytokine regulation of endothelin-1 release from bovine aortic endothelial cells. *J Cardiovasc Pharmacol* 1995;**26 Suppl 3**:S56-58.
44. Goetz KL, Wang BC, Madwed JB, Zhu JL, Leadley RJ, Jr. Cardiovascular, renal, and endocrine responses to intravenous endothelin in conscious dogs. *Am J Physiol* 1988;**255**:R1064-1068.

45. Miller WL, Redfield MM, Burnett JC, Jr. Integrated cardiac, renal, and endocrine actions of endothelin. *J Clin Invest* 1989;**83**:317-320.
46. Yang LL, Gros R, Kabir MG, Sadi A, Gotlieb AI, Husain M, Stewart DJ. Conditional cardiac overexpression of endothelin-1 induces inflammation and dilated cardiomyopathy in mice. *Circulation* 2004;**109**:255-261.
47. Pall ML. The NO/ONOO-cycle as the central cause of heart failure. *Int J Mol Sci* 2013;**14**:22274-22330.
48. Tatsumi T, Matoba S, Kawahara A, Keira N, Shiraishi J, Akashi K, Kobara M, Tanaka T, Katamura M, Nakagawa C, Ohta B, Shirayama T, Takeda K, Asayama J, Fliss H, Nakagawa M. Cytokine-induced nitric oxide production inhibits mitochondrial energy production and impairs contractile function in rat cardiac myocytes. *J Am Coll Cardiol* 2000;**35**:1338-1346.
49. Tsujino M, Hirata Y, Imai T, Kanno K, Eguchi S, Ito H, Marumo F. Induction of nitric oxide synthase gene by interleukin-1 beta in cultured rat cardiocytes. *Circulation* 1994;**90**:375-383.
50. Frustaci A, Petrosillo N, Vizza D, Francone M, Badagliacca R, Verardo R, Fedele F, Ippolito G, Chimenti C. Myocardial and microvascular inflammation/infection in patients with HIV-associated pulmonary artery hypertension. *AIDS* 2014;**28**:2541-2549.
51. Steen VD, Medsger TA. Changes in causes of death in systemic sclerosis, 1972-2002. *Ann Rheum Dis* 2007;**66**:940-944.
52. Tedford RJ, Mudd JO, Girgis RE, Mathai SC, Zaiman AL, Housten-Harris T, Boyce D, Kelemen BW, Bacher AC, Shah AA, Hummers LK, Wigley FM, Russell SD, Saggar R, Saggar R, Maughan WL, Hassoun PM, Kass DA. Right ventricular dysfunction in systemic sclerosis-associated pulmonary arterial hypertension. *Circ Heart Fail* 2013;**6**:953-963.
53. Overbeek MJ, Lankhaar JW, Westerhof N, Voskuyl AE, Boonstra A, Bronzwaer JG, Marques KM, Smit EF, Dijkmans BA, Vonk-Noordegraaf A. Right ventricular contractility in systemic sclerosis-associated and idiopathic pulmonary arterial hypertension. *Eur Respir J* 2008;**31**:1160-1166.
54. Stenmark KR, Meyrick B, Galie N, Mooi WJ, McMurtry IF. Animal models of pulmonary arterial hypertension: the hope for etiological discovery and pharmacological cure. *Am J Physiol Lung Cell Mol Physiol* 2009;**297**:L1013-1032.
55. Jasmin JF, Lucas M, Cernacek P, Dupuis J. Effectiveness of a nonselective ET(A/B) and a selective ET(A) antagonist in rats with monocrotaline-induced pulmonary hypertension. *Circulation* 2001;**103**:314-318.
56. Taraseviciene-Stewart L, Kasahara Y, Alger L, Hirth P, Mc Mahon G, Waltenberger J, Voelkel NF, Tuder RM. Inhibition of the VEGF receptor 2 combined with chronic hypoxia causes cell death-dependent pulmonary endothelial cell proliferation and severe pulmonary hypertension. *FASEB J* 2001;**15**:427-438.
57. Ahmed LA, Obaid AA, Zaki HF, Agha AM. Role of oxidative stress, inflammation, nitric oxide and transforming growth factor-beta in the protective effect of diosgenin in monocrotaline-induced pulmonary hypertension in rats. *Eur J Pharmacol* 2014;**740**:379-387.
58. Alencar AK, Montes GC, Montagnoli T, Silva AM, Martinez ST, Fraga AG, Wang H, Groban L, Sudo RT, Zapata-Sudo G. Activation of GPER ameliorates experimental pulmonary hypertension in male rats. *Eur J Pharm Sci* 2017;**97**:208-217.

59. Nogueira-Ferreira R, Moreira-Goncalves D, Silva AF, Duarte JA, Leite-Moreira A, Ferreira R, Henriques-Coelho T. Exercise preconditioning prevents MCT-induced right ventricle remodeling through the regulation of TNF superfamily cytokines. *Int J Cardiol* 2016;**203**:858-866.
60. Rice KM, Manne ND, Kolli MB, Wehner PS, Dornon L, Arvapalli R, Selvaraj V, Kumar A, Blough ER. Curcumin nanoparticles attenuate cardiac remodeling due to pulmonary arterial hypertension. *Artif Cells Nanomed Biotechnol* 2016;**44**:1909-1916.
61. Moreira-Goncalves D, Ferreira R, Fonseca H, Padrao AI, Moreno N, Silva AF, Vasques-Novoa F, Goncalves N, Vieira S, Santos M, Amado F, Duarte JA, Leite-Moreira AF, Henriques-Coelho T. Cardioprotective effects of early and late aerobic exercise training in experimental pulmonary arterial hypertension. *Basic Res Cardiol* 2015;**110**:57.
62. Wang JJ, Zuo XR, Xu J, Zhou JY, Kong H, Zeng XN, Xie WP, Cao Q. Evaluation and Treatment of Endoplasmic Reticulum (ER) Stress in Right Ventricular Dysfunction during Monocrotaline-Induced Rat Pulmonary Arterial Hypertension. *Cardiovasc Drugs Ther* 2016;**30**:587-598.
63. Brown MB, Neves E, Long G, Graber J, Gladish B, Wiseman A, Owens M, Fisher AJ, Presson RG, Petrache I, Kline J, Lahm T. High-intensity interval training, but not continuous training, reverses right ventricular hypertrophy and dysfunction in a rat model of pulmonary hypertension. *Am J Physiol Regul Integr Comp Physiol* 2017;**312**:R197-R210.
64. Waehre A, Vistnes M, Sjaastad I, Nygard S, Husberg C, Lunde IG, Aukrust P, Yndestad A, Vinge LE, Behmen D, Neukamm C, Brun H, Thaulow E, Christensen G. Chemokines regulate small leucine-rich proteoglycans in the extracellular matrix of the pressure-overloaded right ventricle. *J Appl Physiol (1985)* 2012;**112**:1372-1382.
65. Novoyatleva T, Schymura Y, Janssen W, Strobl F, Swiercz JM, Patra C, Posern G, Wietelmann A, Zheng TS, Schermuly RT, Engel FB. Deletion of Fn14 receptor protects from right heart fibrosis and dysfunction. *Basic Research in Cardiology* 2013;**108**.
66. Filusch A, Zelniker T, Baumgartner C, Eschricht S, Frey N, Katus HA, Chorianopoulos E. Soluble TWEAK predicts hemodynamic impairment and functional capacity in patients with pulmonary arterial hypertension. *Clin Res Cardiol* 2011;**100**:879-885.
67. Yoshida K, Abe K, Saku K, Sunagawa K. Inhibition of Nuclear Factor-kappaB-Mediated Inflammation Reverses Fibrosis and Improves RV Function in Rats with Pulmonary Artery Banding. *Journal of Cardiac Failure*;**22**:S198.
68. Belhaj A, Dewachter L, Kerbaul F, Brimioulle S, Dewachter C, Naeije R, Rondelet B. Heme oxygenase-1 and inflammation in experimental right ventricular failure on prolonged overcirculation-induced pulmonary hypertension. *PLoS One* 2013;**8**:e69470.
69. Frump AL, Goss KN, Vayl A, Albrecht M, Fisher A, Tursunova R, Fierst J, Whitson J, Cucci AR, Brown MB, Lahm T. Estradiol improves right ventricular function in rats with severe angioproliferative pulmonary hypertension: effects of endogenous and exogenous sex hormones. *Am J Physiol Lung Cell Mol Physiol* 2015;**308**:L873-890.
70. Lambert V, Capderou A, Le Bret E, Rucker-Martin C, Deroubaix E, Gouadon E, Raymond N, Stos B, Serraf A, Renaud JF. Right ventricular failure secondary to chronic overload in congenital heart disease: an experimental model for therapeutic innovation. *J Thorac Cardiovasc Surg* 2010;**139**:1197-1204, 1204 e1191.

71. Ribeiro A, Lindmarker P, Juhlin-Dannfelt A, Johnsson H, Jorfeldt L. Echocardiography Doppler in pulmonary embolism: right ventricular dysfunction as a predictor of mortality rate. *Am Heart J* 1997;**134**:479-487.
72. Goldhaber SZ, Haire WD, Feldstein ML, Miller M, Toltzis R, Smith JL, Taveira da Silva AM, Come PC, Lee RT, Parker JA, et al. Alteplase versus heparin in acute pulmonary embolism: randomised trial assessing right-ventricular function and pulmonary perfusion. *Lancet* 1993;**341**:507-511.
73. Grifoni S, Olivotto I, Cecchini P, Pieralli F, Camaiti A, Santoro G, Conti A, Agnelli G, Berni G. Short-term clinical outcome of patients with acute pulmonary embolism, normal blood pressure, and echocardiographic right ventricular dysfunction. *Circulation* 2000;**101**:2817-2822.
74. Iwadate K, Tanno K, Doi M, Takatori T, Ito Y. Two cases of right ventricular ischemic injury due to massive pulmonary embolism. *Forensic Sci Int* 2001;**116**:189-195.
75. Watts JA, Zagorski J, Gellar MA, Stevinson BG, Kline JA. Cardiac inflammation contributes to right ventricular dysfunction following experimental pulmonary embolism in rats. *J Mol Cell Cardiol* 2006;**41**:296-307.
76. Jones AE, Watts JA, Debelak JP, Thornton LR, Younger JG, Kline JA. Inhibition of prostaglandin synthesis during polystyrene microsphere-induced pulmonary embolism in the rat. *Am J Physiol Lung Cell Mol Physiol* 2003;**284**:L1072-1081.
77. Zagorski J, Gellar MA, Obraztsova M, Kline JA, Watts JA. Inhibition of CINC-1 decreases right ventricular damage caused by experimental pulmonary embolism in rats. *J Immunol* 2007;**179**:7820-7826.
78. Dewachter C, Belhaj A, Rondelet B, Vercruyssen M, Schraufnagel DP, Remmelink M, Brimioulle S, Kerbaul F, Naeije R, Dewachter L. Myocardial inflammation in experimental acute right ventricular failure: Effects of prostacyclin therapy. *J Heart Lung Transplant* 2015;**34**:1334-1345.
79. Dewachter C, Dewachter L, Rondelet B, Fesler P, Brimioulle S, Kerbaul F, Naeije R. Activation of apoptotic pathways in experimental acute afterload-induced right ventricular failure. *Crit Care Med* 2010;**38**:1405-1413.
80. Vikholm P, Schiller P, Hellgren L. A modified Glenn shunt reduces venous congestion during acute right ventricular failure due to pulmonary banding: a randomized experimental study. *Interact Cardiovasc Thorac Surg* 2014;**18**:418-425.
81. Belhaj A, Dewachter L, Rorive S, Remmelink M, Weynand B, Melot C, Galanti L, Hupkens E, Sprockeels T, Dewachter C, Creteur J, McEntee K, Naeije R, Rondelet B. Roles of inflammation and apoptosis in experimental brain death-induced right ventricular failure. *J Heart Lung Transplant* 2016;**35**:1505-1518.
82. Birks EJ, Owen VJ, Burton PB, Bishop AE, Banner NR, Khaghani A, Polak JM, Yacoub MH. Tumor necrosis factor-alpha is expressed in donor heart and predicts right ventricular failure after human heart transplantation. *Circulation* 2000;**102**:326-331.
83. Poon BY, Ward CA, Cooper CB, Giles WR, Burns AR, Kubes P. alpha(4)-integrin mediates neutrophil-induced free radical injury to cardiac myocytes. *J Cell Biol* 2001;**152**:857-866.
84. Simms MG, Walley KR. Activated macrophages decrease rat cardiac myocyte contractility: importance of ICAM-1-dependent adhesion. *Am J Physiol* 1999;**277**:H253-260.

85. Smith CW, Entman ML, Lane CL, Beaudet AL, Ty TI, Youker K, Hawkins HK, Anderson DC. Adherence of neutrophils to canine cardiac myocytes in vitro is dependent on intercellular adhesion molecule-1. *J Clin Invest* 1991;**88**:1216-1223.
86. Davani EY, Dorscheid DR, Lee CH, van Breemen C, Walley KR. Novel regulatory mechanism of cardiomyocyte contractility involving ICAM-1 and the cytoskeleton. *Am J Physiol Heart Circ Physiol* 2004;**287**:H1013-1022.
87. Davani EY, Boyd JH, Dorscheid DR, Wang Y, Meredith A, Chau E, Singhera GK, Walley KR. Cardiac ICAM-1 mediates leukocyte-dependent decreased ventricular contractility in endotoxemic mice. *Cardiovasc Res* 2006;**72**:134-142.
88. Granton JT, Goddard CM, Allard MF, van Eeden S, Walley KR. Leukocytes and decreased left-ventricular contractility during endotoxemia in rabbits. *Am J Respir Crit Care Med* 1997;**155**:1977-1983.
89. Nevers T, Salvador AM, Grodecki-Pena A, Knapp A, Velazquez F, Aronovitz M, Kapur NK, Karas RH, Blanton RM, Alcaide P. Left Ventricular T-Cell Recruitment Contributes to the Pathogenesis of Heart Failure. *Circ Heart Fail* 2015;**8**:776-787.
90. Laroumanie F, Douin-Echinard V, Pozzo J, Lairez O, Tortosa F, Vinel C, Delage C, Calise D, Dutaur M, Parini A, Pizzinat N. CD4+ T cells promote the transition from hypertrophy to heart failure during chronic pressure overload. *Circulation* 2014;**129**:2111-2124.
91. Patten M, Kramer E, Bunemann J, Wenck C, Thoenes M, Wieland T, Long C. Endotoxin and cytokines alter contractile protein expression in cardiac myocytes in vivo. *Pflugers Arch* 2001;**442**:920-927.
92. Moe GW, Marin-Garcia J, Konig A, Goldenthal M, Lu X, Feng Q. In vivo TNF-alpha inhibition ameliorates cardiac mitochondrial dysfunction, oxidative stress, and apoptosis in experimental heart failure. *Am J Physiol Heart Circ Physiol* 2004;**287**:H1813-1820.
93. Paulin R, Sutendra G, Gurtu V, Dromparis P, Haromy A, Provencher S, Bonnet S, Michelakis ED. A miR-208-Mef2 axis drives the decompensation of right ventricular function in pulmonary hypertension. *Circ Res* 2015;**116**:56-69.
94. Liu SJ, Zhou W, Kennedy RH. Suppression of beta-adrenergic responsiveness of L-type Ca2+ current by IL-1beta in rat ventricular myocytes. *Am J Physiol* 1999;**276**:H141-148.
95. Combes A, Frye CS, Lemster BH, Brooks SS, Watkins SC, Feldman AM, McTiernan CF. Chronic exposure to interleukin 1beta induces a delayed and reversible alteration in excitation-contraction coupling of cultured cardiomyocytes. *Pflugers Arch* 2002;**445**:246-256.
96. Schulz R, Panas DL, Catena R, Moncada S, Olley PM, Lopaschuk GD. The role of nitric oxide in cardiac depression induced by interleukin-1 beta and tumour necrosis factor-alpha. *Br J Pharmacol* 1995;**114**:27-34.
97. McTiernan CF, Lemster BH, Frye C, Brooks S, Combes A, Feldman AM. Interleukin-1 beta inhibits phospholamban gene expression in cultured cardiomyocytes. *Circ Res* 1997;**81**:493-503.
98. Villegas S, Villarreal FJ, Dillmann WH. Leukemia Inhibitory Factor and Interleukin-6 downregulate sarcoplasmic reticulum Ca2+ ATPase (SERCA2) in cardiac myocytes. *Basic Res Cardiol* 2000;**95**:47-54.

99. Janssen SP, Gayan-Ramirez G, Van den Bergh A, Herijgers P, Maes K, Verbeken E, Decramer M. Interleukin-6 causes myocardial failure and skeletal muscle atrophy in rats. *Circulation* 2005;**111**:996-1005.
100. Sanada S, Hakuno D, Higgins LJ, Schreiter ER, McKenzie AN, Lee RT. IL-33 and ST2 comprise a critical biomechanically induced and cardioprotective signaling system. *J Clin Invest* 2007;**117**:1538-1549.
101. Weinberg EO, Shimpo M, De Keulenaer GW, MacGillivray C, Tominaga S, Solomon SD, Rouleau JL, Lee RT. Expression and regulation of ST2, an interleukin-1 receptor family member, in cardiomyocytes and myocardial infarction. *Circulation* 2002;**106**:2961-2966.
102. Shah RV, Chen-Tournoux AA, Picard MH, van Kimmenade RR, Januzzi JL. Serum levels of the interleukin-1 receptor family member ST2, cardiac structure and function, and long-term mortality in patients with acute dyspnea. *Circ Heart Fail* 2009;**2**:311-319.
103. Ky B, French B, McCloskey K, Rame JE, McIntosh E, Shahi P, Dries DL, Tang WH, Wu AH, Fang JC, Boxer R, Sweitzer NK, Levy WC, Goldberg LR, Jessup M, Cappola TP. High-sensitivity ST2 for prediction of adverse outcomes in chronic heart failure. *Circ Heart Fail* 2011;**4**:180-187.
104. Carlomagno G, Messalli G, Melillo RM, Stanziola AA, Visciano C, Mercurio V, Imbriaco M, Ghio S, Sofia M, Bonaduce D, Fazio S. Serum soluble ST2 and interleukin-33 levels in patients with pulmonary arterial hypertension. *Int J Cardiol* 2013;**168**:1545-1547.
105. AbouEzzeddine OF, McKie PM, Dunlay SM, Stevens SR, Felker GM, Borlaug BA, Chen HH, Tracy RP, Braunwald E, Redfield MM. Suppression of Tumorigenicity 2 in Heart Failure With Preserved Ejection Fraction. *J Am Heart Assoc* 2017;**6**.
106. Heymans S, Corsten MF, Verhesen W, Carai P, van Leeuwen RE, Custers K, Peters T, Hazebroek M, Stoger L, Wijnands E, Janssen BJ, Creemers EE, Pinto YM, Grimm D, Schurmann N, Vigorito E, Thum T, Stassen F, Yin X, Mayr M, de Windt LJ, Lutgens E, Wouters K, de Winther MP, Zacchigna S, Giacca M, van Bilsen M, Papageorgiou AP, Schroen B. Macrophage microRNA-155 promotes cardiac hypertrophy and failure. *Circulation* 2013;**128**:1420-1432.
107. Koren L, Alishekevitz D, Elhanani O, Nevelsky A, Hai T, Kehat I, Shaked Y, Aronheim A. ATF3-dependent cross-talk between cardiomyocytes and macrophages promotes cardiac maladaptive remodeling. *Int J Cardiol* 2015;**198**:232-240.
108. Thaik CM, Calderone A, Takahashi N, Colucci WS. Interleukin-1 beta modulates the growth and phenotype of neonatal rat cardiac myocytes. *J Clin Invest* 1995;**96**:1093-1099.
109. Wollert KC, Taga T, Saito M, Narazaki M, Kishimoto T, Glembotski CC, Vernallis AB, Heath JK, Pennica D, Wood WI, Chien KR. Cardiotrophin-1 activates a distinct form of cardiac muscle cell hypertrophy. Assembly of sarcomeric units in series VIA gp130/leukemia inhibitory factor receptor-dependent pathways. *J Biol Chem* 1996;**271**:9535-9545.
110. Higuchi Y, Otsu K, Nishida K, Hirotani S, Nakayama H, Yamaguchi O, Matsumura Y, Ueno H, Tada M, Hori M. Involvement of reactive oxygen species-mediated NF-kappa B activation in TNF-alpha-induced cardiomyocyte hypertrophy. *J Mol Cell Cardiol* 2002;**34**:233-240.
111. Yokoyama T, Nakano M, Bednarczyk JL, McIntyre BW, Entman M, Mann DL. Tumor necrosis factor-alpha provokes a hypertrophic growth response in adult cardiac myocytes. *Circulation* 1997;**95**:1247-1252.

112. Bozkurt B, Kribbs SB, Clubb FJ, Jr., Michael LH, Didenko VV, Hornsby PJ, Seta Y, Oral H, Spinale FG, Mann DL. Pathophysiologically relevant concentrations of tumor necrosis factor-alpha promote progressive left ventricular dysfunction and remodeling in rats. *Circulation* 1998;**97**:1382-1391.
113. Novoyatleva T, Janssen W, Wietelmann A, Schermuly RT, Engel FB. TWEAK/Fn14 axis is a positive regulator of cardiac hypertrophy. *Cytokine* 2013;**64**:43-45.
114. Jain M, Jakubowski A, Cui L, Shi J, Su L, Bauer M, Guan J, Lim CC, Naito Y, Thompson JS, Sam F, Ambrose C, Parr M, Crowell T, Lincecum JM, Wang MZ, Hsu YM, Zheng TS, Michaelson JS, Liao R, Burkly LC. A novel role for tumor necrosis factor-like weak inducer of apoptosis (TWEAK) in the development of cardiac dysfunction and failure. *Circulation* 2009;**119**:2058-2068.
115. Zhu J, Liu M, Kennedy RH, Liu SJ. TNF-alpha-induced impairment of mitochondrial integrity and apoptosis mediated by caspase-8 in adult ventricular myocytes. *Cytokine* 2006;**34**:96-105.
116. Krown KA, Page MT, Nguyen C, Zechner D, Gutierrez V, Comstock KL, Glembotski CC, Quintana PJ, Sabbadini RA. Tumor necrosis factor alpha-induced apoptosis in cardiac myocytes. Involvement of the sphingolipid signaling cascade in cardiac cell death. *J Clin Invest* 1996;**98**:2854-2865.
117. Moe KT, Khairunnisa K, Yin NO, Chin-Dusting J, Wong P, Wong MC. Tumor necrosis factor-alpha-induced nuclear factor-kappaB activation in human cardiomyocytes is mediated by NADPH oxidase. *J Physiol Biochem* 2014;**70**:769-779.
118. Awad AE, Kandalam V, Chakrabarti S, Wang X, Penninger JM, Davidge ST, Oudit GY, Kassiri Z. Tumor necrosis factor induces matrix metalloproteinases in cardiomyocytes and cardiofibroblasts differentially via superoxide production in a PI3Kgamma-dependent manner. *Am J Physiol Cell Physiol* 2010;**298**:C679-692.
119. Gao CQ, Sawicki G, Suarez-Pinzon WL, Csont T, Wozniak M, Ferdinandy P, Schulz R. Matrix metalloproteinase-2 mediates cytokine-induced myocardial contractile dysfunction. *Cardiovasc Res* 2003;**57**:426-433.
120. Hamid T, Gu Y, Ortines RV, Bhattacharya C, Wang G, Xuan YT, Prabhu SD. Divergent tumor necrosis factor receptor-related remodeling responses in heart failure: role of nuclear factor-kappaB and inflammatory activation. *Circulation* 2009;**119**:1386-1397.
121. Chen HN, Wang DJ, Ren MY, Wang QL, Sui SJ. TWEAK/Fn14 promotes the proliferation and collagen synthesis of rat cardiac fibroblasts via the NF-small ka, CyrillicB pathway. *Mol Biol Rep* 2012;**39**:8231-8241.
122. Xia Y, Lee K, Li N, Corbett D, Mendoza L, Frangogiannis NG. Characterization of the inflammatory and fibrotic response in a mouse model of cardiac pressure overload. *Histochem Cell Biol* 2009;**131**:471-481.
123. Campbell SE, Janicki JS, Weber KT. Temporal differences in fibroblast proliferation and phenotype expression in response to chronic administration of angiotensin II or aldosterone. *J Mol Cell Cardiol* 1995;**27**:1545-1560.
124. Ma F, Feng J, Zhang C, Li Y, Qi G, Li H, Wu Y, Fu Y, Zhao Y, Chen H, Du J, Tang H. The requirement of CD8+ T cells to initiate and augment acute cardiac inflammatory response to high blood pressure. *J Immunol* 2014;**192**:3365-3373.

125. Koren L, Barash U, Zohar Y, Karin N, Aronheim A. The cardiac maladaptive ATF3-dependent cross-talk between cardiomyocytes and macrophages is mediated by the IFNgamma-CXCL10-CXCR3 axis. *Int J Cardiol* 2017;**228**:394-400.
126. Yoshioka T, Okada T, Maeda Y, Ikeda U, Shimpo M, Nomoto T, Takeuchi K, Nonaka-Sarukawa M, Ito T, Takahashi M, Matsushita T, Mizukami H, Hanazono Y, Kume A, Ookawara S, Kawano M, Ishibashi S, Shimada K, Ozawa K. Adeno-associated virus vector-mediated interleukin-10 gene transfer inhibits atherosclerosis in apolipoprotein E-deficient mice. *Gene Ther* 2004;**11**:1772-1779.
127. Ito T, Okada T, Miyashita H, Nomoto T, Nonaka-Sarukawa M, Uchibori R, Maeda Y, Urabe M, Mizukami H, Kume A, Takahashi M, Ikeda U, Shimada K, Ozawa K. Interleukin-10 expression mediated by an adeno-associated virus vector prevents monocrotaline-induced pulmonary arterial hypertension in rats. *Circ Res* 2007;**101**:734-741.
128. Brown RD, Ambler SK, Mitchell MD, Long CS. The cardiac fibroblast: therapeutic target in myocardial remodeling and failure. *Annu Rev Pharmacol Toxicol* 2005;**45**:657-687.
129. Turner NA, Mughal RS, Warburton P, O'Regan DJ, Ball SG, Porter KE. Mechanism of TNFalpha-induced IL-1alpha, IL-1beta and IL-6 expression in human cardiac fibroblasts: effects of statins and thiazolidinediones. *Cardiovasc Res* 2007;**76**:81-90.
130. Turner NA, Das A, Warburton P, O'Regan DJ, Ball SG, Porter KE. Interleukin-1alpha stimulates proinflammatory cytokine expression in human cardiac myofibroblasts. *Am J Physiol Heart Circ Physiol* 2009;**297**:H1117-1127.
131. Jacobs M, Staufenberger S, Gergs U, Meuter K, Brandstatter K, Hafner M, Ertl G, Schorb W. Tumor necrosis factor-alpha at acute myocardial infarction in rats and effects on cardiac fibroblasts. *J Mol Cell Cardiol* 1999;**31**:1949-1959.
132. Peng J, Gurantz D, Tran V, Cowling RT, Greenberg BH. Tumor necrosis factor-alpha-induced AT1 receptor upregulation enhances angiotensin II-mediated cardiac fibroblast responses that favor fibrosis. *Circ Res* 2002;**91**:1119-1126.
133. Koudssi F, Lopez JE, Villegas S, Long CS. Cardiac fibroblasts arrest at the G1/S restriction point in response to interleukin (IL)-1beta. Evidence for IL-1beta-induced hypophosphorylation of the retinoblastoma protein. *J Biol Chem* 1998;**273**:25796-25803.
134. Yue P, Massie BM, Simpson PC, Long CS. Cytokine expression increases in nonmyocytes from rats with postinfarction heart failure. *Am J Physiol* 1998;**275**:H250-258.
135. Dobaczewski M, Bujak M, Li N, Gonzalez-Quesada C, Mendoza LH, Wang XF, Frangogiannis NG. Smad3 signaling critically regulates fibroblast phenotype and function in healing myocardial infarction. *Circ Res* 2010;**107**:418-428.
136. Westermann D, Lindner D, Kasner M, Zietsch C, Savvatis K, Escher F, von Schlippenbach J, Skurk C, Steendijk P, Riad A, Poller W, Schultheiss HP, Tschope C. Cardiac inflammation contributes to changes in the extracellular matrix in patients with heart failure and normal ejection fraction. *Circ Heart Fail* 2011;**4**:44-52.
137. Harel-Adar T, Ben Mordechai T, Amsalem Y, Feinberg MS, Leor J, Cohen S. Modulation of cardiac macrophages by phosphatidylserine-presenting liposomes improves infarct repair. *Proc Natl Acad Sci U S A* 2011;**108**:1827-1832.

138. Piao L, Fang YH, Parikh K, Ryan JJ, Toth PT, Archer SL. Cardiac glutaminolysis: a maladaptive cancer metabolism pathway in the right ventricle in pulmonary hypertension. *J Mol Med (Berl)* 2013;**91**:1185-1197.
139. Piao L, Fang YH, Cadete VJ, Wietholt C, Urboniene D, Toth PT, Marsboom G, Zhang HJ, Haber I, Rehman J, Lopaschuk GD, Archer SL. The inhibition of pyruvate dehydrogenase kinase improves impaired cardiac function and electrical remodeling in two models of right ventricular hypertrophy: resuscitating the hibernating right ventricle. *J Mol Med (Berl)* 2010;**88**:47-60.
140. Potus F, Malenfant S, Graydon C, Mainguy V, Tremblay E, Breuils-Bonnet S, Ribeiro F, Porlier A, Maltais F, Bonnet S, Provencher S. Impaired angiogenesis and peripheral muscle microcirculation loss contribute to exercise intolerance in pulmonary arterial hypertension. *Am J Respir Crit Care Med* 2014;**190**:318-328.
141. Tamby MC, Chanseaud Y, Humbert M, Fermanian J, Guilpain P, Garcia-de-la-Pena-Lefebvre P, Brunet S, Servettaz A, Weill B, Simonneau G, Guillevin L, Boissier MC, Mouthon L. Anti-endothelial cell antibodies in idiopathic and systemic sclerosis associated pulmonary arterial hypertension. *Thorax* 2005;**60**:765-772.
142. Arends SJ, Damoiseaux J, Duijvestijn A, Debrus-Palmans L, Boomars K, Broers B, Tervaert JW, van Paassen P. Prevalence of anti-endothelial cell antibodies in idiopathic pulmonary arterial hypertension. *Eur Respir J* 2010;**35**:923-925.
143. Dib H, Tamby MC, Bussone G, Regent A, Berezne A, Lafine C, Broussard C, Simonneau G, Guillevin L, Witko-Sarsat V, Humbert M, Mouthon L. Targets of anti-endothelial cell antibodies in pulmonary hypertension and scleroderma. *Eur Respir J* 2012;**39**:1405-1414.
144. van Paassen P, Duijvestijn A, Debrus-Palmans L, Damoiseaux J, Vroomen M, Tervaert JW. Induction of endothelial cell apoptosis by IgG antibodies from SLE patients with nephropathy: a potential role for anti-endothelial cell antibodies. *Ann N Y Acad Sci* 2007;**1108**:147-156.
145. Belizna C, Duijvestijn A, Hamidou M, Tervaert JW. Antiendothelial cell antibodies in vasculitis and connective tissue disease. *Ann Rheum Dis* 2006;**65**:1545-1550.
146. Kondo A, Takahashi K, Mizuno T, Kato A, Hirano D, Yamamoto N, Hayashi H, Koide S, Takahashi H, Hasegawa M, Hiki Y, Yoshida S, Miura K, Yuzawa Y. The Level of IgA Antibodies to Endothelial Cells Correlates with Histological Evidence of Disease Activity in Patients with Lupus Nephritis. *PLoS One* 2016;**11**:e0163085.
147. Arends SJ, Damoiseaux JG, Duijvestijn AM, Debrus-Palmans L, Boomars KA, Brunner-La Rocca HP, Cohen Tervaert JW, van Paassen P. Functional implications of IgG anti-endothelial cell antibodies in pulmonary arterial hypertension. *Autoimmunity* 2013;**46**:463-470.
148. Negi VS, Tripathy NK, Misra R, Nityanand S. Antiendothelial cell antibodies in scleroderma correlate with severe digital ischemia and pulmonary arterial hypertension. *J Rheumatol* 1998;**25**:462-466.
149. Mandavia CH, Aroor AR, Demarco VG, Sowers JR. Molecular and metabolic mechanisms of cardiac dysfunction in diabetes. *Life Sci* 2013;**92**:601-608.

150. Yang J, Park Y, Zhang H, Xu X, Laine GA, Dellsperger KC, Zhang C. Feed-forward signaling of TNF-alpha and NF-kappaB via IKK-beta pathway contributes to insulin resistance and coronary arteriolar dysfunction in type 2 diabetic mice. *Am J Physiol Heart Circ Physiol* 2009;**296**:H1850-1858.
151. Serrano-Marco L, Rodriguez-Calvo R, El Kochairi I, Palomer X, Michalik L, Wahli W, Vazquez-Carrera M. Activation of peroxisome proliferator-activated receptor-beta/-delta (PPAR-beta/-delta) ameliorates insulin signaling and reduces SOCS3 levels by inhibiting STAT3 in interleukin-6-stimulated adipocytes. *Diabetes* 2011;**60**:1990-1999.
152. Nan WQ, Shan TQ, Qian X, Ping W, Bing GA, Ying LL. PPARalpha agonist prevented the apoptosis induced by glucose and fatty acid in neonatal cardiomyocytes. *J Endocrinol Invest* 2011;**34**:271-275.
153. Min W, Bin ZW, Quan ZB, Hui ZJ, Sheng FG. The signal transduction pathway of PKC/NF-kappa B/c-fos may be involved in the influence of high glucose on the cardiomyocytes of neonatal rats. *Cardiovasc Diabetol* 2009;**8**:8.
154. Nishida K, Otsu K. Inflammation and metabolic cardiomyopathy. *Cardiovasc Res* 2017;**113**:389-398.
155. Fuentes-Antras J, Ioan AM, Tunon J, Egido J, Lorenzo O. Activation of toll-like receptors and inflammasome complexes in the diabetic cardiomyopathy-associated inflammation. *Int J Endocrinol* 2014;**2014**:847827.
156. Ko HJ, Zhang Z, Jung DY, Jun JY, Ma Z, Jones KE, Chan SY, Kim JK. Nutrient stress activates inflammation and reduces glucose metabolism by suppressing AMP-activated protein kinase in the heart. *Diabetes* 2009;**58**:2536-2546.
157. Hansmann G, Wagner RA, Schellong S, Perez VA, Urashima T, Wang L, Sheikh AY, Suen RS, Stewart DJ, Rabinovitch M. Pulmonary arterial hypertension is linked to insulin resistance and reversed by peroxisome proliferator-activated receptor-gamma activation. *Circulation* 2007;**115**:1275-1284.
158. West J, Niswender KD, Johnson JA, Pugh ME, Gleaves L, Fessel JP, Hemnes AR. A potential role for insulin resistance in experimental pulmonary hypertension. *Eur Respir J* 2013;**41**:861-871.
159. Agard C, Rolli-Derkinderen M, Dumas-de-La-Roque E, Rio M, Sagan C, Savineau JP, Loirand G, Pacaud P. Protective role of the antidiabetic drug metformin against chronic experimental pulmonary hypertension. *Br J Pharmacol* 2009;**158**:1285-1294.
160. Abernethy AD, Stackhouse K, Hart S, Devendra G, Bashore TM, Dweik R, Krasuski RA. Impact of diabetes in patients with pulmonary hypertension. *Pulm Circ* 2015;**5**:117-123.
161. Benson L, Brittain EL, Pugh ME, Austin ED, Fox K, Wheeler L, Robbins IM, Hemnes AR. Impact of diabetes on survival and right ventricular compensation in pulmonary arterial hypertension. *Pulm Circ* 2014;**4**:311-318.
162. Nunoda S, Genda A, Sugihara N, Nakayama A, Mizuno S, Takeda R. Quantitative approach to the histopathology of the biopsied right ventricular myocardium in patients with diabetes mellitus. *Heart Vessels* 1985;**1**:43-47.
163. Heresi GA, Malin SK, Barnes JW, Tian L, Kirwan JP, Dweik RA. Abnormal Glucose Metabolism and High-Energy Expenditure in Idiopathic Pulmonary Arterial Hypertension. *Ann Am Thorac Soc* 2017;**14**:190-199.

164. Dinarello CA. A clinical perspective of IL-1beta as the gatekeeper of inflammation. *Eur J Immunol* 2011;**41**:1203-1217.
165. Yndestad A, Damas JK, Oie E, Ueland T, Gullestad L, Aukrust P. Systemic inflammation in heart failure--the whys and wherefores. *Heart Fail Rev* 2006;**11**:83-92.
166. Van Tassell BW, Arena RA, Toldo S, Mezzaroma E, Azam T, Seropian IM, Shah K, Canada J, Voelkel NF, Dinarello CA, Abbate A. Enhanced interleukin-1 activity contributes to exercise intolerance in patients with systolic heart failure. *PLoS One* 2012;**7**:e33438.
167. Van Tassell BW, Arena R, Biondi-Zoccai G, McNair Canada J, Oddi C, Abouzaki NA, Jahangiri A, Falcao RA, Kontos MC, Shah KB, Voelkel NF, Dinarello CA, Abbate A. Effects of interleukin-1 blockade with anakinra on aerobic exercise capacity in patients with heart failure and preserved ejection fraction (from the D-HART pilot study). *Am J Cardiol* 2014;**113**:321-327.
168. Van Tassell BW, Abouzaki NA, Oddi Erdle C, Carbone S, Trankle CR, Melchior RD, Turlington JS, Thurber CJ, Christopher S, Dixon DL, Fronk DT, Thomas CS, Rose SW, Buckley LF, Dinarello CA, Biondi-Zoccai G, Abbate A. Interleukin-1 Blockade in Acute Decompensated Heart Failure: A Randomized, Double-Blinded, Placebo-Controlled Pilot Study. *J Cardiovasc Pharmacol* 2016;**67**:544-551.
169. Van Tassell BW, Canada J, Carbone S, Trankle C, Buckley L, Oddi Erdle C, Abouzaki N, Dixon DL, Kadariya D, Dessie S, Christopher S, Billingsley H, Regan J, Bhatnagar A, Viscusi M, Arena R, Lesnefsky EJ, Abbate A. Interleukin-1 Blockade in Recently Decompensated Systolic Heart Failure: the REcently Decompensated Heart failure Anakinra Response Trial (REDHART). *Eur J Heart Fail* 2017.
170. BW VT, J VR, C O, S C, J C, Abouzaki NA, Biondi-Zoccai G, Arena R, Abbate A. Interleukin-1 Blockade in Recently Decompensated Systolic Heart Failure: Study Design of the Recently Decompensated Heart Failure Anakinra Response Trial (RED-HART). *J Clin Trial Cardiol* 2015;**2**:1-8.
171. Dunlay SM, Weston SA, Redfield MM, Killian JM, Roger VL. Tumor necrosis factor-alpha and mortality in heart failure: a community study. *Circulation* 2008;**118**:625-631.
172. Li YY, Feng YQ, Kadokami T, McTiernan CF, Draviam R, Watkins SC, Feldman AM. Myocardial extracellular matrix remodeling in transgenic mice overexpressing tumor necrosis factor alpha can be modulated by anti-tumor necrosis factor alpha therapy. *Proc Natl Acad Sci U S A* 2000;**97**:12746-12751.
173. Chung ES, Packer M, Lo KH, Fasanmade AA, Willerson JT, Anti TNFTACHFI. Randomized, double-blind, placebo-controlled, pilot trial of infliximab, a chimeric monoclonal antibody to tumor necrosis factor-alpha, in patients with moderate-to-severe heart failure: results of the anti-TNF Therapy Against Congestive Heart Failure (ATTACH) trial. *Circulation* 2003;**107**:3133-3140.
174. Mann DL, McMurray JJ, Packer M, Swedberg K, Borer JS, Colucci WS, Djian J, Drexler H, Feldman A, Kober L, Krum H, Liu P, Nieminen M, Tavazzi L, van Veldhuisen DJ, Waldenstrom A, Warren M, Westheim A, Zannad F, Fleming T. Targeted anticytokine therapy in patients with chronic heart failure: results of the Randomized Etanercept Worldwide Evaluation (RENEWAL). *Circulation* 2004;**109**:1594-1602.

175. Fildes JE, Shaw SM, Yonan N, Williams SG. The immune system and chronic heart failure: is the heart in control? *J Am Coll Cardiol* 2009;**53**:1013-1020.
176. Aderka D, Engelmann H, Maor Y, Brakebusch C, Wallach D. Stabilization of the bioactivity of tumor necrosis factor by its soluble receptors. *J Exp Med* 1992;**175**:323-329.
177. Scallon BJ, Trinh H, Nedelman M, Brennan FM, Feldmann M, Ghrayeb J. Functional comparisons of different tumour necrosis factor receptor/IgG fusion proteins. *Cytokine* 1995;**7**:759-770.
178. Pearl JM, Wellmann SA, McNamara JL, Lombardi JP, Wagner CJ, Raake JL, Nelson DP. Bosentan prevents hypoxia-reoxygenation-induced pulmonary hypertension and improves pulmonary function. *Ann Thorac Surg* 1999;**68**:1714-1721; discussion 1721-1712.
179. Packer M, McMurray J, Massie BM, Caspi A, Charlon V, Cohen-Solal A, Kiowski W, Kostuk W, Krum H, Levine B, Rizzon P, Soler J, Swedberg K, Anderson S, Demets DL. Clinical effects of endothelin receptor antagonism with bosentan in patients with severe chronic heart failure: results of a pilot study. *J Card Fail* 2005;**11**:12-20.
180. Wilkins MR, Paul GA, Strange JW, Tunariu N, Gin-Sing W, Banya WA, Westwood MA, Stefanidis A, Ng LL, Pennell DJ, Mohiaddin RH, Nihoyannopoulos P, Gibbs JS. Sildenafil versus Endothelin Receptor Antagonist for Pulmonary Hypertension (SERAPH) study. *Am J Respir Crit Care Med* 2005;**171**:1292-1297.
181. Dai H, Jiang L, Xiao Z, Guang X. ACE2-angiotensin-(1-7)-Mas axis might be a promising therapeutic target for pulmonary arterial hypertension. *Nat Rev Cardiol* 2015;**12**:374.
182. Tallant EA, Ferrario CM, Gallagher PE. Angiotensin-(1-7) inhibits growth of cardiac myocytes through activation of the mas receptor. *Am J Physiol Heart Circ Physiol* 2005;**289**:H1560-1566.
183. Qi Y, Shenoy V, Wong F, Li H, Afzal A, Mocco J, Sumners C, Raizada MK, Katovich MJ. Lentivirus-mediated overexpression of angiotensin-(1-7) attenuated ischaemia-induced cardiac pathophysiology. *Exp Physiol* 2011;**96**:863-874.
184. Mercure C, Yogi A, Callera GE, Aranha AB, Bader M, Ferreira AJ, Santos RA, Walther T, Touyz RM, Reudelhuber TL. Angiotensin(1-7) blunts hypertensive cardiac remodeling by a direct effect on the heart. *Circ Res* 2008;**103**:1319-1326.
185. Loot AE, Roks AJ, Henning RH, Tio RA, Suurmeijer AJ, Boomsma F, van Gilst WH. Angiotensin-(1-7) attenuates the development of heart failure after myocardial infarction in rats. *Circulation* 2002;**105**:1548-1550.
186. Dai H, Gong Y, Xiao Z, Guang X, Yin X. Decreased levels of serum Angiotensin-(1-7) in patients with pulmonary arterial hypertension due to congenital heart disease. *Int J Cardiol* 2014;**176**:1399-1401.
187. Shenoy V, Ferreira AJ, Qi Y, Fraga-Silva RA, Diez-Freire C, Dooies A, Jun JY, Sriramula S, Mariappan N, Pourang D, Venugopal CS, Francis J, Reudelhuber T, Santos RA, Patel JM, Raizada MK, Katovich MJ. The angiotensin-converting enzyme 2/angiogenesis-(1-7)/Mas axis confers cardiopulmonary protection against lung fibrosis and pulmonary hypertension. *Am J Respir Crit Care Med* 2010;**182**:1065-1072.

CHAPTER 8

Reversal of right ventricular remodeling by dichloroacetate is related to inhibition of mitochondria-dependent apoptosis

Xiao-Qing Sun[1, 2], Rui Zhang[2], Hong-Da Zhang[2], Ping Yuan[2], Xiao-Jian Wang[3], Qin-Hua Zhao[2], Lan Wang[2], Rong Jiang[2], Harm Jan Bogaard[1], Zhi-Cheng Jing[2, 3]

[1]Department of Pulmonary Medicine, VU University Medical Center, Amsterdam, The Netherlands [2]Department of Cardio-Pulmonary Circulation, Shanghai Pulmonary Hospital, Tongji University School of Medicine, Shanghai, China [3]State Key Laboratory of Cardiovascular Disease, Fu Wai Hospital, National Center for Cardiovascular Disease, Peking Union Medical College and Chinese Academy Medical Science, Beijing, China

Hypertens Res. 2016 May;39(5):302-311.

ABSTRACT

Most patients with pulmonary arterial hypertension die from right ventricular failure (RVF). Right ventricular (RV) myocardial apoptosis plays an important role in RVF and is regulated by mitochondria. Dichloroacetate (DCA) can improve cardiac function in RVF, but whether it can regulate myocardial apoptosis via mitochondria is still unknown. In this study, we investigated the effects of DCA on myocardial mitochondria, the mitochondrial apoptosis and other aspects of RV remodeling, including fibrosis and capillary rarefaction. RVF was induced in rats by a single subcutaneous injection of monocrotaline. Four weeks later, DCA treatment was started with intraperitoneal injection of 50, 150 or 200 mg/kg/d during 14 days. Compared with saline-treated RVF animals, treatment with DCA resulted in decreased mean pulmonary arterial pressure and total pulmonary resistance (TPR), and increased cardiac output. The expression of pyruvate dehydrogenase kinase was suppressed while pyruvate dehydrogenase expression was upregulated with DCA application. DCA treatment was also associated with restored RV mitochondrial function and a reduction in RV hypertrophy, fibrosis, capillary rarefaction and apoptosis. Mitochondria-dependent apoptosis was involved in DCA regulation of RV. The absent correlation between TPR and main parameters in RV suggests that the effects of DCA in the two organ systems are independent. We conclude that DCA improves cardiac function in experimental RVF partly by reversing RV remodeling, restoring mitochondrial function and regulating mitochondria-dependent apoptosis. The study shows that a fear for increased RV apoptosis with DCA treatment is unnecessary and suggests a potential role of DCA in the treatment of RVF.

KEYWORDS

Apoptosis, mitochondria, pulmonary arterial hypertension, right ventricular failure, right ventricular remodeling

1.INTRODUCTION

Pulmonary arterial hypertension (PAH) is a fatal disease characterized by pulmonary vascular remodeling and a chronically and frequently progressive increase in right ventricle (RV) afterload, causing RV remodeling and RV failure (RVF).[1] Although the initial insult in PAH involves the pulmonary vasculature, RVF is the most important determinant of longevity in patients with PAH.[2] Recent animal data suggests that RV remodeling contributes to the progression of RVF.[3] Many questions, however, regarding the mechanisms underlying RV remodeling remain unanswered. Abnormal RV remodeling may be amenable to therapeutic intervention.

It has become clear that myocardial apoptosis is involved in RV remodeling and plays an important role in RVF.[4] While inhibition of myocardial apoptosis is a viable therapeutic strategy for left ventricular (LV) failure,[5] recent studies indicate that suppressing apoptosis can also be beneficial in experimental RVF.[6,7] Therefore, reducing myocardial apoptosis may provide a new therapeutic strategy in patients with RVF. Meanwhile, it now becomes clear that mitochondria act to integrate diverse proapoptotic stimuli by releasing apoptosis promoting factors such as cytochrome c, Smac/Diablo and the flavoprotein AIF.[8] Given the known role of mitochondria as apoptotic controllers, it is tempting to speculate that therapies targeting mitochondria can regulate RV myocardial apoptosis and improve RV function.

Mitochondrial abnormalities are not only closely related to induction of apoptosis, but also to deregulated metabolism.[9-11] Indeed in RVF, myocardial apoptosis occurs alongside several metabolic changes and may be linked on the level of the mitochondria. Metabolic changes in RVF include increased activity and expression of pyruvate dehydrogenase kinase (PDK), which causes phosphorylation and inhibition of pyruvate dehydrogenase (PDH). PDH phosphorylation inhibits formation of acetyl-CoA and therefore slows the Krebs' cycle, causing an increase in glycolysis relative to glucose oxidation.[12] Even though during short-term stress this metabolic switch seems beneficial, long-term reliance on glycolysis for ATP generation appears insufficient and contributes to the development of RVF.[13] Dichloroacetate (DCA) is a small molecular inhibitor of all four PDK isoforms and has shown promise as a new therapy for RVF.[14,15] By reducing PDH phosphorylation and improving glucose oxidation, DCA improved cardiac output in animal models of RVF.[9,16]

Because DCA not only reverses metabolic derangements but also effectively targets mitochondrial related pathways of apoptosis,[8,17] at least some of DCA's beneficial effects in RVF may come about through modulation of myocardial apoptosis. However, the effect of DCA on RV myocardial apoptosis is not clear. And previous studies on DCA and apoptosis seem inconsistent. A study on pulmonary vasculature suggests that DCA increases mitochondria-dependent apoptosis in pulmonary arterial smooth muscle cell (PASMC) in PAH.[17] Thus it is possible that DCA would also promote RV apoptosis in PAH induced RVF, which would largely limit the application of DCA in PAH. However, an *in vitro* study showed that DCA prevented H_2O_2-induced cell apoptosis in cultured cardiomyocytes.[18] To support DCA treatment on PAH, it is of great importance to figure out the effect of DCA on myocardial apoptosis in RVF *in vivo*. Moreover, recent data show that the development of RVF is also associated with multiple maladaptive RV remodeling including fibrosis, and a decreased RV capillary density,[3] but whether DCA can have an effect on these aspects of experimental RV remodeling is still unknown.

Here we hypothesize that DCA improves cardiac function in PAH induced RVF through a mechanism involving modulation of RV mitochondrial function and mitochondria-dependent apoptosis. Thus, we sought to discover the possible mechanisms underlying the effects of DCA on RVF by 1) evaluating the effects of DCA on RV remodeling including myocardial apoptosis, fibrosis and capillary rarefaction, 2) examining the effects of DCA on mitochondrial structure and function, 3) assessing the mitochondria-dependent apoptotic pathway in RVF by application of DCA.

2. MATERIALS AND METHODS

2.1 Monocrotaline rat model of right ventricular failure

A total of 60 adult male Sprague-Dawley rats (from the Second Military Medical University Affiliated Experimental Animal Center; body weights 250-300 g) were divided into two groups: rats received a single subcutaneous injection of saline (control, n=10), or monocrotaline (MCT, 60 mg/kg, Sigma Aldrich, St. Louis, MO, USA) to induce RVF (n=50).[19] To determine the effects of different DCA doses on the progression of established RVF, four weeks later rats with induced RVF were randomly divided into 4 groups: rats with a daily intraperitoneal injection of saline (MCT-RVF, n=14) or respectively 50, 150 or 200 mg/kg (n=12) DCA (Sigma Aldrich, St. Louis, MO) during 14

days. Then rats were anaesthetized for hemodynamic assessment and RV tissues were separated for further measurements.

All experimental procedures involving animals were executed conforming to the US National Institute of Health regulations (NIH) and were approved by the Institutional Committee for Use and Care of Laboratory Animals of Tongji University.

2.2 Hemodynamic evaluation

Six weeks after receiving a single subcutaneous injection of saline or MCT, all surviving rats (control, 100% survival rate; MCT-RVF, 50% survival rate; DCA 50 mg/kg, 67% survival rate; DCA 150 mg/kg, 75% survival rate; DCA 200 mg/kg, 75% survival rate) were anaesthetized with an intraperitoneal injection of ip sodium pentobarbital (40 mg/kg), and hemodynamic parameters were measured by a polygraph system (PowerLab 8/30; ADInstruments, Bella Vista, NSW, Australia). Adequate anaesthesia was monitored by determining the withdrawal response to a paw pinch and respiration monitoring. After tracheotomy a polyethylene-50 catheter was inserted via the right external jugular vein into the pulmonary artery to assess mean pulmonary arterial pressure (mPAP) and cardiac output (CO). With these values the total pulmonary resistance (TPR=mPAP/CO) was calculated.

2.3 Assessment of right ventricular hypertrophy index

After assessing haemodynamic parameters, the animals were euthanized by removal of the heart under deep anesthesia. After the atria, the pulmonary trunk and the aorta were removed from the excised heart, the RV wall was separated from the LV wall and ventricular septum. Wet weights of the RV, free LV, and ventricular septum were determined. The ratio of RV weight to LV plus septum weight (RV/[LV+S]) was calculated for assessment of RV hypertrophy.[19, 20]

2.4 Histology, TUNEL and DNA laddering

For analysis of RV dimensions, hearts were fixed *in situ*, embedded in paraffin, and stained with haematoxylin and eosin, as described previously.[21] Masson's Trichrome stain was used to assess the degree of fibrosis in cardiac sections. Fibrosis was quantified on digitized images, on which blue stained tissue areas are expressed as percentage of the total surface area.[7] A mean cardiomyocyte cross-sectional area (CSA) was determined in RV cryosections stained with haematoxylin and eosin and the capillary density was determined by Isolectin B4 (Vector) staining.[21] Apoptotic cells

were assessed by the terminal-deoxynucleotidyltransferase-mediated 2′-deoxyuridine 5′-triphosphated nick-end-labeling (TUNEL) method (EMD Millipore, Billerica, MA, USA). Using a magnification rate of 400, the percentages of TUNEL-positive cells were calculated in 10 randomly chosen fields of each section from three animals per group. The procedures of DNA laddering were exactly as described previously.[22]

2.5 Transmission electron microscopy

The ultrastructure of mitochondria was analyzed using transmission electron microscopy, as described previously.[10] Briefly, re-suspended EV pellet (3 μL) was fixed with 2.5% glutaraldehyde, post-fixed in buffered 1% OsO_4 with 1.5% $K_4Fe(CN)_6$, embedded in 1% agar, and processed according to standard Epon812 embedding procedure. Mitochondria were visualized on thin sections (60 nm) with a transmission electron microscope (JEM1230, Japan) at 80 kV.

2.6 Real-time quantitative reverse transcription-polymerase chain reaction (RT-PCR)

Total RNA was isolated from the tissues of three rats per group using Trizol reagent according to the manufacturer's protocol. RNA concentration and purity were measured with a spectrophotometer at A260 and A260/280, respectively. The reverse transcription reaction was performed with the Gene Amp PCR System 9700 (Applied Biosystems, Carlsbad, CA, USA) for the first-strand cDNA synthesis. RT-PCR was performed on an ABI 7500 apparatus (ABI, NY, USA). The sequences of primers used were as follows: lactate dehydrogenase (LDHA), forward: 5'- caaactgctcatcgtctcaaac-3' and reverse: 5'- gcaaccacttccaataactctgt-3'; superoxide dismutase2 (SOD2), forward: 5'-ggcttcaataaggagcaaggt-3' and reverse: 5'- tctcccagttgattacattcca-3'; glyceraldehyde-3-phosphate dehydrogenase (GAPDH), forward: 5'-acagcaacagggtggtggac-3' and reverse: 5'- tttgagggtgcagcgaactt-3'. The PCR conditions were as follows: a pre-denaturing at 95 °C for 30 s, followed by 40 cycles of denaturation at 95 °C for 5 s, annealing/extension at 60 °C for 34 s. A relative amount for each gene examined was obtained from a standard curve generated by plotting the cycle threshold value against the concentration of a serially diluted RNA sample expressing the gene of interest. This amount was normalized to the level of GAPDH mRNA.

2.7 Western blotting

Western blotting was performed using RV lysates from three rats per group. The protein concentration was determined by Pierce BCA Protein Assay Kit (Thermo Fisher,

Waltham, MA, USA) with BSA as the standard. Polyvinylidence fluoride membranes were probed by mouse monoclonal GAPDH (1:8000), rabbit monoclonal PDHα1 (1:1000), rabbit polyclonal Bax (1:1000), Bcl-2 (1:1000), LDHA (1:1000) and cleaved caspase-9 (1:1000) from Cell Signaling Technology Inc. (Beverly, MA, USA); rabbit monoclonal PDK2 (1:500) and polyclonal active caspase-3 (1:200), mouse monoclonal SOD2 (1:2000, Abcam, Cambridge, United Kingdom); rabbit polyclonal PDK4 (1:1000, Sigma-Aldrich, Poole, United Kingdom) and goat polyclonal PDHα2 (1:200, Santa Cruz Biotechnology Inc., Dallas, TX, USA) antibodies overnight with constant shaking at 4 °C. After washing 3 times for 10 minutes in TBS-T buffer, membranes were incubated with an appropriate horseradish-peroxidase-conjugated antibody and enhanced chemiluminescence reagent (Thermo Fisher, Waltham, MA, USA). Band intensities were determined using Quantity One software from Bio-Rad (Hercules, CA, USA). All measurements were replicated at least three times.

2.8 Measurements of mitochondrial cytochrome c release into cytosol

Measurements of cytosolic cytochrome c were achieved by subcellular fractionation and Western blotting with cytochrome c antibody (1:1000, Cell Signaling Technology, Inc. Beverly, MA, USA) as described previously.[23] The purity of the cytosolic fractions was validated by Western blotting using antibodies to cytochrome c oxidase subunit IV (COX IV; 1:1000, Cell Signaling Technology, Inc. Beverly, MA, USA).

2.9 Statistical analysis

Data were presented as mean ± standard deviation (SD) and were analyzed using one-way analysis of variance (ANOVA) with Bonferroni post hoc comparisons. Correlations between TPR and RV parameters were calculated using Spearman correlation coefficients. A value of $P<0.05$ was accepted as an indication of statistical significance. All statistical computations were performed using the Statistical Package for the Social Sciences version 13.0 software (SPSS, Inc., Chicago, IL, USA).

3. RESULTS

3.1 Dichloroacetate improved haemodynamic parameters in MCT induced RVF rats

After two weeks of treatment with DCA, there was no evident difference in the body weight between the MCT-RVF group and DCA groups, or between the three DCA treatment groups of different dosages. Rats challenged with MCT consistently developed

significant PAH, with higher mPAP and TPR, and lower CO. DCA treatment resulted in a marked reduction in mPAP by 29%, 32% and 36% after application of respectively 50, 150 and 200 mg/kg (Figure 1A). CO was reduced in the MCT group compared with the control group (81±6.3 versus 184±11.5, P<0.001, Figure 1B) and DCA improved CO by 45%, 65%, and 78% in MCT-induced RVF rats after application of respectively 50, 150 and 200 mg/kg (Figure 1B). In addition, treatment with DCA 50, 150 and 200 mg/kg resulted in a marked reduction in TPR by respectively 52%, 57% and 58% (Figure 1C), and no significant differences were found between the treatment groups.

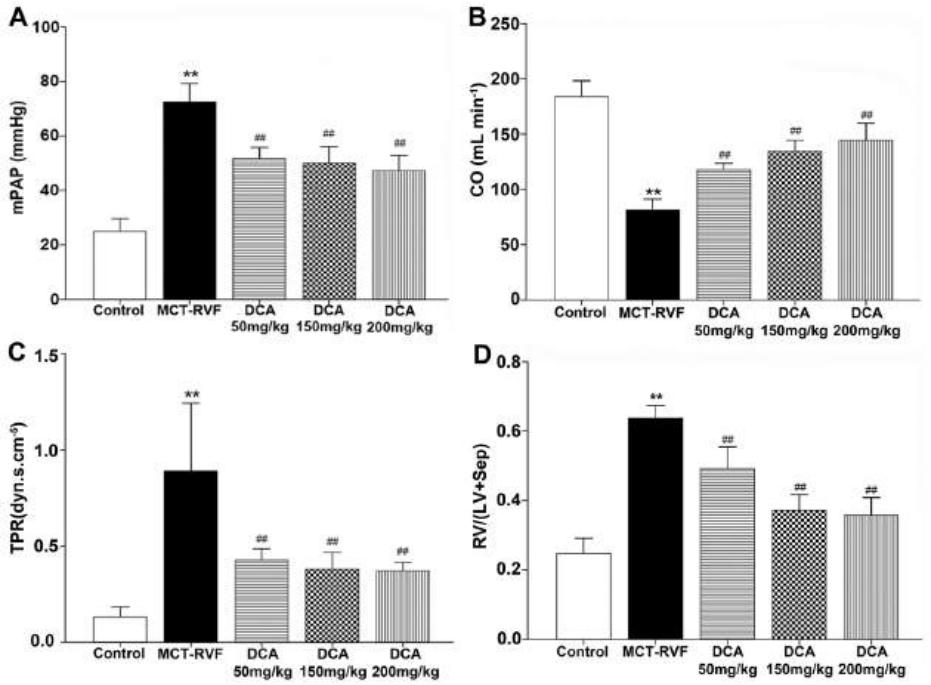

Figure 1. DCA improves haemodynamics and cardiac function in MCT induced RVF.
(A) Mean pulmonary artery pressure (mPAP); (B) Cardiac output (CO); (C) Total pulmonary resistance (TPR); (D) the ratio of free wall of RV weight to LV+Sep weight. Data shown are means ± SD of 7-10 rats per group. **P<0.001: Compared with control group; ##P<0.001: Compared with MCT-RVF group. MCT-RVF, Monocrotaline induced right ventricular failure group; DCA 50 mg/kg, Dichloroacetate 50 mg/kg/day group; DCA 150 mg/kg, Dichloroacetate 150 mg/kg/day group; DCA 150 mg/kg, Dichloroacetate 200 mg/kg/day group.

3.2 Dichloroacetate reversed RV remodeling in RVF

As shown by the ratio of RV weight to LV plus septum weight (RV/[LV+S]), there was significantly less hypertrophy in DCA-treated animals than in saline-treated MCT animals (Figure 1D). To further evaluate the effect of DCA treatment on RV remodeling, we performed a morphometric analysis of RV myocytes CSA, RV fibrosis, capillary density and myocardial apoptosis in these five groups of rats. DCA treatment significantly reduced RV CSA that was otherwise enlarged in MCT rats (Figures 2A and 2D). Moreover, RVF resulted in a loss of RV capillaries (Figures 2B and 2E). In contrast, DCA treatment partly recovered the normal density of RV capillaries (Figures 2B and 2E). Additionally, the RV of MCT rats developed a high degree of fibrosis, and DCA treatment markedly reduced the overall fibrosis in RV (Figures 2C and 2F).

3.3 Dichloroacetate inhibited RV myocardial apoptosis in RVF

To determine whether DCA can reverse RV remodeling by inhibiting apoptosis in RV myocytes, TUNEL staining and DNA laddering were used. The percentage of TUNEL-positive nuclei was significantly greater in the MCT-RVF group (Figure 3B) compared with the control group (Figure 3A), and DCA treatment reduced the TUNEL-positive nuclei percentage (Figures 3C-F). Moreover, a weak pattern of DNA laddering was observed in both the control and DCA groups, but a much stronger DNA laddering pattern was found in the MCT-RVF group (Figure 3G).

3.4 Dichloroacetate improved RV myocardial mitochondrial function in RVF

Transmission electron microscopy of the RV cardiomyocytes demonstrated that the mitochondrial ultrastructure in MCT-induced RVF tissues was highly abnormal, including swelling and a decreased number of mitochondria (Figure 4A). Moreover, in comparison to the controls, MCT-induced RVF tissues revealed medullary sheath-like degeneration, dissolution of the myofilaments, broken Z-lines and an irregular pattern of transverse striations (Figure 4A). Although these abnormalities were also present in the DCA 50 mg/kg treatment group, the defects in mitochondrial shape, size and number were obviously alleviated in the DCA 150 mg/kg and 200 mg/kg treatment groups (Figure 4A).

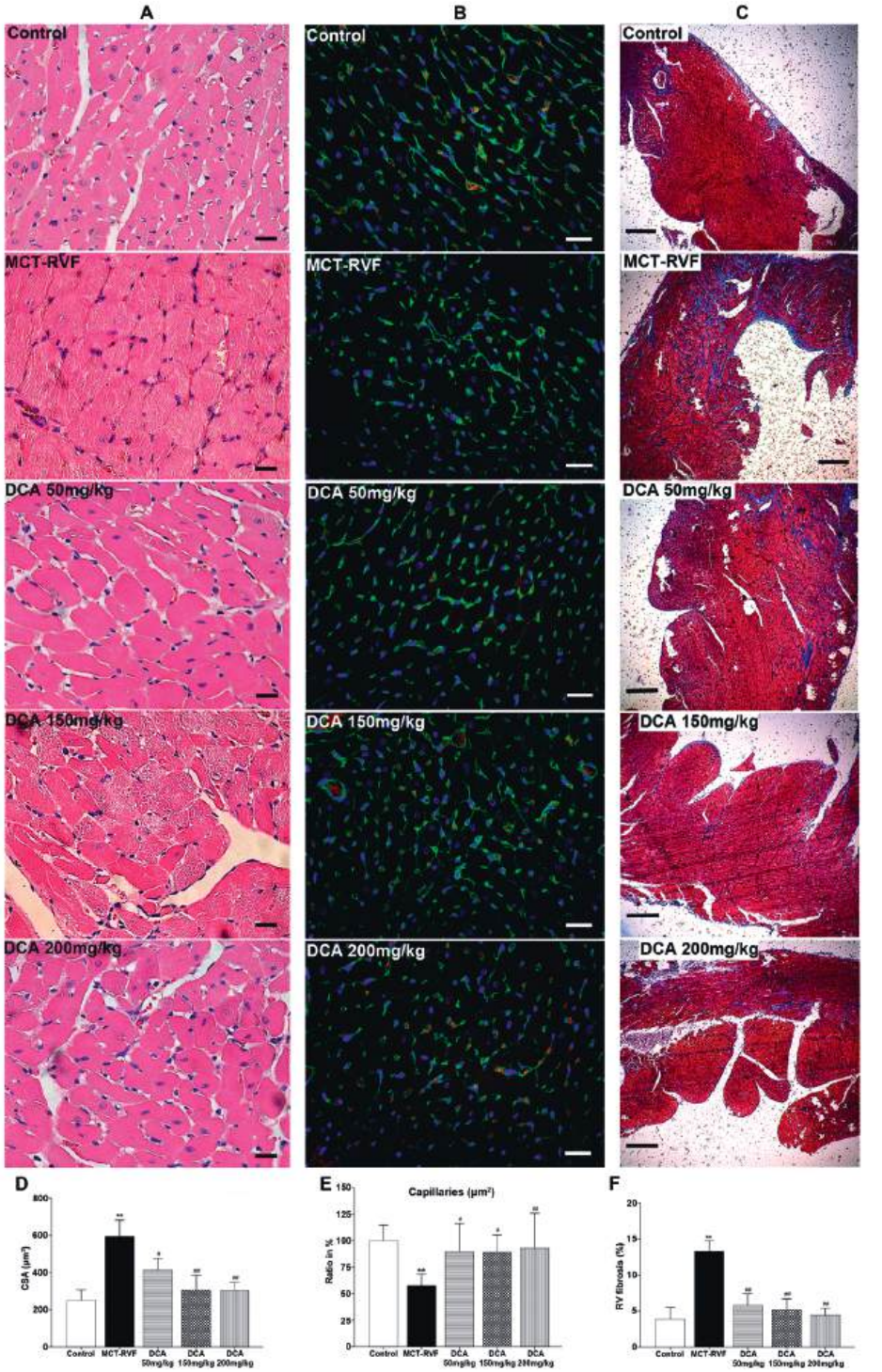
A
B
C
Control
MCT-RVF
DCA 50mg/kg
DCA 150mg/kg
DCA 200mg/kg
D
CSA (μm²)
E
Capillaries (μm²)
Ratio in %
F
RV fibrosis (%)
Control
MCT-RVF
DCA 50mg/kg
DCA 150mg/kg
DCA 200mg/kg

Figure 2. DCA partly reversed RV remodeling in RVF.
(A) Haematoxylin and eosin staining of in situ fixed RV sections; bar=20μm. (B) RV cryosections stained with isolectin B4 (blood vessels, red), WGA (cell membranes, green), and nuclei (DAPI, blue), scale bar: 20μm. (C)Fibrotic areas are shown by Masson trichrome stain, scale bar: 100μm. (D) Quantitative analysis of mean cross sectional area (CSA) of RV cardiomyocytes. (E) Capillaries to area (μm2) ratio. (F) Fibrosis quantification (blue-stained areas expressed as percentage of total RV surface area) of digitized images. *P<0.05, **P<0.001: Compared with control group; #P<0.05, ##P<0.001: Compared with MCT-RVF group.

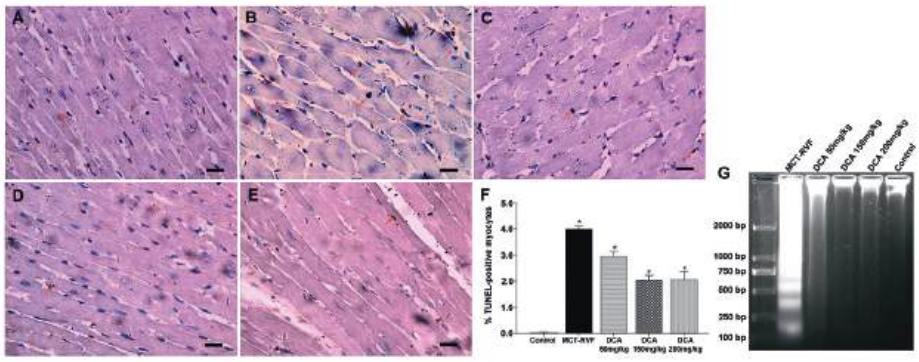

Figure 3. Dichloroacetate inhibited myocardial apoptosis in RVF
A-E) In situ detection of cardiac myocyte apoptosis was detected by TUNEL assay. Compared with control group (A), RV myocardial apoptosis in RVF rats was enhanced (B), and DCA 50 mg/kg (C), 150 mg/kg (D) and 200 mg/kg (E) inhibited the apoptosis; scale bar: 20 μm. (F) Quantitative changes in the incidence of myocardial apoptosis in RV among various treatment groups. The percentages of TUNEL-positive cells were calculated in 10 randomly chosen fields of each section at ×400 magnification. *P<0.05: Compared with control group; #P<0.05: Compared with MCT-RVF group. (G) Representative DNA laddering of various treatment groups.

Western blotting results demonstrated that both PDK2 and PDK4 proteins were upregulated in MCT-RVF rats. DCA reduced the protein expression of PDK2 and PDK4 (Figures 4C and 4F). However, the protein expression of PDK1 was unaltered in MCT-RVF rats, and DCA had no effect on PDK1 expression (Figures 4C and 4F). Accordingly, both PDHα1 and PDHα2 protein expression, which were depressed in the MCT-RVF group, were increased by DCA treatment (Figures 4C and 4F).

To further determine the effects of DCA on mitochondrial function, leakage of cytochrome c from mitochondria, SOD2 and LDHA expression were examined. The absence of COX IV in the cytosolic fractions confirmed that the cytosolic preparations were free of mitochondrial contamination. Compared to the control group, leakage of the cytochrome c from the mitochondria to the cytosol increased in MCT rats (Figures 4E and 4G). DCA treatment decreased the leakage of cytochrome c from the mitochondria in RV cardiomyocytes when applied at a dose of 50, 150 and 200 mg/kg/day for two weeks

(Figures 4E and 4G). Moreover, the gene expression of SOD2 in RV from saline MCT rats was significantly lower than that from the control group (Figure 4B), and was increased toward normal in all three DCA treatment groups (Figure 4B). Consistently, the SOD2 protein expression was also decreased in the MCT group and increased in the DCA groups (Figures 4D and 4G). Additionally, while LDHA gene expression was upregulated in MCT rats compared with the control group, the upregulation was suppressed in both the DCA 150 mg/kg and 200 mg/kg groups (Figure 4B). Accordingly, Western blotting showed that its protein expression was also markedly increased in the MCT group and decreased in the DCA treatment groups with doses of 150 or 200 mg/kg (Figures 4D and 4G).

3.5 Dichloroacetate reduced RV cardiomyocytes apoptosis by regulating the mitochondria-dependent apoptotic pathway

As shown by TUNEL staining and DNA laddering, RV myocardial apoptosis increased in the MCT-induced RVF while it was suppressed by DCA treatment (Figures 3F and 3G). Furthermore, to determine whether mitochondria-dependent apoptosis was involved, we detected the critical proteins by Western blotting.

Since Bcl-2 family member proteins mediate the mitochondrial apoptotic pathway, we examined the effect of DCA on Bcl-2 and Bax expression (Figure 5A). The expression of Bcl-2 protein was repressed in the MCT-RVF group compared with the control group, while DCA 150 mg/kg and 200 mg/kg significantly upregulated Bcl-2 protein expression (Figures 5A and 5B). In contrast, Bax protein increased in the MCT-RVF group and was effectively suppressed by DCA in all three treatment groups (Figures 5A and 5B).

Moreover, as was shown above by cytosolic Western blotting, leakage of the caspase activator cytochrome c from the mitochondria to the cytosal was enhanced in MCT rats. Also, DCA treatment attenuated the leakage of cytochrome c from the mitochondria in RV cardiomyocytes (Figures 4E and 4G). Caspase-9 is an initiator caspase in the mitochondrial apoptotic pathway. We measured the cleaved caspase-9 protein by Western blotting. An increase in the amount of cleaved caspase-9 was observed in the MCT-RVF group, while treatment with DCA evidently decreased the level of caspase-9 (Figures 5A and 5B). Accordingly, active caspase-3 protein significantly increased in MCT-RVF rats, and DCA treatment decreased the level of this protein (Figures 5A and 5B). Additionally, caspase-3 activity was evidently lower in DCA treated rats compared to MCT-RVF rats (Figure 5C). In agreement with the results of active caspase-3, PARP cleavage increased in MCT-induced RVF rats, and decreased markedly in all the DCA groups (Figures 5A and 5B).

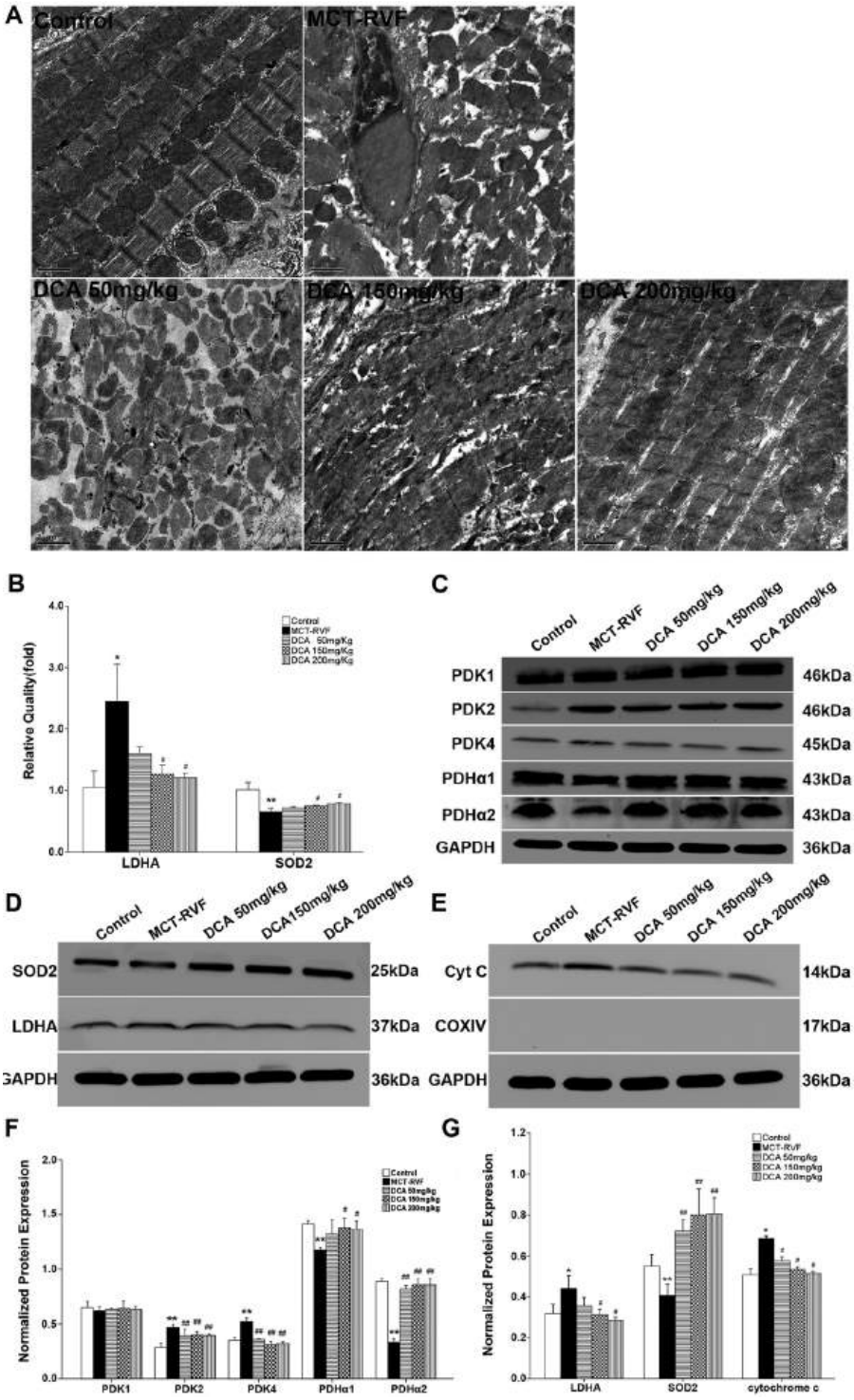
A
Control
MCT-RVF
DCA 50mg/kg
DCA 150mg/kg
DCA 200mg/kg
B
Relative Quality(fold)
Control
MCT-RVF
DCA 50mg/Kg
DCA 150mg/Kg
DCA 200mg/Kg
LDHA
SOD2
C
Control
MCT-RVF
DCA 50mg/kg
DCA 150mg/kg
DCA 200mg/kg
PDK1
PDK2
PDK4
PDHα1
PDHα2
GAPDH
46kDa
46kDa
45kDa
43kDa
43kDa
36kDa
D
Control
MCT-RVF
DCA 50mg/kg
DCA150mg/kg
DCA 200mg/kg
SOD2
LDHA
GAPDH
25kDa
37kDa
36kDa
E
Control
MCT-RVF
DCA 50mg/kg
DCA 150mg/kg
DCA 200mg/kg
Cyt C
COXIV
GAPDH
14kDa
17kDa
36kDa
F
Normalized Protein Expression
PDK1
PDK2
PDK4
PDHα1
PDHα2
G
Normalized Protein Expression
LDHA
SOD2
cytochrome c

Figure 4. Dichloroacetate restored myocardial mitochondrial function in RVF
(A) DCA partly reversed the abnormal mitochondrial ultrastructure in MCT-induced RVF, Scale bar=1μm. (B) Real-time PCR showed that DCA inhibited the mRNA expression of LDHA and upregulated that of SOD2. (C) Western blots showed that increased PDK2 and PDK4 expression in RV myocytes in RVF was reduced by DCA, while decreased PDHα1 and PDHα2 expression was upregulated by DCA. The expression of PDK1 was unaltered in RVF and was not influenced by DCA. (D) Western blots showed that DCA inhibited the protein expression of LDHA and upregulated that of SOD2. (E) Western blots of cytosolic fractions from various treatment groups show accumulation of cytochrome c in RVF and that can be significantly suppressed by DCA. (F, G) Densitometries are shown for three rats per group, and the measurements were replicated at least three times. The gels are representative of one rat in each group from one of three separate experiments. GAPDH in the immunoblot is shown as a loading control. *P<0.05, **P<0.001: Compared with control group; #P<0.05, ##P<0.001: Compared with MCT-RVF group.

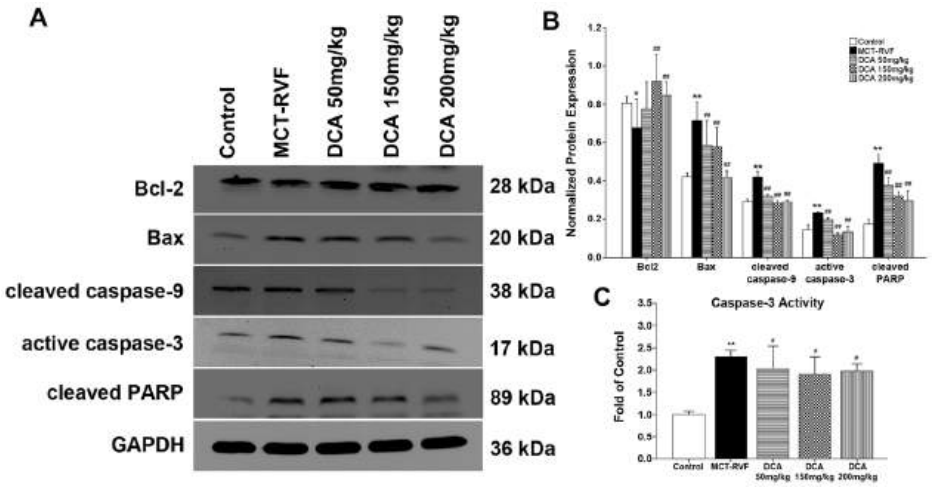

Figure 5. DCA regulated myocardial apoptosis in RVF via mitochondrial apoptotic pathway
(A-B) Western blot analysis of ventricular lysates shows increased levels of BAX, cleaved caspase 9, active caspase 3, cleaved PARP and decreased Bcl-2 in MCT induced RVF group. DCA treatment significantly up-regulated Bcl-2 levels, suppressed MCT induced changes in the BAX levels and attenuated activation of caspases in RVF. (C) caspase-3 activity increased in RVF and decreased after the treatment of DCA. GAPDH in the immunoblot is shown as a loading control. *P<0.05, **P<0.001: Compared with control group; #P<0.05, ##P<0.001: Compared with MCT-RVF group.

3.6 The effect of different DCA doses on RV was independent from changes in TPR.

DCA has been reported to have effects on pulmonary vascular remodeling in MCT rats.[17] Since mPAP in this study was lower with DCA treatment, it could be argued that all the RV beneficial effects of DCA were mediated by a reduction in afterload. To correct for the effects of afterload in the 50 mg/kg, 150 mg/kg and 200 mg/kg DCA treatment groups, we calculated the correlations between TPR and the main RV parameters for the groups with different DCA doses. The effect of DCA on cytochrome c release from RV mitochondria did not correlate significantly with TPR (Figure 6A). Accordingly, in RVF

under the treatment of DCA, no correlation was found between TPR and normalized protein expression changes of cleaved caspase-9, active caspase-3 or cleaved PARP (Figures 6B-6D).

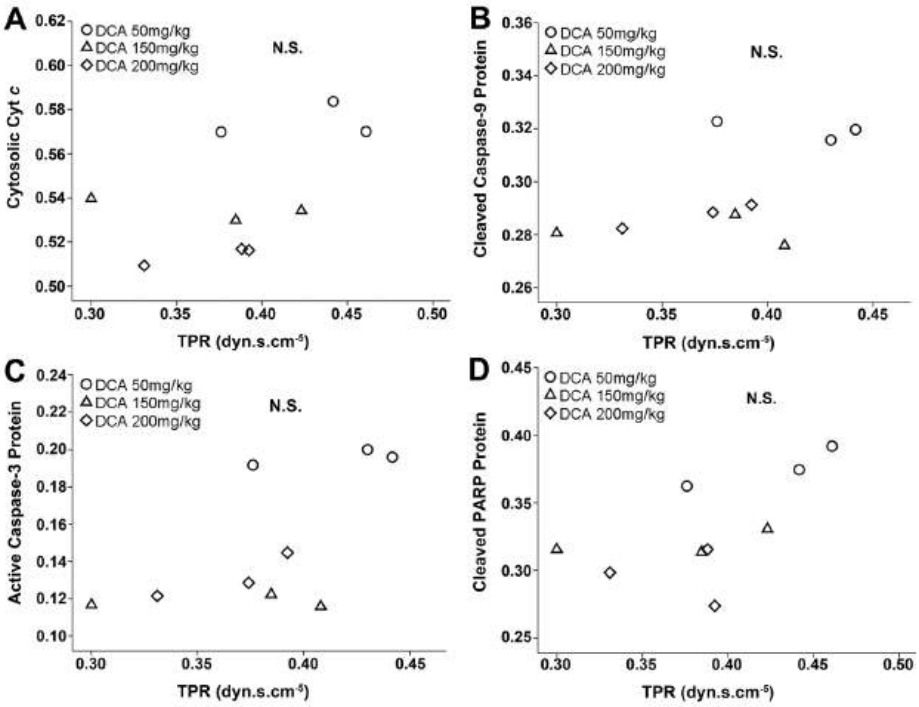

Figure 6. The effect of different DCA doses on RV was independent from changes in TPR. (A)The effect of DCA on cytochrome c release from RV mitochondria did not correlate significantly with total pulmonary resistance (TPR). (B, C, D) The normalized protein expression changes of cleaved caspase-9, active caspase-3 and cleaved PARP in RVF under the treatment of DCA did not correlate significantly with TPR. N.S.: not significant. Correlations between TPR and RV parameters were calculated using Spearman correlation coefficients.

4. DISCUSSION

This study provides novel insight into the mechanism of mitochondria targeted therapy for PAH induced RVF, showing that treatment with DCA is associated not only with an increased level of oxidative metabolism, but also with reduced RV myocardial apoptosis and restored mitochondrial function. These findings are important because they show that a fear for increased RV myocardial apoptosis with DCA is unnecessary, as DCA promotes PASMC apoptosis in PAH. Moreover, DCA has a positive effect on

haemodynamics, RV myocardial fibrosis and capillary rarefaction, metabolism and cardiac function, supporting the potential role of the drug for the treatment of PAH induced RVF.

While DCA is known to have benefits on RVF by regression of pulmonary vascular remodeling,[17] a recent study also suggested that DCA has direct effects on the RV by enhancing glucose oxidation and restoring RV repolarization.[9] In our study, we evaluated the effect of DCA treatment on RVF with different doses, by applying 50 mg/kg, 150 mg/kg and 200 mg/kg. Significant differences were found in the effects of DCA between treatment groups with different doses. Although there is a potential toxicity related to a high dosage of DCA, this probably is not an issue here as no significant differences are found between the body weight of the rats in the three different groups. Besides, the dosage for long term DCA treatment on patients with mitochondrial diseases can be 50 mg/kg, which is well tolerated. This dosage equals to about 300 mg/kg in rats, which is more than the used dosage.[24,25] To further evaluate the direct effects of DCA on RV, we calculated the correlations between the critical parameters in RV and TPR in the treatment groups with different DCA doses, and no correlation was found between TPR and the main parameters in RV including cytochrome c release, cleaved caspase-9, active caspase-3 and cleaved PARP protein expression. The absence of a correlation shows that there is a different DCA dose-response relationship for the effects in the lungs and for the effects in the heart, suggesting that the effects of DCA in the two organ systems are independent. Furthermore, we demonstrated for the first time in the MCT induced RVF rat model that DCA significantly improved mitochondrial function by restoring mitochondrial structural abnormalities, reducing the cytochrome c release from mitochondria, upregulating the expression of SOD2 and reducing the expression of LDHA compared with untreated MCT-RVF models. Moreover, DCA reversed maladaptive RV remodeling including increased RV myocardial apoptosis and fibrosis, and decreased RV capillary density. Furthermore, we confirmed that DCA suppressed RV myocardial apoptosis by modulating the mitochondria-dependent apoptotic pathway. These results suggest that DCA has its direct benefits on RVF by improving mitochondrial function, inhibiting mitochondria-dependent apoptotic pathway, and reversing maladaptive RV remodeling.

Accumulating evidence suggests that RVF is partly attributable to metabolic derangements and mitochondrial defects.[9,10,26] The activity and expression of PDK is increased in RVF, which phosphorylates and inhibits PDH. Phosphorylated PDH inhibits

formation of acetyl-CoA and slows the Krebs' cycle, causing an increase in glycolysis and a decrease in glucose oxidation.[12] In agreement with a previous study,[16] our study shows that the expression of both PDK2 and PDK4 is increased in MCT-induced RVF rats and that DCA significantly suppressed this expression. However, PDK1 expression was unaltered in RVF and DCA had no evident effect on it. A possible reason is that the PDK isoforms have a different transcriptional regulation. PDK1 transcription is activated by hypoxia-induced factor 1α (HIF-1α), while PDK4 activation is mediated by the forkhead transcription factor (FOXO1).[9,27] Even though it has been demonstrated that the PDK activation in the lung in PAH is stimulated by redox-mediated activation of HIF-1α,[28] the expression of HIF-1α, mRNA or protein is unchanged in RVF while FOXO1 is found to be increased significantly,[9] which is consistent with our PDK results. Accordingly expression of PDHα1 and PDHα2 was repressed in RVF models and was upregulated by DCA, which is in agreement with a previous study demonstrating that DCA reduced the phosphorylation of PDH.[10] Moreover, it has been recognized that deregulated metabolism contributes to the mitochondrial abnormalities,[11] which exacerbate the low oxygen condition and the abnormal metabolism.[9,10] Considering the interconnectedness of metabolism and mitochondria, we further measured the effect of DCA on mitochondrial structure by transmission electron microscopy and its effect on mitochondrial function by assessing the release of cytochrome c and the expression of SOD2 and LDHA. Consistent with a previous study,[10] transmission electron microscopy of the RV cardiomyocytes revealed abnormalities in the MCT-treated group that were not visible in the control group. We observed reversal of these abnormalities with DCA treatment. Moreover, the benefits of DCA on mitochondrial function were partly reflected by reduced cytochrome c release, reduced LDHA expression and increased SOD2 expression. LDHA is a key enzyme involved in both glycolysis and acidosis and DCA can protect mitochondria from acidosis by suppressing this enzyme. Therefore our study for the first time suggests that DCA can attenuate mitochondrial abnormalities and improve mitochondrial function.

Mitochondria are considered to play a vital role in both cardiac remodeling and heart failure,[12,29,30] and multiple lines of evidence indicate that the progression of RVF is associated with RV remodeling, including upregulated RV myocardial apoptosis, fibrosis and decreased RV capillary density.[3] In the early stages of the disease, RV remodeling is mostly an adaptive response, but as the disease progresses, the RV dilates and RVF eventually occurs (maladaptive RV remodeling).[31] Therefore we measured the effects of the mitochondria targeted therapy DCA on RV myocardial

apoptosis by TUNEL staining and DNA laddering. RV fibrosis and capillary density were determined by picro-Sirius redstaining and Isolectin B4 staining, respectively. Here we show that DCA can reduce myocardial apoptosis in PAH induced RVF *in vivo*, as confirmed by a previous *in vitro* study which suggests that DCA suppresses apoptosis in cardiomyocytes.[18] Moreover, DCA reduced fibrosis and capillary rarefaction in RV, indicating that DCA improves cardiac function and attenuates RVF partly by reversing the maladaptive RV remodeling. However, the mechanisms underlying the reverse of RV remodeling need to be further studied. It is reported that the vascular endothelial growth factor (VEGF) expression decreases in RVF, which could cause the capillary growth to lag behind the cardiomyocyte growth, inducing capillary rarefaction.[3] Since a recent study on neuroblastoma cells suggested that the expression of VEGF could be influenced by PDK4,[32] it is reasonable to speculate that VEGF may be involved in the effect of DCA on RV capillary density.

Furthermore, considering the interconnectedness of apoptosis and mitochondria,[8] here we mainly focused on the DCA regulation of myocardial apoptosis. Myocardial apoptosis plays a role in RV disease progression.[4] Apoptosis is rare in the normal heart with one apoptotic cardiomyocyte in 10^4 to 10^5 cells.[33] However, apoptotic rates increase to up to 1 in 400 in human heart failure.[34,35] Apoptosis rates vary in animal models, with rates as high as 14% in ischemia/reperfusion and lower than 1% in chronic pressure overload.[36] The rate of RV myocardial apoptosis is upregulated after pulmonary artery banding in rats.[37,38] Even very low rates of apoptosis have been shown to cause lethal dilated cardiomyopathy in a mouse model.[39] It was also found that apoptotic signals can stimulate ventricular hypertrophy.[40] The Bcl-2/Bax ratio is known to determine cell apoptotic fate.[41,42] In our study, the Bcl-2/Bax ratio was reduced significantly in RV cardiomyocytes in the MCT-RVF group compared with the control group, and DCA significantly upregulated the ratio. Apoptosis detections by TUNEL and DNA laddering were consistent with the dramatic alterations of Bcl-2/Bax. Our study supports the hypothesis that apoptosis might be involved in a critical mechanism in the RV remodeling during the progression of pulmonary hypertension. Furthermore, we examined the expression and activity of some critical proteins related to the mitochondria-dependent apoptotic to determine the mechanisms underlying the effect of DCA on RV myocardial apoptosis. The expression of both cleaved caspase-9 and active caspase-3 as well as the activity of caspase-3 were enhanced in MCT-RVF, and were suppressed by DCA. Accordingly, PARP cleavage as the substrate of active caspase-3 increased in the MCT-RVF group, and decreased markedly in all the DCA

groups. So here, for the first time, we demonstrated that DCA improved cardiac function by inhibiting apoptosis in RV cardiomyocytes *in vivo* through a mechanism that involves the mitochondria-dependent pathway. This result seems to contradict the previous observation in the lung, where DCA acts to increase the mitochondria-dependent apoptosis in PASMCs.[17] However, our observation is partly in agreement with another study on congestive heart failure, which shows that DCA prevents H_2O_2-induced cell apoptosis in cultured cardiomyocytes.[18] It suggests the possibility that DCA may have different effect on PASMCs and RV cardiomyocytes, but the underlying mechanism needs to be further studied. In addition to Bcl-2/Bax, other upstream molecules may also be involved in the effect of DCA on myocardial apoptosis via other mechanisms. Previous studies suggest that mitochondrial reactive oxygen species (mROS) increase in RVF, which oxidizes and thus activates apoptosis molecules like p53.[43] In combination with our work which demonstrated that DCA increased the expression of SOD2 and improved the mitochondrial function in RVF, which plays a crucial role in cleaning mROS,[44] DCA may possibly reduce the expression of p53 or other apoptosis molecules.

Although here we show that the cardioprotective actions of DCA are accompanied by a number of cellular and molecular changes in RVF, improved mitochondrial function and reduced RV cardiomyocyte apoptosis, more mechanistic studies are required to determine how mitochondria targeted therapy in general and DCA in particular have a direct effect on PAH induced RVF. Our study was also limited since it only included one animal model of RVF. Direct effect of DCA on RV could be further proved by performing other animal models of RVF, such as the pulmonary artery banding rats, and vascular endothelial growth factor receptor antagonist SU5416 and chronic hypoxia induced RVF rats. In addition, there may be other possible mechanisms underlying the effect of DCA on RV apoptosis. A study on the congestive heart failure rat model suggests that DCA improves cardiac function and increases the survival of the animals by activating the pentose phosphate pathway in rat heart. Moreover, DCA decreased oxidative stress and attenuated H_2O_2-induced myocyte cell death by activating the pentose phosphate pathway.[18] Therefore other mechanisms underlying the effects of DCA on RV remodeling are worthwhile to be further studied.

Concluding, our results show that DCA has a direct effect on RV and reverses maladaptive RV remodeling in RVF by suppressing RV myocardial fibrosis, increasing RV capillary density, and inhibiting myocardial apoptosis via mitochondria-dependent

apoptotic pathway by restoring mitochondrial functional and structural abnormalities. The present study clearly shows that a fear for increased RV myocardial apoptosis with DCA treatment is unnecessary, which provides a new theoretical basis for the use of DCA in the management of PAH and RVF in the clinic.

DISCLOSURES

Z.-C.J. has acted as a consultant to and a member of scientific advisory boards for companies including Actelion, Bayer Schering, Pfizer and United Therapeutics, in addition to working as an investigator in trials involving these companies. No other author has any conflict of interest to declare regarding the content of this paper.

REFERENCES

1. Ikeda S, Satoh K, Kikuchi N, Miyata S, Suzuki K, Omura J, Shimizu T, Kobayashi K, Kobayashi K, Fukumoto Y, Sakata Y, Shimokawa H. Crucial role of Rho-Kinase in pressure overload–induced right ventricular hypertrophy and dysfunction in mice. Arterioscler Thromb Vasc Biol 2014; 34: 1260-1271.
2. van Wolferen SA, Marcus JT, Boonstra A, Marques KM, Bronzwaer JG, Spreeuwenberg MD, Postmus PE, Vonk-Noordegraaf A. Prognostic value of right ventricular mass, volume, and function in idiopathic pulmonary arterial hypertension. Eur Heart J 2007; 28: 1250-1257.
3. Bogaard HJ, Natarajan R, Henderson SC, Long CS, Kraskauskas D, Smithson L, Ockaili R, McCord JM, Voelkel NF. Chronic pulmonary artery pressure elevation is insufficient to explain right heart failure. Circulation 2009; 120: 1951-1960.
4. Campian ME, Verberne HJ, Hardziyenka M, de Bruin K, Selwaness M, van den Hoff MJ, Ruijter JM, van Eck-Smit BL, de Bakker JM, Tan HL. Serial noninvasive assessment of apoptosis during right ventricular disease progression in rats. J Nucl Med 2009; 50: 1371-1377.
5. Dorn GW. Apoptotic and non-apoptotic programmed cardiomyocyte death in ventricular remodelling. Cardiovasc Res 2008; 81: 465-473.
6. Zuo XR, Wang Q, Cao Q, Yu YZ, Wang H, Bi LQ, Xie WP, Wang H. Nicorandil prevents right ventricular remodeling by inhibiting apoptosis and lowering pressure overload in rats with pulmonary arterial hypertension. PLoS One 2012; 7: e44485.
7. Bogaard HJ, Natarajan R, Mizuno S, Abbate A, Chang PJ, Chau VQ, Hoke NN, Kraskauskas D, Kasper M, Salloum FN, Voelkel NF. Adrenergic receptor blockade reverses right heart remodeling and dysfunction in pulmonary hypertensive rats. Am J Respir Cirt Care Med 2010; 182: 652-660.
8. Adrain C, Martin SJ. The mitochondrial apoptosome: a killer unleashed by the cytochrome seas. Trends Biochem Sci 2001; 26: 390-397.
9. Piao L, Sidhu VK, Fang YH, Ryan JJ, Parikh KS, Hong Z, Toth PT, Morrow E, Kutty S, Lopaschuk GD, Archer SL. FOXO1-mediated upregulation of pyruvate dehydrogenase kinase-4 (PDK4) decreases glucose oxidation and impairs right ventricular function in pulmonary hypertension: therapeutic benefits of dichloroacetate. J Mol Med (Berl) 2013; 91: 333-346.
10. Piao L, Fang YH, Cadete VJ, Wietholt C, Urboniene D, Toth PT, Marsboom G, Zhang HJ, Haber I, Rehman J, Lopaschuk GD, Archer SL. The inhibition of pyruvate dehydrogenase kinase improves impaired cardiac function and electrical remodeling in two models of right ventricular hypertrophy: resuscitating the hibernating right ventricle. J Mol Med (Berl) 2010; 88: 47-60.
11. Gomez-Arroyo J, Mizuno S, Szczepanek K, Van Tassell B, Natarajan R, dos Remedios CG, Drake JI, Farkas L, Kraskauskas D, Wijesinghe DS, Chalfant CE, Bigbee J, Abbate A, Lesnefsky EJ, Bogaard HJ, Voelkel NF. Metabolic gene remodeling and mitochondrial dysfunction in failing right ventricular hypertrophy due to pulmonary arterial hypertension. Circ Heart Fail 2013; 6: 136-144.
12. Sugden MC, Langdown ML, Harris RA, Holness MJ. Expression and regulation of pyruvate dehydrogenase kinase isoforms in the developing rat heart and in adulthood: role of thyroid hormone status and lipid supply. Biochem J 2000; 352: 731-738.

13. Neubauer S. The failing heart-an engine out of fuel. N Engl J Med 2007; 356: 1140-1151.
14. Stacpoole PW. The pharmacology of dichloroacetate. Metabolism 1989; 38: 1124-1144.
15. Piao L, Marsboom G, Archer SL. Mitochondrial metabolic adaptation in right ventricular hypertrophy and failure. J Mol Med (Berl) 2010; 88: 1011-1020.
16. Finck BN, Kelly DP. PGC-1 coactivators: inducible regulators of energy metabolism in health and disease. J Clin Invest 2006; 116: 615-622.
17. McMurtry MS, Bonnet S, Wu X, Dyck JR, Haromy A, Hashimoto K, Michelakis ED. Dichloroacetate prevents and reverses pulmonary hypertension by inducing pulmonary artery smooth muscle cell apoptosis. Circ Res 2004; 95: 830-840.
18. Kato T, Niizuma S, Inuzuka Y, Kawashima T, Okuda J, Tamaki Y, Iwanaga Y, Narazaki M, Matsuda T, Soga T, Kita T, Kimura T, Shioi T. Analysis of metabolic remodeling in compensated left ventricular hypertrophy and heart failure. Circ Heart Fail 2010; 3: 420-430.
19. Guo Q, Huang JA, Yamamura A, Yamamura H, Zimnicka AM, Fernandez R, Yuan JX. Inhibition of the Ca(2+)-sensing receptor rescues pulmonary hypertension in rats and mice. Hypertens Res 2014; 37: 116-124.
20. Cowan KN, Heilbut A, Humpl T, Lam C, Ito S, Rabinovitch M. Complete reversal of fatal pulmonary hypertension in rats by a serine elastase inhibitor. Nat Med 2000; 6: 698-702.
21. Ricke-Hoch M, Bultmann I, Stapel B, Condorelli G, Rinas U, Sliwa K, Scherr M, Hilfiker-Kleiner D. Opposing roles of Akt and STAT3 in the protection of the maternal heart from peripartum stress. Cardiovasc Res 2014; 101: 587-596.
22. Li J, Zhang DS, Ye JC, Li CM, Qi M, Liang DD, Xu XR, Xu L, Liu Y, Zhang H, Zhang YY, Deng FF, Feng J, Shi D, Chen JJ, Li L, Chen G, Sun YF, Peng LY, Chen YH. Dynamin-2 mediates heart failure by modulating Ca2+-dependent cardiomyocyte apoptosis. Int J Cardiol 2013; 168: 2109-2119.
23. Sinha-Hikim I, Shen R, Nzenwa I, Gelfand R, Mahata SK, Sinha-Hikim AP. Minocycline suppresses oxidative stress and attenuates fetal cardiac myocyte apoptosis triggered by in uterococaine exposure. Apoptosis 2011; 16: 563-573.
24. Barshop BA, Naviaux RK, McGowan KA, Levine F, Nyhan WL, Loupis-Geller A, Haas RH. Chronic treatment of mitochondrial disease patients with dichloroacetate. Mol Genet Metab 2004; 83: 138-149.
25. Reagan-Shaw S, Nihal M, Ahmad N. Dose translation from animal to human studies revisited. FASEB J 2008; 22: 659-661.
26. Fang YH, Piao L, Hong Z, Toth PT, Marsboom G, Bache-Wiig P, Rehman J, Archer SL. Therapeutic inhibition of fatty acid oxidation in right ventricular hypertrophy: exploiting Randle's cycle. J Mol Med (Berl) 2012; 90: 31-43.
27. Kim JW, Tchernyshyov I, Semenza GL, Dang CV. HIF-1-mediated expression of pyruvate dehydrogenase kinase: a metabolic switch required for cellular adaptation to hypoxia. Cell Metab 2006; 3: 177-185.
28. Marsboom G, Wietholt C, Haney CR, Toth PT, Ryan JJ, Morrow E, Thenappan T, Bache-Wiig P, Piao L, Paul J, Chen CT, Archer SL. Lung (1)(8)F-fluorodeoxyglucose positron emission tomography for diagnosis and monitoring of pulmonary arterial hypertension. Am J Respir Crit Care Med 2012; 185: 670-679.

29. Tsutsui H, Kinugawa S, Matsushima S. Mitochondrial oxidative stressand dysfunction in myocardial remodelling. Cardiovasc Res 2009; 81: 449-456.
30. Rodrigues JQ, da Silva ED Jr, de Magalhães Galvão K, Miranda-Ferreira R, Caricati-Neto A, Jurkiewicz NH, Garcia AG, Jurkiewicz A. Differential regulation of atrial contraction by P1 and P2 purinoceptors in normotensive and spontaneously hypertensive rats. Hypertens Res 2014; 37: 210-219.
31. Haddad F, Ashley E, Michelakis ED. New insights for the diagnosis and management of right ventricular failure, from molecular imaging to targeted right ventricular therapy. Curr Opin Cardiol 2010; 25: 131-140.
32. Rellinger EJ, Romain C, Choi S, Qiao J, Chung DH. Silencing gastrin-releasing peptide receptor suppresses key regulators of aerobic glycolysis in neuroblastoma cells. Pediatr Blood Cancer 2015; 62: 581-586.
33. Soonpaa MH, Field LJ. Survey of studies examining mammalian cardiomyocyte DNA synthesis. Circ Res 1998; 83: 15-26.
34. Hein S, Arnon E, Kostin S, Schönburg M, Elsässer A, Polyakova V, Bauer EP, Klövekorn WP, Schaper J. Progression from compensated hypertrophy to failure in the pressure-overloaded human heart: structural deterioration and compensatory mechanisms. Circulation 2003; 107: 984-991.
35. Olivetti G, Abbi R, Quaini F, Kajstura J, Cheng W, Nitahara JA, Quaini E, Di Loreto C, Beltrami CA, Krajewski S, Reed JC, Anversa P. Apoptosis in the failing human heart. N Engl J Med 1997; 336: 1131-1141.
36. Kang PM, Izumo S. Apoptosis and heart failure: a critical review of the literature. Circ Res 2000; 86: 1107-1113.
37. Ikeda S, Hamada M, Hiwada K. Cardiomyocyte apoptosis with enhanced expression of P53 and Bax in right ventricle after pulmonary arterial banding. Life Sci 1999; 65: 925-933.
38. Braun MU, Szalai P, Strasser RH, Borst MM. Right ventricular hypertrophy and apoptosis after pulmonary artery banding: regulation of PKC isozymes. Cardiovasc Res 2003; 59: 658-667.
39. Wencker D, Chandra M, Nguyen K, Miao W, Garantziotis S, Factor SM, Shirani J, Armstrong RC, Kitsis RN. A mechanistic role for cardiac myocyte apoptosis in heart failure. J Clin Invest 2003; 111: 1497-1504.
40. Hirotani S, Otsu K, Nishida K, Higuchi Y, Morita T, Nakayama H, Yamaguchi O, Mano T, Matsumura Y, Ueno H, Tada M, Hori M. Involvement of nuclear factor-kappaB and apoptosis signal-regulating kinase 1 in G-protein-coupled receptor agonist-induced cardiomyocyte hypertrophy. Circulation 2002; 105: 509-515.
41. Gross A. BCL-2 proteins: regulators of the mitochondrial apoptotic program. IUBMB Life 2001; 52: 231-236.
42. Adams JM, Cory S. The Bcl-2 protein family: arbiters of cell survival. Science 1998; 281: 1322-1326.
43. B Liu, Y Chen, DK St Clair. ROS and p53: a versatile partnership. Free Radic Biol Med 2008; 44: 1529-1535.
44. Pias EK, Ekshyyan OY, Rhoads CA, Fuseler J, Harrison L, Aw TY. Differential effects of superoxide dismutase isoform expression on hydroperoxide-induced apoptosis in PC-12 cells. J Biol Chem 2003; 278: 13294-13301.

CHAPTER 9

Increased MAO-A activity promotes progression of pulmonary arterial hypertension

Xiao-Qing Sun[1]*, Eva L Peters[1,2]*, Ingrid Schalij[1], Julie Birkmose Axelsen[3], Stine Andersen[3], Kondababu Kurakula[4], Maria Catalina Gomez-Puerto[5], Robert Szulcek[1], Xiaoke Pan[1], Denielli da Silva Goncalves Bos[1], Roy EJ Schiepers[1], Asger Andersen[3], Marie-José Goumans[4], Anton Vonk-Noordegraaf[1], Willem J van der Laarse[2], Frances S de Man[1], Harm Jan Bogaard[1]

**Authors contributed equally to this work.*

[1]Pulmonary Medicine, Amsterdam Cardiovascular Sciences, Amsterdam UMC, Vrije Universiteit Amsterdam, Amsterdam, The Netherlands; [2]Department of Physiology, Amsterdam UMC, Vrije Universiteit Amsterdam, Amsterdam, The Netherlands; [3]Institute of Clinical Medicine, Department of Cardiology, Aarhus University Hospital, Denmark; [4]Department of Cell and Chemical Biology, Laboratory for Cardiovascular Cell Biology, Leiden University Medical Center, Leiden, The Netherlands. [5]Department of Cell and Chemical Biology and Oncode Institute, Leiden University Medical Center, Leiden, The Netherlands.

Am J Respir Cell Mol Biol. 2020 Dec 2.

ABSTRACT

RATIONALE: Monoamine oxidases (MAO), a class of enzymes bound to the outer mitochondrial membrane, are important sources of reactive oxygen species. Increased MAO-A activity in endothelial cells and cardiomyocytes contributes to vascular dysfunction and progression of left heart failure.

OBJECTIVES: We hypothesized that inhibition of MAO-A can be used to treat pulmonary arterial hypertension (PAH) and right ventricular (RV) failure.

METHODS: MAO-A level in PAH patient lung and RV samples was compared to non-PAH donors. Experimental PAH was induced in male Sprague-Dawley rats by Sugen 5416 and hypoxia (SuHx), and RV failure was induced in male Wistar rats by pulmonary trunk banding (PTB). Animals were randomized to receive either saline or MAO-A inhibitor clorgyline 10 mg/kg. Echocardiography and RV catheterization was performed, heart and lung tissues were collected for further analysis.

MEASUREMENTS AND MAIN RESULTS: We found increased MAO-A expression in the pulmonary vasculature of PAH patients and in experimental PH induced by SuHx. Cardiac MAO-A expression and activity was increased in SuHx- and PTB-induced RV failure. Clorgyline treatment reduced RV afterload and pulmonary vascular remodelling in SuHx rats, through reduced pulmonary vascular proliferation and oxidative stress. Moreover, clorgyline improved RV stiffness, relaxation and reversed RV hypertrophy in SuHx rats. In PTB rats, clorgyline had no direct effect on the RV. Our study reveals the role of MAO-A in the progression of PAH.

CONCLUSIONS: Collectively, these findings indicated that MAO-A may be involved in pulmonary vascular remodeling and consecutive RV failure.

Key Words: Pulmonary arterial hypertension, right ventricular failure, monoamine oxidase A, oxidative stress

INTRODUCTION

Pulmonary arterial hypertension (PAH) is a fatal disease characterized by pulmonary vascular remodelling, increased right ventricular (RV) afterload and ultimately RV failure (1). Despite advances in treatment, current therapies are ineffective in stopping the disease progression (2). Therefore, new treatments are urgently needed. Reactive oxygen species (ROS)-mediated oxidative damage plays an important role in pulmonary vascular dysfunction and RV failure, and therefore therapies targeting the major ROS sources have been propagated (3).

ROS can be produced from multiple intracellular sources, and some have been identified to play important roles in PAH (3). Recently, an additional mitochondrial enzyme, monoamine oxidase (MAO), was found to be a major ROS source, with pathophysiological relevance in multiple cardiovascular diseases (4, 5). On the contrary to other ROS sources, MAO inhibitors are available and used in the clinic for the treatment of mood disorders, Parkinson's disease, and Alzheimer's disease (6). MAOs are flavoenzymes bound to the outer membrane of mitochondria, which oxidize neurotransmitters and biogenic amines, thereby producing H_2O_2 and aldehyde. MAOs have two isoforms, MAO-A and MAO-B, which have different distributions, structures, inhibitor sensitivities and substrate affinities (6). While MAO-A and MAO-B are equally present in the lungs, MAO-A is the predominant isoform in cardiomyocytes of human and rodents (7, 8).

MAO-A catalyzes preferentially serotonin (5-HT) and norepinephrine (NE), two monoamines with widely recognized roles in PAH (4, 9). Both plasma and lung endothelial cell (EC) derived 5-HT are increased in PAH patients, thus increasing substrate availability for MAO-A (10, 11). 5-HT is mostly metabolized by MAO-A in hepatic and lung ECs and induces ROS production (9). However, a role of MAO-A in lung ECs in PAH can be speculated. MAO-A activity was found to contribute to impaired vascular relaxation in ECs and increased proliferation in smooth muscle cells (SMCs) in different vascular diseases (12, 13), but its role remains unknown in the pulmonary vasculature in PAH. Apart from 5-HT, increased plasma NE was found in PAH patients with end-stage heart failure, contributing to increased activity of the sympathetic nervous system (SNS) (14). In cardiomyocytes, NE can induce a rise in MAO-A with markedly increased ROS and trigger hypertrophy (15). In various experimental models of heart failure, MAO-A inhibition was found to be beneficial, including those based on

ischemia/reperfusion injury (16, 17), left ventricular (LV) pressure overload (15, 18) and diabetes (19, 20). However, the role of MAO-A in the RV is unknown.

Here we investigated the involvement of MAO-A and its impact on PAH and RV failure. Our results show that MAO-A expression is increased in the media and intima layers, but not in whole lung lysates of PAH patients and that MAO-A inhibitor has significant therapeutic effects in experimental PAH. Collectively, our findings suggest that MAO-A inhibition may be involved in pulmonary vascular remodeling.

METHODS

Human samples, cell culture and siRNA transfections

Human sample collection was approved by the local ethics committees at Amsterdam UMC (Amsterdam, the Netherlands) and written informed consent was obtained. Details are in the online supplement.

SuHx rat model of pulmonary arterial hypertension

SuHx rats was induced as described previously (21). Animals were randomized to receive clorgyline (started with 10 mg/kg, followed by 2 mg/kg, Sigma-Aldrich) or saline by intraperitoneal injection four times from week 8 to week 10. The study was approved by an independent local animal ethic committee at Amsterdam UMC (Amsterdam, the Netherlands, study number VU-FYS13-01A4), and were carried out in compliance with guidelines issued by the Dutch government. Details are in the online supplement.

PTB rat model of RV failure

PTB rats was induced as described previously (22). PTB animals were randomized to receive clorgyline (started with 10 mg/kg, followed by 2 mg/kg, Sigma-Aldrich) or saline by intraperitoneal injection 3 times per week from week 2 to week 7. All experiments with PTB rats were in accordance with the Danish law for animal research (Danish Ministry of Justice , authorization number 2016-15-0201-01040) and approved by the Institutional Ethics Review Board. Details are in the online supplement.

Echocardiography and RV catheterization

All animals underwent echocardiographic assessments and RV catheterization as published previously (21, 22). See the online supplement for details.

Histology, western blot, MAO-A, and ATPase activity

See the online supplement for details.

Statistics

Statistical analyses were performed using Prism for Windows (GraphPad 8 Software). p-values < 0.05 were considered significant. All statistical tests used two-sided tests of significance. Data are presented as mean ± SEM. Details are in the online supplement.

RESULTS

MAO-A is increased in the pulmonary vasculatures of PAH patients.

To investigate the expression pattern of MAO-A in human PAH lungs, we performed immunofluorescence staining on paraffin sections of patients with end-stage PAH. We found that MAO-A was expressed in several cell types in the lungs, including ECs, SMCs, fibroblasts and epithelial cells (Fig. 1A, Supplement Fig. E1). To determine the expression of MAO-A, we performed fluorescence quantification. We found that MAO-A expression in the pulmonary vasculatures of PAH patients was increased in the intima as well as in the media layer (Fig. 1B, C, Supplement Fig. E1). However, we did not observe increased MAO-A expression in human whole lung lysates (Fig. 1D, E).

Moreover, we did not observe differences in MAO-A expression in primary cultures of microvascular ECs (MVECs) or PAECs derived from PAH patients and controls (Supplement: Fig. E2A, B).

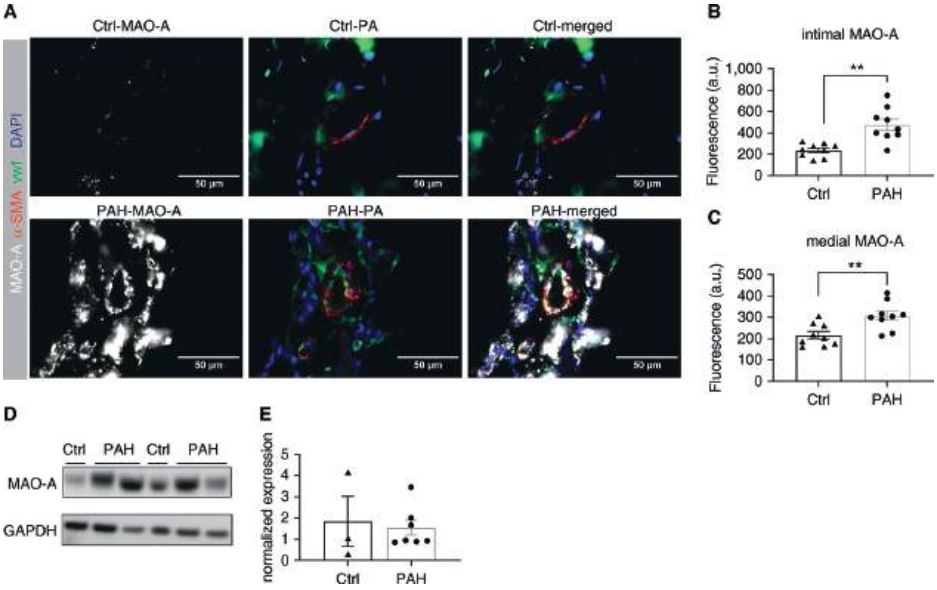

Figure 1. MAO-A expression is increased in the pulmonary vasculatures of PAH patients. **(A)** Representative lung immunofluorescence staining for MAO-A of ctrl donors and end stage PAH patients. α-SM (red), vwF (green) and DAPI (blue) were co-stained with MAO-A (white). Scale bar 50 µm. **(B, C)** Quantification of fluorescence reveals increased MAO-A expression in the intima and media layers of the pulmonary vasculatures of PAH patients. n = 9. **(D)** Representative images of western blot on human lung homogenates for MAO-A, with GAPDH as loading control. **(E)** Quantification of western blot shows that MAO-A expression in whole lung homogenates has no difference between ctrl donors and end stage PAH patients. All data are presented as mean ± SEM; Unpaired t-test. **p<0.01. PA: pulmonary artery.

MAO-A is increased in the pulmonary vasculatures of SuHx-PAH rat model.

Consistent with the findings in the tissues from PAH patients, MAO-A expression was increased in the intima and media layers of the pulmonary vasculature of SuHx-PAH rats at 10 weeks into the disease (Fig. 2A-C). Moreover, as shown by histochemistry on lung cryosections, MAO-A activity was increased in the pulmonary vasculatures of SuHx rats at week 10 (Fig. 2D). However, MAO-A protein expression was unaltered in whole lung tissue (Fig. 2E, Supplement: Fig. E3A, B).

MAO-A is increased in the RV of experimental models but not in PAH patients.

To investigate the expression and activity of MAO-A in the RV of PAH patients, we performed western blots on homogenates of the RV from patients with end-stage PAH and from controls (patients with myocardial infarction outside the RV). MAO-A expression was not increased in the RV of PH patients compared to control (Fig. 3A). In addition, enzyme histochemistry revealed no differences in MAO-A activity (Fig. 3B).

MAO-A activity and expression were markedly increased in the RV of SuHx-PAH rats (Fig. 3C, D), as well as in the RV of PTB rats (Fig. 3E, F).

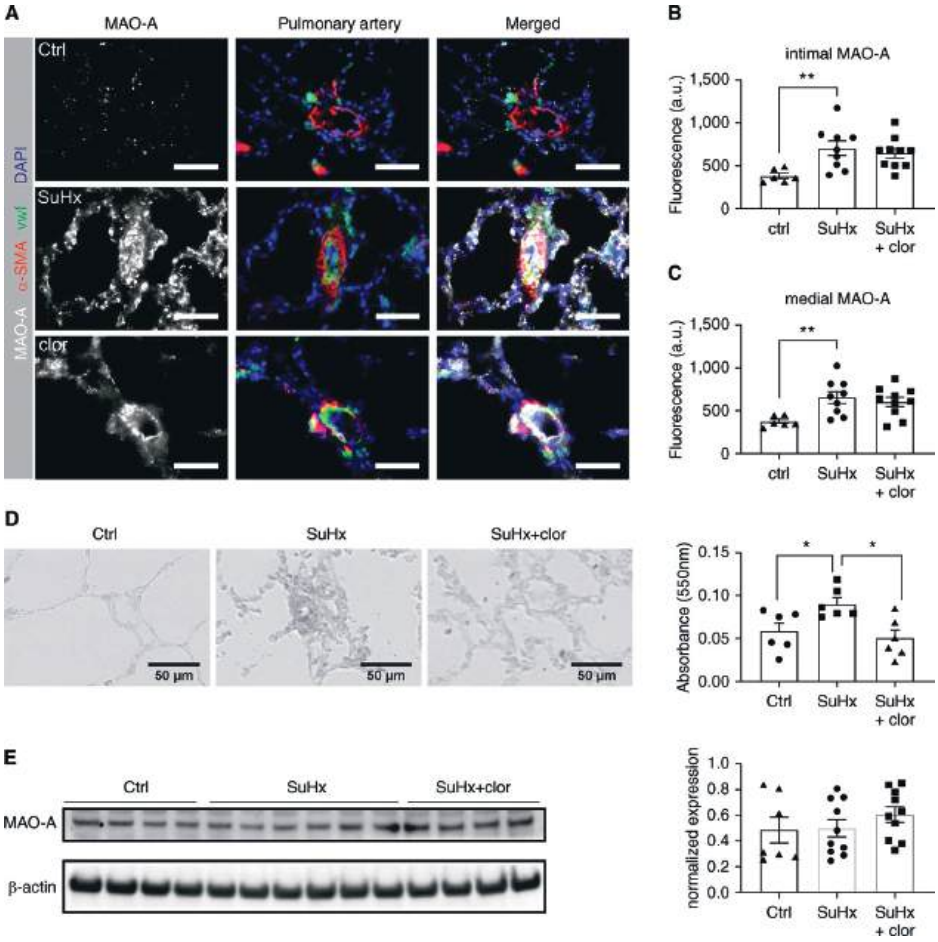

Figure 2. MAO-A is increased in the pulmonary vasculatures of SuHx rats.
(A) Representative lung immunofluorescence staining for MAO-A from ctrl, SuHx and SuHx+clorgyline groups. Scale bar 50 µm. **(B, C)** Quantification of fluorescence shows increased MAO-A expression in the intima and media layers of the pulmonary vasculatures of SuHx rats. No difference in MAO-A expression was observed by clorgyline treatment. Ctrl: n = 6, SuHx: n = 9, SuHx+clor: n = 10. **(D)** Lung histochemistry staining shows increased MAO-A activity in the lungs from SuHx rats and reduced after clorgyline treatment. Scale bar 50 µm. Incubation time: 4 hours. Ctrl: n = 6, SuHx: n = 6, SuHx+clor: n = 6. **(E)** Western blot on lung lysates shows unaltered MAO-A expression between ctrl, SuHx and clorgyline treated rats, with β-actin as loading control. ctrl: n = 7, SuHx: n = 10, SuHx+clor: n = 10. All data are presented as mean ± SEM; One-way ANOVA followed by Bonferroni posthoc comparison between ctrl and SuHx, SuHx and SuHx+clor. *p<0.05, **p<0.01.

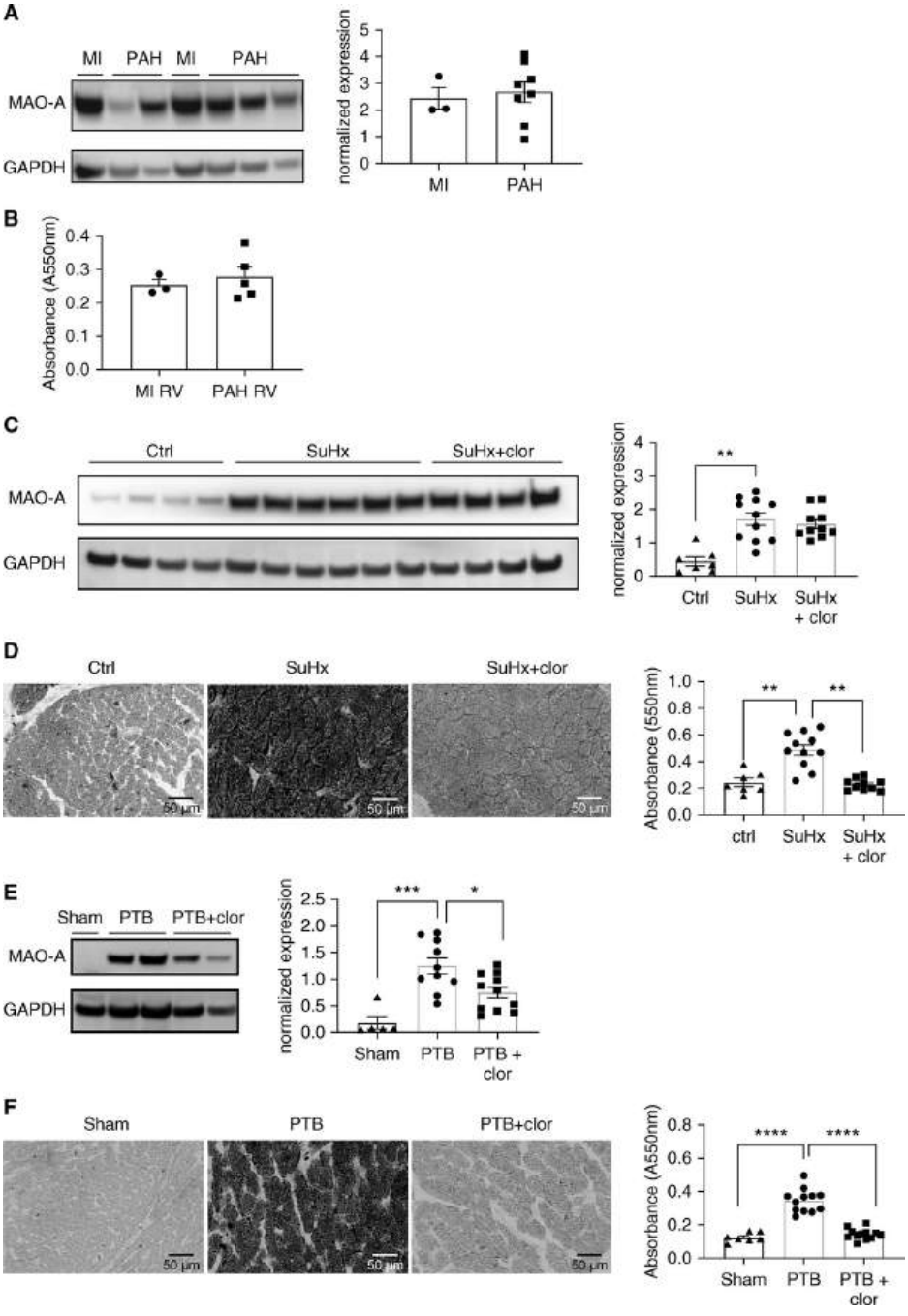
A
MI
PAH
MI
PAH
MAO-A
GAPDH
normalized expression
MI
PAH
B
Absorbance (A550nm)
MI RV
PAH RV
C
Ctrl
SuHx
SuHx+clor
MAO-A
GAPDH
normalized expression
Ctrl
SuHx
SuHx + clor
D
Ctrl
SuHx
SuHx+clor
50 µm
Absorbance (550nm)
ctrl
SuHx
SuHx + clor
E
Sham
PTB
PTB+clor
MAO-A
GAPDH
normalized expression
Sham
PTB
PTB + clor
F
Sham
PTB
PTB+clor
50 µm
Absorbance (A550nm)
Sham
PTB
PTB + clor

Figure 3. MAO-A is increased in the RV from experimental PAH.
(A) Western blot analysis reveals that MAO-A expression has no difference in the RVs between end stage PAH patients and MI patients. MI: n = 3; PH: n = 8. **(B)** Histochemistry staining reveals no difference in MAO-A activity between the RVs from PAH patients and MI patients. Scale bar 50 μm. Incubation time: 90 minutes. MI: n = 3; PH: n = 5. **(C)** MAO-A expression was increased in the RV from SuHx rats, and it was not affected by clorgyline treatment. ctrl: n = 7, SuHx: n = 11, SuHx+clor: n = 10. **(D)** MAO-A activity was increased in SuHx RV compared to ctrl RV, and it was normalized by clorgyline treatment. Scale bar 50 μm. Incubation time: 90 minutes. ctrl: n = 7, SuHx: n = 11, SuHx+clor: n = 10. **(E)** MAO-A expression was increased in the RV from PTB rats. Sham: n = 5, PTB: n = 10, PTB+clor: n = 11. **(F)** MAO-A activity was increased in the RV from PTB rats, and it was normalized after clorgyline treatment. Scale bar 50 μm. Incubation time: 60 minutes. Sham: n = 7, PTB: n = 12, PTB+clor: n = 12. All data are presented as mean ± SEM; One-way ANOVA followed by Bonferroni posthoc comparison between ctrl and SuHx, SuHx and SuHx+clor. *p<0.05, **p<0.01, ***p<0.001, ****p<0.0001. MI: myocardial infarction.

Clorgyline treatment reduces RV afterload by reversing pulmonary vascular remodeling in SuHx-PAH rats

To assess the therapeutic effect of MAO-A inhibition, we chose the irreversible MAO-A inhibitor clorgyline. Two weeks treatment with clorgyline reduced MAO-A activity in the PAH lungs (Fig. 2D), and left MAO-A protein expression unaltered (Fig. 2A-C,E). As shown by pressure-volume analysis, clorgyline reduced RV systolic pressure (RVSP) and arterial elastance (Ea) in SuHx rats (Fig. 4A). Consistently, as revealed by echocardiography analysis, clorgyline reduced total pulmonary resistance (TPR) (Fig. 4B). To further elucidate the origin of the reduced RV afterload, we measured pulmonary vascular remodeling (Fig. 4C). Clorgyline increased the percentage of open vessels, and reduced the remodeled and occluded vessels (Fig. 4D). Further quantification on the thickness of the pulmonary vascular layers revealed that clorgyline reversed vascular remodeling in the intima layer, but not the media layer (Fig. 4E, F). Consistently, as shown by PCNA immunofluorescence, clorgyline reduced proliferation in the intima layer, without affecting the proliferation of medial PASMCs (Fig. 4G-I). Cleaved caspase-3 western blots of whole lung lysates revealed no differences in apoptotic rates after clorgyline treatment (Fig. 4J).

Clorgyline treatment reduces oxidative stress in the pulmonary vasculatures of SuHx-PAH rats

Since MAO-A is an important ROS source (4, 5), we examined the effect of clorgyline on oxidative stress. Immunofluorescence staining with anti-8-Oxo-2'-deoxyguanosine (8-OHdG) revealed increased oxidative stress in the lungs and pulmonary vasculatures of SuHx rats, and clorgyline normalized oxidative stress in the pulmonary vasculatures (Fig. 5A, B). However, no differences in 8-OHdG or nitrotyrosine levels in whole lung tissues were found after clorgyline treatment (Fig. 5C, D).

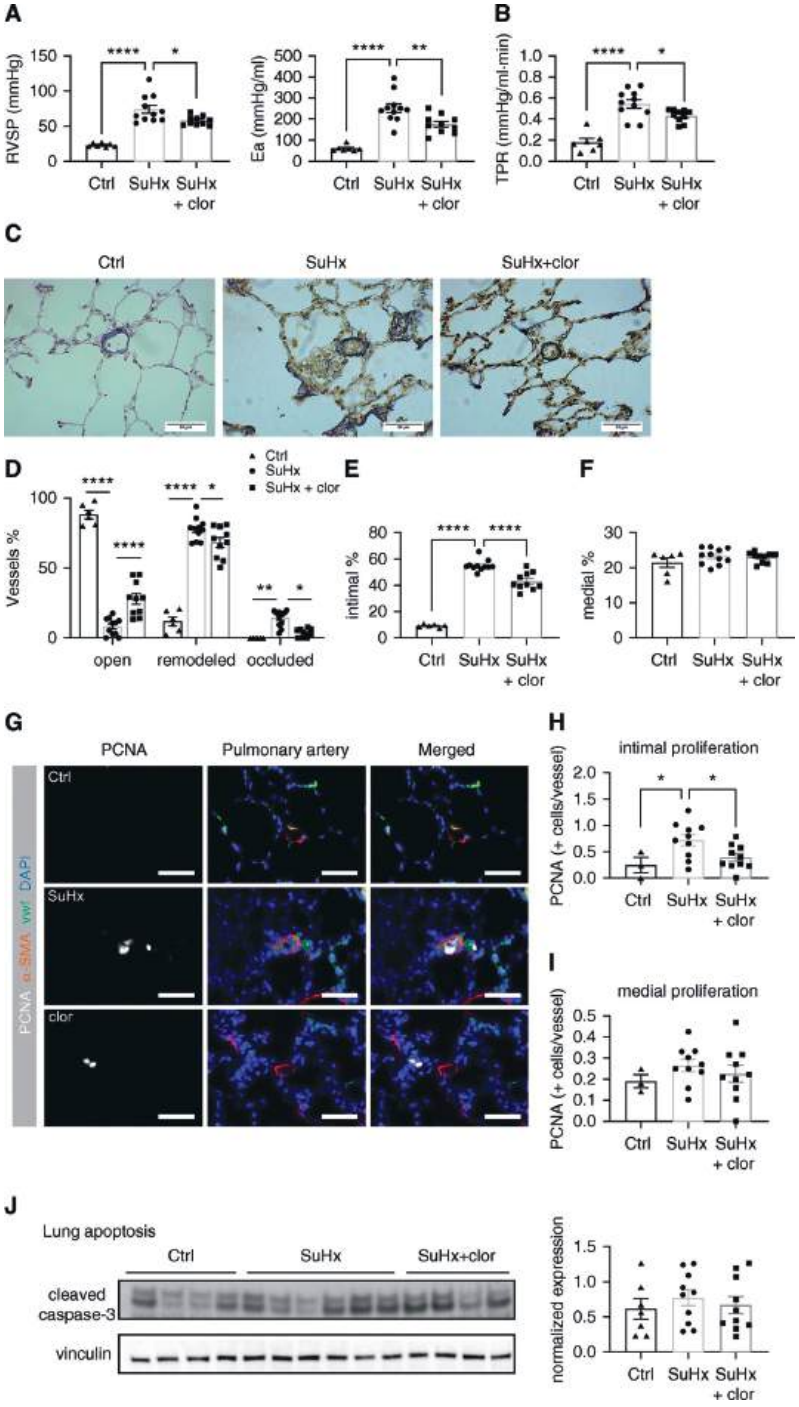

Figure 4. Clorgyline treatment reduced RV afterload in SuHx rats by reversing pulmonary vascular remodeling and proliferation.

Figure 4. (continued)
(A) Pressure-volume loop analysis reveals decreased RVSP and RV afterload (Ea) after clorgyline treatment. ctrl: n = 7, SuHx: n = 11, SuHx+clor: n = 10. **(B)** Echocardiography analysis reveals reduced TPR after clorgyline treatment. ctrl: n = 7, SuHx: n = 11, SuHx+clor: n = 10. **(C)** Representative images of pulmonary vasculatures by elastic van Gieson staining. Scale bar 50 µm. **(D-F)** Quantification of the histology images shows increased open vessels, reduced remodeled and occluded vessels in the lungs (D), reduced intima layer thickness (E), and unchanged media layer thickness (F) after clorgyline treatment. ctrl: n = 6, SuHx: n = 11, SuHx+clor: n = 10. **(G)** Representative lung immunofluorescence staining for proliferation with PCNA. α-SM (red), vwF (green) and DAPI (blue) were co-stained with PCNA (white). Scale bar 50 µm. **(H, I)** Quantification of PCNA positive cells shows reduced proliferation in intima layer of pulmonary vasculatures after clorgyline treatment, but not in the media layer. ctrl: n = 3, SuHx: n = 10, SuHx+clor: n = 10. **(J)** Western blot analysis on whole lung homogenates shows no difference in apoptotic rates between the groups. ctrl: n = 7, SuHx: n = 10, SuHx+clor: n = 10. All data are presented as mean ± SEM; One-way ANOVA followed by Bonferroni posthoc comparison between ctrl and SuHx, SuHx and SuHx+clor. *p<0.05, **p<0.01, ****p<0.0001.

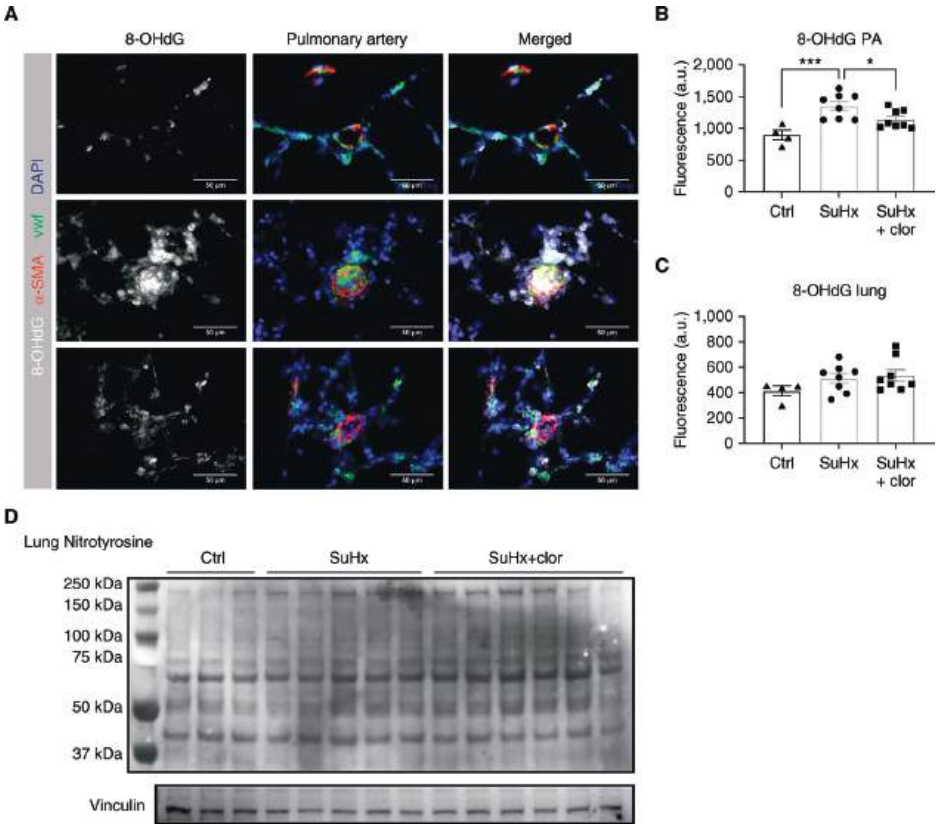

Figure 5. Clorgyline treatment reduced pulmonary vascular oxidative stress in SuHx rats.
(A) Representative lung immunofluorescence staining for oxidative stress with 8-OHdG. α-SM (red), vwF (green) and DAPI (blue) were co-stained with 8-OHdG (white). Scale bar 50 µm. **(B)** Quantification of fluorescence within the pulmonary vasculatures shows increased 8-OHdG in SuHx group compared to ctrl, and it was reduced by clorgyline. ctrl: n = 4, SuHx: n = 8, SuHx+clor: n = 8. **(C)** Quantification of 8-OHdG fluorescence shows no difference in the whole lung area between the groups. ctrl: n = 4, SuHx: n = 8, SuHx+clor: n = 8. **(D)** Western blot for oxidative stress with nitrotyrosine on whole lung

Figure 5. *(continued)*
homogenates did not reveal any difference between ctrl and SuHx rats, or between SuHx rats and SuHx rats treated with clorgyline. All data are presented as mean ± SEM; One-way ANOVA followed by Bonferroni posthoc comparison between ctrl and SuHx, SuHx and SuHx+clor. *p<0.05, ***p<0.001.

Clorgyline treatment improves RV stiffness, relaxation and RV hypertrophy in SuHx-PAH rats.

Consistent with the findings in the lungs, clorgyline normalized MAO-A activity in the RV of SuHx rats, while MAO-A protein expression was unaffected (Fig. 3C, D). Clorgyline improved RV stiffness and relaxation, as shown by reduced end diastolic elastance (Eed) and dP/dt(min), respectively (Fig. 6A). While dP/dt(max) was reduced by clorgyline, no difference was observed in load-independent RV contractility, as shown by end systolic elastance (Ees) (Supplement: Fig. E4A, Fig. 6A). Further echocardiography analysis showed no differences in tricuspid annular plane systolic excursion (TAPSE), RV end diastolic diameter (RVEDD), stoke volume (SV) (Fig. 6B), heart rate (HR) or cardiac output (CO) (data not shown).

Clorgyline reversed RV hypertrophy as shown by reduced Fulton index and RV myocardial cross-sectional area (CSA) (Fig. 6C-E). By contrast, clorgyline had no effect on RV fibrosis, apoptosis or inflammation (Fig. 6F, G, Supplement: Fig. E4B, C).

Clorgyline treatment has no direct effects on RV dysfunction induced by PTB

To investigate the direct effects of MAO-A inhibitor on the RV, we treated PTB rats with clorgyline. Clorgyline decreased not only MAO-A activity, but also expression (Fig. 3E, F, Supplement: Fig. E5A). As expected, pressure-volume loop analysis showed increased RVSP and RV afterload in PTB rats (Supplement: Fig. E5B). Body weight at the end of the study was lower in clorgyline treated rats (data not shown), therefore we used body surface area (BSA) to index all hemodynamic parameters where applicable (23). Signs of RV dysfunction in PTB rats were confirmed by decreased TAPSE and RV relaxation (dP/dt min), while RV stiffness (Eed index), contractility (Ees index) and SV index (SVI) were preserved (Fig.7 A, B), as well as HR and the resulting CO (data not shown). No difference was observed in RV function due to clorgyline treatment (Fig. 7A, B, Supplement: Fig. E5B).

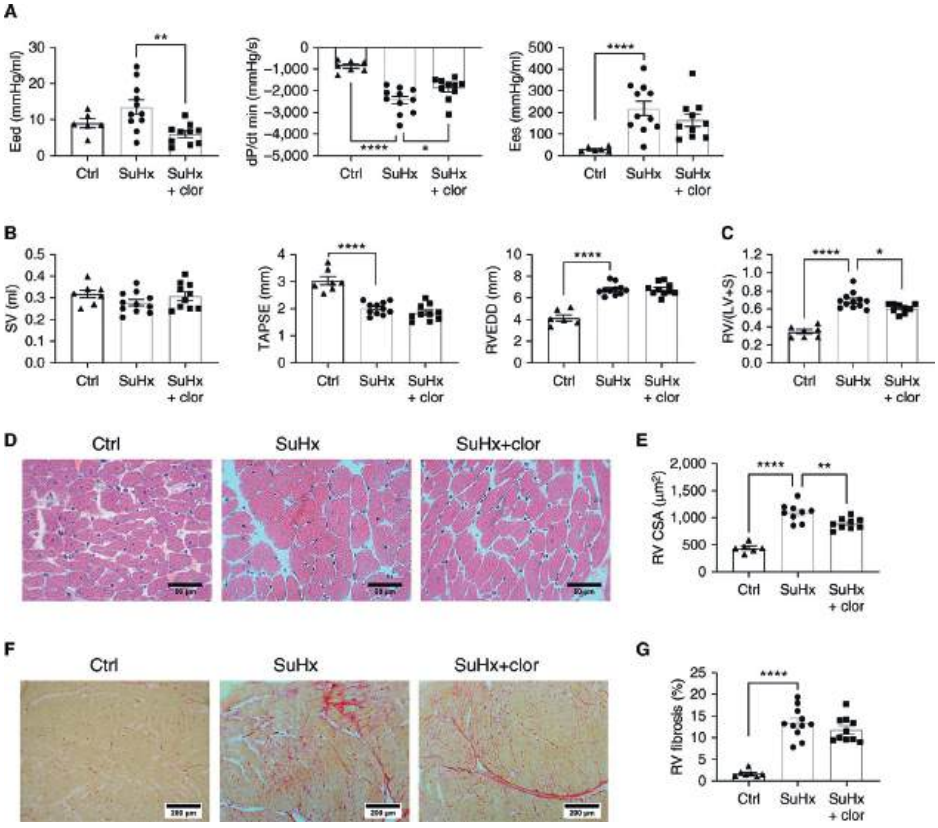

Figure 6. Clorgyline treatment improved RV stiffness, relaxation and RV hypertrophy in SuHx rats. **(A)** Pressure-volume loop analysis reveals that clorgyline reduced RV stiffness (Eed) and improved RV relaxation (dp/dt min). No difference was observed in RV contractility (Ees). Eed and Ees, ctrl: n = 6, SuHx: n = 11, SuHx+clor: n = 10. dp/dt min, ctrl: n = 7, SuHx: n = 11, SuHx+clor: n = 10. **(B)** No difference was observed in SV, TAPSE and RVEDD after clorgyline treatment by echocardiography analysis. ctrl: n = 7, SuHx: n = 11, SuHx+clor: n = 10. **(C)** Clorgyline treatment reduced Fulton index. ctrl: n = 7, SuHx: n = 12, SuHx+clor: n = 9. **(D)** Representative images of RV cardiomyocytes by H&E staining. Scale bar 50 µm. **(E)** Clorgyline reduced RV hypertrophy as shown by reduced RV myocardial CSA. ctrl: n = 6, SuHx: n = 9, SuHx+clor: n = 9. **(F)** Representative images of RV fibrosis by picrosirius red staining. Scale bar 200 µm. **(G)** No difference was observed by RV fibrosis quantification. ctrl: n = 7, SuHx: n = 11, SuHx+clor: n = 10. All data are presented as mean ± SEM; One-way ANOVA followed by Bonferroni posthoc comparison between ctrl and SuHx, SuHx and SuHx+clor. *p<0.05, **p<0.01.

Further measurement of RV remodeling revealed that clorgyline did not delay the progression of RV dilation, as shown by unaltered RVEDD index (RVEDDI) and RV end systolic diameter index (RVESDI) over time (Fig. 7A). RV hypertrophy was confirmed in PTB rats as shown by increased Fulton index and RV myocardial CSA, and no difference

was found after clorgyline treatment (Fig. 7C-E). RV fibrosis and RV apoptosis were not significantly increased in PTB rats, and were not affected by clorgyline (Fig. 7E-G).

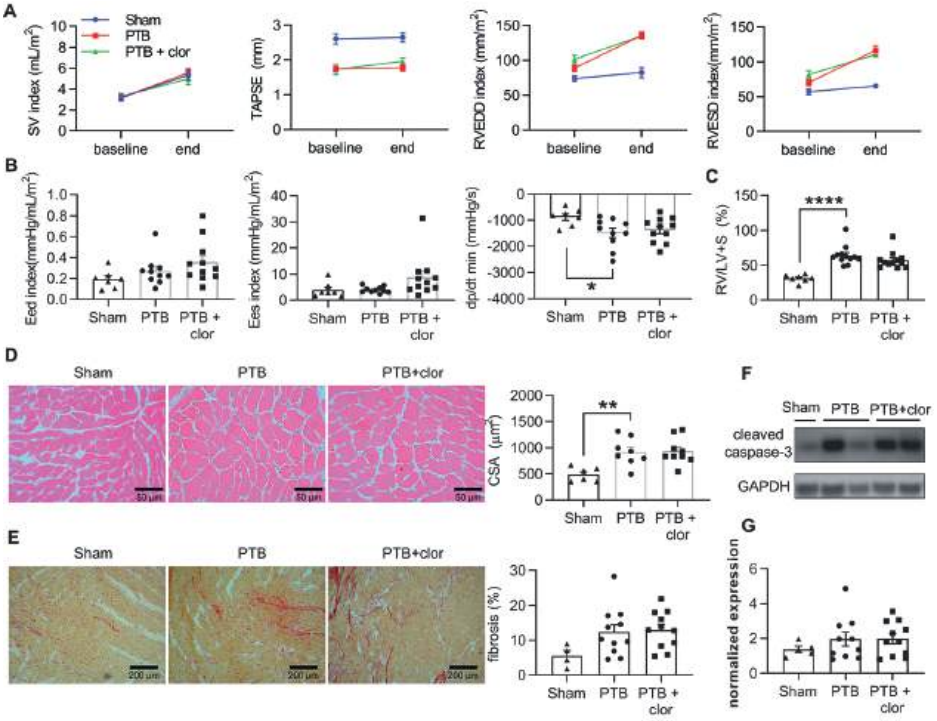

Figure 7. Clorgyline treatment has no detrimental effect on PTB induced RVF rats.
(A) Echocardiography reveals unaltered RV function as shown by SV index and TAPSE (Sham: n = 7, PTB: n = 12, PTB+clor: n = 12), and unaltered RV remodeling as shown by RVEDD index and RVESD index (Sham: n = 7, PTB: n = 11, PTB+clor: n = 12). **(B)** No difference was observed by clorgyline treatment in RV stiffness (Eed index), RV contractility (Ees index) and RV relaxation (dp/dt min), as shown by pressure-volume loop analysis. Sham: n = 7, PTB: n = 10, PTB+clor: n = 11. **(C)** Clogyline did not affect Fulton index. Sham: n = 7, PTB: n = 12, PTB+clor: n = 12. **(D)** Representative images of RV cardiomyocytes by H&E staining. Scale bar 50 μm. RV hypertrophy was observed in PTB rats by quantification of RV myocardial CSA, and it was not affected by clorgyline treatment. Sham: n = 6, PTB: n = 8, PTB+clor: n = 9. **(E)** Representative images of RV fibrosis by picrosirius red staining. Scale bar 200 μm. No difference was observed in RV fibrosis between the groups. Sham: n = 6, PTB: n = 12, PTB+clor: n = 12. **(F)** Representative images of cleaved caspase-3 western blot on RV homogenates, with GAPDH as loading control. **(G)** Quantification of cleaved caspase-3 reveals that RV apoptosis has no difference between the groups. All data are presented as mean ± SEM; One-way ANOVA followed by Bonferroni posthoc comparison between ctrl and PTB, PTB and PTB+clor. Kruskal-wallis test followed by Dunn's multiple comparison test was used for data that was not normally distributed. Two-way ANOVA for repeated measurements followed by Sidak's post-hoc was used for repeated data of echocardiography analysis. *p<0.05, **p<0.01, ****p<0.0001.

Since MAO-A is bound to the outer mitochondrial membrane, produced ROS has its effects on the mitochondria (24). No differences in mitochondrial efficiency were found between the groups (Supplement: Fig. E5C). Collectively, we found that clorgyline had neither a beneficial nor detrimental effect on the RV in PTB rats.

DISCUSSION

In the present study, we demonstrated for the first time that MAO-A is increased in the pulmonary vasculature of PAH patients. Moreover, our data indicate that increased pulmonary vascular MAO-A activity is involved in the progression of PAH, and that MAO-A inhibition may help to reverse pulmonary vascular remodeling, thereby benefiting the RV.

MAO-A up-regulation in the pulmonary vasculature in PAH

Previous studies have demonstrated that MAOs can be detected in several tissues, including the human and rodent lungs and heart (7, 8, 12). Consistent with these findings, we found that MAO-A was widely present in human and rat lungs and expressed within all layers of the vascular wall.

Increased vascular MAO-A activity has been implicated in different vascular diseases, including experimentally induced hypertension, inflammation and diabetes (12, 25-27). 5-HT, one of the main substrates of MAO-A is increased in PAH patients and experimentally induced PH, and plays a crucial role (10, 28). 5-HT is mostly metabolized into 5-Hydroxyindoleacetic acid (5-HIAA) by MAO-A in hepatic and lung ECs. A previous study suggested a normal or increased 5-HT metabolism in PAH patients, as plasma 5-HIAA remained elevated in PAH patients before and during epoprostenol treatment, which was expected to reduce platelet release of 5-HT (10). Consistently, here we show for the first time that MAO-A expression is up-regulated in the intima and media layers of the pulmonary vasculature of PAH patients, as well as in rats with experimentally induced PAH. Consistent with a previous study (8), we found that MAO-A is expressed in several other, non-vascular cell types in the lungs. However, upregulation of MAO-A could not be confirmed in whole lung lysates from PAH patients or rats with SuHx-induced PAH, nor in isolated MVECs and PAECs derived from PAH patient lungs. This study is the first to show increased MAO-A activity in the pulmonary vessels in experimental PAH. However, we were not able to perform activity measurements in

human lungs because no cryosection samples were available. Therefore, the role of MAO-A in human PAH remains uncertain, and further studies are needed to investigate the relevance of MAO-A inhibition as a therapeutic target.

MAO-A inhibitor as treatment for experimentally induced PH

In PAH, increased ROS production has been found to be one of the stimuli responsible for pulmonary vascular remodeling, through EC dysfunction and SMC proliferation (29). Due to the intense cross-talk between different ROS sources in the cell, inhibition of a single ROS source is able to abolish oxidative stress, which make MAOs promising treatment targets for diseases related to oxidative injury (30, 31). Increased MAO-A in diseased vessels can impair vasorelaxation by increasing ROS production, and inhibiting MAO-A can reduce ROS formation, increase cyclic guanosine monophosphate levels and restore vasorelaxation (25-27). More interestingly, increased MAO-A can induce proliferation in SMCs by increasing ROS production, which is a key feature of pulmonary vascular remodeling in PAH (13, 32). Based on those evidences, here we chose to test an irreversible MAO-A inhibitor clorgyline on SuHx induced PAH rat model, which can selectively inhibit MAO-A activity at a low concentration (6). As expected, we found that clorgyline reduced MAO-A activity in the lungs and RVs in the rats, and partly reversed established PAH in SuHx rats as shown by reduced RVSP, RV afterload and TPR. Moreover, clorgyline is beneficial to the RV as shown by reduced RV stiffness, improved RV relaxation and reversed RV hypertrophy in SuHx rats.

Further histology analysis revealed that clorgyline reversed pulmonary vascular remodeling, in particular the intima layer remodeling, indicating the role of MAO-A in EC function in PAH. It is further supported by our finding that clorgyline reduced proliferation in the intima layer of the pulmonary vasculatures. Moreover, we found that clorgyline reduced pulmonary vascular oxidative stress *in vivo* as shown by decreased 8-OHdG level. Our results on the intima layer of the vessels are in line with previous findings of reduced H_2O_2 production in the endothelium *ex vivo* upon clorgyline administration (26, 27). As such, the role of H_2O_2 as a stimulus for EC proliferation was confirmed (33).

Though it was shown by a previous study that clorgyline reduced proliferation in rabbit femoral SMCs and human PASMCs, in this study no difference was observed in the media layer remodeling after clorgyline treatment, neither in the media layer proliferation (13, 34). This might be due to the short period of the treatment. In addition

to increased ROS production, it has to be noticed that increased MAO-A can also produce aldehyde, which is toxic for the biological system and associated with oxidative stress (35). Therefore, aldehyde could be also involved in the mechanisms underlying the effects of clorgyline treatment.

MAO-A up-regulation in the RV in PAH

Here we find for the first time that MAO-A expression and activity is upregulated in the RV in experimental PAH and RV failure (SuHx and PTB). This finding is in line with a previous study reporting that MAO-A activity is up-regulated in the RV wall and isolated papillary muscles of monocrotaline (MCT) induced PH rats (36). The up-regulation of MAO-A in cardiomyocytes can be explained by the hyperactivation of SNS and renin angiotension-aldosterone system (RAAS), as revealed by several studies on experimentally induced LV failure models (15, 37). Similarly, in PAH patients and experimentally induced PH, hyperactivation of SNS and RAAS has also been observed (38, 39). NE, as a main substrate of MAO-A, was found to be increased in the plasma of PAH patients with end-stage heart failure, and it is correlated with pulmonary artery pressure, cardiac index and pulmonary vascular resistance in PAH patients (14, 40, 41). Moreover, NE was found to induce a rise in MAO-A expression with markedly increased ROS production in cardiomyocytes (15).

Here we compared RV MAO-A level of end-stage PAH patients with MI (outside the RV) patients and were unable to confirm the strong upregulation of MAO-A as observed in the animal models. Several factors may have contributed to the apparent discrepancy between the animal and human data. Firstly, we used autopsy tissue from patients, which represents end-stage RV failure, whereas the SuHx and PTB rats all survived until the end of the experiment and thus represent less severe RV failure. Secondly, limitations in tissue harvesting protocols, variable intervals between time of death and autopsy, and prolonged storage of human samples at -80°C may have affected MAO-A levels in autopsy specimens. Moreover, in rodent hearts MAO-A is expressed much more than MAO-B, whereas in the human heart MAO-A and -B are equally active (8, 42). Therefore, the relative role of cardiac MAO-A could be different in humans and rats. Further research into the contribution of both MAO-A and -B and their interactions should reveal their relative importance in humans.

MAO-A inhibitor as treatment on the RV in PAH

In PAH, the survival is determined by the condition of the RV rather than the degree of pulmonary vascular resistance (43). Therefore, it is important for drugs used in the treatment of PAH to be beneficial or at least non-toxic to the RV. Multiple studies highlighted MAO-A as an important source of ROS in the myocardium (15-17). Both pharmacological and genetic inhibition of MAO-A was found to be beneficial in various experimental heart failure, including those based on ischemia/reperfusion injury (16, 17), LV pressure overload (15, 18) and diabetes (19, 20). More interestingly, it was shown that clorgyline can decrease the basal rate of oxygen consumption of RV papillary muscles in MCT induced PH rats (36). At the other end of the scale, cardiac-specific MAO-A overexpression enhanced H_2O_2 formation leading to cardiomyocyte necrosis and ventricular failure with mitochondrial impairment (18). In this study, we found that clorgyline is beneficial to the RV in SuHx-PAH rats, by reducing stiffness, improving relaxation and reducing hypertrophy. Though fibrosis and apoptosis are closely related to oxidative stress, here we did not find any effect of clorgyline on SuHx RV fibrosis or apoptosis, which could be due to the short treatment duration of 2 weeks.

A previous study showed that LV hypertrophy was exacerbated in MAO-A knockout mice subjected to transverse aortic constriction (TAC) due to hyperactivation of 5-HT2A receptors (44). Therefore, despite the improved RV function found in the SuHx-PAH model, it is crucial to confirm the safety of MAO-A inhibitor on the RV. Here we treated PTB rats with clorgyline to investigate the direct effect on the RV. Unlike the results on SuHx-PAH or TAC model, we did not observe any beneficial or detrimental effects of clorgyline on the RV. Therefore, the beneficial effects of clorgyline on the RV of SuHx rats can be mainly due to reduced RV afterload, and possibly reduced RV oxidative stress. A previous study revealed that RV oxidative stress is largely increased in SuHx RV but unchanged in PTB (45), which may explain the negative findings on RV fibrosis and apoptosis, which are closely related to oxidative stress. Besides the different responses to pressure overload between RV and LV (46), it has to be noted that the starting time point of the drug administration in this study is different from the studies on TAC model. In this reversal study, clorgyline treatment started two weeks after PTB surgery, when the rats showed signs of RV dysfunction, while clorgyline was given to the TAC mice directly after TAC surgery as prevention.

Limitations

Clorgyline is no longer used in the clinic due to the "cheese-effect", which can cause hypertensive crises after ingestion of food rich in tyramine (6). Although it limits the direct translation to the clinic, we believe it is justified for this proof of principle study, as clorgyline is a specific and selective MAO-A inhibitor. The introduction of a new generation of reversible MAO-A inhibitors can avoid the adverse cheese effect. Therefore, it is worth for future research to test those clinically approved new generation MAO-A inhibitors in combination with other PAH drugs, as well as the development of lung-specific delivery methods to achieve efficiency at low drug concentration.

The use of human samples obtained at autopsy clearly has limitations. The duration of storage of the cardiac samples ranged between 2-12 years at -80°C before analysis of MAO-A activity and expression. Also, the exact times between death and autopsy are unknown. However, MAO-A expression and activity is closely regulated by neurohormonal activity which is known to be increased in PAH. Therefore, the present results on the inhibition of MAO-A activity may still be of clinical significance in PAH patients.

The present study used two animal models. The SuHx rat model was used to investigate the effect of MAO-A inhibition on the pulmonary vasculature, and the PTB rat model to study the effect of MAO-A inhibition on RV failure. We believe that a treatment study with MCT rats may not add much valuable information, since the SuHx model provides a much better representation of vascular findings in human PAH.

CONCLUSION

In conclusion, MAO-A is increased locally in the pulmonary vasculatures of PAH patients and in the pulmonary vasculature and RV of experimentally induced PH models. Treatment with MAO-A inhibitor clorgyline can partly reverse RV afterload and pulmonary vascular remodeling in established experimental PH by reducing pulmonary vascular proliferation and oxidative stress. Importantly, while it has no direct effect on cardiac function, it is beneficial to the RV by reducing RV afterload. Collectively, MAO-A seems to be involved in pulmonary vascular remodeling and further investigations should reveal the relevance of MAO-A in different stages of human PAH.

ACKNOWLEDGMENTS

The authors wish to thank Peter ten Dijke for his input and discussion.

FUNDING

HJB, AVN and FSdM were supported by the Netherlands CardioVascular Research Initiative: the Dutch Heart Foundation, Dutch Federation of University Medical Centers, the Netherlands Organization for Health Research and Development, and the Royal Netherlands Academy of Sciences (CVON-2012-08 PHAEDRA, CVON-2018-29 PHAEDRA-IMPACT, CVON-2017-10 Dolphin-Genesis). HJB and AVN were supported by research grants from Actelion, GSK and Ferrer (Therabel). EP, XS, AVN and FSdM were further supported by The Netherlands Organization for Scientific Research (NWO-VICI: 918.16.610, NWO-VIDI: 917.18.338). FSdM was supported by the Dutch Heart Foundation Dekker senior post-doc grant (2018T059).

REFERENCES

1. Rubin LJ. Primary pulmonary hypertension. *N Engl J Med* 1997; 336: 111-117.
2. Lajoie AC, Lauziere G, Lega JC, Lacasse Y, Martin S, Simard S, Bonnet S, Provencher S. Combination therapy versus monotherapy for pulmonary arterial hypertension: a meta-analysis. *Lancet Respir Med* 2016; 4: 291-305.
3. Fulton DJR, Li X, Bordan Z, Haigh S, Bentley A, Chen F, Barman SA. Reactive Oxygen and Nitrogen Species in the Development of Pulmonary Hypertension. *Antioxidants (Basel)* 2017; 6.
4. Kaludercic N, Mialet-Perez J, Paolocci N, Parini A, Di Lisa F. Monoamine oxidases as sources of oxidants in the heart. *J Mol Cell Cardiol* 2014; 73: 34-42.
5. Deshwal S, Di Sante M, Di Lisa F, Kaludercic N. Emerging role of monoamine oxidase as a therapeutic target for cardiovascular disease. *Curr Opin Pharmacol* 2017; 33: 64-69.
6. Youdim MB, Edmondson D, Tipton KF. The therapeutic potential of monoamine oxidase inhibitors. *Nat Rev Neurosci* 2006; 7: 295-309.
7. Holschneider DP, Kumazawa T, Chen K, Shih JC. Tissue-specific effects of estrogen on monoamine oxidase A and B in the rat. *Life Sci* 1998; 63: 155-160.
8. Sivasubramaniam SD, Finch CC, Rodriguez MJ, Mahy N, Billett EE. A comparative study of the expression of monoamine oxidase-A and -B mRNA and protein in non-CNS human tissues. *Cell Tissue Res* 2003; 313: 291-300.
9. MacLean MMR. The serotonin hypothesis in pulmonary hypertension revisited: targets for novel therapies (2017 Grover Conference Series). *Pulm Circ* 2018; 8: 2045894018759125.
10. Kereveur A, Callebert J, Humbert M, Herve P, Simonneau G, Launay JM, Drouet L. High plasma serotonin levels in primary pulmonary hypertension. Effect of long-term epoprostenol (prostacyclin) therapy. *Arterioscler Thromb Vasc Biol* 2000; 20: 2233-2239.
11. Eddahibi S, Guignabert C, Barlier-Mur AM, Dewachter L, Fadel E, Dartevelle P, Humbert M, Simonneau G, Hanoun N, Saurini F, Hamon M, Adnot S. Cross talk between endothelial and smooth muscle cells in pulmonary hypertension: critical role for serotonin-induced smooth muscle hyperplasia. *Circulation* 2006; 113: 1857-1864.
12. Lighezan R, Sturza A, Duicu OM, Ceausu RA, Vaduva A, Gaspar M, Feier H, Vaida M, Ivan V, Lighezan D, Muntean DM, Mornos C. Monoamine oxidase inhibition improves vascular function in mammary arteries from nondiabetic and diabetic patients with coronary heart disease. *Can J Physiol Pharmacol* 2016; 94: 1040-1047.
13. Coatrieux C, Sanson M, Negre-Salvayre A, Parini A, Hannun Y, Itohara S, Salvayre R, Auge N. MAO-A-induced mitogenic signaling is mediated by reactive oxygen species, MMP-2, and the sphingolipid pathway. *Free Radic Biol Med* 2007; 43: 80-89.
14. Mak S, Witte KK, Al-Hesayen A, Granton JJ, Parker JD. Cardiac sympathetic activation in patients with pulmonary arterial hypertension. *Am J Physiol Regul Integr Comp Physiol* 2012; 302: R1153-1157.
15. Kaludercic N, Takimoto E, Nagayama T, Feng N, Lai EW, Bedja D, Chen K, Gabrielson KL, Blakely RD, Shih JC, Pacak K, Kass DA, Di Lisa F, Paolocci N. Monoamine oxidase A-mediated enhanced catabolism of norepinephrine contributes to adverse remodeling and pump failure in hearts with pressure overload. *Circ Res* 2010; 106: 193-202.

16. Bianchi P, Kunduzova O, Masini E, Cambon C, Bani D, Raimondi L, Seguelas MH, Nistri S, Colucci W, Leducq N, Parini A. Oxidative stress by monoamine oxidase mediates receptor-independent cardiomyocyte apoptosis by serotonin and postischemic myocardial injury. *Circulation* 2005; 112: 3297-3305.
17. Pchejetski D, Kunduzova O, Dayon A, Calise D, Seguelas MH, Leducq N, Seif I, Parini A, Cuvillier O. Oxidative stress-dependent sphingosine kinase-1 inhibition mediates monoamine oxidase A-associated cardiac cell apoptosis. *Circ Res* 2007; 100: 41-49.
18. Villeneuve C, Guilbeau-Frugier C, Sicard P, Lairez O, Ordener C, Duparc T, De Paulis D, Couderc B, Spreux-Varoquaux O, Tortosa F, Garnier A, Knauf C, Valet P, Borchi E, Nediani C, Gharib A, Ovize M, Delisle MB, Parini A, Mialet-Perez J. p53-PGC-1alpha pathway mediates oxidative mitochondrial damage and cardiomyocyte necrosis induced by monoamine oxidase-A upregulation: role in chronic left ventricular dysfunction in mice. *Antioxid Redox Signal* 2013; 18: 5-18.
19. Umbarkar P, Singh S, Arkat S, Bodhankar SL, Lohidasan S, Sitasawad SL. Monoamine oxidase-A is an important source of oxidative stress and promotes cardiac dysfunction, apoptosis, and fibrosis in diabetic cardiomyopathy. *Free Radic Biol Med* 2015; 87: 263-273.
20. Deshwal S, Forkink M, Hu CH, Buonincontri G, Antonucci S, Di Sante M, Murphy MP, Paolocci N, Mochly-Rosen D, Krieg T, Di Lisa F, Kaludercic N. Monoamine oxidase-dependent endoplasmic reticulum-mitochondria dysfunction and mast cell degranulation lead to adverse cardiac remodeling in diabetes. *Cell Death Differ* 2018; 25: 1671-1685.
21. Kurakula K, Sun XQ, Happe C, da Silva Goncalves Bos D, Szulcek R, Schalij I, Wiesmeijer KC, Lodder K, Tu L, Guignabert C, de Vries CJM, de Man FS, Vonk Noordegraaf A, Ten Dijke P, Goumans MJ, Bogaard HJ. Prevention of progression of pulmonary hypertension by the Nur77 agonist 6-mercaptopurine: role of BMP signalling. *Eur Respir J* 2019; 54.
22. Andersen S, Axelsen JB, Ringgaard S, Nyengaard JR, Hyldebrandt JA, Bogaard HJ, de Man FS, Nielsen-Kudsk JE, Andersen A. Effects of combined angiotensin II receptor antagonism and neprilysin inhibition in experimental pulmonary hypertension and right ventricular failure. *Int J Cardiol* 2019; 293: 203-210.
23. Gouma E, Simos Y, Verginadis I, Lykoudis E, Evangelou A, Karkabounas S. A simple procedure for estimation of total body surface area and determination of a new value of Meeh's constant in rats. *Lab Anim* 2012; 46: 40-45.
24. Hauptmann N, Grimsby J, Shih JC, Cadenas E. The metabolism of tyramine by monoamine oxidase A/B causes oxidative damage to mitochondrial DNA. *Arch Biochem Biophys* 1996; 335: 295-304.
25. Poon CC, Seto SW, Au AL, Zhang Q, Li RW, Lee WY, Leung GP, Kong SK, Yeung JH, Ngai SM, Ho HP, Lee SM, Chan SW, Kwan YW. Mitochondrial monoamine oxidase-A-mediated hydrogen peroxide generation enhances 5-hydroxytryptamine-induced contraction of rat basilar artery. *Br J Pharmacol* 2010; 161: 1086-1098.
26. Sturza A, Leisegang MS, Babelova A, Schroder K, Benkhoff S, Loot AE, Fleming I, Schulz R, Muntean DM, Brandes RP. Monoamine oxidases are mediators of endothelial dysfunction in the mouse aorta. *Hypertension* 2013; 62: 140-146.

27. Sturza A, Duicu OM, Vaduva A, Danila MD, Noveanu L, Varro A, Muntean DM. Monoamine oxidases are novel sources of cardiovascular oxidative stress in experimental diabetes. *Can J Physiol Pharmacol* 2015; 93: 555-561.
28. Hervé P LJ, Scrobohaci ML, Brenot F, Simonneau G, Petitpretz P, Poubeau P, Cerrina J, Duroux P, Drouet L. Increased plasma serotonin in primary pulmonary hypertension. *Am J Med* 1995; 99: 249-254.
29. Aggarwal S, Gross CM, Sharma S, Fineman JR, Black SM. Reactive oxygen species in pulmonary vascular remodeling. *Compr Physiol* 2013; 3: 1011-1034.
30. Kaludercic N, Carpi A, Menabo R, Di Lisa F, Paolocci N. Monoamine oxidases (MAO) in the pathogenesis of heart failure and ischemia/reperfusion injury. *Biochim Biophys Acta* 2011; 1813: 1323-1332.
31. Duicu OM, Lighezan R, Sturza A, Ceausu RA, Borza C, Vaduva A, Noveanu L, Gaspar M, Ionac A, Feier H, Muntean DM, Mornos C. Monoamine Oxidases as Potential Contributors to Oxidative Stress in Diabetes: Time for a Study in Patients Undergoing Heart Surgery. *Biomed Res Int* 2015; 2015: 515437.
32. Toshner M, Voswinckel R, Southwood M, Al-Lamki R, Howard LS, Marchesan D, Yang J, Suntharalingam J, Soon E, Exley A, Stewart S, Hecker M, Zhu Z, Gehling U, Seeger W, Pepke-Zaba J, Morrell NW. Evidence of dysfunction of endothelial progenitors in pulmonary arterial hypertension. *Am J Respir Crit Care Med* 2009; 180: 780-787.
33. Porter KM, Kang BY, Adesina SE, Murphy TC, Hart CM, Sutliff RL. Chronic hypoxia promotes pulmonary artery endothelial cell proliferation through H2O2-induced 5-lipoxygenase. *PLoS One* 2014; 9: e98532.
34. Lawrie A, Spiekerkoetter E, Martinez EC, Ambartsumian N, Sheward WJ, MacLean MR, Harmar AJ, Schmidt AM, Lukanidin E, Rabinovitch M. Interdependent serotonin transporter and receptor pathways regulate S100A4/Mts1, a gene associated with pulmonary vascular disease. *Circ Res* 2005; 97: 227-235.
35. Chen CH, Budas GR, Churchill EN, Disatnik MH, Hurley TD, Mochly-Rosen D. Activation of aldehyde dehydrogenase-2 reduces ischemic damage to the heart. *Science* 2008; 321: 1493-1495.
36. van Eif VW, Bogaards SJ, van der Laarse WJ. Intrinsic cardiac adrenergic (ICA) cell density and MAO-A activity in failing rat hearts. *J Muscle Res Cell Motil* 2014; 35: 47-53.
37. Raasch W BT, Gieselberg A, Dendorfer A, Dominiak P. Angiotensin I-converting enzyme inhibition increases cardiac catecholamine content and reduces monoamine oxidase activity via an angiotensin type 1 receptor-mediated mechanism. *J Pharmacol Exp Ther* 2002; 300: 428-434.
38. Ciarka A, Doan V, Velez-Roa S, Naeije R, van de Borne P. Prognostic significance of sympathetic nervous system activation in pulmonary arterial hypertension. *Am J Respir Crit Care Med* 2010; 181: 1269-1275.
39. Piao L, Fang YH, Parikh KS, Ryan JJ, D'Souza KM, Theccanat T, Toth PT, Pogoriler J, Paul J, Blaxall BC, Akhter SA, Archer SL. GRK2-mediated inhibition of adrenergic and dopaminergic signaling in right ventricular hypertrophy: therapeutic implications in pulmonary hypertension. *Circulation* 2012; 126: 2859-2869.

40. Nootens M, Kaufmann E, Rector T, Toher C, Judd D, Francis GS, Rich S. Neurohormonal activation in patients with right ventricular failure from pulmonary hypertension: Relation to hemodynamic variables and endothelin levels. *Journal of the American College of Cardiology* 1995; 26: 1581-1585.
41. Nagaya N, Nishikimi T, Uematsu M, Satoh T, Kyotani S, Sakamaki F, Kakishita M, Fukushima K, Okano Y, Nakanishi N, Miyatake K, Kangawa K. Plasma brain natriuretic peptide as a prognostic indicator in patients with primary pulmonary hypertension. *Circulation* 2000; 102: 865-870.
42. Saura J, Kettler R, Da Prada M, Richards JG. Quantitative enzyme radioautography with 3H-Ro 41-1049 and 3H-Ro 19-6327 in vitro: localization and abundance of MAO-A and MAO-B in rat CNS, peripheral organs, and human brain. *J Neurosci* 1992; 12: 1977-1999.
43. Mauritz GJ, Kind T, Marcus JT, Bogaard HJ, van de Veerdonk M, Postmus PE, Boonstra A, Westerhof N, Vonk-Noordegraaf A. Progressive changes in right ventricular geometric shortening and long-term survival in pulmonary arterial hypertension. *Chest* 2012; 141: 935-943.
44. Lairez O, Calise D, Bianchi P, Ordener C, Spreux-Varoquaux O, Guilbeau-Frugier C, Escourrou G, Seif I, Roncalli J, Pizzinat N, Galinier M, Parini A, Mialet-Perez J. Genetic deletion of MAO-A promotes serotonin-dependent ventricular hypertrophy by pressure overload. *J Mol Cell Cardiol* 2009; 46: 587-595.
45. Bogaard HJ, Natarajan R, Henderson SC, Long CS, Kraskauskas D, Smithson L, Ockaili R, McCord JM, Voelkel NF. Chronic pulmonary artery pressure elevation is insufficient to explain right heart failure. *Circulation* 2009; 120: 1951-1960.
46. Zungu-Edmondson M, Suzuki YJ. Differential stress response mechanisms in right and left ventricles. *J Rare Dis Res Treat* 2016; 1: 39-45.

SUPPLEMENTAL FIGURES

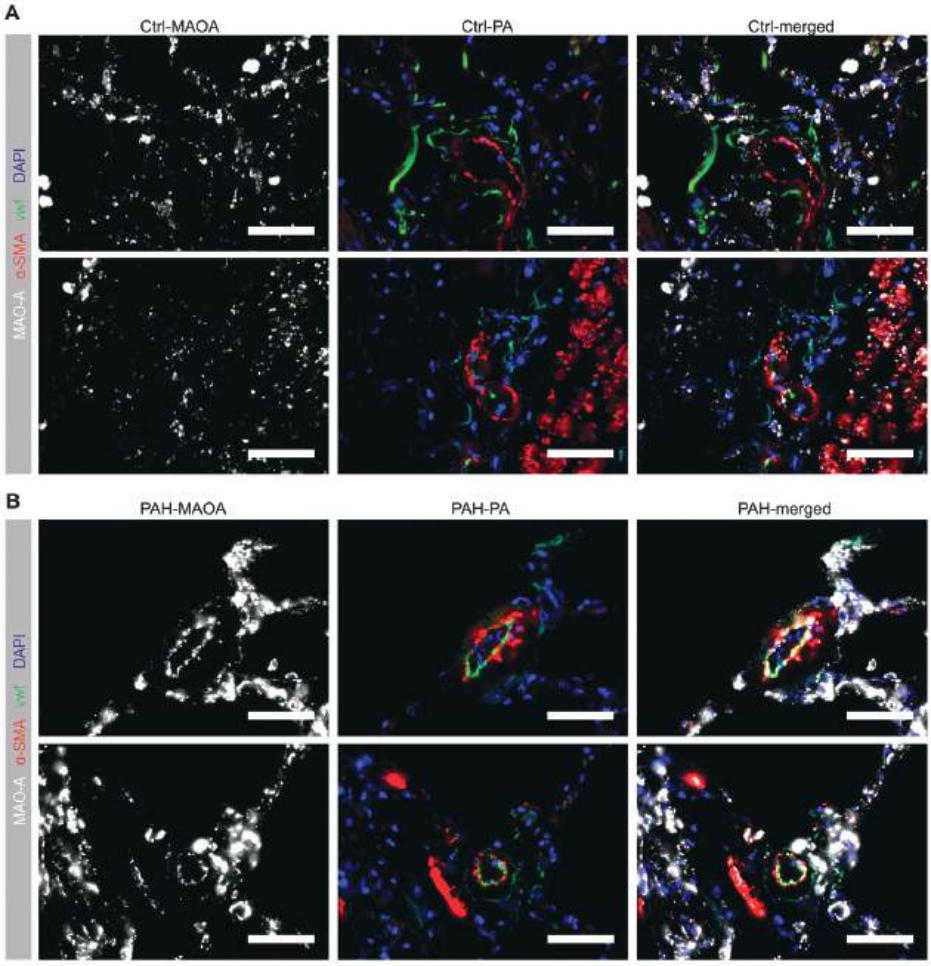

Figure E1. Representative images of MAO-A immunofluorescence staining in human lungs. Representative lung immunofluorescence staining for MAO-A of ctrl donors (A) and end stage PAH patients (B). α-SM (red), vwF (green) and DAPI (blue) were co-stained with MAO-A (white). Scale bar 50 μm.

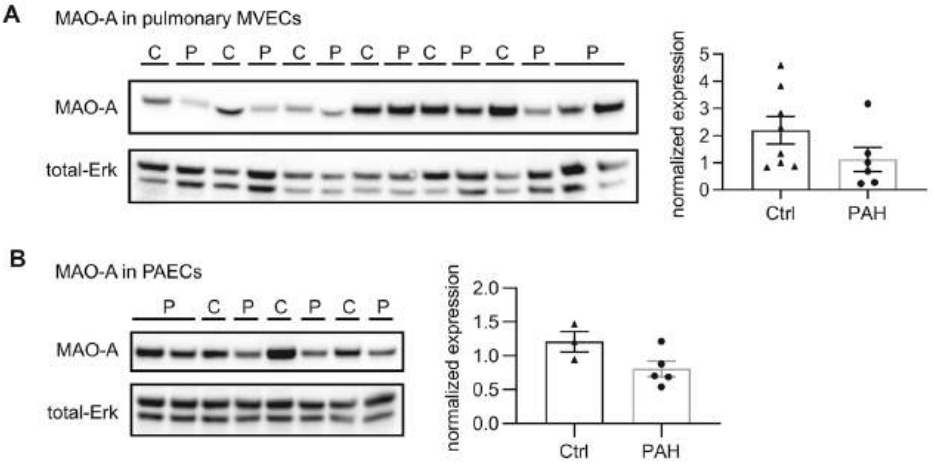

Figure E2. MAO-A expression in ECs of PAH patients.
Western blot analysis shows no difference in MAO-A expression in pulmonary MVECs (A) or PAECs (B) between non-PAH and PAH patients, with total-Erk as loading control. (A) Ctrl: n = 8, PAH: n = 6. (B) Ctrl: n = 3, PAH: n = 5. All data are presented as mean ± SEM. Unpaired t-test.

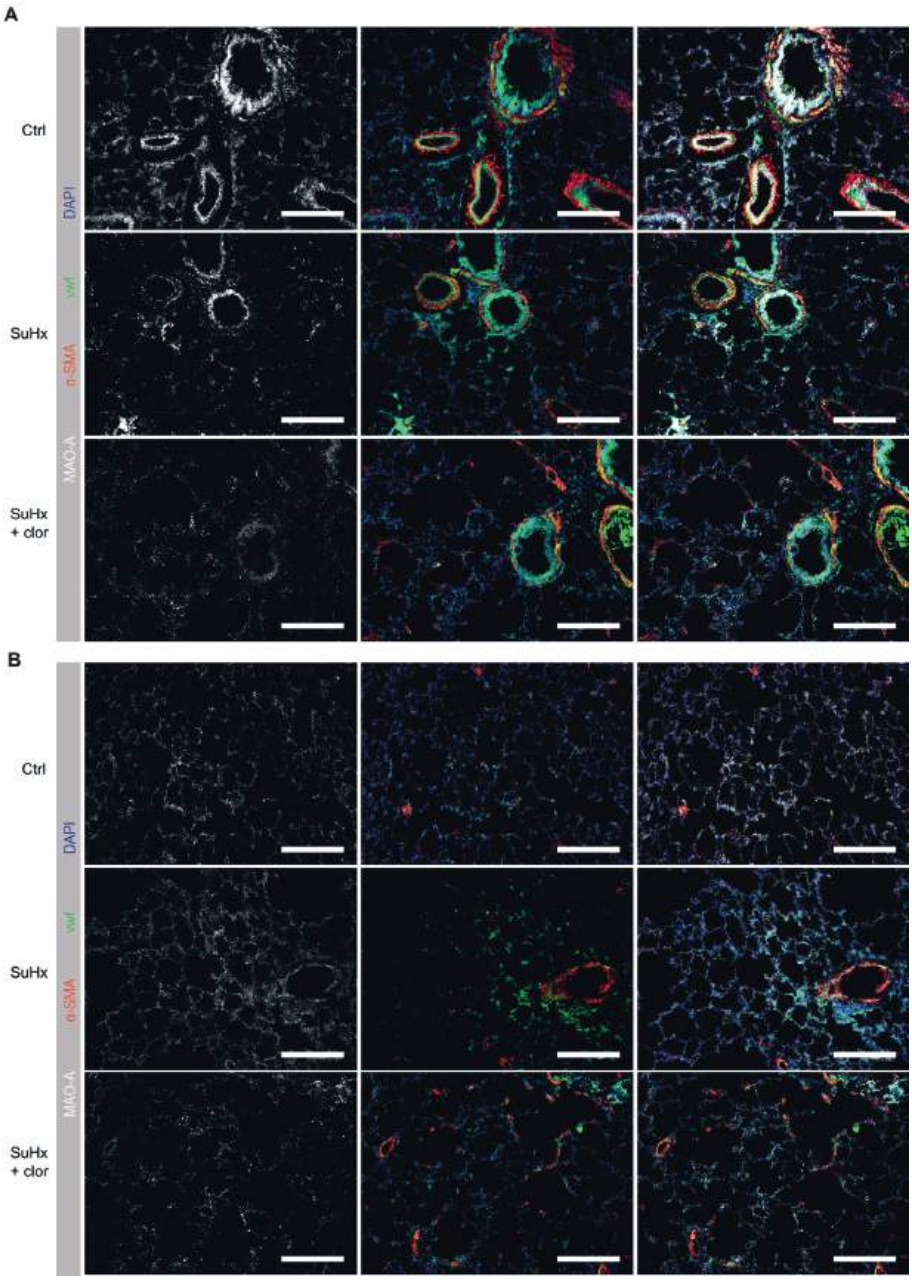

Figure E3. MAO-A expression on whole lung tissue

(A, B) Representative lung immunofluorescence staining for MAO-A of ctrl rats, SuHx rats, and SuHx rats with clorgyline treatment. α-SM (red), vwF (green) and DAPI (blue) were co-stained with MAO-A (white). Scale bar 200 μm.

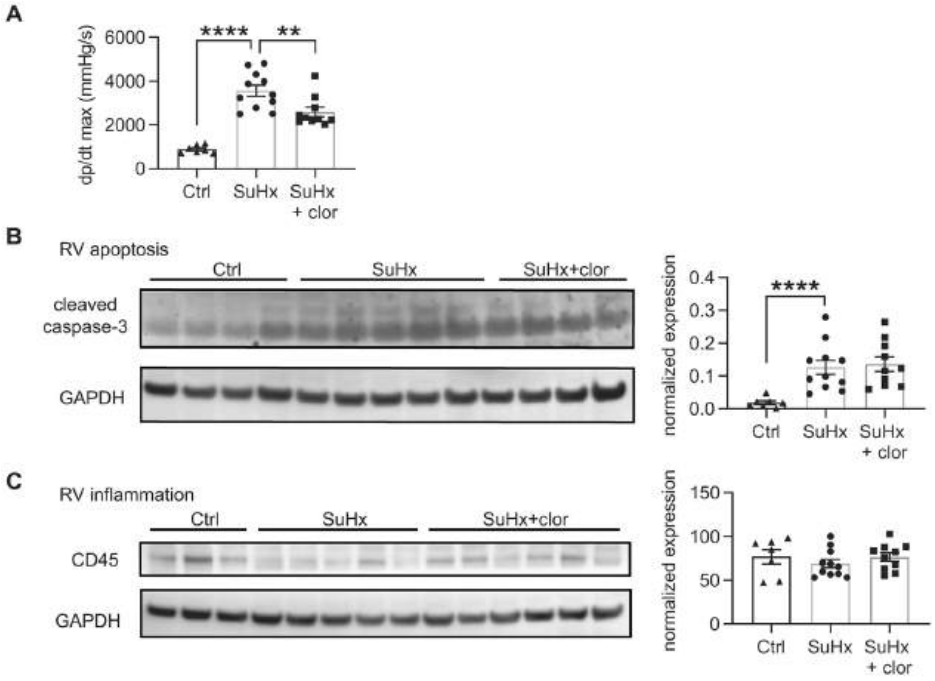

Figure E4. Clogyline treatment on SuHx-PAH rats.

(A) Pressure-volume analysis shows decreased dp/dt max. ctrl: n = 7, SuHx: n = 11, SuHx+clor: n = 10. (B) Western blot analysis on the RV shows no difference in apoptosis between the groups. n = 7, SuHx: n = 11, SuHx+clor: n = 10. (C) Western blot analysis on the RV shows no difference in inflammation between the groups. n = 7, SuHx: n = 11, SuHx+clor: n = 10. All data are presented as mean ± SEM; One-way ANOVA followed by Bonferroni posthoc comparison between ctrl and SuHx, SuHx and SuHx+clor. ** p<0,01.

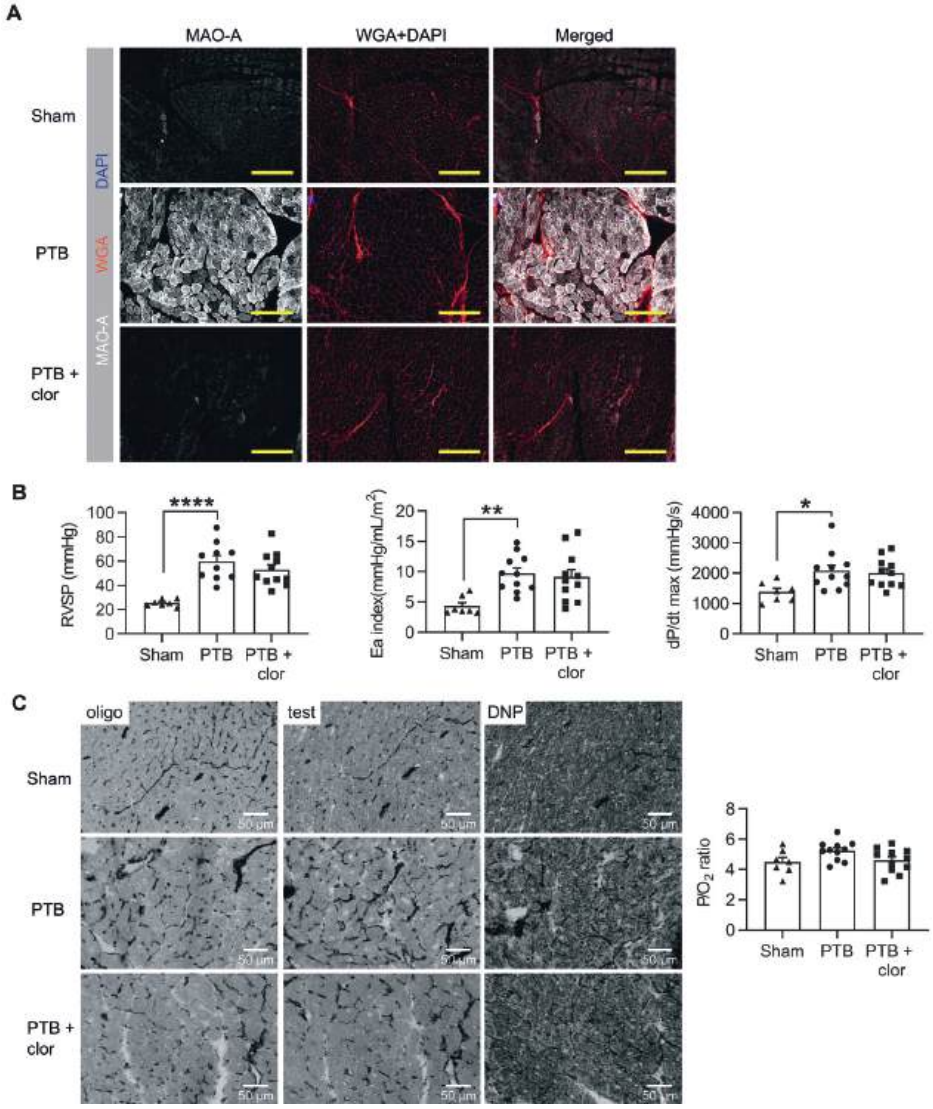

Figure E5: Clorgyline treatment on PTB rats.

(A) Representative RV immunofluorescence staining for MAO-A of Sham, PTB, and PTB rats with clorgyline treatment. WGA (red) and DAPI (blue) were co-stained with MAO-A (white). Scale bar 200 µm. (B) Pressure-volume analysis shows increased RVSP, Ea index and dp/dt max in PTB rats, and clorgyline had no effect on those parameters. RVSP, Sham: n = 7, PTB: n = 10, PTB+clor: n = 11. Ea index and dp/dt max, Sham: n = 7, PTB: n = 11, PTB+clor: n = 11. (C) Mitochondrial efficiency was assessed by measuring the background, actual and maximal mitochondrial ATPase activity in serial cryosections of the RV, of which P/O2 ratio was estimated. Scale bar 50 µm. With the theoretical maximal P/O2 being 6.3, all groups were in the normal range with no difference between the groups. Sham: n = 7, PTB: n = 11, PTB+clor: n = 11. All data are presented as mean ± SEM; One-way ANOVA followed by Bonferroni posthoc comparison between ctrl and PTB, PTB and PTB+clor. SDH: succinate dehydrogenase.

SUPPLEMENTAL METHODS

Human lung and RV samples

Human lung and heart sample collection was approved by the local ethics committees at the Amsterdam UMC (Amsterdam, the Netherlands) and written informed consent was obtained. Control lung tissues on paraffin slides were obtained from healthy donors died from accidents. Control pulmonary arteries for ECs isolation were obtained from patients undergoing surgery for lung carcinoma, which were distant from the malignant lesion and were dissected by a pathologist. PAH lung tissues on paraffin slides and pulmonary arteries for ECs isolation were obtained from idiopathic PAH and heritable PAH patients undergoing lung transplantation. Isolation and culturing of MVECs and PAECs from control and PAH patients was described previously (1). RV tissue samples from PAH and MI patients (with MI outside the RV), and frozen lung samples from PAH were collected at autopsy and provided by the biobank of the Amsterdam UMC, location VUmc (biobank protocols BUP2018-15, RES18-249, RES18-461 and RES20-238). Frozen lung samples from controls were taken from patients with (suspicion of) a tumor as far away as possible from the tumor. The time of storage for the cardiac tissue ranged between 2-12 years at -80°C before analysis of MAO-A activity and expression. The exact times between death and autopsy are unknown. For two cases there were 2 days between death and autopsy, for two cases autopsy was done on the next day. For the remainder of the patients, autopsy was done on the day of death. The storage time and time between death and autopsy for frozen lung samples is unknown.

SuHx rat model of pulmonary arterial hypertension

Male Sprague-Dawley rats (n = 24, Charles River) were used throughout the experiment. Rats were housed in standard conditions and food and water was available *ad libitum*. SU5416 + Hypoxia (SuHx)-mediated PAH was induced according to previously published protocol (2, 3). Briefly, rats were subjected to a single subcutaneous injection of SU5416 (25 mg/kg, Tocris Bioscience) followed by a 4-week transient exposure to 10% hypoxia and 4 weeks of normoxic re-exposure. After randomization (treatment vs vehicle), animals were divided into two groups receiving clorgyline (SuHx+clor, n = 12, started with 10 mg/kg for the first time, followed by 2 mg/kg for the rest, Sigma-Aldrich) or vehicle (SuHx, n = 12, saline) by intraperitoneal injection four times from week 8 to week 10. At the end of the experiment, rats were anaesthetized for hemodynamic assessment via echocardiography and RV catheterization, after which rats were exsanguinated. Due to loss of rats, hemodynamic data was collected from 11 rats in SuHx group and 10 rats

in SuHx+clor group. Both lung and cardiac tissues were separated for further analysis. Data of healthy male Sprague-Dawley rats was collected from a previous published study of our group as control (ctrl, n = 7) (2).

PTB rat model of RV failure

Male Wistar rats (n = 36, Janvier Labs, Le Genest-Saint-Isle) underwent either surgery to place a clip around the pulmonary artery with a diameter of 0.6 mm (PTB) or sham surgery (n=8), according to previously published protocols (4). Four animals died shortly after the surgery, 1 sham animal died during baseline echo for unknown reasons. Temgesic was given for 3 days in drinking water after the surgery. Baseline echo was performed 2 weeks after the surgery. One day after the baseline echo, PTB animals were randomized into two groups receiving clorgyline (n = 12, started with 10 mg/kg for the first time, followed by 2 mg/kg, Sigma-Aldrich) or saline (n = 12) by intraperitoneal injection 3 times per week from week 2 to week 7. At the end of the experiment, rats were anaesthetized for hemodynamic assessment via echocardiography and RV catheterization, after which rats were exsanguinated. Cardiac tissues were separated for further analysis.

Echocardiography

All animals underwent echocardiographic assessments (For rats in SuHx study: Prosound SSD-4000 system equipped with a 13-MHz linear transducer UST-5542, Aloka, Tokyo, Japan; For rats in PTB study: A Vevo 2100 echocardiographic system with a 21-MHz linear array transducer, Visual Sonics, Canada) as published previously (4, 5), to measure RVEDD, RVESD, TAPSE, SV, heart rate, pulmonary artery acceleration time, and cycle length after the treatment. Analysis of echocardiography in the PTB study was done blinded.

RV catheterization

Animals were anaesthetized for open-chest RV catheterization (AD Instruments and Millar Instruments) as previously described (3). RVSP was determined from steady state measurement, as well as RV afterload (Ea). Pressure-volume loops after vena-cava occlusion were obtained and used to derive Ees and Eed.

Relative wall thickness of pulmonary arterioles

At the end of experiment, lungs were inflated with an 1% solution of low-melt-agarose and fixed in formalin (overnight) and embedded in paraffin. To determine the pulmonary vascular remodelling, paraffin embedded 5-µm-thick lung sections were stained with Elastic van Gieson to measure the relative wall thickness of pulmonary arterioles (PA), as well as the intimal and medial wall thickness separately, as described previously. Minimally thirty transversally pulmonary arterioles cut, with an outer diameter between 25 and 100 µm, randomly distributed over the lungs, were measured.

Right ventricular hypertrophy

To assess the extent of RV hypertrophy, the heart was removed and the RV free wall was separated from the LV and ventricular septum. Wet weights of the RV, free LV and septum were determined separately, and the ratio of RV weight to LV plus septum weight (RV/[LV+S]) was calculated for RV hypertrophy. For further analysis of RV hypertrophy, 5-µm-thick sections of frozen cardiac tissues (transversally cut) were stained with haematoxylin and eosin, and a mean cardiomyocyte CSA was assessed by measuring minimally thirty cardiomyocytes at the level of the nucleus, randomly distributed over the ventricles.

Right ventricular fibrosis

For analysis of RV fibrosis, 5-µm-thick sections of frozen cardiac tissues were stained with picrosirius red. Level of fibrosis was expressed as the percentage of tissue area positive for collagen compared to total area.

Immunofluorescence staining

Human and rat lung tissues were fixed and stained as previously described (3, 6). Briefly, 5-µm-thick lung paraffin sections were deparaffinized and rehydrated. Sections were boiled for 40 min in Vector® Antigen Unmasking Solution (Vector) using a pressure cooker. After blocking with goat serum 10% (ThermoFisher Scientific), sections were incubated overnight at 4°C with primary antibodies directed against MAO-A (1:50; ab126751, Abcam, Cambridge, UK), or PCNA antibody (1:100; sc-7907, Santa Cruz Biotechnology, Dallas, TX), or 8-OHdG (1:150; bs-1278R, Bioss Antibodies), co-stained with von willebrand factor (1:1000; ab8822, Abcam, Cambridge, UK), and alpha smooth muscle actin (1:1000; Sigma-Aldrich, St. Louis, MO). All sections were mounted with ProLong® Gold antifade reagent (Invitrogen) containing DAPI.

Immunofluorescence quantification

Images were acquired on a Marianas digital imaging microscopy workstation (Intelligent Imaging Innovations (3i), Denver, CO). SlideBook imaging analysis software (SlideBook 6, 3i) was used to semi-automatically quantify the images. Pulmonary vascular MAO-A and 8-OHdG mean relative fluorescence intensity was semi-automatically quantified and measured over twenty vessels. Proliferative cells were quantified by counting positive cells with a positive (PCNA) signal per vessel.

MAO-A activity

MAO-A activity was measured in 5 µm thick heart or lung cryosections by calibrated enzyme histochemistry, as described before (7). Briefly, sections were incubated in PBS containing 0.4 mM tetranitroblue tetrazolium chloride and 6.25 mM tryptamine hydrochloride at 37 °C in a stainless-steel box. Oxygen saturated with water vapor was gently flowing into the box during the incubation. The reaction was stopped in 10 mM HCl and the sections were mounted in glycerin gelatin. MAO-A activity is measured as the absorbance of formazan produced in the sections. This method is specific to the MAO-A isoform, as pretreatment with the MAO-A inhibitor clorgyline inhibits the activity completely (7) (and confirmed by us, not shown). Also, clorgyline is highly specific to MAO-A (8, 9).

ATPase activity

Reverse F_1F_O ATPase activity was estimated using enzyme histochemistry on 5 µm thick cryosections of the apical part of the RV as described (10, 11). F_1F_O was measured by precipitating P_i released from ATP as $Pb_3(PO_4)_2$ in the section when pump is operating in reverse mode. The precipitate is converted to PbS, which can be measured with a microdensitometer. The activity is proportional to the proton permeability of the inner membrane: maximum activity is obtained in the presence of DNP (positive control) whereas background ATPase activity is obtained in the presence of oligomycin. Increased proton permeability increases basal oxygen consumption and reduces ATP/O_2.

Shortly, serial cryosections were incubated either in the presence of oligomycin to determine background ATPase activity, 2,4-DNP, or normal incubation medium and all in the presence of ATP. By using 6.3 as theoretical maximal P/O_2 ratio, the actual P/O_2 ratio was estimated from the ratio of the actual and maximal F_1F_O ATPase activity, corrected for the background activity. This method is validated in heart muscle only (11), therefore we did not perform the staining in lung tissues.

Protein expression by western blot

Lung and RV tissue of the rats was homogenized in radioimmunoprecipitation assay (RIPA) buffer containing phosphatase and protease inhibitors (Sigma-Aldrich). The protein concentration was quantified by the Pierce 660 nm protein assay kit (Thermo Scientific, Rockford, USA). 20 μg protein was used to detect the expression of MAO-A (1:1000; ab126751; Abcam), PCNA (1:1000; sc-7907; Santa Cruz Biotechnology, Dallas, TX, USA), nitrotyrosine (1:2000; ab126751; Abcam), cleaved caspase-3 (1:1000; 9611; cell signaling Technology Inc. Beverly, MA, USA), CD45 (1:500; sc-53045; Santa Cruz Biotechnology, Dallas, TX, USA) with primary antibody incubation at 4°C overnight, followed by appropriate secondary antibody incubation. The protein amount was normalized by vinculin (1:500; sc-5573; Santa Cruz Biotechnology, Dallas, TX, USA) or GAPDH (1:50000; G9295; Sigma-Aldrich) as loading control.

Statistics

Statistical analyses were performed using Prism for Windows (GraphPad 8 Software). Normality of data was checked and either log-transformation or non-parametric test was performed if data was not normally distributed. Unpaired student's t-tests were used for comparisons between two groups. Multiple comparisons were assessed by one-way ANOVA, followed by Bonferroni's post-hoc test. Two-way ANOVA for repeated measurements followed by Sidak's post-hoc was used for repeated data of echocardiography analysis. Kruskal-wallis test followed by Dunn's multiple comparison test was used for data that was not normally distributed. p-values < 0.05 were considered significant. All statistical tests used two-sided tests of significance. Data are presented as mean ± SEM.

REFERENCES

1. Szulcek R, Happe CM, Rol N, Fontijn RD, Dickhoff C, Hartemink KJ, Grunberg K, Tu L, Timens W, Nossent GD, Paul MA, Leyen TA, Horrevoets AJ, de Man FS, Guignabert C, Yu PB, Vonk-Noordegraaf A, van Nieuw Amerongen GP, Bogaard HJ. Delayed Microvascular Shear Adaptation in Pulmonary Arterial Hypertension. Role of Platelet Endothelial Cell Adhesion Molecule-1 Cleavage. *Am J Respir Crit Care Med* 2016; 193: 1410-1420.
2. da Silva Goncalves Bos D, Van Der Bruggen CEE, Kurakula K, Sun XQ, Casali KR, Casali AG, Rol N, Szulcek R, Dos Remedios C, Guignabert C, Tu L, Dorfmuller P, Humbert M, Wijnker PJM, Kuster DWD, van der Velden J, Goumans MJ, Bogaard HJ, Vonk-Noordegraaf A, de Man FS, Handoko ML. Contribution of Impaired Parasympathetic Activity to Right Ventricular Dysfunction and Pulmonary Vascular Remodeling in Pulmonary Arterial Hypertension. *Circulation* 2018; 137: 910-924.
3. Kurakula K, Sun XQ, Happe C, da Silva Goncalves Bos D, Szulcek R, Schalij I, Wiesmeijer KC, Lodder K, Tu L, Guignabert C, de Vries CJM, de Man FS, Vonk Noordegraaf A, Ten Dijke P, Goumans MJ, Bogaard HJ. Prevention of progression of pulmonary hypertension by the Nur77 agonist 6-mercaptopurine: role of BMP signalling. *Eur Respir J* 2019; 54.
4. Andersen S, Axelsen JB, Ringgaard S, Nyengaard JR, Hyldebrandt JA, Bogaard HJ, de Man FS, Nielsen-Kudsk JE, Andersen A. Effects of combined angiotensin II receptor antagonism and neprilysin inhibition in experimental pulmonary hypertension and right ventricular failure. *Int J Cardiol* 2019; 293: 203-210.
5. de Raaf MA, Kroeze Y, Middelman A, de Man FS, de Jong H, Vonk-Noordegraaf A, de Korte C, Voelkel NF, Homberg J, Bogaard HJ. Serotonin transporter is not required for the development of severe pulmonary hypertension in the Sugen hypoxia rat model. *Am J Physiol Lung Cell Mol Physiol* 2015; 309: L1164-1173.
6. Duim SN, Kurakula K, Goumans MJ, Kruithof BP. Cardiac endothelial cells express Wilms' tumor-1: Wt1 expression in the developing, adult and infarcted heart. *Journal of molecular and cellular cardiology* 2015; 81: 127-135.
7. van Eif VW, Bogaards SJ, van der Laarse WJ. Intrinsic cardiac adrenergic (ICA) cell density and MAO-A activity in failing rat hearts. *J Muscle Res Cell Motil* 2014; 35: 47-53.
8. Geha RM, Rebrin I, Chen K, Shih JC. Substrate and inhibitor specificities for human monoamine oxidase A and B are influenced by a single amino acid. *J Biol Chem* 2001; 276: 9877-9882.
9. Ma J, Yoshimura M, Yamashita E, Nakagawa A, Ito A, Tsukihara T. Structure of rat monoamine oxidase A and its specific recognitions for substrates and inhibitors. *J Mol Biol* 2004; 338: 103-114.
10. Meijer AEFH, Vloedman AHT. The histochemical characterization of the coupling state of skeletal muscle mitochondria. *Histochemistry* 1980; 69: 217-232.
11. Peters EL, Comerford D, Vaz FM, van der Laarse WJ. Meijer and Vloedman's histochemical demonstration of mitochondrial coupling obeys Lambert–Beer's law in the myocardium. *Histochemistry and Cell Biology* 2019; 151: 85-90.

Part V

Summary and general discussion

CHAPTER 10

Summary and further perspectives

SUMMARY AND FURTHER PERSPECTIVES

Pulmonary hypertension (PH) is a disease characterized by an increased blood pressure in the pulmonary vascular system, ultimately leading to right ventricular failure (RVF) and premature death.[1] Pulmonary arterial hypertension (PAH), PH group 1, is defined by an increase in mean pulmonary artery pressure (mPAP) ≥ 20 mmHg, pulmonary wedge pressure ≤ 15 mmHg, and pulmonary vascular resistance > 3 wood units measured by right heart catheterization.[2, 3]

This thesis aimed to investigate novel promising treatment strategies for PAH and PAH induced RVF, based on multiple pathological mechanisms underlying the disease. I investigated drugs impacting on the bone morphogenetic protein type 2 receptor (BMPR2) signaling pathway (***Chapter 2-4***), on growth factor signaling (***Chapter 5***), on histone acetylation (***Chapter 6***), as well as several therapeutic strategies specifically targeting the RV (***Chapter 7-9***).

Table 1. Summary of the PAH novel treatment strategies studied in this thesis.

novel treatment	pathway	pulmonary vasculature		RV
		intima layer	media layer	
6-MP	BMPR2	√	√	×
MnTBAP	BMPR2	√	√	NS
nintedanib	growth factors	×	×	√
quisinostat	HDACs	√	×	×
DCA	PDKs	NS	NS	√
clorgyline	MAO-A	√	×	×

6-MP: 6-mercaptopurine; MnTBAP: manganese (III) tetrakis (4-benzoic acid) porphyrin; DCA: dicholoroacetate; BMPR2: bone morphogenetic protein type 2 receptor; HDACs: histone deacetylases; PDKs: pyruvate dehydrogenase kinases; MAO-A: monoamine oxidase A. √: effective; ×: without any effect; NS: not studied in this thesis.

BMPR2 pathway in PAH

Impaired BMPR2 signaling not only occurs in hereditary PAH (hPAH) patients, but also in non-hereditary forms of PAH.[4, 5] Restoring the BMPR2 signaling pathway could be of interest and as new treatment options are emerging, it is of utmost importance that the PAH animal models reflect the pathology in human PAH. Therefore, in ***Chapter 2***, BMPR2 expression and downstream phosphorylation of Smads and downstream targets were evaluated in two commonly used PAH animal models and were compared with

human PAH. Whole lung protein expression was assessed by western blot analysis and localized vascular expression was assessed by immunofluorescence staining. We found that monocrotaline (MCT) and Sugen+hypoxia (SuHx) induced PAH rat models express altered BMPR2, but in a different way compared to human PAH. However, the protein expression of the downstream signal transduction via Smads was similarly affected in both PAH models and PAH patients. Future studies should be performed to reveal the different regulatory mechanisms underlying BMP/Smad signaling between PAH animal models and PAH patients, including the imbalance between BMPR2 and TGF-β signaling pathway.

In ***Chapter 3*** and ***Chapter 4***, we used 6-mercaptopurine (6-MP) and Manganese (III) tetrakis (4-benzoic acid) porphyrin (MnTBAP) to modulate BMPR2 signaling and treat animals with experimental PAH. As one of the oldest immunosuppressive drugs, 6-MP does not only affect inflammatory cells by hampering purine synthesis, but also regulates a wide range of biological processes by activating the orphan nuclear receptor Nur77.[6] In ***Chapter 3***, we found that Nur77 expression is down-regulated in lungs and pulmonary microvascular endothelial cells (MVECs) of PAH patients, and involved in the pathogenesis of PAH by regulating EC proliferation, inflammation and BMPR2/Smad signaling. Pharmacological activation of Nur77 with 6-MP prevented and reversed pulmonary vascular remodeling in SuHx PAH rats by reducing proliferation, inflammation and by up-regulating BMPR2/Smad signaling in the lungs.

MnTBAP, a synthetic metalloporphyrin with antioxidant and anti-inflammatory effects,[7-9] was shown to inhibit the turn-over of BMPR2 in human umbilical vein endothelial cells.[10] In ***Chapter 4***, we found that MnTBAP can increase BMPR2 levels in MVECs isolated from PAH patients, and that chronic treatment with MnTBAP can reduce RV afterload and pulmonary vascular remodeling in SuHx PAH rats, resulting in improved cardiac function. This study provided evidence for the promising role of superoxide dismutase mimetics as PAH treatment options.

Taken together, Chapters 3 and 4 highlight the benefits of enhancing/increasing BMPR2 signaling to treat PAH. While MnTBAP has not been approved to be used in humans, 6-MP is one of the oldest immunosuppressive drugs approved to treat various auto immune and chronic inflammatory diseases such as inflammatory bowel disease, rheumatoid arthritis, hematologic malignancies, chronic active hepatitis, and lupus nephritis.[11-13] As RV function is an important concern in the field of PAH treatment,

our group further confirmed the safety of 6-MP treatment on the RV, by using a RV dysfunction rat model induced by PAB.[14] Based on these findings, our group initiated an open-label, proof-of-concept, single-center study of 6-MP treatment in 15 PAH patients to evaluate the efficacy and safety. In accordance with the findings in ***Chapter 3***, this proof-of-concept study showed that 6-MP treatment decreased pulmonary vascular resistance (PVR) in PAH patients coinciding with an increased *BMPR2* mRNA expression in peripheral blood mononuclear cells (PBMCs).[15] However, the magnitude of PVR reduction was relatively small, leading to no improvement in New York Heart Association (NYHA) functional class, 6-minute-walk distance (6MWD) or N-terminal pro-brain natriuretic peptide (NT-proBNP) concentrations. More importantly, the dosing schemes of 6-MP used in this study were found to have an unfavorable risk/benefit ratio in PAH patients, as frequency and severity of side effects were higher than reported and expected.[15] Therefore, future studies are needed to improve the dosing schemes of 6-MP treatment or evaluate other thiopurine analogs in PAH patients.

Moreover, future research should address to what extent 6-MP and MnTBAP have an add on effect in patients already treated with other PAH drugs. It is also needed to assess the effects of BMPR2 modulating therapies on RV function. BMPR2 signaling plays a role in the RV and PAH patients with BMPR2 mutation have a diminished RV function compared to PAH patients carrying the wild-type BMPR2 gene.[16] Moreover, other compounds/metabolites or other delivery methods may achieve similar or even better effects with lower toxicity.

Other promising treatment targets in PAH

Dysregulated signaling of growth factors, particularly platelet derived growth factor (PDGF), fibroblast growth factor (FGF), vascular endothelial growth factor (VEGF), and TGF-β, contributes to remodeling observed in PAH in both the pulmonary vasculature and the RV.[17, 18] In ***Chapter 5***, we tested the effects in experimental PAH of nintedanib, a drug which targets PDGF-, FGF-, and VEGF-mediated proliferation in pulmonary fibroblasts and TGF-β-mediated transformation of fibroblasts to myofibroblasts.[19-21] We found that nintedanib inhibited proliferation of MVECs from normal subjects but not from PAH patients. Nintedanib also failed to reduce RV afterload or pulmonary vascular remodeling in SuHx PAH rats. Interestingly, despite lack of effects on the lungs, nintedanib treatment benefited the RV of PAH rats by reducing RV hypertrophy and collagen content. Collectively, nintedanib has favorable effects on the RV but does not reverse pulmonary vascular remodeling in PAH. As an approved treatment

of idiopathic pulmonary fibrosis (IPF), nintedanib is worth to be further evaluated by future studies on associated PH in patients with IPF.

Histone deacetylases (HDACs) are key enzymes in histone modification and by removing acetyl groups HDACs regulate key cellular processes including proliferation, apoptosis and inflammation.[22, 23] Abnormal HDAC expression and activity have been shown to play a role in PAH, however, the role of HDAC inhibitors as novel therapeutic options for PAH remains unpredictable. In ***Chapter 6***, we assessed the effects of quisinostat on experimental PAH. Quisinostat is a novel second generation HDAC inhibitor with a boosted pharmacodynamic response pattern and enhanced HDAC inhibitory efficacy.[24] While increased HDAC1 expression was found in MVECs isolated from PAH patients, quisinostat reduced proliferation and inflammation in these cells by inhibiting the activity of HDACs. Chronic treatment with quisinostat reduced intima layer remodeling in SuHx rats and in rats with PAH induced by MCT and increased shunt flow. Quisinostat had no effects on the RV of a RVF rat model induced by pulmonary artery banding (PAB). Taken together, the treatment effects of quisinostat are limited to the pulmonary vasculature, without a danger of cardiotoxicity.

Promising treatment strategies targeting the RV

Although the initial insult in PAH involves the pulmonary vasculature, RVF is the most important determinant of mortality in patients with PAH.[25] Many questions, however, regarding the mechanisms underlying RVF remain unclear. In ***Chapter 7***, we reviewed the role of cardiac inflammation in RVF and the possible therapeutic strategies for RVF by reducing inflammation. Consistent with many other types of heart failure, cardiac inflammation, triggered by systemic and local stressors, has been shown in RVF patients as well as in RVF animal models. RV inflammation likely contributes to impaired RV contractility, maladaptive remodeling and a vicious circle between RV and pulmonary vascular injury. Although the potential to improve RV function through anti-inflammatory therapy has not been tested, this approach has been applied clinically in left ventricular failure patients, with variable success. Because inflammation plays a dual role in the development of both pulmonary vascular pathology and RVF, anti-inflammatory therapies may have a potential double benefit in patients with PAH and associated RVF.

The survival of PAH patients is determined by the condition of the RV.[26] Therefore, the goal of translational research in PAH is to identify drugs that reverse pulmonary

vascular remodeling and are beneficial or at least non-toxic to the RV. In ***Chapter 8***, we assessed the effects of dichloroacetate (DCA) on RV myocardial apoptosis in the MCT rat model. As an inhibitor of pyruvate dehydrogenase kinase (PDK), DCA has been shown as a promising new therapy for RV failure, while studies on DCA and apoptosis have generated contradicting results. We found that DCA treatment can benefit the RV not only by increasing oxidative metabolism, but also by reducing RV myocardial apoptosis and restoring mitochondrial function. These findings are important, because they show that a fear for increased RV apoptosis with DCA is unnecessary, as DCA promotes PASMC apoptosis in PAH. These findings support DCA as a promising treatment for PAH in the clinic. Though we only evaluated the effect of DCA on the RV in this thesis, it was shown by previous studies that DCA can reverse pulmonary vascular remodeling in PAH rat models.[27, 28] Based on the pre-clinical findings, an open labeled, proof-of-concept, dose-finding clinical trial with DCA treatment was conducted in PAH patients. 4-month treatment with DCA reduced mPAP, pulmonary vascular resistance and improved functional capacity, but with a range of individual responses.[29] Interestingly, lack of clinical response is associated with the presence of functional variants of *SIRT3* and *UCP2*, which can cause PDK-independent mitochondrial suppression.[29] Therefore, future studies are needed to identify genetic variants and other factors that may induce PDK-independent mitochondrial dysfunction. Consistently future clinical trials are required to enroll PAH patients based on related assessments to promote DCA as a novel precision medicine for PAH.

In ***Chapter 9***, we aimed to study the role of monoamine oxidase A (MAO-A) in pulmonary vascular remodeling and RV dysfunction in PAH. As a mitochondrial enzyme, MAO-A is a major source of reactive oxygen species (ROS) with pathophysiological relevance in multiple cardiovascular diseases.[30, 31] We found increased MAO-A expression in the pulmonary vasculature of PAH patients and SuHx PAH rats, as well as in the RV of SuHx- and PAB-induced RVF rats. Pharmacological inhibition of MAO-A with clorgyline reduced RV afterload and pulmonary vascular remodeling in SuHx rats by reducing ROS. However, it had no independent effects on the RV of the PAB rat model, while it benefited the RV of SuHx rats by affecting the lung. Collectively, MAO-A seems to be involved in the pathophysiology of PAH. Based on this finding, it is worth for future search to test clinically approved new generation MAO-A inhibitors in combination with other PAH drugs to promote the direct translation to the clinic.

Novel promising treatment strategies for PAH

In this thesis, the effects of six novel treatment strategies were assessed on experimentally induced PAH: 6-MP, MnTBAP, nintedanib, quisinostat, DCA and clorgyline, as described in ***Table 1.*** Among the six novel treatments, 6-MP, MnTBAP, quisinostat and clorgyline were found to reduce RV afterload and reverse pulmonary vascular remodeling in rat models with established PAH. Compared to quisinostat and clorgyline treatment, which can only reverse remodeling in the intima layer, 6-MP and MnTBAP were shown to normalize RV afterload at a better level with reversed pulmonary vascular remodeling in both intima and media layers. Consistent with the reduced RV afterload, 6-MP and MnTBAP were shown to have more benefits to the RV compared to quisinostat and clogyline. Taken together, among all the novel treatments described in this thesis, 6-MP and MnTBAP can be considered as promising therapeutic options for PAH by modulation of BMPR2 pathway, which can reverse pulmonary vascular remodeling and thus benefit the RV.

This thesis represents a drug pipeline for future treatments of PAH, via modulation of multiple pathological mechanisms. Based on previous findings, we chose these five pathways as promising treatment targets for PAH, to see the potential of each modulation. Taken together, our findings emphasized the role of the BMPR2 pathway as a promising therapeutic target and as a focus for future clinical trials. BMPR2 signaling has a protective role in the vascular wall by promoting the survival of PAECs, inhibiting PASMCs proliferation and triggering anti-inflammatory responses.[32-34] Consistent with our findings in Chapter 3 and 4, other studies have also shown that modulation of the BMPR2 pathway at multiple levels can benefit experimental PAH, including genetic-based therapies, transcriptional and translational regulation, protein activity and SMAD downstream signaling modulation.[35] Upregulating BMPR2 by adenoviral BMPR2 gene delivery to the pulmonary vascular endothelium is beneficial to experimental PAH.[36] As a ligand of BMPR2, BMP9 was found to prevent apoptosis and enhance the integrity of ECs from PAH patients, and therapeutic BMP9 delivery can prevent and reverse PAH in animal models.[37] Treatment with FK506 and chloroquine have also been shown to reverse PAH in animal models by increasing BMPR2 signaling.[38, 39] Taken together, our findings and other preclinical evidence support the concept that modulation of BMPR2 signaling pathway could provide promising therapeutic options for PAH.

However, there are still multiple challenges for these BMPR2 targeted strategies to be used to the benefit of PAH patients. A growing number of treatment strategies targeting BMPR2 signaling are currently being evaluated in clinical trials. Compared to the promising findings in experimental PAH, most BMPR2 targeted strategies have lacked efficacy in clinical trials and were associated with a considerable risk of side effects. Treatment with low-dose FK506 was tested in three patients with end-stage PAH for 12 months improved NYHA functional class, 6MWD and NT-proBNP, and increased BMPR2 expression in PBMCs.[40] Based on this, a further randomized, double-blind, single-center phase IIa trial with low-dose FK506 was performed on 20 PAH patients with NYHA functional class II/III. While low-level FK506 was generally well tolerated, it had no effect on 6MWD, NT-proBNP or RV function.[41] The clinical trial with 6-MP performed by our group shows promising effects on PVR and *BMPR2* mRNA level in PBMCs. However, the magnitude of PVR reduction was relatively small, leading to no improvement in NYHA functional class, 6MWD or NT-proBNP concentrations.[15] These clinical findings suggest the necessity of a more personalized approach for PAH patients, which takes into account the types of gene mutations, BMPR2 levels, inflammation, cardiac function, proliferation and infections. For example, as a recent study revealed that *GDF2* mutations result in reduced BMP9 and loss of function, it could be promising to initiate a BMP9 clinical trial specifically for PAH patients with *GDF2* mutations.[42] Ataluren, a drug that induces ribosomal read through of nonsense mutations, was found to restore BMPR2 signaling *in vitro,* which may offer the possibility of personalized therapy for the subset of PAH patients with this type of mutation.[43-45] Moreover, it has to be noted in the clinical trial with FK506, that despite the overall lack of improvement after FK506 treatment, some patients responded with a pronounced increase in BMPR2 expression as well as improvements in 6MWD and cardiac function. This suggests that BMPR2 levels at baseline may provide a promising standard to select PAH subgroups to receive BMPR2 targeted treatments.[41] Because 6-MP and FK506 are immunosuppressive drugs, it could be promising to enroll PAH patients based on baseline inflammatory levels for further clinical trials. Interestingly, as a recent study revealed that radioligand 3′-deoxy-3′-[18F]-fluorothymidine positron emission tomography imaging can be used to report hyper-proliferation in PAH patients,[46] it is possible for future clinical trials to select PAH patients with hyper-proliferation, and thus develop a precision medicine approach with BMPR2 targeted treatments. In addition, newly developed preclinical methods, such as lung or vessel on a chip, .[47] could further improve the pipeline of BMPR2 modifying compounds.

Besides lack of efficacy, side effects of the BMPR2 targeted drugs on PAH patients can also bring challenges for their use in the clinic. Recent studies revealed that BMP9 could harm endothelium by inducing aberrant endothelial-to-mesenchymal transition and calcification in the presence of an inflammatory stimulus.[48, 49] Moreover, as mentioned above, the clinical trial with 6-MP treatment reported frequent and severe side effects on PAH patients, although the dosage of 6-MP used in this study was generally well tolerated by patients with inflammatory bowel disease.[15, 50] Therefore, despite the promising findings of 6-MP on decreased PVR and increased *BMPR2* mRNA level in PBMCs, its role as an add-on treatment for PAH patients is still unfavorable. Moreover, while BMPR2 signaling exhibits multiple functions in organ regeneration and tissue homeostasis, most of the BMPR2 targeted strategies are systemically applied and not specifically acting on pulmonary vascular cells, which may rise the risk for long-term use. Besides improvements in dosing schemes, the development of lung-specific delivery methods for BMPR2 targeted drugs would be helpful to achieve efficient pulmonary efficacy at low drug concentrations, such as the inhaled formulation of iloprost given by ProDose™ and I-neb AAD nebulizers.[51]

Limitations

The conclusions outlined in this thesis are partly based on the use of a limited number of PAH animal models. The treatment effects of 6-MP, nintedanib, MAO-A inhibitor and MnTBAP on pulmonary vasculatures were only confirmed in the SuHx rat model. Confirmation of these findings in additional PAH animal models would be helpful to further study mechanisms of effect of these different novel treatments. Therapeutics targeting the BMPR2 signaling pathway are preferentially investigated in multiple animal models, as both the SuHx and the MCT rat model recapitulate only parts of BMPR2 signaling in human situation, as shown in Chapter 2. Moreover, direct effects of some treatments on the RV are still uncertain, since we didn't include the PAB model in all studies. My thesis is focused on treatment effects on pulmonary ECs, because ECs play a crucial role in PAH through hyperproliferation and secretion of factors such as inflammatory cytokines and growth factors, which in turn affect PASMCs and fibroblasts. Future studies are needed to reveal the direct effect of the novel treatments on other cell types involved in PAH, such as PASMCs, pericytes and fibroblasts. Finally, no single or combination of animal models can fully recapitulate PAH in humans. Innovative preclinical methods, such as lung or vessel on a chip and 3D engineered heart tissue of the RV, may further improve the evaluation of novel drugs.

Some treatment options tested in this thesis, particularly MnTBAP and clorgyline, are not directly available in the clinic because of potential side-effects. While the studies in this thesis were justified to show proof of principle, it is still worthwhile to further test the related treatment options working through similar mechanisms. An additional factor limiting the clinical translation of my findings is the fact that full dose ranges of the different drugs were not studied. In Chapter 3, we studied the effects on SuHx rats of 6-MP in doses of 1, 7,5 and 15 mg/kg. Although 1 mg/kg 6-MP prevented the development of PAH, it failed to reverse pulmonary vascular remodeling in rats with established PAH. While 15 mg/kg 6-MP suppressed bone marrow function, 7,5 mg/kg 6-MP partly reversed PAH without obvious side effects. In other chapters, doses were based on prior studies in different animal models and full dose finding was not done. Finally, to promote the direct translation to the clinic, it is desirable to test novel treatment options in rats already on treatment with a combination of approved PAH drugs.

Summary and Conclusion

This thesis investigated novel promising treatment strategies for PAH and PAH induced RV failure, based on multiple pathological mechanisms underlying the disease, including BMPR2 signaling, growth factor, HDACs, inflammation, oxidative stress and mitochondrial metabolism. Taken together, this thesis highlighted the promising role of restoring BMPR2 signaling pathway in PAH treatment by reversing pulmonary vascular remodeling and thus benefiting the RV, as well as the benefits of inhibiting HDACs and MAO-A to the lung. Moreover, this thesis demonstrated the benefits of inhibiting growth factors, inflammation and apoptosis to the RV. However, there are still multiple challenges for these novel promising strategies to be used to the benefit of PAH patients, due to lack of efficacy in clinical trials and a considerable risk of side effects. Therefore, future clinical studies are needed to develop a more personalized approach for PAH patients, improve dosing schemes and develop lung-specific delivery methods.

REFERENCES

1. Vonk Noordegraaf A, Groeneveldt JA and Bogaard HJ. Pulmonary hypertension. *Eur Respir Rev*. 2016;25:4-11.
2. Condon DF, Nickel NP, Anderson R, Mirza S and de Jesus Perez VA. The 6th World Symposium on Pulmonary Hypertension: what's old is new. *F1000Res*. 2019;8.
3. Simonneau G, Montani D, Celermajer DS, Denton CP, Gatzoulis MA, Krowka M, Williams PG and Souza R. Haemodynamic definitions and updated clinical classification of pulmonary hypertension. *Eur Respir J*. 2019;53.
4. Yang J, Davies RJ, Southwood M, Long L, Yang X, Sobolewski A, Upton PD, Trembath RC and Morrell NW. Mutations in bone morphogenetic protein type II receptor cause dysregulation of Id gene expression in pulmonary artery smooth muscle cells: implications for familial pulmonary arterial hypertension. *Circ Res*. 2008;102:1212-21.
5. Atkinson C, Stewart S, Upton PD, Machado R, Thomson JR, Trembath RC and Morrell NW. Primary pulmonary hypertension is associated with reduced pulmonary vascular expression of type II bone morphogenetic protein receptor. *Circulation*. 2002;105:1672-8.
6. Wansa KD, Harris JM, Yan G, Ordentlich P and Muscat GE. The AF-1 domain of the orphan nuclear receptor NOR-1 mediates trans-activation, coactivator recruitment, and activation by the purine anti-metabolite 6-mercaptopurine. *The Journal of biological chemistry*. 2003;278:24776-90.
7. Suresh MV, Yu B, Lakshminrusimha S, Machado-Aranda D, Talarico N, Zeng L, Davidson BA, Pennathur S and Raghavendran K. The protective role of MnTBAP in oxidant-mediated injury and inflammation in a rat model of lung contusion. *Surgery*. 2013;154:980-90.
8. Bi X, Wang J, Liu Y, Wang Y and Ding W. MnTBAP treatment ameliorates aldosterone-induced renal injury by regulating mitochondrial dysfunction and NLRP3 inflammasome signalling. *Am J Transl Res*. 2018;10:3504-3513.
9. Batinic-Haberle I, Cuzzocrea S, Reboucas JS, Ferrer-Sueta G, Mazzon E, Di Paola R, Radi R, Spasojevic I, Benov L and Salvemini D. Pure MnTBAP selectively scavenges peroxynitrite over superoxide: comparison of pure and commercial MnTBAP samples to MnTE-2-PyP in two models of oxidative stress injury, an SOD-specific Escherichia coli model and carrageenan-induced pleurisy. *Free Radic Biol Med*. 2009;46:192-201.
10. Zhou Q, Einert M, Schmitt H, Wang Z, Pankratz F, Olivier CB, Bode C, Liao JK and Moser M. MnTBAP increases BMPR-II expression in endothelial cells and attenuates vascular inflammation. *Vascul Pharmacol*. 2016;84:67-73.
11. Srinivasan R and Lichtenstein GR. Recent developments in the pharmacological treatment of Crohn's disease. *Expert opinion on investigational drugs*. 2004;13:373-91.
12. Kumar SS, Athimoolam S and Sridhar B. XRD, vibrational spectra and quantum chemical studies of an anticancer drug: 6-Mercaptopurine. *Spectrochim Acta A Mol Biomol Spectrosc*. 2015;146:204-13.
13. Tidd DM and Paterson AR. A biochemical mechanism for the delayed cytotoxic reaction of 6-mercaptopurine. *Cancer research*. 1974;34:738-46.

14. Axelsen JB, Andersen S, Sun XQ, Ringgaard S, Hyldebrandt JA, Kurakula K, Goumans MJ, de Man FS, Nielsen-Kudsk JE, Bogaard HJ and Andersen A. Effects of 6-mercaptopurine in pressure overload induced right heart failure. *PLoS One*. 2019;14:e0225122.
15. Botros L, Szulcek R, Jansen SMA, Kurakula K, Goumans MTH, van Kuilenburg ABP, Vonk Noordegraaf A, de Man FS, Aman J and Bogaard HJ. The Effects of Mercaptopurine on Pulmonary Vascular Resistance and BMPR2 Expression in Pulmonary Arterial Hypertension. *Am J Respir Crit Care Med*. 2020;202:296-299.
16. van der Bruggen CE, Happé CM, Dorfmüller P, Trip P, Spruijt OA, Rol N, Hoevenaars FP, Houweling AC, Girerd B, Marcus JT, Mercier O, Humbert M, Handoko ML, van der Velden J, Vonk Noordegraaf A, Bogaard HJ, Goumans MJ and de Man FS. Bone Morphogenetic Protein Receptor Type 2 Mutation in Pulmonary Arterial Hypertension: A View on the Right Ventricle. *Circulation*. 2016;133:1747-60.
17. Hassoun PM, Mouthon L, Barberà JA, Eddahibi S, Flores SC, Grimminger F, Jones PL, Maitland ML, Michelakis ED, Morrell NW, Newman JH, Rabinovitch M, Schermuly R, Stenmark KR, Voelkel NF, Yuan JX and Humbert M. Inflammation, growth factors, and pulmonary vascular remodeling. *J Am Coll Cardiol*. 2009;54:S10-9.
18. Godinas L, Guignabert C, Seferian A, Perros F, Bergot E, Sibille Y, Humbert M and Montani D. Tyrosine kinase inhibitors in pulmonary arterial hypertension: a double-edge sword? *Semin Respir Crit Care Med*. 2013;34:714-24.
19. Wollin L, Wex E, Pautsch A, Schnapp G, Hostettler KE, Stowasser S and Kolb M. Mode of action of nintedanib in the treatment of idiopathic pulmonary fibrosis. *Eur Respir J*. 2015;45:1434-45.
20. Bendstrup E, Wuyts W, Alfaro T, Chaudhuri N, Cornelissen R, Kreuter M, Melgaard Nielsen K, Münster AB, Myllärniemi M, Ravaglia C, Vanuytsel T and Wijsenbeek M. Nintedanib in Idiopathic Pulmonary Fibrosis: Practical Management Recommendations for Potential Adverse Events. *Respiration; international review of thoracic diseases*. 2019;97:173-184.
21. Wollin L, Maillet I, Quesniaux V, Holweg A and Ryffel B. Antifibrotic and anti-inflammatory activity of the tyrosine kinase inhibitor nintedanib in experimental models of lung fibrosis. *The Journal of pharmacology and experimental therapeutics*. 2014;349:209-20.
22. Gatla HR, Muniraj N, Thevkar P, Yavvari S, Sukhavasi S and Makena MR. Regulation of Chemokines and Cytokines by Histone Deacetylases and an Update on Histone Decetylase Inhibitors in Human Diseases. *International journal of molecular sciences*. 2019;20.
23. Glaser KB, Li J, Staver MJ, Wei RQ, Albert DH and Davidsen SK. Role of class I and class II histone deacetylases in carcinoma cells using siRNA. *Biochemical and biophysical research communications*. 2003;310:529-36.
24. Arts J, King P, Marien A, Floren W, Belien A, Janssen L, Pilatte I, Roux B, Decrane L, Gilissen R, Hickson I, Vreys V, Cox E, Bol K, Talloen W, Goris I, Andries L, Du Jardin M, Janicot M, Page M, van Emelen K and Angibaud P. JNJ-26481585, a novel "second-generation" oral histone deacetylase inhibitor, shows broad-spectrum preclinical antitumoral activity. *Clin Cancer Res*. 2009;15:6841-51.
25. van Wolferen SA, Marcus JT, Boonstra A, Marques KM, Bronzwaer JG, Spreeuwenberg MD, Postmus PE and Vonk-Noordegraaf A. Prognostic value of right ventricular mass, volume, and function in idiopathic pulmonary arterial hypertension. *European heart journal*. 2007;28:1250-7.

26. Mauritz GJ, Kind T, Marcus JT, Bogaard HJ, van de Veerdonk M, Postmus PE, Boonstra A, Westerhof N and Vonk-Noordegraaf A. Progressive changes in right ventricular geometric shortening and long-term survival in pulmonary arterial hypertension. *Chest*. 2012;141:935-943.
27. Piao L, Sidhu VK, Fang YH, Ryan JJ, Parikh KS, Hong Z, Toth PT, Morrow E, Kutty S, Lopaschuk GD and Archer SL. FOXO1-mediated upregulation of pyruvate dehydrogenase kinase-4 (PDK4) decreases glucose oxidation and impairs right ventricular function in pulmonary hypertension: therapeutic benefits of dichloroacetate. *Journal of molecular medicine (Berlin, Germany)*. 2013;91:333-46.
28. McMurtry MS, Bonnet S, Wu X, Dyck JR, Haromy A, Hashimoto K and Michelakis ED. Dichloroacetate prevents and reverses pulmonary hypertension by inducing pulmonary artery smooth muscle cell apoptosis. *Circ Res*. 2004;95:830-40.
29. Michelakis ED, Gurtu V, Webster L, Barnes G, Watson G, Howard L, Cupitt J, Paterson I, Thompson RB, Chow K, O'Regan DP, Zhao L, Wharton J, Kiely DG, Kinnaird A, Boukouris AE, White C, Nagendran J, Freed DH, Wort SJ, Gibbs JSR and Wilkins MR. Inhibition of pyruvate dehydrogenase kinase improves pulmonary arterial hypertension in genetically susceptible patients. *Sci Transl Med*. 2017;9.
30. Kaludercic N, Mialet-Perez J, Paolocci N, Parini A and Di Lisa F. Monoamine oxidases as sources of oxidants in the heart. *J Mol Cell Cardiol*. 2014;73:34-42.
31. Deshwal S, Di Sante M, Di Lisa F and Kaludercic N. Emerging role of monoamine oxidase as a therapeutic target for cardiovascular disease. *Curr Opin Pharmacol*. 2017;33:64-69.
32. Soon E, Crosby A, Southwood M, Yang P, Tajsic T, Toshner M, Appleby S, Shanahan CM, Bloch KD, Pepke-Zaba J, Upton P and Morrell NW. Bone morphogenetic protein receptor type II deficiency and increased inflammatory cytokine production. A gateway to pulmonary arterial hypertension. *Am J Respir Crit Care Med*. 2015;192:859-72.
33. de Jesus Perez VA, Alastalo TP, Wu JC, Axelrod JD, Cooke JP, Amieva M and Rabinovitch M. Bone morphogenetic protein 2 induces pulmonary angiogenesis via Wnt-beta-catenin and Wnt-RhoA-Rac1 pathways. *J Cell Biol*. 2009;184:83-99.
34. Hansmann G, de Jesus Perez VA, Alastalo TP, Alvira CM, Guignabert C, Bekker JM, Schellong S, Urashima T, Wang L, Morrell NW and Rabinovitch M. An antiproliferative BMP-2/PPARgamma/apoE axis in human and murine SMCs and its role in pulmonary hypertension. *J Clin Invest*. 2008;118:1846-57.
35. Orriols M, Gomez-Puerto MC and Ten Dijke P. BMP type II receptor as a therapeutic target in pulmonary arterial hypertension. *Cell Mol Life Sci*. 2017;74:2979-2995.
36. Reynolds AM, Holmes MD, Danilov SM and Reynolds PN. Targeted gene delivery of BMPR2 attenuates pulmonary hypertension. *Eur Respir J*. 2012;39:329-43.
37. Long L, Ormiston ML, Yang X, Southwood M, Graf S, Machado RD, Mueller M, Kinzel B, Yung LM, Wilkinson JM, Moore SD, Drake KM, Aldred MA, Yu PB, Upton PD and Morrell NW. Selective enhancement of endothelial BMPR-II with BMP9 reverses pulmonary arterial hypertension. *Nature medicine*. 2015;21:777-85.

38. Spiekerkoetter E, Tian X, Cai J, Hopper RK, Sudheendra D, Li CG, El-Bizri N, Sawada H, Haghighat R, Chan R, Haghighat L, de Jesus Perez V, Wang L, Reddy S, Zhao M, Bernstein D, Solow-Cordero DE, Beachy PA, Wandless TJ, Ten Dijke P and Rabinovitch M. FK506 activates BMPR2, rescues endothelial dysfunction, and reverses pulmonary hypertension. *J Clin Invest*. 2013;123:3600-13.
39. Long L, Yang X, Southwood M, Lu J, Marciniak SJ, Dunmore BJ and Morrell NW. Chloroquine prevents progression of experimental pulmonary hypertension via inhibition of autophagy and lysosomal bone morphogenetic protein type II receptor degradation. *Circ Res*. 2013;112:1159-70.
40. Spiekerkoetter E, Sung YK, Sudheendra D, Bill M, Aldred MA, van de Veerdonk MC, Vonk Noordegraaf A, Long-Boyle J, Dash R, Yang PC, Lawrie A, Swift AJ, Rabinovitch M and Zamanian RT. Low-Dose FK506 (Tacrolimus) in End-Stage Pulmonary Arterial Hypertension. *Am J Respir Crit Care Med*. 2015;192:254-7.
41. Spiekerkoetter E, Sung YK, Sudheendra D, Scott V, Del Rosario P, Bill M, Haddad F, Long-Boyle J, Hedlin H and Zamanian RT. Randomised placebo-controlled safety and tolerability trial of FK506 (tacrolimus) for pulmonary arterial hypertension. *Eur Respir J*. 2017;50.
42. Hodgson J, Swietlik EM, Salmon RM, Hadinnapola C, Nikolic I, Wharton J, Guo J, Liley J, Haimel M, Bleda M, Southgate L, Machado RD, Martin JM, Treacy CM, Yates K, Daugherty LC, Shamardina O, Whitehorn D, Holden S, Bogaard HJ, Church C, Coghlan G, Condliffe R, Corris PA, Danesino C, Eyries M, Gall H, Ghio S, Ghofrani HA, Gibbs JSR, Girerd B, Houweling AC, Howard L, Humbert M, Kiely DG, Kovacs G, Lawrie A, MacKenzie Ross RV, Moledina S, Montani D, Olschewski A, Olschewski H, Ouwehand WH, Peacock AJ, Pepke-Zaba J, Prokopenko I, Rhodes CJ, Scelsi L, Seeger W, Soubrier F, Suntharalingam J, Toshner MR, Trembath RC, Vonk Noordegraaf A, Wort SJ, Wilkins MR, Yu PB, Li W, Graf S, Upton PD and Morrell NW. Characterization of GDF2 Mutations and Levels of BMP9 and BMP10 in Pulmonary Arterial Hypertension. *Am J Respir Crit Care Med*. 2020;201:575-585.
43. Drake KM, Dunmore BJ, McNelly LN, Morrell NW and Aldred MA. Correction of nonsense BMPR2 and SMAD9 mutations by ataluren in pulmonary arterial hypertension. *American journal of respiratory cell and molecular biology*. 2013;49:403-9.
44. Austin ED, Phillips JA, Cogan JD, Hamid R, Yu C, Stanton KC, Phillips CA, Wheeler LA, Robbins IM, Newman JH and Loyd JE. Truncating and missense BMPR2 mutations differentially affect the severity of heritable pulmonary arterial hypertension. *Respiratory research*. 2009;10:87.
45. Girerd B, Montani D, Eyries M, Yaici A, Sztrymf B, Coulet F, Sitbon O, Simonneau G, Soubrier F and Humbert M. Absence of influence of gender and BMPR2 mutation type on clinical phenotypes of pulmonary arterial hypertension. *Respiratory research*. 2010;11:73.
46. Ashek A, Spruijt OA, Harms HJ, Lammertsma AA, Cupitt J, Dubois O, Wharton J, Dabral S, Pullamsetti SS, Huisman MC, Frings V, Boellaard R, de Man FS, Botros L, Jansen S, Vonk Noordegraaf A, Wilkins MR, Bogaard HJ and Zhao L. 3'-Deoxy-3'-[18F]Fluorothymidine Positron Emission Tomography Depicts Heterogeneous Proliferation Pathology in Idiopathic Pulmonary Arterial Hypertension Patient Lung. *Circ Cardiovasc Imaging*. 2018;11:e007402.

47. Esch EW, Bahinski A and Huh D. Organs-on-chips at the frontiers of drug discovery. *Nature reviews Drug discovery*. 2015;14:248-60.
48. Szulcek R, Sanchez-Duffhues G, Rol N, Pan X, Tsonaka R, Dickhoff C, Yung LM, Manz XD, Kurakula K, Kielbasa SM, Mei H, Timens W, Yu PB, Bogaard HJ and Goumans MJ. Exacerbated inflammatory signaling underlies aberrant response to BMP9 in pulmonary arterial hypertension lung endothelial cells. *Angiogenesis*. 2020;23:699-714.
49. Sanchez-Duffhues G, Garcia de Vinuesa A, van de Pol V, Geerts ME, de Vries MR, Janson SG, van Dam H, Lindeman JH, Goumans MJ and Ten Dijke P. Inflammation induces endothelial-to-mesenchymal transition and promotes vascular calcification through downregulation of BMPR2. *J Pathol*. 2019;247:333-346.
50. van Gennep S, Konté K, Meijer B, Heymans MW, D'Haens GR, Löwenberg M and de Boer NKH. Systematic review with meta-analysis: risk factors for thiopurine-induced leukopenia in IBD. *Alimentary pharmacology & therapeutics*. 2019;50:484-506.
51. Olschewski H, Simonneau G, Galiè N, Higenbottam T, Naeije R, Rubin LJ, Nikkho S, Speich R, Hoeper MM, Behr J, Winkler J, Sitbon O, Popov W, Ghofrani HA, Manes A, Kiely DG, Ewert R, Meyer A, Corris PA, Delcroix M, Gomez-Sanchez M, Siedentop H and Seeger W. Inhaled iloprost for severe pulmonary hypertension. *The New England journal of medicine*. 2002;347:322-9.

CHAPTER 11

Nederlandse Samenvatting
Chinese summary
List of Publications
Acknowledgements
About the author

NEDERLANDSE SAMENVATTING

Pulmonale arteriële hypertensie (PAH) is een ziekte die wordt gekenmerkt door progressieve vernauwing van de bloedvaten in de long. Door de vernauwing van de bloedvaten ontstaat er een verhoogde werkdruk voor de rechter hartkamer. De rechter hartkamer (rechter ventrikel, RV) heeft als functie zuurstofarm bloed door de longen te pompen. De linker hartkamer pompt dit zuurstofrijke bloed daarna door het gehele lichaam. Deze bloedsomlopen worden ook wel de kleine en grote bloedsomloop genoemd.

Dit proefschrift gaat over nieuwe veelbelovende therapieën voor PAH en RV dysfunctie, inclusief therapieën gericht op BMPR2 signalering (***Hoofdstuk 2-4***), groeifactoren (***Hoofdstuk 5***), histone deacetylasen (HDACs) (***Hoofdstuk 6***), en therapieën gericht op het RV (***Hoofdstuk 7-9***).

Deel 1: De rol van BMPR2 signalering in PAH

Bij erfelijke vormen van PAH worden in 80% van de gevallen genetische mutaties van het *BMPR2* gengevonden. BMPR2 is een onderdeel van TGF-β receptor familie, en is verantwoordelijk voor de aansturing van vele cellulaire processen zoals celdeling (proliferatie) en inflammatie. PAH patiënten met een *BMPR2* mutatie hebben een slechtere prognose dan patiënten zonder mutaties.

Hoofdstuk 2 onderzoekt de expressie en activiteit van BMPR2 signalering in PAH patiënten en PAH diermodellen. Binnen het PAH onderzoek hebben we de beschikking over meerdere diermodellen. Hier onderzochten we de expressie van BMPR2 in twee veelgebruikte diermodellen. Dit met als doel om het meest accurate diermodel te vinden en zo translatie van data naar de humane situatie te verbeteren. BMPR2 receptor expressie is verminderd in de longvaten van patiënten met idiopathische en erfelijke PAH. Bij de diermodellen konden we deze resultaten niet repliceren maar waren downstream targets van deze receptor wel gelijk aangedaan.

Hoofdstuk 3 richt zich op het verband tussen Nur77 en BMPR2 op de longen in PAH patiënten en diermodel. Nur77 is een orphan nuclear receptor, welke verantwoordelijk is voor de aansturing van vele cellulaire processen en signalering zoals proliferatie, inflammatie en TGF-β signalering. We vonden dat een verminderde Nur77 activiteit in PAH longen en endotheelcellen leidt tot minder BMPR2 expressie. In een PAH diermodel

werd Nur77 geactiveerd door middel van 6-mercaptopurine (6-MP) toediening, wat leidde tot een verminderde vaatremodelering in longweefsel, overleving van de ziekte en een verhoogde BMPR2 expressie.

In ***Hoofdstuk 4*** worden de effecten van MnTBAP op BMPR2 op PAH endotheelcellen onderzocht en de potentiele therapeutische waarde op PAH diermodel bestudeerd. MnTBAP is een remmer van oxidatieve stress, en eerder onderzoek heeft gevonden dat MnTBAP de BMPR2 receptor expressie kan verhogen in endotheelcellen van de navelstrengader. We vonden dat MnTBAP de expressie van BMPR2 receptor heeft verhoogd in endotheelcellen die zijn geïsoleerd uit de longen van overleden of getransplanteerde PAH patiënten. In een PAH diermodel leidde MnTBAP toediening tot verminderde vaatremodelering in longweefsel en overleving van de ziekte.

Deel 2: Andere nieuwe veelbelovende therapieën voor PAH

Verstoorde signalering in endotheelcellen van PAH patiënten is belangrijk voor behangdelingen gericht op groeifactoren, zoals besproken in ***Hoofdstuk 5***. Hoewel proliferatie van gezonde endotheelcellen wordt geremd door nintedanib, een tyrosine-kinase remmer gericht op VEGF, PDGF, FGF en TGF-β signalering, wordt dit effect niet gezien in PAH endotheelcellen. Er werd ook geen effect van nintedanib geobserveerd op vaatremodelering in longweefsel van een PAH diermodel. Wel vonden wij onverwacht een verbetering op RV dilatatie, mogelijk door fibrose remming in het hart. Deze studie suggereert dat nintedanib, een medicament goedgekeurd voor patiënten met idiopathische pulmonale fibrose (IPF), veilig kan worden gebruikt in de context van pulmonale hypertensie geassocieerd met IPF.

In ***Hoofdstuk 6*** hebben we het effect van quisinostat, een HDACs remmer, op PAH endotheelcellen getest en de potentiele therapeutische waarde op drie diermodellen bestudeerd. Eerder onderzoek heeft omgekeerde effecten aangetoond van HDACs remmers als behandelingen voor PAH diermodellen. Quisinostat is een nieuwe tweede generatie remmer van HDACs met lange farmacodynamische respons. We vonden dat proliferatie en inflammatie van PAH endotheelcellen worden geremd door quisinostat, net zoals vaatremodelering in longweefsel van PAH diermodellen. Er werd geen effect van quisinostat geobserveerd op het hart van diermodel met RV dysfunctie.

Deel 3: Veelbelovende therapieën gericht op het RV

RV functie is een belangrijke prognostische factor voor het verloop van PAH. In ***Hoofdstuk 7*** wordt de rol van inflammatie in het RV beschreven. Inflammatie in het hart, zoals beschreven is in veel andere vormen van hartfalen, komt ook voor in het RV van PAH patiënten en in diermodellen van RV falen. RV inflammatie draagt waarschijnlijk bij aan verslechterde RV contractiliteit, RV remodelering en aan de vicieuze cirkel tussen RV falen en schade aan longvaten. Anti-inflammatoire therapieën zijn klinisch getest in patiënten met LV falen, met wisselend succes. Het is echter nooit getest of anti-inflammatoire therapieën de RV functie kunnen verbeteren. Omdat inflammatie een rol speelt bij zowel het ontstaan van vasculaire schade in de longen en bij RV falen, zou een anti-inflammatoire therapie op beide een gunstig effect kunnen hebben in patiënten met PAH en RV falen.

In ***Hoofdstuk 8*** hebben we gekeken naar de effecten van dichlooracetaat (DCA) op apoptose in het RV, in een diermodel van PAH. DCA remt pyruvaat dehydrogenase kinases (PDKs) en bleek in eerdere studies een veelbelovende nieuwe therapie voor PAH en RV falen. Echter, studies naar het effect van DCA op apoptose laten wisselende resultaten zien. In een rat-model van PAH hebben we gevonden dat behandeling met DCA een gunstig effect heeft op het RV, niet alleen door apoptose in het RV te verminderen en mitochondriële functie te verbeteren. Dit is een belangrijke bevinding, omdat het laat zien dat DCA niet zorgt voor een toename in apoptose in het RV, terwijl DCA wel apoptose stimuleert in de longen. Dit ondersteunt het idee dat DCA inderdaad een veelbelovende behandeling is voor PAH patiënten.

In ***Hoofdstuk 9*** hebben we bestudeerd wat de rol van monoamine oxidase A (MAO-A) bij de vasculaire remodelering en RV falen in PAH. Als mitochondrieel enzym is MAO-A een grote bron van oxidatieve stress. MAO-A speelt een rol in de pathofysiologie van verschillende cardiovasculaire aandoeningen. Wij hebben gevonden dat de expressie van MAO-A is toegenomen in de longvaten van PAH patiënten en in een diermodel, en daarnaast ook in het RV van twee diermodellen van RV falen. Farmacologische inhibitie van MAO-A met clorgyline verlaagde de nabelasting op het RV. Het verminderde ook de remodelering van de longvaten, door oxidatieve stress en proliferatie te verlagen. MAO-A inhibitie had echter geen direct effect op het RV, en het gunstige effect op het RV in het diermodel van PAH is te wijten aan verbeteringen in de longvaten. Concluderend lijkt MAO-A betrokken te zijn bij de pathofysiologie van PAH.

中文总结

肺高血压 (pulmonary hypertension, PH) 是一类常见肺血管疾病, 其主要病理生理学特征是静息状态下肺动脉压力升高, 同时合并不同程度右心功能衰竭。肺动脉高压 (pulmonary arterial hypertension, PAH) 为孤立性肺动脉压力升高, 而左心房与肺静脉压力正常, 主要由肺小动脉重构导致肺血管阻力增加, 且不合并慢性呼吸系统疾病、慢性血栓栓塞性疾病及其它未知因素导致的肺高血压。PAH属于肺高血压第一大类, 其血流动力学诊断标准为右心导管测量平均肺动脉压力≥20 mmHg, 同时肺小动脉楔压≤15 mmHg及肺血管阻力>3 Wood单位。

本论文旨在探索与研究针对PAH以及右心功能衰竭的新型治疗药物, 其筛选基于PAH的多种不同发病机制, 包括骨形态生成蛋白2型受体 (BMPR2, 论文**第2–4章节**) , 生长因子 (论文**第5章节) ,** 组蛋白乙酰化 (论文**第6章节**) , 以及针对右心的靶点治疗 (论文**第7–9章节**) 。

骨形态生成蛋白2型受体 (BMPR2) 与肺动脉高压

BMPR2信号通路在PAH发病机制中有重要作用, 而基于BMPR2通路的新型治疗方案在近年来受到很大关注。因此, 阐明BMPR2信号通路在PAH动物模型与PAH患者肺血管中表达的一致性对于相关转化医学研究非常关键。在本论文**第二章节**中, 我们分别研究了BMPR2及其下游信号通路在PAH动物模型与患者肺组织及肺血管中的表达。本研究发现BMPR2在PAH动物模型中表达异常, 然而与PAH患者相比却有所不同。对BMPR2通路的进一步研究发现, BMPR2下游信号通路Smads在PAH动物模型与PAH患者肺血管中的表达具有一致性, 但造成BMPR2与其下游信号表达不同的原因仍需进一步研究。本章节为进一步研究BMPR2通路与PAH发病机制提供了新思路, 并且为以BMPR2通路作为PAH新型治疗方案的转化医学研究提供了重要参考。

在本论文**第三与第四章节**中, 我们分别研究了基于BMPR2通路的两种药物, 6–巯基嘌呤 (6–MP) 与锰卟啉 (MnTBAP) 在实验型PAH中的潜在治疗作用。6–MP是一种广泛使用的抗白血病药剂和免疫抑制药, 不仅能够抑制嘌呤合成, 还能够通过激活孤儿核受体Nur77调节细胞增殖, 凋亡与炎症反应等。在**第三章节**中, 我们通过研究发现, Nur77在PAH患者的肺组织中表达下调, 且与PAH肺动脉内皮细胞的增殖, 炎症反应及BMPR2信号通路的调节密切相关。根据此结果, 我们进一步研究了6–MP作为Nur77激活药物对PAH动物模型的治疗作用, 并发现6–MP不

仅对动物模型中PAH的发病具有预防作用，且可在PAH动物模型中降低右心后负荷，部分逆转肺动脉重构，抑制炎症反应并激活BMPR2信号通路。本章节阐明了Nur77在PAH发病机制中的重要作用，并揭示Nur77可作为具有潜力的PAH新型治疗靶点。

MnTBAP 是一种新型具有稳定性和细胞渗透性的超氧化物歧化酶模拟物，具有抗氧化性及抗炎性。以往研究表明，MnTBAP可上调BMPR2在人脐静脉内皮细胞中的表达。在**第三章节**中，我们发现MnTBAP可同样上调BMPR2在PAH患者肺动脉内皮细胞中的表达，而MnTBAP在PAH动物模型中治疗效果显著，可降低右心后负荷，部分逆转肺动脉重构，并降低氧化应激造成的肺血管损伤。本章节通过研究超氧化物歧化酶模拟物在肺动脉内皮细胞中对BMPR2的调节，揭示了其作为PAH新型治疗手段的可能性。

生长因子，组蛋白乙酰酶与肺动脉高压

已有的研究表明，多种生长因子失调在PAH发病机制中有重要作用，包括血小板衍生生长因子PDGF，成纤维细胞生长因子FGF，血管内皮细胞生长因子VEGF，以及转化生长因子TGF–β。在本论文**第五章节**中，我们研究了尼达尼布（nintedanib）对PAH的治疗作用。尼达尼布为一种新一代治疗癌症及特发性肺纤维化的口服药物，对PDGF–，FGF–，VEGF–，以及TGF–β引起的肺成纤维细胞增殖及分化有抑制作用。本研究发现，尼达尼布可抑制正常肺血管内皮细胞增殖，然而对PAH患者肺血管内皮细胞增殖并无作用。同样，在PAH动物模型中，尼达尼布治疗无法逆转肺动脉重构。然而，进一步对右心的研究表明，尼达尼布可部分逆转右心室肥厚及纤维化。此研究证实了尼达尼布对右心重构的治疗作用，为尼达尼布应用于特发性肺纤维化相关PH的治疗提供了依据。

组蛋白脱乙酰酶（HDACs）是一类蛋白酶，通过对染色体的结构修饰和基因表达的调控,在细胞生物活动中发挥着重要作用，包括调节细胞增殖，凋亡和炎症反应等。以往研究表明，HDACs活性异常参与PAH发病机制，然而HDACs抑制剂对PAH的治疗效果及对右心的安全性具有不确定性。在本论文**第六章节**中，我们研究了第二代新型HDACs抑制剂quisinostat对实验性PAH的治疗效果。不同于其它HDACs抑制剂，quisinostat具有更加长效的药物动力学反应，并对PAH相关HDAC亚型具有更强的抑制作用。本能研究发现，quisinostat不仅能抑制PAH肺血管内皮细胞增殖及炎症反应，且能够在两种PAH动物模型中部分逆转肺动脉重

构。进一步对右心的检测发现，quisinostat对右心功能及重构没有直接作用。此研究证实了新型HDACs抑制剂quisinostat对实验性PAH的治疗作用，且证实了其治疗对右心的安全性。

针对右心的新型靶点治疗

PAH虽然以肺血管损伤为始发因素，但决定PAH患者生存时间长短的最重要因素却是右心功能。最近的研究表明，右心异常重构是引发并促进右心衰竭的重要因素，然而其重构的复杂机制依然未知，而寻找逆转重构的靶点治疗方法成为目前PAH领域研究热点。在本论文**第七章节**中，我们通过文献综述回顾了炎症反应在促进右心衰竭中的作用。以往研究在右心衰竭患者及动物模型中均找到了右心炎症反应增加的证据，且发现右心炎症可损害右心室收缩功能，并对促进右心重构、肺血管与右心损伤之间的恶性循环起重要作用。尽管抗炎治疗对右心功能的作用尚不明确，但已有临床研究表明其对改善左心衰竭有显著作用。考虑到炎症反应在肺血管与右心损伤中的双重作用，我们认为抗炎治疗可成为具有潜力的PAH及右心衰竭治疗靶点。

本论文**第八章节**对二氯乙酸钠（DCA）治疗在右心重构中的作用进行了研究。作为丙酮酸脱氢酶激酶抑制剂，DCA治疗被以往研究证实对实验性PAH及右心衰竭有改善作用，然而DCA对不同来源细胞凋亡的作用具有不确定性，因而DCA治疗对右心的安全性具有不确定性。本研究结果表明，DCA治疗不仅能够在PAH动物模型改善心脏功能，还能够抑制心肌细胞凋亡并改善线粒体形态与功能。本研究充分证实了DCA治疗对右心的安全性，为DCA治疗PAH开展临床研究提供了重要依据。

本论文**第九章节**旨在研究单胺氧化酶A（MAO–A）在PAH肺血管重构及右心衰竭发病机制中的作用。MAO–A存在于细胞的线粒体外膜上，是产生活性氧化物的主要来源之一，在多种心血管疾病的发病机制中有重要作用。本研究结果表明，MAO–A不仅在PAH患者及动物模型肺血管中表达升高，且在两种右心衰竭动物模型的右心组织中表达与活性均升高。MAO–A抑制剂clorgyline可在PAH动物模型中降低右心后负荷，部分逆转肺动脉重构并抑制肺血管增殖与氧化应激损伤。对右心的进一步研究表明，clorgyline只可通过逆转肺血管重构改善右心功能，对右心功能及重构本身并无直接作用。本研究首次发现了MAO–A在PAH肺血管及右心的高表达，并揭示了MAO–A在PAH发病机制中的可能作用。

LIST OF PUBLICATIONS

Sun XQ, Abbate A, Bogaard HJ. Role of cardiac inflammation in right ventricular failure. *Cardiovasc Res* 2017, 113(12): 1441-1452. (Review)

Jujo-Sanada T #, **Sun XQ #,** Happé CM , Guignabert C, Tu L, Schalij I, de Man FS, Bogaard HJ, Goumans MJ, Kurakula K. Altered TGFB/SMAD signaling in human and rat models of pulmonary hypertension: an old target needs attention. *Cells.* 2021, 10(1):84.

Sun XQ #, Peters EL #, Schalij I, Axelsen JB, Andersen S, Kurakula K, Gomez-Puerto MC, Szulcek R, Pan X, da Silva Gonçalves Bos D, Schiepers REJ, Andersen A, Goumans MJ, Vonk Noordegraaf A, van der Laarse WJ, de Man FS, Bogaard HJ. Increased MAO-A activity promotes progression of pulmonary arterial hypertension. *Am J Respir Cell Mol Biol* 2020, Dec 2.

Gomez-Puerto MC #, **Sun XQ #,** Schalij I, Orriols M, Szulcek R, Pan X, Goumans MJ, Bogaard HJ, Zhou Q and ten Dijke P. MnTBAP reverses pulmonary vascular remodeling and improves cardiac function in experimental pulmonary arterial hypertension. *Int J Mol Sci*. 2020, 21(11): 4130.

Kurakula K #, **Sun XQ #**, Happé C, da Silva Goncalves Bos D, Szulcek R, Schalij I, Wiesmeijer KC, Lodder K, Tu L, Guignabert C, de Vries CJM, de Man FS, Vonk Noordegraaf A, Ten Dijke P, Goumans MJ, Bogaard HJ. Prevention of progression of pulmonary hypertension by the Nur77 agonist 6-mercaptopurine: role of BMP signalling. *Eur Respir J*. 2019, 54(3): 1802400.

Sun XQ, Zhang R, Zhang HD, Yuan P, Wang XJ, Zhao QH, Wang L, Jiang R, Jan Bogaard H, Jing ZC. Reversal of right ventricular remodeling by dichloroacetate is related to inhibition of mitochondria-dependent apoptosis. *Hypertens Res* 2016, 39(5): 302-311.

Sun XQ #, Kurakula K #, Hagdorn QAJ, Van der Feen DE, ten Dijke P, Ingrid Schalij, Peters EL, Berger RM, Goumans MJ, Bogaard HJ. Selective inhibition of Histone deacetylases by quisinostat reverses vascular remodelling in experimental pulmonary hypertension. (In preparation)

Happé CM #, Kurakula K #, **Sun XQ**, Bos D, Rol N, Guignabert C, Tu L, Schalij I, Wiesmeijer CC, Vonk-Noordegraaf A, ten Dijke P, de Man FS, Bogaard HJ, Goumans MJ. The BMP receptor 2 in pulmonary arterial hypertension: when and where the animal model matches the patient. *Cells.* 2020, 9(6): 1422.

Rol N #, de Raaf MA #, **Sun XQ**, Kuiper VP, da Silva Gonçalves Bos D, Happé C, Kurakula K, Dickhoff C, Thuillet R, Tu L, Guignabert C, Schalij I, Lodder K, Pan X, Herrmann FE, van Nieuw Amerongen GP, Koolwijk P, Vonk-Noordegraaf A, de Man FS, Wollin L, Goumans MJ, Szulcek R, Bogaard HJ. Nintedanib improves cardiac fibrosis but leaves pulmonary vascular remodeling unaltered in experimental pulmonary hypertension. *Cardiovasc Res.* 2019, 115(2):432-439.

Zhang R, Wang XJ, Zhang HD, **Sun XQ**, Zhao QH, Wang L, He J, Jiang X, Liu JM, Jing ZC. Profiling nitric-oxide metabolites in patients with idiopathic pulmonary arterial hypertension. *Eur Respir J* 2016, 48(5): 1386-1395.

Bós D, Van Der Bruggen CEE, Kurakula K, **Sun XQ**, Casali KR, Casali AG, Rol N, Szulcek R, Dos Remedios C, Guignabert C, Tu L, Dorfmüller P, Humbert M, Wijnker PJM, Kuster DWD, van der Velden J, Goumans MJ, Bogaard HJ, Vonk-Noordegraaf A, de Man FS, Handoko ML. Contribution of impaired parasympathetic activity to right ventricular dysfunction and pulmonary vascular remodeling in pulmonary arterial hypertension. *Circulation.* 2018, 137(9): 910-924.

Axelsen JB, Andersen S, **Sun XQ**, Ringgaard S, Hyldebrandt JA, Kurakula K, Goumans MJ, de Man FS, Nielsen-Kudsk JE, Bogaard HJ, Andersen A. Effects of 6-mercaptopurine in pressure overload induced right heart failure. *PLoS One.* 2019 Nov 12;14(11): e0225122.

Bogaard HJ, Legchenko E, Chaudhary KR, **Sun XQ**, Stewart DJ, Hansmann G. Emphysema is - at the most - only a Mild Phenotype in the Sugen-Hypoxia Rat Model of Pulmonary Arterial Hypertension. *Am J Respir Crit Care Med.* 2019 Aug 22.

Bogaard HJ, Legchenko E, Ackermann M, Kühnel MP, Jonigk DD, Chaudhary KR, **Sun X**, Stewart DJ, Hansmann G. The Adult Sprague-Dawley Sugen-Hypoxia Rat Is Still "the One:" A Model of Group 1 Pulmonary Hypertension: Reply to Le Cras and Abman. *Am J Respir Crit Care Med.* 2019 Nov 26.

 # shared first authorship

ACKNOWLEDGEMENT

I still remember the first day I arrived at the Netherlands, full of curiosity and confusion. Time flies! I feel really lucky to have had the opportunity to do my Ph.D here in the Netherlands and get to know you all, my most kind supervisors, colleagues and friends. Thanks to you all, I had a wonderful time here all these years!

To my promotor, dear Harm Jan, thank you for giving me the amazing opportunity to start my research adventure here in the Netherlands. I still remember the first time when we met at Pudong Airport in Shanghai, I was very nervous. But you gave me lots of encouragement on my English and manuscript. At Shanghai Pulmonary Hospital, I was impressed not only by your research presentation, but also the care and warmth you showed towards the patients. During the 5 years working in your research team, you have always been supportive, helpful and encouraging, just as you showed on the first day. I experienced various troubles during my research. However, thanks to you, my research life got much easier under your support. I feel so lucky to have you as my supervisor!

Dear MJ, I am so happy to have you as my promotor together with Harm Jan! I always admire your knowledge background and sharp mind as a scientist. You once said that you feel very lucky, because your hobby and your job are about the same thing, research and science. It is very impressive and motivates me a lot to enjoy research itself, not just to complete it as a task. You are always very supportive to my research, and willing to hear and respond to my opinions. Even when I have unwise ideas sometimes, you always give positive feedback and explain things with lots of patience. Thanks a lot for all your support!

Dear Frances, I am really lucky to have you as my daily supervisor and co-promotor! As my supervisor, I experienced your strict and critical side. However, your help and positive attitude helped me along the way. I surely learned a lot from you. Your useful and constrictive suggestions on my research have been instrumental to the success. More importantly, you encouraged me a lot to think with an analytical and critical mind. This was certainly a personal challenge, given the educational climate of my home country. I sincerely believe that my experiences under your supervision will prove to be helpful in my future research career. I am thankful for all your help. To me, both you and MJ are my idol as female scientists in this field.

Anton, many thanks for giving me the opportunity to come to The Netherlands and do my internship. When I started the planning to do research internship abroad, you were the first one I emailed, and surprisingly got your reply within just one hour. It meant a lot for me, which was a great encouragement. I find it rather pitiful that we did not find much time to discuss my research together. But every time during my presentations, you can always give me very constructive suggestions and supportive comments. You have all my gratitude for your support. But what I will miss the most, are the BBQ parties in your charming garden.

I would like to thank everyone in my thesis reading and defense committee: Prof. Bianca Brundel, Prof. Sébastien Bonnet, Prof. Rudolf de Boer, associate Prof. Asger Andersen, associate Prof. Beatrijs Bartelds and assistant Prof. Gonzalo Sánchez-Duffhues. Each one of you have been of tremendous help, I very much appreciate your involvement and efforts.

I would like to thank Prof. Sébastien Bonnet in particular, for offering me the wonderful opportunity to work at your group and continue my research career in Quebec, Canada. I am really looking forward to this adventure, to working with you at this wonderful group and doing nice research!

I would like to thank Prof. Peter ten Dijke and Catalina at LUMC. Dear Prof. Peter ten Dijke, the first time when I met you at the Pheadra meeting, I was already impressed by your kindness, being helpful and easy-going. I feel very lucky to have had the opportunities to work with you, and you can always gave practical and useful comments to my manuscripts. Thank you very much for all the great help to my research. Dear Catalina, I am really happy to get the chance to accomplish MnTBAP study with you! Your hard-working style and your passion to research are very impressive to me. I really enjoyed it to work with you.

I would like to thank my collaborators at Aarhus University Hospital Denmark, associate Prof. Asger Andersen, Stine and Julie. Dear associate Prof. Asger Andersen, thank you very much for offering me the opportunity to do research at your lab! Besides, I really like your video about PTB model, which I have watched many times and learned a lot. Stine and Julie, thanks for helping me and Eva when we were in Aarhus. It was of great fun to work with you. I enjoyed a lot with you girls at those delicious food markets and the Tupperware party!

My good friends, colleagues and first-year supervisors Deni, Chris and Babu. Dear Deni and Chris, I am so happy that Harm Jan asked you two to supervise me during my internship. The beginning is always the most difficult part, but you both helped me out so much that I could easily build up my life here. You two helped me not only with research, but also with searching for housing, a bike and friends. You are both the friends that I cherish, you mean a lot to me. I miss all the super spicy food with Chris and all the Brazilian barbecue with Deni! Dear Babu, I am really happy to have so many collaborations with you, and achieved much success together. I learned a lot from you and really appreciate all your help. Besides being a good collaborator, I see you as my steady and good friend. I hope that our paths in the future will cross again, and that we may enjoy further collaboration opportunities.

I would like to thank my teammates for animal studies, Eva and Ingrid. Dear Eva, it is really exciting to accomplish the difficult MAO-A journey with you! Though we experienced many failures, I feel proud that we finally accomplished this long journey together while supporting each other. The two months in Denmark with you are unforgettable. The days were rainy and dark, but you could always come up with something fun to add colors to life, museums, national parks, played "basketball" game with the lab clothes, made photos hiding in the closet, funny workouts... Dear Ingrid, I got so much help from you during the 5 years, with every project, thanks so much! You are an amazing animal research expert! I could always feel relieved for any animal experiment when you were around. I really enjoyed working with you, I will miss those long days we spent together at UPC. It was such a relieve for me and Eva when you went to Aarhus to help us. We had such "gezellige momenten" together in Aarhus at that cold dark night!

I would like to thank everyone in our PH research team: Willem, Jurjan, Robert, Berend, Xue, Aida, Kim, Taka, Keimei, Mo, Liza, Eva, Ingrid, Pan, Rowan, Chris, Deni, Nina, Onno, Cathelijne, Anna, Diewertje, Joanne, Josien, Natalia, Samara, Jessie, Chermaine, Jelco. A special thanks to our great technicians: Ingrid, Pan and Rowan; to our very helpful secretaries: Ella, Anny, Ellen and Irma; to dear Willem for the great support for MAO-A study; to dear Aida, Xue and Kim for the great help at the lab; to dear Taka for achieving the success together on TGF study; and to dear Robert for the great help at the lab and with my job hunting.

I would like to thank the physiology department: Jolanda, Bianca, Coen, Reinier, Diederik, Peter, Pieter, Ed, Alice, Isabelle, Victor, Josien. Dear Jolanda, I very much admire your great passion for research and your sharp mind during research discussions. However, to me your taste for fashion and design is most captivating. Thanks for all your encouragement and support! Dear Bianca, I am so glad that you can be the chair of my thesis reading committee, thank you so much for all the effort and help! Dear Coen, thanks for considering me for the position in the US, and thanks for all the kind advices for me! Dear Reinier, thanks for the advices during my job hunting, and thanks for training us for running, I had so much fun to join your running team! A special thanks to the very helpful technicians: Ruud, Sylvia, Pedro, Jeroen, Jan, Zeineb, Max, Michiel, Anoek and Kim; to the very kind secretaries: Aimee and Jessica; to Isabelle for helping me with Ph.D application process; and to Duncan for helping with all kinds of software issues.

Thanks to the UPC employees, especially Rika, Joëlle, Carla, Jerry and all the other UPC-employees who have helped us during weekends, thanks for the great help and support for our animal studies.

I would like thank all my dear colleagues and friends at the lab: Larissa, Maike, Stefan, Diewertje, Jisca, Phat, Rio, Veerle, Vanessa, Martijn, Pedro, Natalija, Zeineb, Max, Ricardo, Kennedy, Edgar, Alex, Aref, Denise, Marit, Babara, Vasco. A special thanks to my desk "neighbors" Phat, Xue, Veerle and Jisca. I had so much fun sitting next to you guys! I miss the big magic jar of Phat, always full of chocolate and candies.

Dear Mo, Taka, Elisa, Chris, Veerle, Aida, Rio, Phat, Xue, thank you guys for giving me an unforgettable, exciting hotpot party of 30s birthday!! I cannot help to put a big smile on my face every time when I look at these dinner photos with you guys, the Rio strategies for all-you-can-eat, the incredible high spicy level of Chris, and the super low spicy level of most of you guys...I am looking forward to having hotpot with you guys again! And Keimei, I am so glad that you joined us for hotpot years ago during your visit, and really happy that you become now a part of this lab!

My dear friends Rahana and Richard, Elisa and Matteo, I am so happy to have you lovely couples as my friends and witnessed your sweetest moment of the wedding. I hope we can get together very soon to have dinner and drinks. To another lovely couple, my dear friends Deni and Marcelo, I am really happy for you that you are finally settling down

in Brazil after so many years. I am looking forward to hearing about your wedding moment! My dear friend Octavia, I was so happy to meet you at Deni's party! You are a cheerful and energetic person with a lot of happy laughter. We had great fun together during those single days, dancing at music festival and going to movies. I am really happy for you that you have such a lovely family with Marcin! And thanks for your help during my job hunting!

I would like to give a special shout-out and thanks to Rahana and Eva. You have been of so much help and support during my defense. I feel both honored and grateful that you have been at side during the final act of my thesis.

Thanks to dear Mechelina, August and Tirsa, always treat me with a lot of love, care and warmth. You can always make me feel like at home. I enjoy so much to be with the lovely "gezellige" family. I am very grateful for all that you have done for me. Special thanks to my dear Ivor, how wonderful life is while you are by my side! You bring me so much love, support and great happiness. I am so much looking forward to experiencing a lot of wonderful things in the world together with you and sharing everything in life with you!

For my dear Chinese friends in the Netherlands

感谢在同一个实验室的中国小伙伴们! 活力四射阿潘潘, 你是我来荷兰后认识的第一个中国人, 意义非凡呢, 你就是实验室的一道阳光, 既带来开心快乐做实验还又特别给力, 有你在可真好! 文艺清新有格调的小旭旭, 好多难忘快乐的时光, 想念跟你一起胡吃海喝, 一起练剑道痛苦地憋笑, 还有在黑灯瞎火中摸索着骑车的日子! 知识渊博又趣味十足的华姐, 跟你一起刹不住的畅聊谈天说地可真爽, 我会格外想念你的咖啡和华姐夫的番茄烧牛肉! 温柔智慧的Deli姐, 是暖心大姐姐, 总能在我有困难的时候给我很大安慰, 还教会了我摘野韭菜, 做美味的野韭菜大包子! 潇洒走四方的小金金, 你总是那么乐观积极独立, 给了我很大鼓舞, 还有你的水饺大盘鸡, 全荷兰无敌! 还有我善解人意的老乡学妹思雨, 特想跟你一起边吃火锅边聊天, 再来一盘狼人杀, 咱还可以约在石家庄走起, 想想就老激动了! 还有最近才来到我们实验室的袁师弟, 积极上进又努力, 肯定前途无量, 要好好享受荷兰的日子哈!

感谢我在荷兰结交的中国小伙伴们, 你们的相伴给我在荷兰的日子平添了好多色彩! 文艺青年蔡博士+摄影师, 以及特别想看斗牛的辉哥, 真想念咱们一起去开会

的日子, 在马德里街头闲逛、拍大片、吃吃喝喝地中海风味, 还能顺便交流 (吐嘈) 下学术问题。还有时尚达人小鹤鹤, 只要在各种论坛、课程遇见你, 便顿时不枯燥了, 想念跟你和蔡博在Papendal下课后一起谈天说地的时光。还有乌得勒支的小伙伴媛媛, 好开心在徒步活动的时候遇见你, 一聊就是一路, 还有在你家一起包饺子、玩游戏, 特别美好的回忆, 祝你在荷兰要快快乐乐、一切都顺利哦!

For my dear supervisors in China

荆志成主任 北京协和医院

荆主任, 我一直非常荣幸自己是您的学生! 不仅仅因为您在肺血管领域作出的卓越贡献, 更因为您对待事业, 对待人生的态度。在跟随您学习的日子里, 充分体会到您对待患者的耐心细致, 对待科研的严谨求实, 对待每一位学生的认真负责。您一直是我们学生心目中的骄傲和榜样。我希望自己能在肺血管疾病研究领域继续走下去, 还期望有机会能跟您学习更多, 更期待有朝一日能够给您争光, 不负您的教导!

张锐老师 上海肺科医院

张老师, 您是我在肺动脉高压基础研究领域的启蒙老师, 对我来说意义非凡, 弥足珍贵! 作为从临床转到基础研究的学生, 当年我对基础研究所知甚少, 几乎等同于一张白纸。多亏了您在理论上耐心的辅导, 在实验室手把手的教学, 才把我一点一点领上基础科研的道路。非常感谢您对我如此悉心的指导! 期待将来有机会跟张老师合作, 继续向张老师学习!

For my loving parents

特别感谢我的爸爸妈妈, 感谢你们给予我无条件的支持、关爱和鼓励, 提醒我以脚踏实地的本心面对顺境, 又开导我以强大而韧性十足的内心面对挫折。感谢你们给予我充分的自由和信任, 让我有机会追求自己喜欢的生活, 又鼓励我追求自己擅长并热爱的工作。感谢你们给予我平等、温馨的家庭氛围, 人生中各种问题我们都可以一起交流、探讨、反省, 内心一起成长。特别感谢你们做我坚定强大的后盾! 爱你们!

ABOUT THE AUTHOR

Xiaoqing Sun was born on 13th December 1989 in Lanling, Linyi City, Shandong province, China. In 2007, after her graduation from NO.24 High School of Shi Jiazhuang City, Hebei Province, she got the opportunity to study at the Tongji University Shanghai, where she was enrolled in the 8-year medical program.

After finalizing her studies at the Tongji University in 2013, Xiaoqing continued her educational career by studying cardiovascular diseases. It was during this time while being under the supervision of Prof. Zhicheng Jing, that Xiaoqing developed a keen interest in the research field of pulmonary hypertension.

Two years later, in 2015, Xiaoqing managed to get an internship scholarship from the Tongji University. She used this scholarship to do an internship in the Netherlands and started her research training at the VU Medical Center and at the Leiden University Medical Center. Xiaoqing focused on the novel treatment of pulmonary hypertension, under the supervision of Prof. Harm-Jan Bogaard. Xiaoqing returned to Shanghai after this internship in order to defend her thesis. The thesis carried the title: ''The Effect of Dichloroacetate on Experimental Pulmonary Arterial Hypertension Induced Right Ventricular Failure''. This concluded her studies at the Tongji University for which she received the doctor's degree in Medicine.

Roughly one year later in July 2016, Xiaoqing got the opportunity to extend her research career as Ph.D. candidate. The VU Medical Center in Amsterdam offered Xiaoqing an challenging but interesting opportunity under the supervision of Prof. Harm Jan Bogaard, Prof Marie-José Goumans and associate Prof. Frances de Man.

Upon receiving her Ph.D. degree, Xiaoqing will continue her efforts in the field of pulmonary hypertension. She will pursue the position as postdoc researcher at the Canadian University: ''Université Laval'', under the supervision of Prof. Sébastien Bonnet.